SYNTHESIS OF HIGHLY CRYSTALLINE MULTILAYERES STRUCTURES OF BNNTs AS A POTENTIAL NEUTRON SENSING ELEMENT

PERVAIZ AHMAD

FACULTY OF SCIENCE
UNIVERSITY OF MALAYA
KUALA LUMPUR

2016

SYNTHESIS OF HIGHLY CRYSTALLINE MULTILAYERES STRUCTURES OF BNNTs AS A POTENTIAL NEUTRON SENSING ELEMENT

PERVAIZ AHMAD

THESIS SUBMITTED IN FULFILMENT OF THE REQUIREMENTS FOR THE DEGREE OF DOCTOR OF PHILOSOPHY

FACULTY OF SCIENCE
UNIVERSITY OF MALAYA
KUALA LUMPUR

2016

UNIVERSITY OF MALAYA
ORIGINAL LITERARY WORK DECLARATION

Name of Candidate: Pervaiz Ahmad

Registration/Matric No: SHC130059

Name of Degree: Doctor of Philosophy

Title of Thesis:

Synthesis of Highly Crystalline Multilayers Structures of BNNTs as a Potential Neutron Sensing Element

Field of Study: Experimental Physics

I do solemnly and sincerely declare that:

(1) I am the sole author/writer of this Work;
(2) This Work is original;
(3) Any use of any work in which copyright exists was done by way of fair dealing and for permitted purposes and any excerpt or extract from, or reference to or reproduction of any copyright work has been disclosed expressly and sufficiently and the title of the Work and its authorship have been acknowledged in this Work;
(4) I do not have any actual knowledge nor do I ought reasonably to know that the making of this work constitutes an infringement of any copyright work;
(5) I hereby assign all and every rights in the copyright to this Work to the University of Malaya ("UM"), who henceforth shall be owner of the copyright in this Work and that any reproduction or use in any form or by any means whatsoever is prohibited without the written consent of UM having been first had and obtained;
(6) I am fully aware that if in the course of making this Work I have infringed any copyright whether intentionally or otherwise, I may be subject to legal action or any other action as may be determined by UM.

Candidate's Signature Date:

Subscribed and solemnly declared before,

Witness's Signature Date:

Name:

Designation:

UNIVERSITI MALAYA

PERAKUAN KEASLIAN PENULISAN

Nama: Pervaiz Ahmad

No. Pendaftaran/Matrik: SHC130059

Nama Ijazah: Doktor Falsafah

Tajuk Tesis:

Sintesis Multilayers Highly Crystalline Structures daripada BNNTs sebagai Potensi Neutron Sensing Element

Bidang Penyelidikan: Fizik eksperimen

Saya dengan sesungguhnya dan sebenarnya mengaku bahawa:

(1) Saya adalah satu-satunya pengarang/penulis Hasil Kerja ini;
(2) Hasil Kerja ini adalah asli;
(3) Apa-apa penggunaan mana-mana hasil kerja yang mengandungi hakcipta telah dilakukan secara urusan yang wajar dan bagi maksud yang dibenarkan dan apa-apa petikan, ekstrak, rujukan atau pengeluaran semula daripada atau kepada mana-mana hasil kerja yang mengandungi hakcipta telah dinyatakan dengan sejelasnya dan secukupnya dan satu pengiktirafan tajuk hasil kerja tersebut dan pengarang/penulisnya telah dilakukan di dalam Hasil Kerja ini;
(4) Saya tidak mempunyai apa-apa pengetahuan sebenar atau patut semunasabahnya tahu bahawa penghasilan Hasil Kerja ini melanggar suatu hakcipta hasil kerja yang lain;
(5) Saya dengan ini menyerahkan kesemua dan tiap-tiap hak yang terkandung di dalam hakcipta Hasil Kerja ini kepada Universiti Malaya ("UM") yang seterusnya mula dari sekarang adalah tuan punya kepada hakcipta di dalam Hasil Kerja ini dan apa-apa pengeluaran semula atau penggunaan dalam apa jua bentuk atau dengan apa juga cara sekalipun adalah dilarang tanpa terlebih dahulu mendapat kebenaran bertulis dari UM;
(6) Saya sedar sepenuhnya sekiranya dalam masa penghasilan Hasil Kerja ini saya telah melanggar suatu hakcipta hasil kerja yang lain sama ada dengan niat atau sebaliknya, saya boleh dikenakan tindakan undang-undang atau apa-apa tindakan lain sebagaimana yang diputuskan oleh UM.

Tandatangan Calon Tarikh:

Diperbuat dan sesungguhnya diakui di hadapan,

Tandatangan Saksi Tarikh:

Nama:

Jawatan:

ABSTRACT

We developed a simple and cost-effective Argon supported thermal CVD technique for the synthesis of h-BN nanostructures. Our developed technique for the synthesis of boron nitride nanotubes (BNNTs) is about 18 % less expensive as compared to the known simplest CVD techniques and 25 – 35 % to any other technique with respect to the cost of experimental setups and other accessories. The optimization of experimental parameters and slight modification of our Argon supported thermal CVD technique leads to the synthesis of different types, size, morphologies and shapes of h-BN nanostructures such as BNNTs, BNNWs, BNMTs and BNNS etc. Change in precursors and substrate nature resulted in different morphologies and formats of BNNTs, whereas the change of reaction atmosphere from Argon to Ammonia resulted in the synthesis of BNMTs. The decrease in the growth duration (60 min → 30 min) and arrangement of vapor – liquid – solid (VLS) growth mechanism resulted in the synthesis of BNNWs, whereas an increase in the growth duration (60 min → 90 min) in the presence of ammonia as a reaction atmosphere resulted in the formation of BNNS. FESEM, EDX, HR-TEM, XPS and Raman are used as characterization tools to study the morphology, size, internal structure, elemental compositions and phase of the final product, respectively. The synthesized nanostructures of h-BN have importance not only in the field of biomedical or microelectronic mechanical systems but also in the developments of solid state neutron detectors with higher detection efficiency.

ABSTRAK

Kami membangunkan teknik CVD haba mudah dan kos efektif Argon disokong untuk sintesis nano h-BN. teknik yang dibangunkan untuk sintesis nanotube boron nitrida (BNNTs) adalah kira-kira 18% lebih murah berbanding dengan teknik yang dikenali mudah CVD dan 25 - 35% untuk mana-mana teknik lain yang berkenaan dengan kos setup eksperimen dan aksesori lain. Pengoptimuman parameter eksperimen dan pengubahsuaian sedikit Argon kami disokong teknik CVD haba membawa kepada sintesis jenis, saiz, morfologi dan bentuk nano h-BN seperti BNNTs, BNNWs, BNMTs dan BNNS dan lain-lain Perubahan prekursor dan sifat substrat mengakibatkan morfologi dan format BNNTs yang berlainan, manakala perubahan suasana reaksi daripada Argon untuk Ammonia menyebabkan sintesis BNMTs. Pengurangan Tempoh pertumbuhan (60 min → 30 min) dan susunan wap - cecair - mekanisme pepejal (VLS) pertumbuhan menyebabkan sintesis BNNWs, manakala peningkatan dalam tempoh pertumbuhan (60 min → 90 min) di hadapan ammonia sebagai suasana reaksi mengakibatkan pembentukan BNNS. FESEM, EDX, HR-TEM, XPS dan Raman digunakan sebagai alat pencirian untuk mengkaji morfologi, saiz, struktur dalaman, komposisi unsur dan fasa produk akhir, masing-masing. The nano disintesis daripada h-BN mempunyai kepentingan bukan sahaja dalam bidang sistem mekanikal bioperubatan atau mikroelektronik tetapi juga dalam perkembangan pengesan neutron keadaan pepejal dengan kecekapan pengesanan yang lebih tinggi.

ACKNOWLEDGEMENTS

I am extremely thankful to Almighty ALLAH (S.W.T.) who blessed me with the ability to accomplish my research. After ALLAH Almighty and HIS Blessings, I am very much grateful for the contributions of the following people in my research work in the current thesis:

My supervisors at Department of Physics, Faculty of Science, University of Malaya, Associate Professor Dr. Mayeen Uddin Khandaker and Professor Dr. Yusoff Mohd Amin for their guidance and support throughout my studies.

Former post-doc research fellow at Department of Physics, Faculty of Science, University of Malaya, Dr. Ziaul Raza Khan for his support and encouragement in the early stage of my experimental work.

My friend at Interdisciplinary Research Centre in Biomedical Materials (IRCBM) COMSATS Institute of Information Technology, Lahore Pakistan, Dr. Nawshad Muhammad for explaining the chemical aspect of the products synthesized in the experimental work.

Bright Sparks Program (BSP) University of Malaya and University of Malaya research grants: RP006D-13AFR and PG076-2014A for the financial assistance.

My mother, Husan Zari, grandfather, late. Khurram Khan, younger sisters, Seamayat Akram and Nazish Akram and other family members and friends for their moral support and encouragement.

TABLE OF CONTENTS

LIST OF FIGURES

LIST OF SYMBOLS AND ABBREVIATIONS

SYMBOLS

Symbols	Definition
nm	Nanometer (10^{-9} m)
µm	Micrometer (10^{-6} m)
eV	Electron Volt (1.6 x 10^{-19} J)
°C	Degree Celsius
Ar	Argon
h	Hour
sccm	Standard cubic centimeter per minute (flow unit)
B	Boron
MgO	Magnesium Oxide
FeO	Iron Oxide

ABBREVIATIONS

BN	:	Boron nitride	4
h-BN	:	Hexagonal boron nitride	4
c-BN	:	Cubic boron nitride	4
w-BN	:	Wurtzite boron nitride	4
BNNTs	:	Boron nitride nanotubes	5
^{10}BNNTs	:	Boron-10 nitride nanotubes	5
BNNWs	:	Boron nitride nanowires	5
BNMTs	:	Boron nitride microtubes	5

BNNS	Boron nitride nanosheets	5
BNNF	Boron nitride nanofibers	5
BNNR	Boron nitride nanorod	5
CNTs	Carbon nanotubes	5
CMTs	Carbon microtubes	10
CVD	Chemical Vapor Deposition	15

CHAPTER 1

INTRODUCTION

The property of a material describes how it behaves under certain conditions. Properties of materials are usually measured by looking at large (~10^{23}) aggregations of atoms or molecules. But, it is very interesting to mention that nanoscale substances exhibit different properties than their macroscale counterparts (Cao, 2004). The followings are considered as the key factors for understanding the nanoscale-related properties:

(a) Dominance of electromagnetic forces: Since the mass of nanoscale objects is so small, gravity becomes negligible. In fact, gravitational force is a function of mass and distance, and is thus weak between (low-mass) nanosized particles. On the other hand, electromagnetic force is a function of charge and distance is not affected by mass, so it can be very strong for nanosized particles (Hotze, Phenrat, & Lowry, 2010).

(b) Importance of quantum mechanical models: Classical mechanical models that we use to understand the macroscale substances break down for the very small (nanoscale) particles and for the very fast speed (near the speed of light) phenomena. On the other hand, Quantum mechanics better describes phenomena that classical physics cannot, like the probability (instead of certainty) of where an electron will be found (Hotze et al., 2010).

(c) Higher surface area to volume ratio: It is interesting to mention that by decreasing the particle size, the amount of surface area increases (Gubin, 2009). The three-part graphic on the **Fig. 1.1** illustrates how, for the same volume, the surface area increases simply by cutting the cube. Each of the three blocks has the same total volume, but the block that has the most cuts has a far greater amount of surfaces area. This is an important concept since it effects how well a material can interact with other things. As for instance, which will cool a glass of water faster: Two ice cubes, or the same two ice cubes (same volume of ice) that have been crushed.

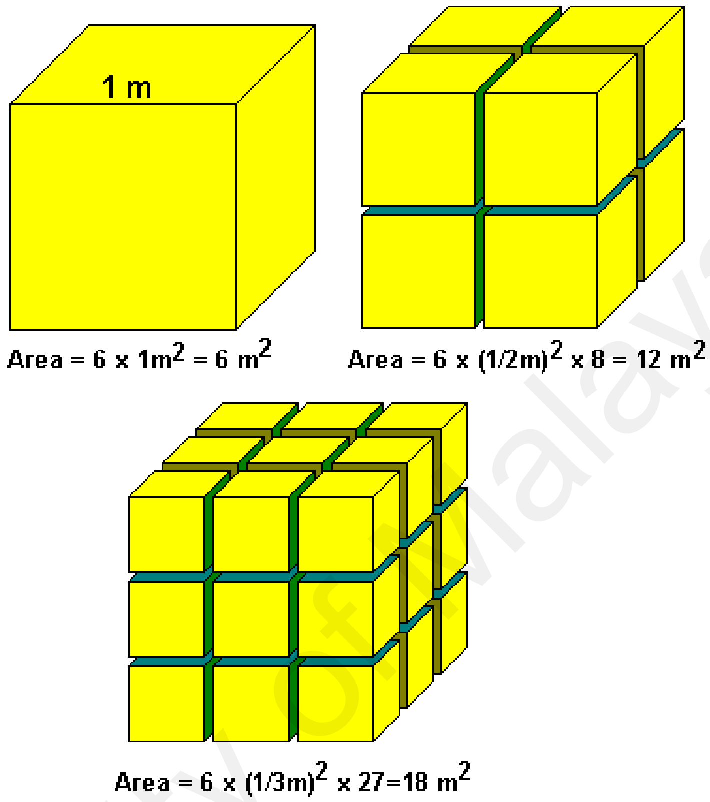

Figure 1.1: Increase of surface area to volume ratio.

(d) Random (Brownian) molecular motion is significant: At the macroscale, one can barely see the movement of constituent particles or why they moves, i.e., random motion is much smaller than the size of the particle. On the other hand, tiny particles, such as dust, are in a constant state of motion when seen through microscope because they are being batted about by collisions with small molecules. These small molecules are in constant random motion due to their kinetic energy, and they bounce the larger particle around, and thus, this motion is large when compared to the size of the particle (Maragó et al., 2010).

Although, reduction of size play a key role for a drastic change of material properties but many other factors such as arrangement of atoms and/or molecules in the particles, how they are bonded together, charge, shape etc. also responsible for such changes. However, the basic properties of materials that changed with the sizes are identified as follows:

(a) Optical (e.g. color, transparency): In the bulk structure of a material, the particles are so small that electrons cannot move freely. Because of the movement is restricted, the particles react differently with light. As an example, bulk gold appears yellow in color while nano-sized gold appears red in color (Zhang et al., 2009).

(b) Electrical (e.g. conductivity): Electrical properties of materials are based on the movement of electrons and the spaces, or "holes," they leave behind. The electronic properties of a nanotube depend on the direction in which the sheet was rolled up. Some nanotubes are metals with high electrical conductivity, while others are semiconductors with relatively large band gaps. Which one it becomes depends on way that it is rolled (also called the "chirality" of the nanotube"). If it's rolled so that its hexagons line up straight along the tube's axis, the nanotube acts as a metal. If it's rolled on the diagonal, so the hexagons spiral along the axis, it acts as a semiconductor (Cao, 2004).

(c) Physical (e.g. hardness, melting point): At the macroscale, the majority of the atoms lie almost inside the object. Note that even in a solid, the atoms are not really "fixed" in place but vibrating around a fixed point. In liquids, the atoms also rotate and move past each other in space (translational motion) though they do not have enough energy to completely overcome the intermolecular forces and move apart as in a gas. At the nanoscale, the majority of the atoms are splitted in between the inside and the surface of the object. That means, the percentage of atoms that lie on the surface are very insignificant compared to the inside ones. A smaller object will have a significantly greater percentage of its atoms on the surface of the object. Since surface atoms need less energy to move (because they are in contact with fewer atoms of the substance), the total energy needed to overcome the intermolecular forces hold them “fixed” is less and thus the melting point is lower.

(d) Chemical (e.g. reactivity, reaction rates): As particles get smaller, their surface area to volume ratio gets larger. With more surface area for the same volume, these small particles react much faster because more surface area provides more reaction sites for the same volume, leading to more chemical reactivity (Cao, 2004).

In fact, the properties (optical, electrical, physical, mechanical and chemical etc.) of nanostructured materials that show great differences from their bulk counterpart are due to the electrons and holes confinement (Lauret et al., 2005), surface effects, and geometrical confinement of the phonon. Since the physico-chemical properties of materials can be tailored by controlling their size and shape at the nanoscale, scientific community find greater interest for the synthesis of various nanostructured materials leading to improved and/or novel applications.

Boron nitride (BN) has become a very lucrative material for different applications in the modern world due to its favorable properties: hardness, high melting point, low dielectric constant, wide band gap and high cross-sections for thermal neutron etc. It exists in three different crystalline forms; hexagonal (h-BN), cubic (c-BN) and wurtzite (w-BN). Hexagonal boron nitride (h-BN) is the normal phase of BN that is stable at room temperature and pressure. Structurally it is identical to graphite, however, the carbons atoms are replaced by alternative boron and nitrogen atoms (Pakdel et al., 2012). Natural Boron (B) in h-BN is found to contain ~ 20 % of ^{10}B and ~ 80 % of ^{11}B (Han rt al., 2006). The variation of isotopic ratio of ^{10}B and ^{11}B in h-BN and other B-based compounds can significantly alter their physical properties (Matsuoka *et al.*, 2004), this fact led the researchers towards the synthesis of different nanostructures of h-BN: boron nitride nanotubes (BNNTs), boron-10 nitride nanotubes (^{10}BNNTs), boron nitride nanowires (BNNWs), boron nitride microtubes (BNMTs), boron nitride nanosheets (BNNS), boron nitride nanofibres (BNNF), boron nitride nanorod (BNNR) etc.

BNNTs are the hollow cylindrical structures or rolled up sheet of h-BN (as shown in **Fig. 1.2** (Golberg et al., 2010)) with diameter in the nanoscale range and length up to and above several micrometers (Chen et al., 2005). They were theoretically predicted in 1994 (Rubio, Corkill, & Cohen, 1994), and experimentally discovered in 1995 (Chopra et al., 1995). The discovery of BNNTs has opened up new ways for making devices with excellent properties. The properties of BNNTs are almost similar to Carbon Nanotubes (CNTs). However, CNTs can be a conductor or semiconductor dependent on the chirality or helicity. Whereas BNNTs are large band gap semiconductors independent of helicity (Ishigami, Aloni, & Zettl, 2003).

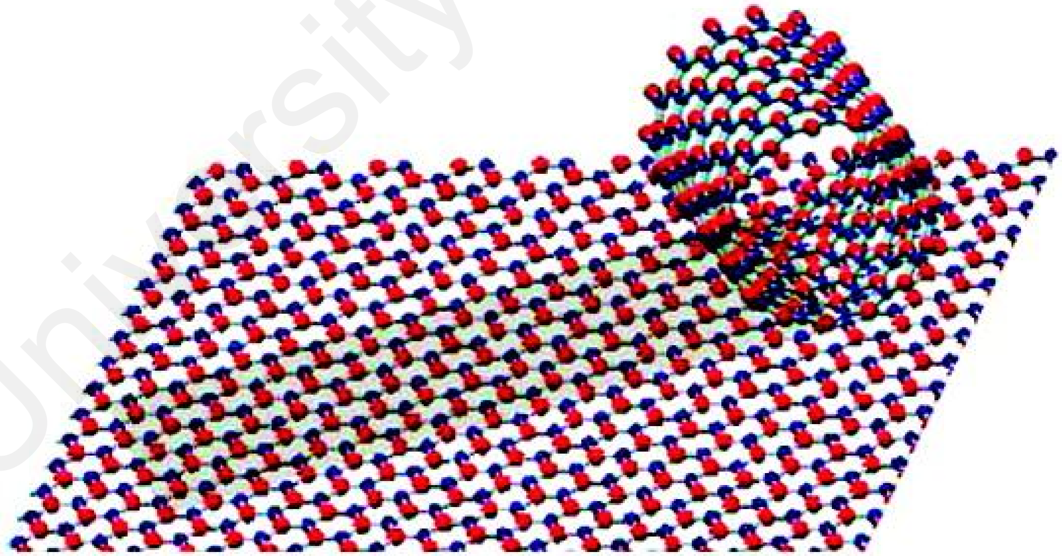

Figure 1.2: Mono-atomic h-BN layer wrapped up in the form of single layer BNNT (Golberg et al., 2010).

BNNTs have attractive magnetic properties. The theoretical calculations indicated that they (BNNTs) have spontaneous magnetization that can be induced through carbon-doping, which can be achieved by substitution of either B or N atoms (Wu et al., 2005). BNNTs have intrinsic magnetism that can be induced by their open ends. The magnetic moment thus produced is dependent on the chirality of the tube (Kolodiazhnyi & Golberg, 2005; Li et al., 2008; Oku & Kuno, 2003). As a result of this magnetism, BNNTs produce spin-splitting effect combined with spin-polarization. This property has made it a very important material for different applications in the field of nanoscale spintronic devices e.g. spin polarized emitters etc. (Hao et al., 2006; Ryu et al., 2008; Zhou & Duan, 2007). The spontaneous magnetization can also be induced in BNNTs (Zhang & Guo, 2009) via fluorination or dopant substitution. Fluorination of BNNTs can further be used to modify the electronic and transport properties of the BNNTs. The fluorinated BNNTs, thus developed, find potential applications in nanoelectronics (Zhou et al., 2006).

The possible role of BNNTs as an insulating protective shield has also been observed in the development of nanocables from semiconducting nanowires (Jang et al., 2006; Suenaga et al., 1997; Tang et al., 2002; Yin et al., 2004; Zhang et al., 1998; Zhu et al., 2003). It has been successfully explored for applications in the field of engineering ceramics and polymeric composites (Bansal, Hurst, & Choi, 2006). It is experimentally observed that the superplasticity of engineering ceramics increases to a great extent with the addition of BNNTs (Huang et al., 2007). Due to the dipolar nature of B-N bond in BNNTs, they result in stronger adsorption of hydrogen. Therefore, BNNTs are considered a very important material for hydrogen storage applications (Durgun, Jang, & Ciraci, 2007; Hu, Kan, & Yang, 2007; Leela Mohana Reddy, Tanur, & Walker, 2010; Mpourmpakis & Froudakis, 2007; Shevlin & Guo, 2007). A change in properties in molecular and solid state electronic devices has also been observed due to the dipolar nature of the B-N bond. It is further responsible for changing the optical properties of materials in the systems (Akdim, Pachter, Duan, & Adams, 2003; Wang, Tsai, & Chou, 1997). Several studies on photoluminescence and cathodoluminescence properties of materials have shown that BNNTs are suitable to emit violet and ultra-violet light. It has been found that the emission peaks normally depend on the internal structure of the samples. Consequently, several peaks/emission lines have been observed at ~230 nm, ~279 nm, ~338 nm, and ~460 nm by different researchers (Chen et al., 2002; Berzina et al., 2006; Berzina et al., 2005; Chen et al., 2007; Chen, Chen, Liu et al., 2007; Han et al., 2008; Jaffrennou et al., 2007; Oku, Koi, & Suganuma et al., 2008; Silly et al., 2007; Tang, Bando, Zhi, & Golberg et al., 2007; Wu et al., 2004).

Biocompatibility of any nanomaterial needs to be tested before using it within a particular bio-medical application. The biocompatibility tests on BNNTs were first initiated by Ciofani et al. (Ciofani et al., 2009; Ciofani et al., 2008; Ciofani, Raffa, Yu, *et al.*, 2009). The obtained results indicated BNNTs to be a very useful material for different biomedical applications such as therapeutic or diagnostic etc. due to their possible non-cytotoxic nature (Chen et al., 2009; Ciofani et al., 2010; Jang et al., 2006; Tang et al., 2002; Yin et al., 2004). In boron nitride capture therapy, they (BNNTs) are proposed to be the boron carriers (Wang, Lee, & Yap, 2010). Upon injection, they are transferred into the tumor cell, produces localized charge particles by the interaction of neutron from an external source. These charge particles may be used to kill the tumor and cure the patient. The uniform distribution of Fe_3O_4 nanoparticles on the BNNTs surface introduced magnetic behavior in BNNTs. This behavior of BNNTs might be very useful in Micro Electro Mechanical System (MEMS) and targeted drug delivery (Liao & Koide, 2011; Wang et al., 2010).

BNNT is a large band gap semiconductor with improved bulk properties, and can be effectively used as a neutron sensing element in a solid state neutron detector. Hexagonal

Boron nitride (h-BN) has high cross-section for thermal neutron. In the conventional solid state detector, a layer of semiconductor material is deposited on the top of neutron sensitive material such as h-BN. This layer is used for the production of electron-hole pair due to interaction of thermal neutron (Li, Dahal, Majety et al., 2011). Thus, if h-BN is replaced by BNNTs (with ^{10}B-enrichement), the efficiency of the neutron detector is predicted to be far better than its bulk counterpart. BNNTs have highly crystalline multilayered structures that make it more suitable to be used as solid state neutron detector with higher detection efficiency (Ahmad, Khandaker, & Amin, 2015b). On the other hand, since BNNT is itself a semiconductor, no other semiconductor layer is required to be deposited on the neutron sensitive surface such as BNNTs or h-BN. The as produced charge particles (due to interaction of neutron) are utilized within the same material (Li et al., 2011). Thus, the extra kinetic energy of the charged particles that was previously needed to accelerate them to reach into semiconductor layers can now be saved and utilized for an increasing production of electron-hole pairs. As a result, a neutron detector based on BNNTs will have high sensitivity and greater efficiency than any other existed solid state or semiconductor based neutron detector (Ahmad, Mohamed, & Burhanudin, 2012).

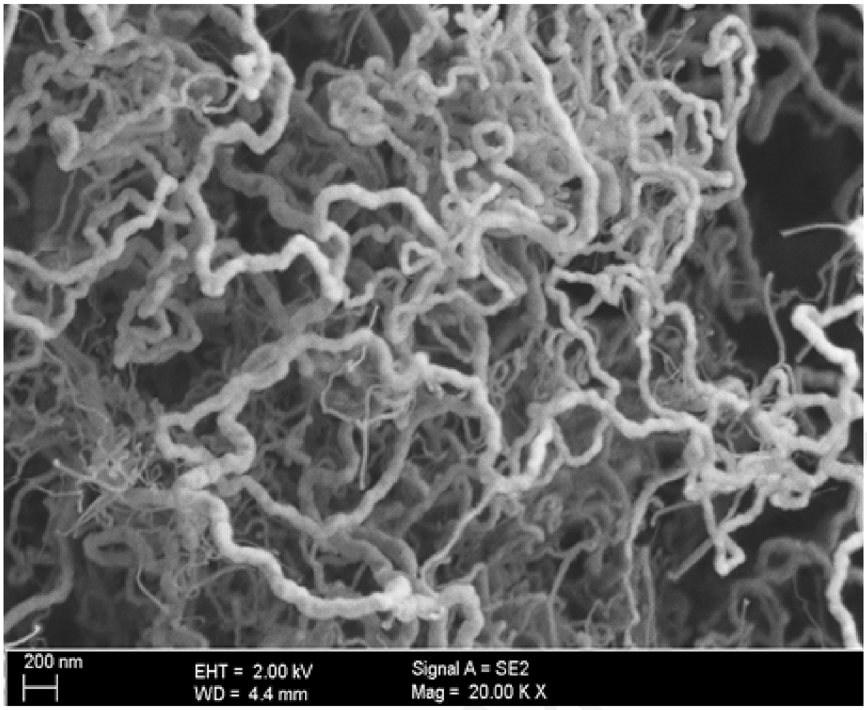

Figure 1.3: FESEM micrograph of BNNWs synthesized by Ahmad et al. (Ahmad, Khandaker, Khan, et al., 2014).

BNNWs are the reduced or low dimensional structures of h-BN. Unlike BNNTs, BNNWs are the filled cylindrical structure of h-BN with at least one dimension in the nanoscale range. An apparent morphology of BNNWs via a FESEM micrograph is shown in **Fig. 1.3**. (Ahmad, Khandaker, Khan et al., 2014). Like CNTs and BNNTs, it is also very important nanostructured material for different applications in small scale devices. It has almost the same applications in the different field of modern technology as BNNTs (Ahmad, Khandaker, Khan, et al., 2014).

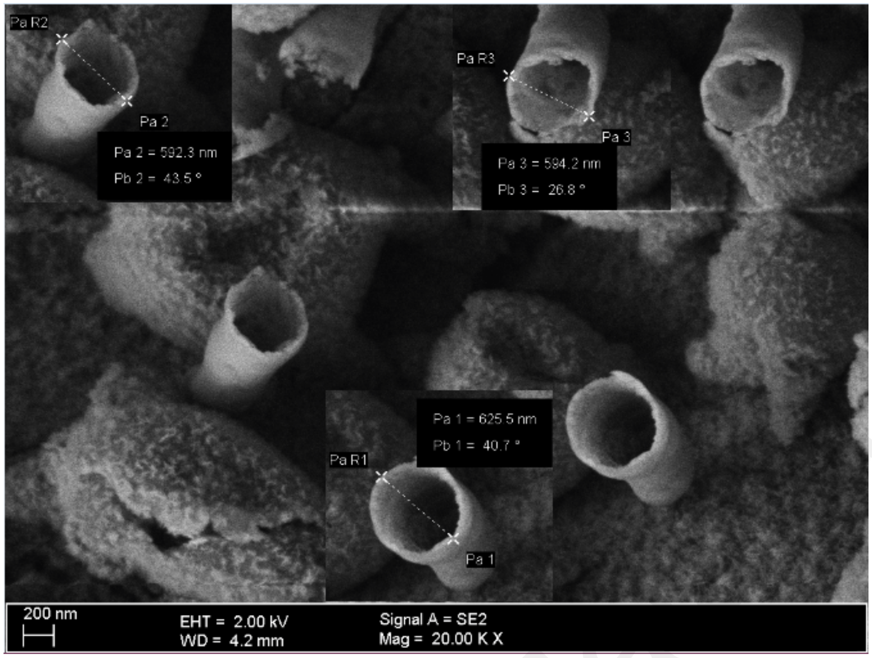

Figure 1.4: FESEM micrograph shows pipe-like morphologies of BNMTs (Ahmad, Khandaker, et al., 2015).

BNMTs are the pipe like morphologies of hexagonal Boron nitride (h-BN) with diameter and length in micro-scale and walls thickness in the range from 1 to 100 nm. Here (in the present study) the wall thicknesses mean the difference of external diameter and internal diameter of the tube/pipe. The unique pipe-like morphology (as shown in **Fig. 1.4**. (Ahmad, Khandaker, Amin et al., 2015) with larger internal space and length in micro-scale range offers exceptional applications as a carrier of larger size bio-molecules in the field of biomedical, and inorganic nanoparticles in micro-reactors, micro-fluids devices and targeted drug delivery systems. Previously Carbon microtubes (CMTs) have been suggested for this purpose (Goldberger, Fan, & Yang, 2006; Hu et al., 2004; Lin et al., 2012), however; the excellent properties of BNMTs such as diameter independency make it more suitable as compared to CMTs. The nano-size walls-thickness of BNMTs also combine the excellent properties of nanoscale materials due to the electron and holes confinement (Golberg, Bando, Tang et al., 2010), surface effects and geometrical confinement of the phonon. (Grossman, Zettl, & Wagner, 2009; Huang et al., 2011) The novel morphology of the BNMTs with larger internal space and nanoscale walls can further enhance it effects during neutron capture therapy to kill the tumor cell and cure the patient. The larger internal space helps in carrying larger scale bio-molecules or medicine to the tumor site (like CMTs). This condition may help to protect the healthy tissues and control the side effects during the destruction of tumor cell due to the contact of charged particles produced by the interaction of a neutron with BNMTs from an external source (Goldberger et al., 2006; Hu et al., 2004; Lin et al., 2012). The study on solid state neutron detector suggests that a 200 μm thick ^{10}B enriched h-BN layer can capture 98.5% of the neutron as compared to the one made of 1 mm thick natural h-BN. It has further been suggested that the development of multiple ^{10}B enriched h-BN layer (epilayer) with improved crystallinity can enhance the neutron detection efficiency up to 100% (Li et al., 2011). The study on BNNTs and BNMTs showed that, these materials are multi-layer structures of h-BN with highly crystalline nature (Oku, Narita, & Nishiwaki, 2004). Though ^{10}B enrichment of these materials is not confirmed still they are believed to be an excellent choice for neutron sensing applications in solid state neutron detector due to their nanoscale properties (Ahmad *et al.,* 2012). BNMTs, are made of h-BN layers with thin-walls, have high chemical stability, excellent mechanical properties and high thermal conductivity. All these properties make it very useful material in the fabrication of different electronic devices that can be used in high temperature environment. BNMTs, as compared to BNNTs, have better crystallinity due to their reduced wall curvatures. Also, they exhibit an intense deep Ultra Violet (UV) emission, which can be observed even at room temperature (Huang et al., 2009).

Boron nitride nanosheets (BNNSs) are the two dimensional nanostructure of h-BN with excellent physiochemical properties. The structure of BNNS is similar to the nanosheets of graphene, however, in case of BNNS alternative Boron and nitrogen atoms substitutes for carbon atoms. The 2D structure, thus developed, is shown in **Fig.1.2**. In addition to its similar mechanical properties and thermal conductivity to graphene (Wang et al., 2011), BN has some excellent properties as compared to its carbon counterpart. These properties included: a constant band gap of 5 - 6 eV, thermal stability, higher chemical inertness and resistance to oxidation etc. (Zhi, Bando, Tang et al., 2008). All these properties have made BNNS a very useful and attractive material for use in a wide range of applications. The devices, thus, developed with BNNS will be highly capable of operating in oxidative and high temperature environment. Further, it can be used as insulating composites of high mechanical properties and thermal conductivity (Golberg et al., 2007; Wang et al., 2011) material.

1.1 Research Problem Investigated

The potential applications of different nanostructures of h-BN are found to depend on the quality and quantity of the final product which further depends on the synthesis techniques (Ahmad et al., 2015; Zhi, Bando, Tang et al., 2010). Most of the earlier techniques were either found to operate at a very high temperature (Chopra et al., 1995) or needed toxic and health risky precursors (Lourie et al., 2000; Ma, Bando, & Sato et al., 2001; Wang et al., 2014) or involved complex and lengthy experimental procedures (Ahmad et al., 2015; Özmen et al., 2013; Seo et al., 2013; Tay et al., 2015). Furthermore, along with the lower quality of the final products, the cost of the experimental set up and the required expertise to easily operate the experiments are also some of the main problems in the development of h-BN nanostructures. Beside this, different nanostructures of h-BN (BNNTs, BNNWs and BNMTs etc.) were reported by various authors (Deepak et al., 2002; Golberg et al., 2010; Huang et al., 2009; Huang et al., 2011; Lee et al., 2008; Lin et al., 2012; Pakdel et al., 2011) with the use of same experimental parameters. Thus, in these works either one or other nanostructure is produced as an undesired product or impurity with the targeted ones. This has created further confusions and delay in the synthesis of a particular nanostructure of h-BN with well-defined experimental parameters.

In the current study, excessive experimental work have been done to address the aforementioned problems. In this regard, a simple and cost-effective experimental set up is developed that operates at a relative low temperature with toxic free precursors and synthesizes pure h-BN nanostructures.

1.2 Objectives

In the current study, experimental approaches have been used to discover a suitable and more reliable solution for the existed problems in the synthesis of different nanostructures of h-BN. In this regard, the current thesis is based on the following main objectives:

1. To develop a simple and cost-effective experimental technique that enables an easy synthesis of different nanostructures of h-BN with minimum resources. The effects of precursor’s nature on size and morphology of h-BN nanostructures and techniques for the synthesis of vertically aligned h-BN nanostructures will also be investigated.
2. To study the main experimental parameters responsible for the synthesis of different nanostructures of h-BN or ^{10}h-BN.
3. To study the synthesis of ^{10}h-BN nanostructures and its potential use as a neutron sensing element.

1.3 Account of Research Progress

This thesis consists of total four chapter: CHAPTER 1 (Introduction), CHAPTER 2 (Literature review in the form of a published review paper), CHAPTER 3 (In the form of eight published papers) and CHAPTER 4 (Conclusions). The contents of this thesis and the findings of each published paper is linked and briefly described as follows:

Publication 1 served as literature review of the current thesis. It describes the properties and potential applications of BNNTs in different fields of bio-medical, MEMs and solid state neutron detectors. The review analyzed the old synthesis techniques for the BNNTs and the as-produced impurities in the form of bulk h-BN, BNNWs, BNMTs and BNNS etc. Chemical vapour deposition (CVD) is shown to produce relatively pure BNNTs as compared to the existing old techniques. BNNTs or bulk h-BN reported via different types of CVD varies in quality, quantity, size and morphology of the final product. In this regard, the role and importance of certain experimental parameters such as experimental set up, precursor's types, temperature, growth mechanism and substrate types etc. have also been studied. The variation or difficulties in CVD techniques with respect to different experimental parameters leads to the development of Argon-supported thermal CVD which not only become a simple technique for BNNTs synthesis but also provides effective logics for the synthesis of BNNWs, BNMTs and BNNS etc.

Publication 2 is based on the study of BNNTs synthesis via Argon-supported thermal CVD technique. In this technique, a conventional horizontal dual zone quartz tube furnace along with one end closed quartz test tube is used as a major part of the experimental set up. Amorphous Boron powder, MgO and γ- Fe_2O_3 nanopowder of 99.9+ % purities were used as precursors and Argon gas as a reaction atmosphere instead of vacuum. This technique has made the BNNTs synthesis simple and ~ 18 % cost-effective as compared to the simplest CVD technique and 25 – 35 % as compared to any other technique.

Publication 3 is the comprehensive study of BNNTs multiple synthesis from a single precursors. The aim of this study is to analyze the effect of precursor's nature on the size and morphology of the final product. For this purpose, BNNTs are first synthesized from the fresh precursor's materials via our Argon-supported thermal CVD technique, and the BNNTs were further synthesized using the residual materials left after first and second experimental run. The product, thus obtained, was characterized for the required analysis. The characterized results showed that the present work can be a step towards continues and large scale synthesis of lengthy and high quality BNNTs.

Publication 4 describes the synthesis and mechanism of vertically aligned BNNTs by combining the concepts and logics that were used for the synthesis of vertically aligned CNTs and pattern growth of BNNTs. In the light of previous concept and logics, a thin alumina layer is deposited at the top of Si substrate via an e-beam evaporator. Nucleation sites are produced in the as-deposited layer of the substrate due to ammonia etching. The as-produced nucleation sites helps in growing vertically aligned BNNTs. Vertically aligned BNNTs have an advantage that it can be used for its potential application without any further purification.

Publication 5 deals with the synthesis of highly crystalline multilayered structure of ^{10}BNNTs via replacement of natural boron with boron-10 in the precursors. The product, thus, synthesized via Argon-supported thermal CVD is proposed to have 100 % neutron detection efficiency if use as a sensing element in a solid state neutron detector.

Publication 6 is related with the synthesis of highly crystalline BNNWs. Unlike various complex and extensive experimental procedures available in the literature, a simple experimental technique has been developed to synthesize BNNWs on Si substrates in a short growth duration of 30 min via vapor – liquid – solid (VLS) growth mechanism.

This work reveals that a modified CVD technique and short growth duration is suitable to synthesis nanowires with tens of nanometers in diameter.

Publication 7 explains the synthesis and characterization of pipe-like morphologies of BNMTs. The method and logics used in the present study are relatively different and easier in comparison to previously synthesized BNNTs, BNMTs and boron-carbon-nitride microtubes regarding the choice of precursors, experimental set up and reaction atmosphere. It further explains the growth mechanism and logics that how the current microtubes are differing from the one synthesized in the literature.

Publication 8 includes a study on the synthesis of BNMTs and formation of BNNSs. The work explains the synthesis of cone-like morphologies of BNMTs and describes the possible reasons for the formation of BNNSs. In this work, it has been found that the elimination of vacuum or inert gases as an internal environment causes the material to grow in the form of microtubes instead of nanotubes. Further, it has been noted that the elongation of growth duration resulted in the development of one particular structure to another structure (i.e. from microtubes to nano-sheet). The growth continue smoothly as long as the precursors are available in a particular growth duration. The unavailability of the growth precursors causes the microtubes walls to become thinner and thinner until it becomes a sheet. More structure of nanoscale BN can be synthesized with further changes in the experimental parameters. The synthesized BNMTs are found to be of great importance as a neutron sensing element in a solid state neutron detector, neutron capture therapy, micro-fluids devices and targeted drug delivery etc.

Publication 9 describes the synthesis of vertically aligned boron nitride nanosheets (BNNS). In order to make the synthesis easier and safe, a very simple technique is introduced in the present study. In this technique BNNS are synthesized in a conventional horizontal dual zone quartz tube furnace at 1200 °C. The as-synthesized BNNS look like spread out cotton packs, has highly crystalline nature with an interlayer spacing of 0.34 nm. It has been noted that nature of internal environment of the chamber (horizontal quartz tube furnace) and growth duration play a key role in the synthesis of BNNS. However, the nature of the substrate and role of the as-formed catalysts or their alloys in the absence of vacuum or Ar free environment cannot be ignored. The synthesized BNNS can be used in the development of devices which will be capable of operating in oxidative and high temperature environment.

Finally, CHAPTER 4 drawn conclusions from the work done in the current thesis and specify future directions for further exploration in the same field including the commercialization of the synthesized products and their potential applications in different field of modern science and technology.

CHAPTER 2

LITERATURE REVIEW

The relevant literature about the synthesis and potential applications of h-BN nanostructures has been searched and organized in the form of a review paper. This review paper has already been published in institute of scientific information (ISI) indexed (Q1) Journal, “RSC Advances”. The literature review chapter in the current thesis is based on this review paper. A brief description of the contents of this publication is already given in Section 1.3 of Chapter 1 (1st Publication).

Publication 1st is the reprint of our paper: P. Ahmad, M.U. Khandaker, Z.R. Khan and Y.M. Amin, “Synthesis of boron nitride nanotubes via chemical vapour deposition: a comprehensive review”, *RSC Advances*, *Volume 5*, *Issue 44, 2015*, *pages 35116-35137*.

RSC Advances

REVIEW

Cite this: *RSC Adv.*, 2015, **5**, 35116

Received 27th January 2015
Accepted 10th April 2015

DOI: 10.1039/c5ra01594d

www.rsc.org/advances

Synthesis of boron nitride nanotubes *via* chemical vapour deposition: a comprehensive review

Pervaiz Ahmad, Mayeen Uddin Khandaker,* Ziaul Raza Khan and Yusoff Mohd Amin

Boron nitride nanotubes (BNNTs) have been synthesized by various methods over the last two decades. Among the various growth techniques, chemical vapor deposition (CVD) is one of the best methods for the synthesis of BNNTs in terms of quality and quantity. It offers relatively easy control of different growth parameters such as growth mechanism, experimental set up, precursor variables, catalyst type and temperature, and hence has become very convenient to grow BNNTs with desired size and morphologies leading to various advanced applications. Here, we present a comprehensive review on BNNT growth by CVD techniques ranging from catalytic to plasma assisted CVD. Moreover, the importance of certain variables for an efficient production of BNNTs, and their effects on the size and morphology of the tubes are also discussed elaborately.

1 Introduction

BNNTs, cylindrical structures of hexagonal boron nitride (h-BN) having diameter in the range of 1–100 nm and length up to several micrometers,[1–3] were theoretically predicted in 1994,[4,5] and experimentally discovered in 1995.[6] The discovery of BNNTs has opened new ways for making devices with excellent properties. The structure and mechanical properties of BNNTs are similar to carbon nanotubes (CNTs), however CNTs can be conductors or semiconductors depending on the chirality or helicity whereas BNNTs are large band gap semiconductors independent of helicity.[7–13] This difference in the electronic structure of these nanostructure materials results in different luminescence emissions. For example BNNTs emit violet or ultraviolet luminescence when excited by electron or photons,[14–19] whereas CNTs emit infrared light with wavelength dependent on the chirality of the tube.[20–24] Moreover, BNNTs are found to be chemically stable and highly resistant to oxidation.[25,26] Therefore it can be effectively utilized in fabrication of

---

Department of Physics, Faculty of Science, University of Malaya, 50603 Kuala Lumpur, Malaysia. E-mail: mu_khandaker@yahoo.com; mu_khandaker@um.edu.my; Fax: +60379674146; Tel: +601115402880

Pervaiz Ahmad obtained his M.Phil. degree in Solid State Physics in 2011 from the Centre of Excellence in Solid State Physic, University of Punjab, PAKISTAN. Currently (Session: 2013–2014) he is pursuing his Ph.D. degree in Physics from the Department of Physics, Faculty of Science, University of Malaya, MALAYSIA. His areas of expertise include: synthesis and characterization of h-BN nanostructures (BNNTs, BNNWs, BNMTs and BNNS etc.*), CNTs and iron oxide nanoparticles for their potential application in the field of radiation sensing, biomedical and microelectronic mechanical systems (MEMs),* etc.

Associate Prof. Dr. Mayeen Uddin Khandaker obtained his Ph.D. from the department of Physics, Kyungpook National University, South Korea. Previously, he served in numerous institutions like the Korea Atomic Energy Research Institute, the International Atomic Energy Agency and American International University-Bangladesh, etc. *Currently (2010 – onwards), he is working in the Department of Physics, University of Malaya, Malaysia. His areas of expertise include: synthesis and characterization of nanostructured materials, production of radionuclides for medical and industrial applications, measurement of natural radioactivity in food and environment and development of optical fibre based TLDs for dosimetry applications.*

different devices that can be used in high temperature environments.[26–33]

BNNTs have attractive magnetic properties. The theoretical calculations indicated that they (BNNTs) have spontaneous magnetization that can be induced through carbon-doping, which can be achieved by substitution of either B or N atoms.[34] BNNTs have intrinsic magnetism that can be induced by their open ends. The magnetic movement thus produced is dependent on the chirality of the tube.[35–37] As a result of this magnetism BNNTs produce spin-splitting effect combined with spin-polarization. This property has made it a very important material for different applications in the field of nanoscale spintronics devices *e.g.* spin polarized emitters *etc.*[38–40] Spontaneous magnetization *via* fluorination or dopant substitution can also be induced in BNNTs.[41] Fluorination of BNNTs can further be used to modify the electronic and transport properties of the BNNTs. The fluorinated BNNTs thus developed have potential applications in nanoelectronics.[42]

The possible role of BNNTs as insulating protective shield has also been observed in the development of nanocables from semiconducting nanowires.[2,43–47] It has been successfully explored for applications in the field of engineering ceramics and polymeric composites.[48] It is experimentally observed that the superplasticity of engineering ceramics increases to a great extent with the addition of BNNTs.[49] Due to dipolar nature of B–N bond in BNNTs, they result in stronger adsorption of hydrogen. Therefore they are considered a very important material for hydrogen storage applications.[50–54] A change in properties in molecular and solid state electronic devices has also been observed due to dipolar nature of the B–N bond. It is further responsible for changing the optical properties of materials in the systems.[7,55] Research based on the studies of photoluminescence and cathodoluminescence properties of the materials have shown that BNNTs are effective violet and ultraviolet light emission material. It has been found that the emission peaks normally depend on the samples. On this basis, peaks have been observed at ~230 nm, ~279 nm, ~338 nm and ~460 nm by different researchers.[17,18,56–64]

Biocompatibility of any nanomaterial need to be tested before using it within a particular bio-medical application. The biocompatibility tests on BNNTs were first initiated by Ciofani *et al.*[65–68] The obtained results indicated BNNTs to be a very useful material for different biomedical applications such as therapeutic or diagnostic *etc.* due to their possible non-cytotoxic nature.[43–45,69,70] In boron nitride capture therapy, they are proposed to be the boron carriers.[71] Upon injection, they are transferred into the tumor cell, produces localized charge particles by the interaction of neutron from an external source. These charge particles may be used to kill the tumor and cure the patient. The uniform distribution of Fe_3O_4 nanoparticles on the BNNTs surface introduced magnetic behavior in BNNTs. This behavior of BNNTs might be very useful in Micro Electro Mechanical System (MEMS) and targeted drug delivery.[71,72]

BNNT is a large band gap semiconductor with improved bulk properties, can be effectively used as a neutron sensing element in a solid state neutron detector.[73] h-BN has a large cross-section for thermal neutron. In a solid state detector, a layer of semiconductor material is deposited on the top of neutron sensitive material. This layer is used for the production of electron–hole pair due to interaction of thermal neutron.[74] Thus, if h-BN is replaced by BNNTs (with ^{10}B-enrichement), the efficiency of the neutron detector is predicted to be far better than its bulk counterpart. BNNTs have highly crystalline multilayers structure that make it more suitable for a solid state neutron detector with higher detection efficiency.[75] Being semiconductor, no other semiconductor layer is required to be deposited on BNNTs or h-BN surface. The as produced charge particles (due to interaction of neutron) are utilized within the same material.[74] Thus the extra kinetic energy of the charged particles that was previously needed to accelerate them to semiconductor layers can now be saved and utilized for an increasing production of electron–hole pairs. Thus a neutron detector based on BNNTs will have high sensitivity and greater efficiency than any other existed solid state or semiconductor based neutron detector.[76]

All of the aforementioned BNNTs applications in different fields are dependent on its purity, size and alignment which in turn depend on the synthesis methods. The synthesis methods

Dr. Ziaul Raza Khan obtained his Ph.D. degree in Physics from Jamia Milia Islamia India. He was a Post-Doctoral Research Fellow at the Low Dimensional Material Research Centre, Department of Physics, University of Malaya, Malaysia. Currently (2015) he is working as an Assistant Professor at the College of Science, University of Hail, Saudi Arabia. His Areas of expertise include: Growth of II–VI semiconductor thin films, Si NWs, SiC thin films and boron nitride nanostructures.

Prof. Dr. Yusoff Mohd Amin obtained his Ph.D. degree in Physics from Birmingham, UK. Currently (2015), he is working as a Professor at the Department of Physics, University of Malaya, Malaysia. His areas of expertise include: synthesis and characterization of h-BN nanostructures (BNNTs, BNNWs, BNMTs and BNNS, etc.*), CNTs, production, detection and applications of radionuclides in nuclear medicine and industry, radiation detection and measurement.*

that are being used for producing BNNTs are arc-discharge, laser ablation, template synthesis, auto clave and ball milling *etc.*[20] Beside high temperature, toxic precursors and complex and lengthy experimental procedures, these techniques were difficult to be followed by other researchers. Furthermore, different precursor's materials were found as impurities in the final product. These impurities are very difficult to separate from the final product.

CVD has been recognized as the most effective technique for the synthesis of high quality and large scale production of CNTs.[77] This technique has not only increased the production or quality of the CNTs but has also provided simple mechanism for its growth in vertically aligned format.[78] The effectiveness of this technique in CNTs synthesis also attracted the attention of the earlier researchers working on the synthesis of BNNTs. For the first time CVD was introduced to synthesize pure BNNTs from borazine as precursors. Though somehow pure BNNTs were obtained in the temperature range of 1000–1100 °C *via* this technique,[79] however, due to toxic nature of borazine, the as-used technique was not further employed with borazine as precursors. The usefulness of CVD technique for BNNTs synthesis with high quality is further considered by other researchers. In this regard, they not only developed their own CVD techniques but also introduced most effective non-toxic precursors. Thus, the major developments in CVD synthesis of BNNTs can be categorized in three main stages. The first stage is from Tang *et al.* (2002)[80] to Zhi *et al.* (2005).[81] During this stage B, MgO and FeO were developed as effective precursors for high yield synthesis of BNNTs *via* Boron Oxide CVD (BOCVD) technique in an inductive furnace. The growth of the BNNTs was assumed to have followed "Vapor Liquid Solid (VLS) Growth Mechanism".[82] According to this mechanism (in the case of BNNTs), the reaction of the precursors powders at a particular temperature produce B_2O_2 vapors and nanosize liquid or partially melted catalysts particles. Later on, when the partial vapor pressures of these catalysts are sufficiently increased they are condensed on the substrate. The as formed B_2O_2 vapor reacts with N_2 from NH_3 gas and form BN-species. These species are then diffused in to the condensed catalysts and aggregates with the passage of time until it supersaturates and precipitates in the form of BNNTs.[83]

The second stage is from Zhi *et al.*[81] (2005) to Lee *et al.* (2008).[84] During this stage, a conventional horizontal tube furnace is used to replace the induction furnace. Furthermore, a particular ratio (2 : 1 : 1, 4 : 1 : 1) of the precursors (B, MgO, FeO) was used to grow pure BNNTs directly on Si/SiO_2 substrate in a temperature range of 1100–1200 °C. The whole process thus developed was named as TCVD. The third stage is from Lee *et al.* (2008)[84] to Ahmad *et al.*[85] (2015). In this stage, the TCVD technique is further simplified with the use of argon gas (as a reaction atmosphere) as an alternative for vacuum or evacuation. As a result the process developed is called, "argon supported TCVD". This simplification has not only reduced the required expertise and cost for the experimental set up but has also helped in growing longer BNNTs due to anti-oxidant quality of argon gas.

The complete description of CVD techniques: it comparison with earlier existed technique, its different types and importance of different experimental parameters in a particular CVD technique is given in the coming sections.

2 BNNTs synthesis methods

After being theoretically predicted in 1994 by A. Rubio and X. Blase *et al.*,[4,5] arc-discharge was the first method employed for the synthesis of BNNTs. Single and multi-walls BNNTs (MWBNNTs) formed by this method had high crystallinity but the final product was found to contain BN onions and cages *etc.* as impurities.[6,20] Due to insulating nature of BN materials, they were not suitable to use as electrodes. Therefore other conductive compounds of boron, such as ZrB_2 and Yb_6 were used as electrode during the arc-discharge synthesis of BNNTs.[47,86] MWBNNTs synthesized *via* this technique were found to have diameter in the range of 1–3 nm. Metal particles were found at the tips of BNNTs. These particles were assumed to be responsible for the growth and nucleation of BNNTs by this technique.[87–89]

Laser ablation utilizes almost the same precursors and catalysts at a slightly higher temperature than the arc-discharge but the BNNTs obtained with this technique have the same characteristics as the one obtained with the arc-discharge method.[42,90–92] This technique for the BNNTs growth was first introduced by Golberg *et al.*[93] As precursor, single crystal of cubic BN (target) was heated with the help of CO_2 laser up to 5000 K to obtain MWBNNTs.[93] Later on, h-BN was also used as precursor in this technique[94–99] and both SWBNNTs and MWBNNTs were successfully synthesized. It was found that fabrication of BNNTs *via* this technique can be achieved without catalysts.[94] Highly crystalline BNNTs can be produced with the help of laser ablation, however, BN cones, onions and amorphous boron flakes can easily be found as impurities in the final product.

Template synthesis method uses CNTs substitution reaction[100–105] or porous alumina anodic as a template[106–108] for BNNTs synthesis. In the case of CNTs substitution, B_2O_3 are reacted with CNTs whereas nitrogen or ammonia is used as a protection gas and a nitrogen source. It is a low temperature method as compared to arc-discharge and laser ablation. As a result, the BNNTs produced by this technique have controlled morphology but has carbon in the lattice as an impurity, which is very difficult to remove from the final product.[109–113] In the case of using porous alumina anodic as a template, 2,4,6-trichloroborazine are decomposed at 700–900 °C to fill the pores of alumina with BN material. The product thus obtained showed tubular structures with an average diameter of 280 nm, however, the detailed studies indicated a polycrystalline structure of the obtained BNNTs.[20]

Auto-clave is another low or room temperature technique for synthesis of BNNTs. In this kind of method for BNNTs synthesis, some special types of auto-clave are designed and used. BNNTs produced *via* this technique were found to have diameter in the range of 30–300 nm and length up to 5 micrometer. Though, this technique had produced BNNTs in different morphologies with thin walls and large inner space, however it yields poor quality and small quantity of the final product (BNNTs). Furthermore, BN cages and B were found as impurities in the synthesized BNNTs.[114–117]

Ball-milling technique for BNNTs synthesis was first developed by Chen *et al.*[118] It gives multi-walled BNNTs (MWBNNTs) in a large quantity at a temperature range of 1000–1200 °C but the quality of the synthesized product was very low and reported B, h-BN and BN-fiber *etc.* as impurities.[118–125]

CVD is a more advanced and easiest technique for the synthesis of large quantity (gram level) of both CNTs and BNNTs with desired applicable properties. The quality of BNNTs is found to depend on the specific method (CVD types) applied for the synthesis. In all these techniques along with standard CVD, partial CVD is also involved combined with other techniques.[6,13,30,42,79–81,116,126–140] Each CVD technique is different from other with respect to the experimental setup, required temperature and types of precursor. A brief summary of all the above techniques is given in the Table 1.

It is clear from Table 1 that though high quality and large quantity of BNNTs can be obtained with CVD technique; however a specific CVD technique with easily available precursors and reaction parameters are still need to be studied in full detail. In this regard an up-to-date development in CVD techniques for BNNTs synthesis are discussed in the next section.

3 Classification of CVD for BNNTs synthesis

The BNNTs are synthesized *via* CVD technique by different groups of researchers. Each group used their own experimental parameters and precursors. As a result the quantity and quality of the synthesized BNNTs were found to vary from group to group. For the purpose of improvement in the results, some of the groups have adopted other techniques combine with CVD.[116,141,142] This fact further notifies the importance of CVD techniques in BNNTs synthesis. In this section, the most prominently used CVD techniques for BNNTs are reviewed. The CVD method has been classified into various sub categories on the basis of growth mechanism, precursor's type and catalysts type for BNNTs synthesis. The classification of CVD for BNNTs synthesis is shown in Fig. 1 and discussed in details in the next section.

3.1 Catalytic CVD

The first group who used CVD successfully for the synthesis of BNNTs was Lourie *et al.* (2000). They used borazine ($B_3N_3H_6$) as the precursor. Ni_2B was found as the most appropriate catalyst among all the other tested catalysts with borazine. A schematic of the proposed rout growth mechanism for BNNTs synthesis is shown in the Fig. 2. Silicon wafer substrate and NiB/Ni_2B catalysts were placed in the center of a tube furnace. The furnace was then heated from 1000–1100 °C. A carrier gas containing borazine was flown into the system for 30 min. At this temperature borazine decomposed and produced BN and H_2. H_2 goes outside through the outlet whereas BN diffuses on nickel boride catalyst particle. With the passage of time BN aggregates leading to super saturation, and consequently result in precipitation of BNNTs on catalyst particle. The BNNTs thus formed have bulbous tips, possessed club like or flag like morphology with a length of approximately 5 μm.[79]

The earlier work on the CVD synthesis of CNTs shows that precursors and catalysts are the two main requisites along with the experimental set up and other parameters.[143] Majority of these technique differ with respect to types and nature of catalysts and some of the experimental parameters.[144–146] For example, CNTs were synthesized *via* CVD technique with methane gas as a precursor, Fe_2O_3/Al_2O_3 as catalyst and Ar gas as a reaction atmosphere to prevent the oxidation of the catalyst. In short, the catalyst was placed in the quartz tube furnace and heated in the presence of Ar gas flow up to 1000 °C. At 1000 °C, the Ar gas flow was replaced with the precursor gas methane and the system was maintained in such a condition for 10 min. After 10 min, the system was brought to room temperature in the presence of Ar gas flow.[143] In the first CVD synthesis of BNNTs, NiB/Ni_2B were used as catalyst and borazine gas as precursor. The substrate and catalysts were heated up to 1000–1100 °C and maintained for 30 min in the presence

Table 1 A summary of different techniques used for BNNTs synthesis

S. no.	Technique	Temperature °C	Advantages	Dis-advantages	References
1	Arc-discharge	~3500	Highly crystalized, both SWBNNTs and MWBNNTs	Containing BN onion and cages like morphologies as impurities	6 and 20
2	Laser ablation	~1200–5000	Highly crystalized, both SWBNNTs and MWBNNTs	Containing BN cones *etc.* as impurities	90–92
3	Template synthesis	750–1580	Having controlled morphology	Containing carbon in lattice as impurities	109–113
4	Auto clave	600	Low temperature	Bad quality, low yield and containing BN cages and B as impurities	114–116
5	Ball milling	1000–1200	Large yield	Low purity with B, h-BN and BN fiber as impurities	118–123
6	CVD	1100–1200	High quality and large quantity up to gram level	Search for a specific method (CVD type) with specific reaction parameters and precursors	6, 13, 79, 116 and 126–135

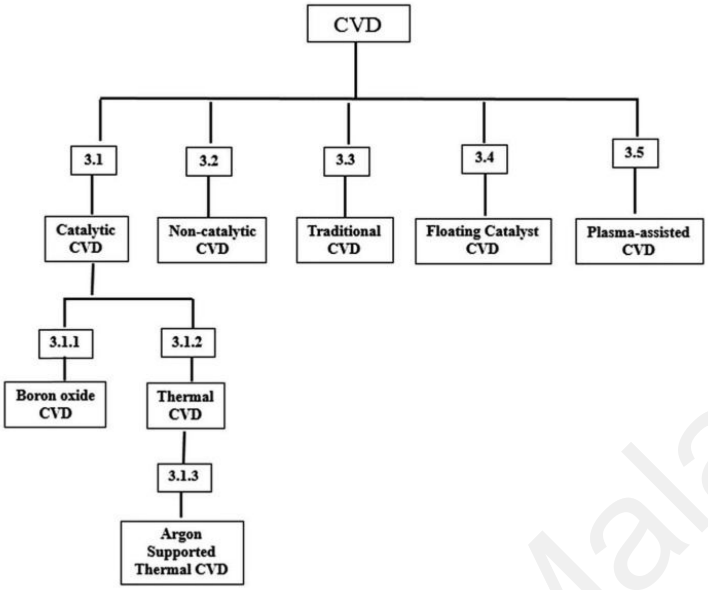

Fig. 1 Block diagram of different CVD methods used for the synthesis of BNNTs.

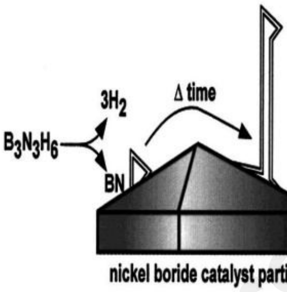

Fig. 2 A depiction of the proposed root growth mechanism.[79]

of borazine-containing carrier gas. Finally the white color product was obtained on the substrate.[79] In order to further improve the quality, quantity and size of the BNNTs *via* catalytic CVD method, it was necessary to avoid toxic gas precursors. The major breakthrough occurred with the use of B and metal oxides as precursors and induction furnace as an experimental set up.[147] Further improvements were sought by the replacement of induction furnace with conventional horizontal tube furnace[84]

If the above pioneer CVD work[79] on the synthesis of BNNTs and the later on major developments[81,84,85,147] are compared with the earlier work on CVD synthesis of CNTs,[143] it would not be difficult to findout that majority of the concepts used in CVD of CNTs and BNNTs are somehow related or linked with each other. But, since both the materials are different, therefore, different types of precursor's powder or gases are used in each technique with different experimental parameters according to the nature of precursor's materials. On these basis the catalytic CVD is further divided into two new categories. The details are mentioned in the following sub-sections.

3.1.1 Boron Oxide CVD (BOCVD). The BOCVD technique for BNNTs synthesis was first developed by Tang *et al.* (2002). The use of carbon-free precursors and induction furnace in this method insured high quality of the synthesized BNNTs. As a precursor boron is used (in each experiment) with different metal oxides in different weight ratios. In this method boron powder react with metal oxides catalysts and form B_xO_y which then reacts with N free radicals from NH_3 at certain temperature and forms BNNTs. In this regard, Tang *et al.* performed different experiment. Each experiment was different from the other by the precursor's type, catalysts, precursor's ratio and the environment in which the precursors and catalysts were used. First, BNNTs were synthesized by heating a mixture of boron and iron oxide powder (1 : 1) in the presence of ammonia gas. It was found that the ratio of the precursors and temperature plays an important role in the structure of the BNNTs.[147] Second, BNNTs were synthesized by heating boron and alumina supported nickel boride catalyst in the presence of N_2 or NH_3 gas at a temperature range of 1100–1300 °C. The BNNTs thus produced have diameter of 5–40 nm and length of several micrometers. Defects in the structure of BNNTs were found at a temperature higher than 1300 °C. However, at a temperature above 1500 °C, no formation of BNNTs was observed.[127] Third, BNNTs were synthesized with a large diameter of up to 70 nm and length greater than 10 μm by heating a mixture of boron and magnesium oxide powder in the presence of NH_3. Boron and MgO were first mixed in a 1 : 1 ratio and then heated at a certain temperature to form B_2O_2 and Mg. Mg was evaporated from the final product whereas the synthesized B_2O_2 reacted with NH_3 to form BNNTs according to VLS growth mechanism. BNNTs thus formed were in the pure form. In a smaller diameter of around 10 nm, the nanotubes were straight with concentric tubular structure containing no defects. Defects were found in the nanotubes with a diameter of about 60 nm.[80]

Zhi *et al.* (2005) further developed the BOCVD technique for high yield synthesis of BNNTs. The details of the synthesis method are mainly similar to the one described elsewhere.[118] However, some modifications were done to obtain high quality results. In short, a mixture of B, FeO and MgO was taken in BN boat and heated in an induction furnace up to 1200 °C. As a result, B_2O_2 vapors were formed. NH_3 was introduced from the top of BN boat. At this temperature NH_3 decomposed into N_2 and H_2. H_2 reacted with oxygen from B_2O_2 and formed water vapors whereas N_2 reacted with boron and formed BNNTs. In this study, it was found that BNNTs can be produced in a temperature range of 1100–1700 °C with an average diameter of ~50 nm and almost no impurity present in the final product. The growth of the BNNTs was catalytic based on VLS model.[81]

Goldberg *et al.* (2010) achieved large scale production of BNNTs up to 2 grams *via* BOCVD method[80] (see in Fig. 3). For high purity of the BNNTs, the design of the induction furnace was optimized. The basic reason for this optimization was to separate boron and metal oxide precursors for the BNNTs synthesis. The BNNTs have a diameter of approximately 50 nm and a length of up to tens of micrometers synthesized in this way.[148]

Huang *et al.* (2011) introduced B and Li_2O as precursor in BOCVD technique, and successfully achieved bulk amount of pure and thin BNNTs. It has been discovered that Li, due to its superior oxidation and promotion effect on the crystallization, played a key role in the large scale synthesis of BNNTs with small diameter. The synthesized BNNTs had an average diameter of sub-10 nm and a length of greater than 10 micrometers.[149]

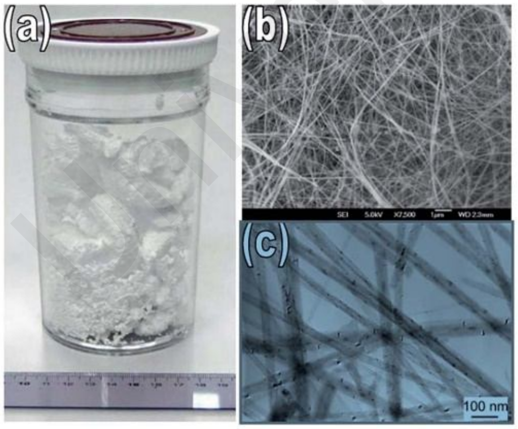

Fig. 3 (a) Image of as synthesized 2 grams BNNTs (b) SEM and (c) TEM image of multiwall BNNTs.[148]

Li *et al.* (2013) tried to enhance the effect of B and Li_2O as precursor *via* further modification in BOCVD technique. The precursors (*i.e.* B and Li_2O[149]) were first ball milled in the presence of NH_3. The ball milled precursors were then moved into a horizontal tube furnace and heated from 2–3 hour in the presence of NH_3 flow. White feather like BNNTs was found inside the boat and on the Silicon substrate. During the milling process the catalyst increased B oxidation and nitridation which was considered to be the possible reason for high yield of BNNTs.[150]

Yamaguchi *et al.* (2013) successfully synthesized 1 g of multiwall BNNTs *via* BOCVD technique reported elsewhere.[49,151–154] The synthesized BNNTs were long up to 1 to 5 μm and external diameter in the range of 40 to 50 nm. The tubes were then subsequently purified at high temperature in the Ar atmosphere. Later on it was utilized for the reinforcement of lightweight aluminum ribbons.[155] The BNNTs synthesized by different researchers *via* BOCVD technique are summarized in Table 2.

Though the introduction of BOCVD was a significant progress regarding the mass production of BNNTs, which led the researchers towards its potential application in nanotechnology.[16,81] However, this technique requires a specific design of induction furnace for achieving higher temperature with high temperature gradient. Further, it was found that this technique cannot be used for coating of BNNTs on Si based substrates without the assistance of other techniques and precursors.

3.1.2 Thermal CVD (TCVD). Lee *et al.* (2008) reported a simple TCVD for the synthesis of BNNTs directly on Si/SiO_2 substrate. The system thus developed is almost the same as previously used for the synthesis of CNTs.[156] However, for obtaining high quality of BNNTs, some changes have been brought in the existed technique. Instead of gaseous precursors and deposited catalysts on the substrate, a mixer of powder precursors and catalysts was used as a starting material. For the first time in BNNTs synthesis, a new concept of growth vapor trapping (GVT) was introduced with the use of one end closed inner test tube. The precursors used were: B, MgO and FeO in a molar ratio of 2 : 1 : 1. All the precursors were put in alumina combustion boat. The boat was placed in one end closed quartz tube. The quartz tube was then pushed inside a quartz chamber. The quartz chamber was first evacuated to ~30 mTorr and then heated up to 1200 °C. At this temperature NH_3 gas was introduced into the chamber at a rate of 200 sccm for one hour. The BNNTs were formed in pure form on the inner walls of the boat and partially vertically aligned on silicon substrate placed on the boat. A view of the as-grown BNNTs is shown in the Fig. 4. The diameter of the tubes was in the range of 10–100 nm with a length of greater than 10 μm. The as-synthesized, partially vertically aligned BNNTs, were not powerful enough to stand against even a small mechanical compression which make them laid horizontally on silicon substrate.[84]

Lee *et al.* (2010) further used his own designed TCVD and obtained pattern growth of BNNTs. Transmission electron microscope (TEM) copper grids were used as pattern. The used precursors were the same as the one mentioned elsewhere,[81,84] but with a different weight ratio of 4 : 1 : 1. The system was

Table 2 Summary of BNNTs grown by various researchers *via* BOCVD

S. no.	Year	Precursors	Precursors ratio	Substrate	Temperature (°C)	Catalysts	Growth mechanism	Final comments	References
1	2002	Boron powder	Not mentioned	Without any substrate	1100–1300	NiB/Al_2O_3	VLS	Diameter 5–40 nm, length several μm with bamboo and polar like BNNTs	127
2	2002	B, MgO	1 : 1	Without any substrate	1300	Mg. Nanoscale catalyst	VLS	Pure, diameter around 10 nm. Defects found in nanotubes with a diameter of about 60 nm	80
3	2005	B, FeO and MgO	Not mentioned	Not mentioned	1100–1700	Fe, Mg	Catalytic growth based on VLS	Diameter 50 nm, no impurity	81
4	2011	B and Li_2O	1 : 1	Not mentioned	1100–1350	Li	Not mentioned	Diameter sub-10 nm, length greater than 10 μm	149
5	2013	B and Li_2O	1 : 1	Si/SiO_2	Not mentioned	Li	Not mentioned	White feather like morphology	150
6	2013	B, FeO and MgO	1 : 1 : 1	Not mentioned	Not mentioned	Mg, Fe	Not mentioned	Diameter 40–50 nm, length 1–5 μm	155

heated in a range of 1100–1200 °C in the presence of NH_3 flow, at a rate of 200–350 sccm for approximately 30 min. The purpose of one end closed small quartz tube was to obtain growth vapor trapping (GVT). For the patterned growth, TEM copper grid was first mounted with the help of adhesive tape on the silicon substrate. Pulse Laser Deposition (PLD) was used to deposit a thin layer of Al_2O_3 film of 30 nm, followed by MgO, Ni or Fe film of 10 nm thicknesses on silicon substrate. After deposition, the TEM grid was removed and the substrate was transferred to the CVD system for the synthesis of BNNTs. The BNNTs formed in this way (have followed base growth mechanism according to VLS model) have diameter of 60 nm and average length of greater than 10 μm, as shown in Fig. 5.[157] The idea used in the initial treatment of the substrate for obtaining the pattern growth[157] is somehow similar to the one used for the synthesis vertically aligned CNTs. However, in case of CNTs Co, Ni or their alloys (Co–Ni) are first deposited at the substrate and then etch with NH_3 to produce nucleation sites for the synthesis of vertically aligned CNTs.[158] Whereas, in the pattern growth of BNNTs Al_2O_3 film, MgO, Ni or Fe film were deposited at the

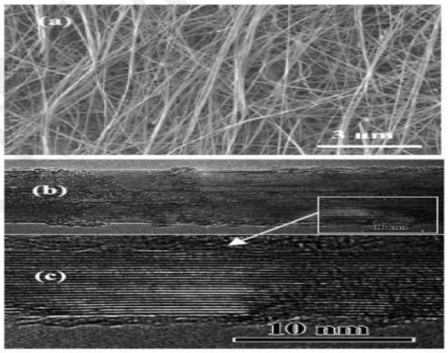

Fig. 4 (a) SEM (b) low and (c) high magnification TEM images of the as-synthesized BNNTs by TCVD.[84]

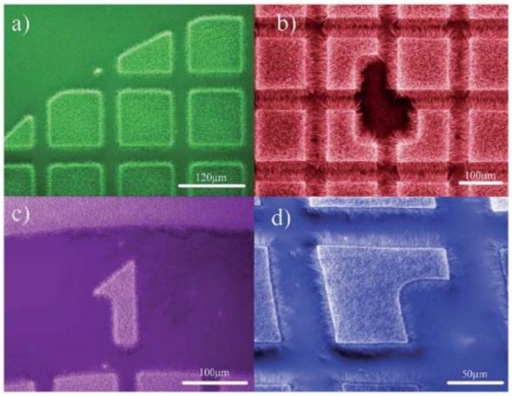

Fig. 5 Partially vertically aligned BNNTs grown in a particular patterned.[157]

substrate surface. No separate NH_3 etching was employed to produce nucleation sites. Therefore, the BNNTs product thus obtained was partially vertically aligned and was not strong enough to stand a slight mechanical compression.[157]

Ferreira *et al.* (2011) used a novel synthesis route based on TCVD technique and successfully synthesized BNNTs from a mixer of amorphous boron powder, ammonium nitrate and hematite. Ammonium nitrate and hematite were used as catalyst. The characterization results showed that the synthesized BNNTs were filled with Fe nanoparticles. Such BNNTs were predicted to be useful in some of the biomedical applications.[159]

Pakdel *et al.* (2012) comprehensively studied the CVD growth of BNNTs in a horizontal electric tube furnace, using B, MgO, and FeO as precursors with different weight ratio of 1 : 1 : 1, 2 : 1 : 1, and 4 : 1 : 1, at a temperature of 1200 °C, 1300 °C and 1400 °C, respectively. The effects of different transition metals or their compounds have been tested as catalysts for the growth of BNNTs. However the results of their reaction with boron were not satisfied. Therefore the precursors were selected following the earlier work by Zhi *et al.* (2005). It was found that the growth temperature and metal oxides content have a significant effect on the structure, morphology and characteristics of the BNNTs. An increase of the temperature above 1200 °C resulted an increase in the tube diameter, and further increase to 1400 °C resulted in a secondary growth of very thin nanotubes. Nanotubes synthesized by using 2 : 1 : 1 ratio of the precursors at 1200 °C and 1300 °C has an average outer diameter of approximately 30 nm and 60 nm, respectively and were uniformly dispersed. At 1400 °C the tubes grown have flower like morphology with a diameter of $\sim$20 nm and $\sim$100 nm. For 1 : 1 : 1 and 4 : 1 : 1 ratio of the precursors, no appreciable result was found at 1200 °C and 1400 °C. However at 1300 °C, the 1 : 1 : 1 ratio has a diameter in the range of $\sim$100–500 nm with flower like morphology, and 4 : 1 : 1 ratio has diameter in the range of $\sim$50–150 nm with entangled curve like morphology. Tip, base-growth or mix-growth mechanism (based on VLS mechanism) was proposed for the growth of the tubes.[83]

Seo *et al.* (2012) combined TCVD with ball milling annealing process and successfully synthesized relatively pure BNNTs (according to VLS mechanism). During this process, the production of impurities was a great concern in the residual material. It was concluded that the reaction parameters such as precursors, temperature and annealing time can sufficiently modify the final product.[160]

Özmen *et al.* (2012) adopted a TCVD method in which BNNTs were synthesized by heating a mixture of boron and iron oxides powder over 900 °C in the presence of NH_3. The temperature and the ratio of B to Fe_2O_3 were found to have a great effect on the crystallinity of the synthesized materials. N_2 produced during the decomposition of NH_3, reacted with Fe_XB_Y, (produced by the reaction of boron with iron oxide) and synthesized BNNTs. Characterization of the samples showed bamboo and hollow cylindrical morphology of the BNNTs with inner diameter in the range of 7 nm to 38 nm.[161] Growth mechanism and physical properties of BNNTs grown *via* TCVD is shown in Table 3.

Though TCVD is a simple technique to grow BNNTs directly on Si/SiO_2 substrate. However, this technique was unable to give a specific idea to get BNNTs with an increasing length. Furthermore, vacuum or evacuation is need as a reaction atmosphere inside the chamber, which require vacuum pump an additional accessory with the conventional horizontal tube furnace. The requirement of the vacuum pump not only increases the cost of the experimental set up but also needed further study about vacuum and extra expertise to run the vacuum pump.

3.1.3 Argon supported TCVD. Ahmad *et al.* (2015) synthesized BNNTs *via* argon supported TCVD technique. Argon gas flow was employed as an alternative for vacuum or evacuation. Ar gas being inert does not react with any material. Its flow through the system helps in the removal of oxygen and dust particles and thus helps in creating a suitable atmosphere for the desired chemical reaction to occur. So it was sought to be a good alternative for the vacuum or evacuation in CVD. Two minutes before the experiment, Ar gas was passed through the system and then a continuous flow was maintained at a rate of 100–200 sccm up to 1100 °C. After the completion of the reaction time Ar gas was again introduced into the system that flew away the water vapors, hydrogen, oxygen and BN species (left behind during the BNNTs synthesis) that might affect the final product quality.

It was found that the flow of Ar gas is playing a significant role in a simple and cost effective synthesis of BNNTs. As an alternative for vacuum, argon gas flow has eliminated the use of vacuum pump, which in other words have made the experimental set up $\sim$18% cost effective as compared to the conventional set up. Thus no extra knowledge or expertise is needed about vacuum or vacuum pump. Furthermore, the anti-oxidant nature of the argon gas prevents the oxidation of the as produced Mg and Fe catalysts, which in other words helps in growing longer BNNTs.[85]

3.2 Non-catalytic CVD

Ma *et al.* (2001) synthesized BNNTs *via* CVD technique, without using any catalyst. Melamine ($C_3N_6H_6$) and boric acid (H_3BO_3) were used as starting materials. These starting materials were first mixed in 2 : 1 ratios to form a hot aqueous solution. This hot solution crystallized into melamine diborate ($C_3N_6H_6 \cdot 2H_3BO_3$) as the CVD system cooled down. After annealing melamine diborate in N_2 environment, B–N–O was formed. It was then heated rapidly in N_2 gas stream to form BNNTs. The multiwalls BNNTs synthesized by this method have 12 concentric layers with inner diameter of 5.2 nm and outer diameter of 13.1 nm. The as-synthesized nanotubes were found to have a length of few micrometers with bulbous tips at the end. These tips were then used to grow the nanotubes.[162]

BNNTs were also synthesized by using α-Al_2O_3 micrometer size particles as the substrate. The purpose of that work was to check the effect of substrate on the final product. The as-synthesized BNNTs were found to have inner diameter of at least 5 nm larger than the one previously described,[162] with the same layers. Thus the substrate was found to affect the diameter of BNNTs

Table 3 Growth mechanisms and physical properties of BNNTs grown by TCVD

S. no.	Year	Precursors	Precursors ratio	Substrate	Temperature (°C)	Catalysts	Growth mechanism	Final comments	References
1	2008	B, MgO and FeO	2 : 1 : 1	Si/SiO_2	1200	FeO, MgO	VLS	Diameter 10–100 nm, length greater than 10 μm	84
2	2010	B, MgO and FeO	4 : 1 : 1	Si/SiO_2	1100–1200	MgO, Ni, or Fe	Base growth according to VLS	Diameter 60 nm, average length greater than 10 μm	157
3	2011	B, NH_4NO_3 Fe_2O_3	15 : 15 : 1	Not mentioned	1300	Fe_2O_3	Not mentioned	BNNTs were filled with Fe nanoparticles	159
4	2012	B, MgO, FeO	1 : 1 : 1, 2 : 1 : 1, 4 : 1 : 1	Si/SiO_2	1200–1400, 1200–1400, 1200–1400	Mg, Fe	Tip-growth. Base growth, mix growth according to VLS mechanism	Diameters ~30 and ~60 nm at 1200 and 1300 with straight morphology. ~10 nm and ~100 nm at 1400 °C with flower-like morphology	83
5	2012	B, MgO, FeO	2 : 1 : 1	Not mentioned	1200	Mg, Fe	VLS	Pure and quantity can be increased *via* milling-annealing + TCVD	160
6	2012	B and Fe_2O_3	15 : 1, 5 : 20	Not mentioned	900–1400	Fe	Not mentioned	BNNTs with bamboo and hollow cylindrical morphology	161

within CVD technique. BNNTs filled with amorphous B–N–O materials were also observed in the final product.[163] Later on it was pointed out by the same group with the help of further experimental work that employing the same CVD technique result in different morphologies of the nanostructures depending on the experimental parameters such as temperature and content of oxygen in the precursor.[164] A summary of BNNTs synthesized *via* non-catalytic CVD is shown in Table 4.

3.3 Traditional CVD

Traditional CVD technique was used to synthesize F-doped BNNTs. A diagram of the experimental setup along

Table 4 Summary of BNNTs synthesized by non-catalytic CVD

S. no.	Year	Precursors	Precursors ratio	Substrate	Temperature (°C)	Catalysts	Growth mechanism	Final comments	References
1	2001	Melamine ($C_3N_6H_6$) and boric acid (H_3BO_3)	1 : 2	Without any substrate	1200	Without any catalyst	Tip growth	BNNTs bulbous tips at the end	162
2	2001	Melamine ($C_3N_6H_6$) and boric acid (H_3BO_3)	1 : 2	α-Al_2O_3	1200	Without any catalyst	Not mentioned	BNNTs filled with amorphous B–N–O materials	163
3	2002	BN powder	Not mentioned	Without any substrate	1700	Not mentioned	Not mentioned	Morphology depends on modification in CVD set up w.r.t. precursor, temperature	164

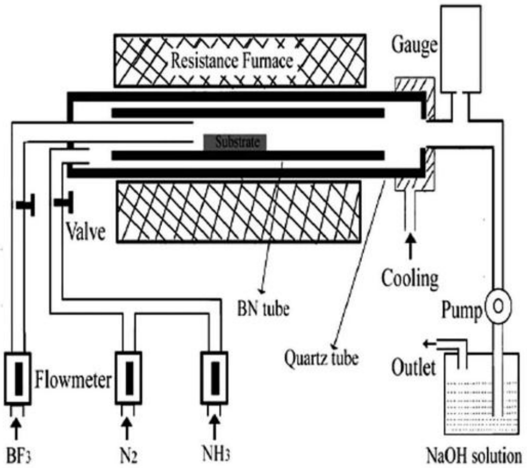

Fig. 6 Traditional CVD setup used in the synthesis of F-doped BNNTs.[165]

experimental parameters and precursors variables is shown in Fig. 6. In this method a Basic BN crystal was first synthesized by using BF_3/NH_3 as precursor. Then at the growth stage, F-atoms were introduced to form F-doped BN crystal. The synthesized F-doped BN crystal had nanotubes like morphology. The length and diameter of the tubes were estimated from the scale shown in the SEM micrograph of the sample, whereas the F-doped BNNTs had a length of few micrometers and diameter in tens of nanometers.[165]

3.4 Floating catalyst CVD

Multiwalls and double-wall BNNTs have been synthesized by floating catalyst CVD with the help of floating nickel catalyst, using two different molecular precursors; amine borane borazine and polyhedral-borane decaborane are separately used in NH_3 atmosphere at 1200 °C and 1300 °C respectively. Both precursors resulted in different size and morphologies of the BNNTs. Double-walls BNNTs synthesized from borazine at 1200 °C were found to be 0.2 μm in length and about 2 nm in diameter. The size of multiwall BNNTs synthesized from decaborane was found to be affected by the temperature. The one synthesized at 1200 °C had inner diameters from ~4–5 nm and outer diameters from ~12–14 nm with a length of ~0.2 μm, whereas the other synthesized at 1300 °C had a length of ~0.6 μm.[166]

Another important CVD technique based on floating catalyst was also introduced[128] later on to obtain good quality and large quantity of BNNTs. It has been successfully used for synthesis of double walled BNNTs. It is found that this technique might be an optimized step toward the continuous growth of BNNTs by CVD technique.[128]

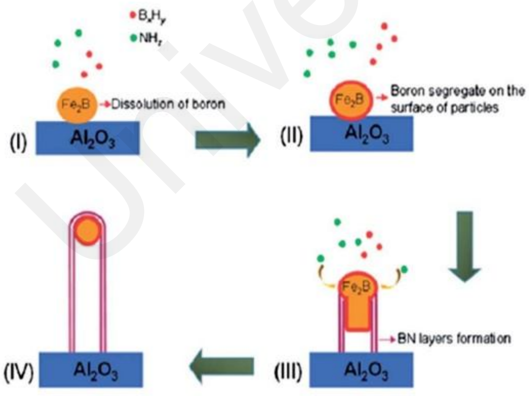

Fig. 7 Different steps involved during the growth of BNNTs *via* plasma-assisted CVD technique.[168]

3.5 Plasma-assisted CVD

Microwave plasma-assisted CVD technique was used to synthesized BNNTs at low substrate temperature by using transition metals as catalyst, and diborane and ammonia as precursors. The nanotubes thus formed have a diameter of less than 10 nm. The morphology and the structure of the nanotubes were found to be strongly affected by the growth condition. Micro-sized Ni dots were used to obtain patterned growth of BNNTs. This patterned growth was considered to be one of the possible ways for the synthesis of BNNTs in the aligned orientation.[167]

Large scale synthesis of BNNTs at low substrate temperature has also been reported by plasma-assisted CVD technique. Diborane and ammonia were used as precursors whereas Fe (powder) was used as supporting catalyst. The yield of BNNTs was found to be increased by the addition of O_2 in the synthesis process. A growth model has also been proposed (as shown in Fig. 7) to properly explain the role of metal catalysts during the synthesis or growth of BNNTs. It was suggested on the basis of the obtained results that this technique can be used to achieve large scale and high quality of BNNTs at low temperature.[168]

The study of all the above CVD techniques showed that the quality, quantity, size and morphology of the BNNTs depend on certain variables like precursor's types, their ratio, temperature, catalyst and growth mechanism *etc.* Therefore all these variables and their importance in different CVD techniques regarding their effect on the final BNNTs products are fully discussed in the next section.

4 Discussion

BNNTs have been synthesized by different CVD techniques. Each technique is different from the other w.r.t. the used experimental set up, precursors, their ratios, substrate, and temperature, catalyst and growth mechanism.[79–81,163] Therefore the final product differ with respect to quality, quantity, size and morphology. The importance of all these parameters is fully discussed in the following sections:

4.1 Importance of B, MgO and FeO as precursors for BNNTs synthesis

BNNTs have been synthesized in different sizes and morphologies by using different precursor's materials. The precursors utilized by the initial groups[20] have although produced pure BNNTs in different sizes and morphologies, however the toxic nature of some of the precursors have made it difficult for other researchers to reproduce BNNTs by the same methods.

A novel method based on VLS[169] mechanism has been proposed and developed by Tang *et al.*[127,132,170] In this method B and MgO were used as precursors. Though pure BNNTs were synthesized from these precursors however to increase the quantity at higher temperature, it resulted in bulk BN flakes. Also the growth of the BNNTs was very slow due to slow catalytic activity of Mg. Furthermore, B and MgO precursors become chemically inactive due to the formation of $Mg_2B_2O_5$ after first experimental run which cannot be used for further synthesis. Thus a major portion of these precursors had been wasted by this way, and only a small portion was utilized for BNNTs synthesis.[81]

Due to the common use of transition metals as catalysts and need of oxygen for B_2O_2 production, FeO has been used with boron powder to obtain a high quality result. However, it was discovered that the chemical reaction effectiveness of B and FeO was not satisfying and very little amount of B_2O_2 was produced in this reaction at a higher temperature. In order to combine the effect of both MgO and FeO, they were collectively used with boron powder, and BNNTs were produced in a wide temperature range of 1100 °C to 1700 °C. No notable impurity or bulk BN flakes were observed in the final product. During this method the growth of the BNNTs stop only when the precursor in the boat is blocked by the initially formed BNNTs at their top. The blockage of the precursors keeps the underneath precursors unreactive. Therefore, when the BNNTs top surface is removed, the remaining precursors can be used for several syntheses. This is the most important advantage of the above precursors (B, MgO, and FeO). It was also found that the quantity of the final product can easily be increased by using a larger size boat.[81]

Later on, some other researchers[83,84] used the above precursors with different weight ratios (1 : 1 : 1, 2 : 1 : 1 and 4 : 1 : 1). The best results *i.e.* BNNTs with diameter from 10–100 nm and length of greater than 10 μm were obtained with 2 : 1 : 1 ratio of the precursors.[83,84]

Further developments regarding quantity and quality of BNNTs (when B, MgO and FeO are used as precursors) were sought by the addition of ball-milling and annealing along with TCVD. In this method the precursors *i.e.* B, MgO and FeO were first ball-milled and then annealed in the presence of reactant gases (nitrogen and ammonia). The obtained results suggested that this combine method (TCVD and ball milling and annealing) can be used to increase the yield of BNNTs and reduces the residual impurities left in the boat which was normally observed by Lee *et al.*[84] by controlling the parameters like temperature, annealing time, ratio of the precursors and types of the reaction gases *etc.*[160] Though efforts have done to brought improvements in the existed method, however the adopted procedure was quite lengthy and relatively difficult to be followed by other researchers relative to the already existed methods.[81,83,84]

Again boron and iron oxide (Fe_2O_3) were used as precursors to synthesized BNNTs. Different weight ratios of B to Fe_2O_3 *i.e.* 15 : 1 and 5 : 1 were used. It was found that the ratio of the precursors has a great effect on the crystallinity of the final product. The crystallinity increases by increasing the weight ratio of boron to iron oxide. The surface area of the as synthesized BNNTs was also found to be affected by the weight ratio of B to Fe_2O_3 and increases by increasing this ratio. It was further found that the color of the final product become darker by decreasing the weight ratio of B to Fe_2O_3.[161] Recently, BNNTs have been synthesized from B, MgO and FeO, according to the procedure mentioned elsewhere.[49,151–154] The as-produced product can easily be functionalized for its potential applications in optical devices.[171–175]

Thus the synthesis of the BNNTs by the above mentioned methods emphasizes the fact that B, MgO and FeO are the most effective precursors for the synthesis of pure BNNTs. This fact has been summarized in the Table 5. According to the analysis shown in the Table 5, there are some disadvantages of using B, MgO and FeO as precursors; however it is also clear that these disadvantages are so minor that they can easily be eliminated.

4.2 Importance of experimental set up

Experimental set up has a key role in a good quality and large quantity of BNNTs synthesis. Different experimental set up have been developed and used for the CVD synthesis of BNNTs. All of these experimental set up consist of either lengthy and complex procedures,[168] or high temperature.[162] Due to which they have not been followed by other researchers. A significant progress has been made in this regard by the development of BOCVD technique.[80,81] This technique employs an induction furnace as an experimental set up to synthesize BNNTs within a temperature range of 1100 to 1700 °C.[81] The major drawback with the induction heating was the effect of temperature to the surrounding growth area, where the increase of the temperature can greatly modify the size and morphology of the BNNTs. This fact has been realized later on, therefore efforts were made on the design of most simple experimental set up where not only temperature can be controlled at the specific growth area but also be used to analyze the growth with increasing temperature.[83,84,157] In this regard the first experimental set up was designed using a conventional horizontal tube furnace with a quartz tube vacuum chamber. It further consisted of a one end closed quartz tube that was placed inside the quartz tube chamber. Precursors were put inside the one end closed quartz tube for the growth of the BNNTs. The system was then sealed and evacuated to a certain level. The precursors were then heated up to 1200 °C and kept for 1 hour at this temperature in the presence of NH_3 flow. BNNTs thus formed were observed inside the boat and on the silicon substrate.[84]

A sketch of such an experimental set up and the BNNTs product obtained is shown in the Fig. 8. It has been

Table 5 Analysis of B, MgO and FeO as an effective precursor for BNNTs synthesis

S. no.	Year	Precursors	Advantages	Dis-advantages
1	2001 (ref. 147), 2005 (ref. 81), 2012 (ref. 161)	B and Fe_2O_3 (ref. 147), B and FeO,[81] B and Fe_2O_3 (ref. 161)	1. High yield of BNNTs by varying precursor ratio from 5 : 1 to 15 : 1 (ref. 161) 2. Increased crystallinity with increasing ratio of B to Fe_2O_3 (ref. 161) 3. Change of BNNTs color with changing ratio of precursor and become darker by reducing the B to Fe_2O_3 ratio[161]	1. Contained α-Fe as impurities[147] 2. Formation of BN bamboo with high concentration of Fe_2O_3 (ref. 147) 3. Produces little B_2O_2 at higher temperature due to unsatisfied chemical reaction effectiveness between B and FeO that result in slow growth rate and lower amount of BNNTs[81]
2	2002, 2002, 2004	B and MgO[127,132,170]	1. Carbon free method[132] 2. Produces pure BNNTs[127,132,170] 3. B and MgO are effective source of B_2O_2 (ref. 81)	1. Results in bulk BN flakes at higher temperature 2. Slow growth due to very slow catalytic activity of Mg 3. B and MgO precursors become chemically inactive due to formation $Mg_2B_2O_5$ after first run[81]
3	2005 (ref. 81), 2008 (ref. 84), 2010 (ref. 157), 2012 (ref. 83)	B, MgO and FeO[81]	1. Pure BNNTs with diameter ∼50 nm can be achieved[81] 2. Temperature has no effect on the purity and diameter of the BNNTs[81] 3. Precursors can be used for several synthesis[81] 4. A larger boat size is helpful in increasing the final product[81] 5. Need a very sample experimental set up[84,157] 6. Diameter of the tube varies from 10–100 nm with length greater than 10 μm[84] 7. Pattern growth is possible in the desire format[157] 8. Allow control growth of BNNTs[157] 9. Desired morphology and diameter can be achieved by changing the precursors ratio and temperature[83]	1. The ratio of the used precursors is not clearly mentioned[81] 2. Need nanoscale catalyst to grow in nano-size diameter[84] 3. Possibility of forming ternary compounds (small amount) like: MgN_2, MgB_2 and Mg–B–N *etc.*, when MgO is used as a catalyst[157]

experimentally verified that the one closed end quartz tube is one of the most important requirement for BNNTs growth by the experimental set up shown in the Fig. 8. In other words, BNNTs growth cannot be achieved if the closed-end quartz tube is replaced with an open-end tube.[84] Later on, the pattern growth of BNNTs has been achieved by using the same experimental set up.[157] Almost the same experimental set up, precursor type (B, Mg, FeO) and ratio (2 : 1 : 1),[84] with some additional treatment (ball-milling) was used for synthesis of BNNTs at a bit higher flow rates of NH_3 and N_2 gases at 1200 °C for 6 hours.[160] Such an experimental set up has also been successful when B and Li_2O were used as precursors.[149,150]

A relatively different experimental set up with respect to the one reported by Lee *et al.*,[84] has been developed to synthesize BNNTs at 1200 °C, 1300 °C and 1400 °C, by using 1 : 1 : 1, 2 : 1 : 1 and 4 : 1 : 1 ratio of B, MgO and FeO as precursors, respectively. In previous experimental set up (Lee *et al.*[84]), the used vacuum chamber and test tube were made of quartz,[84] whereas in the present experimental set up these devices were made of alumina.[83] However, neither in the previous work nor in the present any effect of quartz or alumina (heat gain or loss) has been observed on the final product. Therefore both of the set up are almost the same except the use of one end closed test tube inside the chamber. In Lee *et al.*[84] experimental set up, one end of the test tube was closed and it has been experimentally verified that BNNTs cannot be synthesized if the closed end test tube is replaced by an open end test tube.[84] However in present work, the synthesis of BNNTs have been achieved with an open end test tube,[83] which was experimentally denied by Lee *et al.*[84] High vacuum (evacuation of chamber) and high flow rate of NH_3 (400 sccm compare to 200 sccm) may be the only possible reason for the present results.[83] However none of the two groups have ever considered either the effect of high vacuum or flow rate of NH_3 for possible change in the experimental set up or BNNTs product by using the same precursors.[83,84] Both types of experimental works have been summarized in Table 6.

A sample conventional horizontal quartz tube furnace without any inner one-end closed test tube has been used to

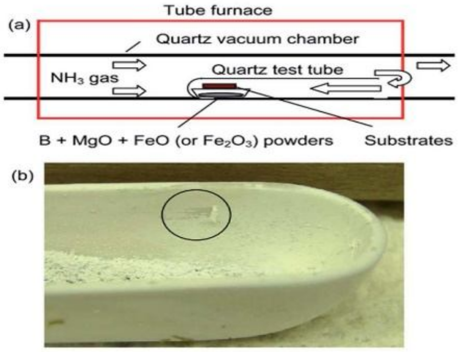

Fig. 8 (a) Sketch of the experimental set up used for BNNTs synthesis at 1200 °C (b) as synthesized BNNT inside alumina boat.[84]

synthesize BNNTs at a temperature lower than 800 °C. However the lengthy and time consuming process involved in the synthesis of the precursors materials, and understanding of the chemical reactions have made it difficult to be followed by other researchers.[176]

The choice of experimental set up changes with change in precursors, and use of Ar gas as an alternative for vacuum. Such changes have been observed by different researchers like Özmen *et al.*[161] Therefore, it is possible that in the near future the above mentioned experimental set up,[83,84] may easily be used with Ar gas as an alternative for vacuum (or evacuation). The use of Ar gas as an alternative for vacuum may not only further simplify the experimental set up but will also make it safe for the user.

4.3 Importance of temperature

Temperature is the most important factor during the synthesis and growth of BNNTs in a CVD technique. Specifically, size and morphology of the BNNTs varies with temperature.[166] The initial group synthesized BNNTs in a temperature range of 1100–1200 °C. The as synthesized BNNTs have flag like morphology with bulbous tip and length of about 5 µm.[79] The yield, diameter and morphology of BNNTs synthesized in a temperature range of 1200–1500 °C changes with increase in temperature. At a temperature below 1350 °C, the BNNTs have wool like structure with diameter 7 to 20 nm. The yield increases when the reaction temperature is fixed at 1250 °C. At this temperature a grey sponge like BNNTs can also be found with diameter 12 to 40 nm.[147] A change in morphology from straight[177] to bamboo,[178] and fiber[179] like has been observed with the change in temperature.[164] Defects were found in the BNNTs structure at a temperature higher than 1300 °C. When the temperature was increased from 1400 °C to 1500 °C, bamboo and polar like morphologies were observed. However, when the temperature was further increased beyond 1500 °C, no formation of BNNTs was reported.[127]

The effect of temperature also depend on the type of precursor used for BNNTs synthesis.[81,149] When B and MgO were used as precursor, good quality of BNNTs was obtained at a temperature below 1100 °C. The yield increased along with the tube diameter at higher temperature. The diameter reached to micron size with further increase in temperature. At a temperature higher than 1250 °C, BN flakes were observed in the final product. When B, MgO and FeO were used as precursors, BNNTs were synthesized in a wide temperature range of 1100 °C to 1700 °C. Higher temperature was found to have no effect on the purity and diameter of as synthesized BNNTs.[81] When B and Li_2O were used as precursors, BNNTs with a smaller diameter were formed at a temperature of 1100 °C. An increase in temperature above 1100 °C resulted in a thick and non-uniform diameter of BNNTs.[149] The temperature effect also varies with precursor's ratio along with precursor's type. For B, MgO and FeO as precursors with 1 : 1 : 1 and 4 : 1 : 1 ratios, no synthesis of BNNTs was reported at 1200 °C and 1400 °C. The synthesis of BNNTs from 1 : 1 : 1 and 4 : 1 : 1 ratio was reported only at 1300 °C. At this temperature the as synthesized BNNTs from 1 : 1 : 1 ratio had semi erect flower like morphology with diameter ~100–500 nm. Whereas the one synthesized from 4 : 1 : 1 ratio had diameter ~50–150 nm with entangled curve like morphology. The BNNTs synthesized from 2 : 1 : 1 ratio of the precursors at 1200 °C had diameter ~30 nm, and were straight and randomly oriented in different directions. When the temperature was increased from 1200 °C to 1300 °C, the morphology remained the same but the diameter increased from ~30 nm to ~60 nm. With further increase in temperature up to 1400 °C both diameter and morphology of the BNNTs changed. At this temperature the BNNTs synthesized have diameter ~20 to ~100 nm with straight flower like morphology.[83] This analysis of BNNTs with increasing temperature[83] is somehow contradicts with the work of Zhi *et al.*,[81] in which higher temperature was found to have no effect on purity

Table 6 Summary of BNNTs synthesized from same precursor but in different experimental set up

						Conventional horizontal tube furnace as experimental set up	
S. no.	Year	Precursors	Vacuum in Torr	Temperature (°C)	NH_3 flow rate in sccm	With one closed-end test tube	With opened end test tube
1	2008	B, MgO, FeO	~30 m Torr	1200	200	BNNTs synthesized with 10–100 nm diameter and length greater than 10 µm	BNNTs cannot be synthesized
2	2012	B, MgO, FeO	~1000 m Torr	1200	400	BNNTs synthesis was not reported	BNNTs synthesized with diameter ~30 nm

and diameter of the as synthesized BNNTs. Change in the experimental set up and ratio of the precursor used may be one of the possible reason for this conflict. However, none of these researchers[81,83] had ever mentioned the experimental set up (to be responsible) to bring a change in size or morphology with the change in temperature.

Temperature is also found to affect the crystallinity and color of the final product in BNNTs synthesis. The crystallinity of the product was found to increase with an increase in temperature. Change in the color and structure of the product was observed with increasing temperature. At 900 °C and 1000 °C, the material was in a particular structure with light brown color. When the temperature was increased to 1100 °C, the product was converted into powder form with brown color. The color changes from brown to grey with particular structure at 1200 °C. A mixer of grey and white color was found at 1300 °C which was converted to only white color at 1400 °C.[161] A concrete description of the temperature effects on size and morphology are summarized in Table 7.

4.4 Importance of catalyst

The use of catalysts is also of great significance in CVD growth of BNNTs. Initially BNNTs were synthesized by using NiB_2 as a catalyst. It was found that the catalysts not only accelerated the growth process but also helped in growing long size nanotubes. The size of the catalyst is also very important in BNNTs growth. It works as a pattern during the growth of BNNTs, and the diameter of the final product was found to be in the range of catalyst size.[79] In other words, the diameter of the tube can be controlled with the help of choosing an appropriate catalyst.[180] BNNTs have also been synthesized without using any catalyst, however the BNNTs thus obtained were smaller in size and lower in quality.[162] Pure BNNTs were produced by the introduction of MgO as a catalyst with B. However the growth of the BNNTs was very slow due to the slow catalytic activity of MgO at higher temperature. Therefore, other transition metals and their compounds have also been excessively searched and used as catalysts with B for BNNTs synthesis.[102,138,181] It has been proved with a series of experiments that the chemical reaction between boron and these catalysts were not effective enough for a satisfied result.[81] FeO reacts with B in the presence of NH_3 to produce BNNTs but its results were also not satisfied at higher temperature. In order to have good results that can further be improved at higher temperature, both FeO and MgO were collectively used with B. Thus high quality of BNNTs were obtained with this combination of precursor.[81] The use of these catalysts was further improved by using them in different ratios with boron in a conventional set up. For the first time the role of MgO and FeO during the BNNTs synthesis and growth was explained in full detail. It was found that MgO and FeO are not only the effective producer of B_2O_2 but also of Mg and Fe nanoparticles. B_2O_2 reacts with NH_3 to synthesize BNNTs whereas Mg and Fe helped in the growth of as synthesized BNNTs.[84,157] The growth stops only when either these catalysts are fully covered by the precursor's material or cut off as a tip from the BNNTs. Later on, the role and effectiveness of these catalysts were further tried by using them in different weight ratio with boron at different temperatures which resulted in different sizes and morphologies of BNNTs.[83] Due to an easy and effective use of MgO and FeO as catalysts with B, they have now become the most effective and conventionally used precursors for BNNTs synthesis till date.[155,160]

Li_2O was also tried as a catalyst with B for BNNTs synthesis due to the superior deoxidation capability of Li compared to Mg. BNNTs thus synthesized were in large quantity. However Li and other species were found in the final product as impurities. Since the experimental set up and steps involved during BNNTs synthesis were a bit complex and time consuming (compared to B, MgO and FeO[84]),[149,150] therefore this catalyst has not been excessively used afterwards. Thus the role of the catalyst is very

Table 7 Summary of temperature effect on size and morphology of BNNTs

			Effect of temperature (°C)		
S. no.	Precursor	Temperature (°C)	Size	Shape or morphology	References
1	$B_3N_3H_6$	1100–1200	Length 5 μm	Flag like	79
2	B and Fe_2O_3	1. Below 1350 2. 1250	1. Diameter 7–20 nm 2. Diameter 12–40 nm	1. Wool like 2. Grey sponge like	147
3	1. BN powder 2. $B_4N_3O_2H$	1700	1. Diameter 10–100 nm and length ~10 μm 2. Diameter 100–200 nm and length ~5 μm	1. Bamboo like 2. Straight cylindrical, tree like and fiber like	164
4	Boron, NiB/Al_2O_3	1400–1500	Diameter 5–40 nm and length several micron	Bamboo and polar like	127
5	1. B and MgO 2. B, MgO, FeO	1. 1250 and above 2. 1100–1700	1. Diameter 1-micron 2. Diameter ~50 nm	1. Bulk BN flakes 2. Straight and randomly aligned	81
6	B, MgO, FeO	1. 1200–1300 2. 1300–1400	1. Diameter ~30 to ~60 nm 2. Diameters of ~20 and ~100 nm	1. Long straight 2. Flower like	83

important in any of CVD technique for BNNTs synthesis. They not only control the size and morphology of BNNTs in CVD techniques but also provides a simple way for the synthesis of other two dimensional (2D) nanostructures of h-BN.

4.5 Importance of growth mechanism

Borazine ($B_3N_3H_6$) was used to successfully synthesized BNNTs for the first time by CVD technique. Root growth mechanism was assumed to have followed during the growth. The full details of this mechanism have already been given along with a figure in Section 3.1.[79] Melamine and boric acid were also used to synthesized BNNTs.[162] The growth mechanism followed was similar to the tip growth model of CNTs.[182,183] Later on BNNTs were synthesized by different CVD techniques. Regardless of the experimental set up and precursor used, BNNTs were assumed to have grown by tip-growth, base-growth or mix-growth model according to VLS mechanism.[80,81,83,84,127,157,169]

In VLS mechanism,[169] the precursor are heated to a certain temperature. At a suitable temperature, the nanosize catalysts either in liquid or partially melted form condensed on the substrate surface. This is usually occurred when their partial vapor pressures is sufficiently enough for this purpose. The as formed BN species then diffuse into the condense catalyst. Which then aggregates with the passage of time and finally becomes supersaturate that leads to the subsequent precipitation of BNNTs.[83]

Beside all of the above factors, the role of under lying substrate is also very important in CVD growth of BNNTs. It has further been noted that its presence is helpful in the rational synthesis of BNNTs.[184,185] Diameter of the as synthesized materials depends on the grain size and morphology of the substrate. By varying the grain size and morphology of the substrate the diameter of the final product can easily be controlled.[186]

5 Role of CVD in growth of 2D h-BN and other nanostructures

In the above sections it has been proved that CVD is the most prominent and reliable technique for the synthesis of pure BNNTs. This leads to further study of the same technique with different types of precursors and experimental parameters for the synthesis of 2D h-BN. However, the progress in this regard is very slow as compared BNNTs. The reason is the improved and excellent properties of BNNTs for its potential applications due to its reduced size and nanoscale dimension.

CVD has successfully been employed in the growth of atomic layers of hybridized h-BN and graphene domains[187] and large scale synthesis of atomic h-BN layers.[188] Ammonia-borane was used as precursor, copper foil as a substrate and Ar/H_2 as a reaction atmosphere. The film of atomic h-BN layers (consisted of 2–5 layers) was deposited at the top of the substrate at 1000 °C in a growth duration of 30–60 min. The adopted method for the synthesis was thus suggested to help in studying the structure and properties of h-BN thin film for its potential applications.[188] To further facilitate the synthesis of h-BN thin film another simple CVD technique is introduced. This technique work at ambient pressure and thus called ambient pressure CVD (APCVD). In this technique, the precursors ($B_3N_3H_6$) vapor are carried to the substrate (polycrystalline Ni) with the help of N_2 gas flow where they are deposited in the form of thin film (h-BN). This was believed to be the low-cost technique in which the growth temperature can be reduced to 400 °C. However, the growth is followed by annealing at 1000 °C that results in the production of high quality h-BN thin film with thickness in the range of 5–50 nm.[189] Though this technique was successful to grow a multilayer (5–50 nm) thin film of h-BN, however, it was unable to control the number of layer to a monolayer and failed to give a specific growth mechanism. These issues have been resolved with the development of low pressure CVD (LPCVD). In this technique Cu foil was used as a substrate and borazane as precursors. Growth in the LPCVD was believed to be surface reaction limited and was hoped to be not affected considerably by the gases flow or substrate surface. However, it was found that the geometry of the substrate has a key role in uniformity of the layers.[190] In this regard, a suitable substrate with smooth and fine surface was predicted to be of great importance.[190]

These progress in CVD synthesis of h-BN thin film and BNNTs shows the potential for further developments in CVD technique with respect to precursor's types, reaction atmosphere, growth duration and experimental set up *etc.* However, the progress is not restricted only to the synthesis of BNNTs or h-BN thin film. The development in CVD for the synthesis of other nanostructures of h-BN cannot be ignored. Ar-supported TCVD was successfully utilized for the synthesis of BNNWs. In this synthesis the relatively short growth duration was considered to be responsible for the synthesis of BNNWs.[73] The concept of Ar-supported TCVD also helped in the successful synthesis of BNMTs. During the synthesis of BNMTs,[191] the precursor's type, ratio and experimental set up used were the same as in the synthesis of BNNTs *via* Ar-supported TCVD,[85] however, in the synthesis of BNMTs, NH_3 gas flow was used as a reaction atmosphere instead of Ar gas. The same concept[191] with an increased growth duration of 90 min (instead of 60 min) was used for the synthesis of BNNS without any further modification.[192]

All these modifications and progress in CVD techniques suggests that CVD is very versatile technique that can be used for the high quality synthesis of any materials or its compounds by carefully optimizing its experimental parameters. This further provides opportunities for the commercialized production of materials and its use for its potential application.

6 Conclusions

Among all the techniques used for BNNTs synthesis, CVD technique has been proven to produce quality and quantity of BNNTs. The quality and quantity of BNNTs depends on the specific type of CVD technique. In each type of CVD technique, experimental set up, types and ratios of the precursor, temperature, catalysts, substrate and growth mechanism are some of the basic experimental parameters that affect the characteristics of the final product. Therefore, optimization of CVD setup for BNNTs synthesis is still an open area of research. The product obtained so far is not yet suitable (regarding quality and quantity) to be effectively used in any application in the real life.

B, MgO and FeO are the most effective precursors and the conventional horizontal tube furnace with one end closed inner test tube is the most commonly used experimental set up. Changes in the precursors (B, MgO and FeO) dimension and home-made experimental set up with Ar (gas) as an alternative for vacuum or evacuation can assist in successful synthesis of longer and cost effective BNNTs *via* a more simple TCVD technique. In addition, the idea of re-using the precursors (B, MgO and FeO), for several synthesis and suggested increase in the final product with increasing boat size, it is further suggested that the quality and quantity of BNNTs can be increased to any desired level by modifying the experimental set up in such a way that the synthesized BNNTs cannot block the precursor in the boat. For this purpose the boat should be replaced by a device (like the one used for concrete mixing) of appropriate size and shape that can keep or separate the as form BNNTs layer, and continuously make a homogeneous mixture of the rest of the precursors for further synthesis. This will not only prevent the top of precursor from blocking due to formation of BNNTs layer but also help to continue syntheses of BNNTs till the precursor are completely utilized.

Acknowledgements

We are extremely grateful to University of Malaya, 50603 Kuala Lumpur Malaysia, Project Number: RG375-15AFR, for providing funds and facilities for our research work.

References

1 X. Chen, X. Gao, H. Zhang, Z. Zhou, W. Hu, G. Pan, H. Zhu, T. Yan and D. Song, Preparation and electrochemical hydrogen storage of boron nitride nanotubes, *J. Phys. Chem. B*, 2005, **109**, 11525–11529.

2 Y. Zhang, K. Suenaga, C. Colliex and S. Iijima, Coaxial nanocable: silicon carbide and silicon oxide sheathed with boron nitride and carbon, *Science*, 1998, **281**, 973–975.

3 S. Chattopadhyay, A. Ganguly, K.-H. Chen and L.-C. Chen, One-dimensional group III-nitrides: growth, properties, and applications in nanosensing and nano-optoelectronics, *Crit. Rev. Solid State Mater. Sci.*, 2009, **34**, 224–279.

4 A. Rubio, J. L. Corkill and M. L. Cohen, Theory of graphitic boron nitride nanotubes, *Phys. Rev. B: Condens. Matter Mater. Phys.*, 1994, **49**, 5081–5084.

5 X. Blase, A. Rubio, S. Louie and M. Cohen, Stability and band gap constancy of boron nitride nanotubes, *Europhys. Lett.*, 1994, **28**, 335–340.

6 N. G. Chopra, R. Luyken, K. Cherrey, V. H. Crespi, M. L. Cohen, S. G. Louie and A. Zettl, Boron nitride nanotubes, *Science*, 1995, **269**, 966–967.

7 B. Akdim, R. Pachter, X. Duan and W. W. Adams, Comparative theoretical study of single-wall carbon and boron-nitride nanotubes, *Phys. Rev. B: Condens. Matter Mater. Phys.*, 2003, **67**, 245404–245408.

8 Z. H. Dong and Y. Song, Transformations of Cold-Compressed Multiwalled Boron Nitride Nanotubes Probed by Infrared Spectroscopy, *J. Phys. Chem. C*, 2010, **114**, 1782–1788.

9 R. S. Lee, J. Gavillet, M. L. de la Chapelle, A. Loiseau, J. L. Cochon, D. Pigache, J. Thibault and F. Willaime, Catalyst-free synthesis of boron nitride single-wall nanotubes with a preferred zig-zag configuration, *Phys. Rev. B: Condens. Matter Mater. Phys.*, 2001, **64**, 121405.

10 C. Y. Zhi, Y. Bando, T. Terao, C. C. Tang, H. Kuwahara and D. Golberg, Towards Thermoconductive, Electrically Insulating Polymeric Composites with Boron Nitride Nanotubes as Fillers, *Adv. Funct. Mater.*, 2009, **19**, 1857–1862.

11 M. Ishigami, J. D. Sau, S. Aloni, M. L. Cohen and A. Zettl, Observation of the giant stark effect in boron-nitride nanotubes, *Phys. Rev. Lett.*, 2005, **94**, 056804.

12 W. L. Wang, Y. Bando, C. Y. Zhi, W. Y. Fu, E. G. Wang and D. Golberg, Aqueous noncovalent functionalization and controlled near-surface carbon doping of multiwalled boron nitride nanotubes, *J. Am. Chem. Soc.*, 2008, **130**, 8144.

13 M. Ishigami, S. Aloni and A. Zettl, Properties of boron nitride nanotubes, in *AIP Conference Proceedings*, 2003, pp. 94–99.

14 J. Lauret, R. Arenal, F. Ducastelle, A. Loiseau, M. Cau, B. Attal-Tretout, E. Rosencher and L. Goux-Capes, Optical transitions in single-wall boron nitride nanotubes, *Phys. Rev. Lett.*, 2005, **94**, 037405.

15 P. Jaffrennou, F. Donatini, J. Barjon, J.-S. Lauret, A. Maguer, B. Attal-Trétout, F. Ducastelle and A. Loiseau, Cathodoluminescence imaging and spectroscopy on a single multiwall boron nitride nanotube, *Chem. Phys. Lett.*, 2007, **442**, 372–375.

16 C. Zhi, Y. Bando, C. Tang, D. Golberg, R. Xie and T. Sekigushi, Phonon characteristics and cathodoluminescence of boron nitride nanotubes, *Appl. Phys. Lett.*, 2005, **86**, 213110.

17 C. Tang, Y. Bando, C. Zhi and D. Golberg, Boron–oxygen luminescence centres in boron–nitrogen systems, *Chem. Commun.*, 2007, 4599–4601.

18 J. Wu, W.-Q. Han, W. Walukiewicz, J. Ager, W. Shan, E. Haller and A. Zettl, Raman Spectroscopy and Time-Resolved Photoluminescence of BN and $B_xC_yN_z$ Nanotubes, *Nano Lett.*, 2004, **4**, 647–650.

19 P. Jaffrennou, J. Barjon, T. Schmid, L. Museur, A. Kanaev, J.-S. Lauret, C. Zhi, C. Tang, Y. Bando and D. Golberg, Near-band-edge recombinations in multiwalled boron nitride nanotubes: cathodoluminescence and photoluminescence spectroscopy measurements, *Phys. Rev. B: Condens. Matter Mater. Phys.*, 2008, **77**, 235422.

20 C. Zhi, Y. Bando, C. Tang and D. Golberg, Boron nitride nanotubes, *Mater. Sci. Eng., R*, 2010, **70**, 92–111.

21 H. Harutyunyan, T. Gokus, A. A. Green, M. C. Hersam, M. Allegrini and A. Hartschuh, Defect-induced photoluminescence from dark excitonic states in individual single-walled carbon nanotubes, *Nano Lett.*, 2009, **9**, 2010–2014.

22 S. Lebedkin, K. Arnold, F. Hennrich, R. Krupke, B. Renker and M. M. Kappes, FTIR-luminescence mapping of dispersed single-walled carbon nanotubes, *New J. Phys.*, 2003, **5**, 140.

23 Y. Murakami, B. Lu, S. Kazaoui, N. Minami, T. Okubo and S. Maruyama, Photoluminescence sidebands of carbon nanotubes below the bright singlet excitonic levels, *Phys. Rev. B: Condens. Matter Mater. Phys.*, 2009, **79**, 195407.

24 M. J. O'connell, S. M. Bachilo, C. B. Huffman, V. C. Moore, M. S. Strano, E. H. Haroz, K. L. Rialon, P. J. Boul, W. H. Noon and C. Kittrell, Band gap fluorescence from individual single-walled carbon nanotubes, *Science*, 2002, **297**, 593–596.

25 B. Yan, C. Park, J. Ihm, G. Zhou, W. Duan and N. Park, Electron Emission Originated from Free-Electron-like States of Alkali-Doped Boron-Nitride Nanotubes, *J. Am. Chem. Soc.*, 2008, **130**, 17012–17015.

26 A. Zettl, C. Chang and G. Begtrup, A new look at thermal properties of nanotubes, *Phys. Status Solidi B*, 2007, **244**, 4181–4183.

27 Y. Chen, J. Zou, S. J. Campbell and G. Le Caer, Boron nitride nanotubes: pronounced resistance to oxidation, *Appl. Phys. Lett.*, 2004, **84**, 2430–2432.

28 D. Golberg, Y. Bando, K. Kurashima and T. Sato, Synthesis and characterization of ropes made of BN multiwalled nanotubes, *Scr. Mater.*, 2001, **44**, 1561–1565.

29 Z. Xu, D. Golberg and Y. Bando, *In situ* TEM-STM recorded kinetics of boron nitride nanotube failure under current flow, *Nano Lett.*, 2009, **9**, 2251–2254.

30 N. Koi, T. Oku, M. Inoue and K. Suganuma, Structures and purification of boron nitride nanotubes synthesized from boron-based powders with iron particles, *J. Mater. Sci.*, 2008, **43**, 2955–2961.

31 J. Yu, B. C. Li, J. Zou and Y. Chen, Influence of nitriding gases on the growth of boron nitride nanotubes, *J. Mater. Sci.*, 2007, **42**, 4025–4030.

32 L. H. Li, Y. Chen and A. M. Glushenkov, Boron nitride nanotube films grown from boron ink painting, *J. Mater. Chem.*, 2010, **20**, 9679–9683.

33 J. Li, G. Zhou, Y. Chen, B. L. Gu and W. H. Duan, Magnetism of C Adatoms on BN Nanostructures: Implications for Functional Nanodevices, *J. Am. Chem. Soc.*, 2009, **131**, 1796–1801.

34 R. Wu, L. Liu, G. Peng and Y. Feng, Magnetism in BN nanotubes induced by carbon doping, *Appl. Phys. Lett.*, 2005, **86**, 122510.

35 F. Li, Z. Zhu, M. Zhao and Y. Xia, *Ab initio* calculations on the magnetic properties of hydrogenated boron nitride nanotubes, *J. Phys. Chem. C*, 2008, **112**, 16231–16235.

36 T. Kolodiazhnyi and D. Golberg, Paramagnetic defects in boron nitride nanostructures, *Chem. Phys. Lett.*, 2005, **413**, 47–51.

37 T. Oku and M. Kuno, Synthesis, argon/hydrogen storage and magnetic properties of boron nitride nanotubes and nanocapsules, *Diamond Relat. Mater.*, 2003, **12**, 840–845.

38 S. Hao, G. Zhou, W. Duan, J. Wu and B.-L. Gu, Tremendous spin-splitting effects in open boron nitride nanotubes: application to nanoscale spintronic devices, *J. Am. Chem. Soc.*, 2006, **128**, 8453–8458.

39 G. Zhou and W. Duan, Spin-polarized electron current from carbon-doped open armchair boron nitride nanotubes: Implication for nano-spintronic devices, *Chem. Phys. Lett.*, 2007, **437**, 83–86.

40 K.-S. Ryu, Y.-I. Kim, J. K. Jung, Y. Chen and C. H. Lee, Dynamics of Natural Spin Defects in Boron Nitride Nanotubes, *J. Nanosci. Nanotechnol.*, 2008, **8**, 5193–5195.

41 Z. H. Zhang and W. L. Guo, Tunable Ferromagnetic Spin Ordering in Boron Nitride Nanotubes with Topological Fluorine Adsorption, *J. Am. Chem. Soc.*, 2009, **131**, 6874–6879.

42 Z. Zhou, J. Zhao, Z. Chen and P. V. R. Schleyer, Atomic and electronic structures of fluorinated BN nanotubes: computational study, *J. Phys. Chem. B*, 2006, **110**, 25678–25685.

43 C. Tang, Y. Bando, T. Sato and K. Kurashima, Uniform boron nitride coatings on silicon carbide nanowires, *Adv. Mater.*, 2002, **14**, 1046–1049.

44 W. S. Jang, S. Y. Kim, J. Lee, J. Park, C. J. Park and C. J. Lee, Triangular GaN–BN core–shell nanocables: synthesis and field emission, *Chem. Phys. Lett.*, 2006, **422**, 41–45.

45 L. W. Yin, Y. Bando, Y. C. Zhu, D. Golberg and M. S. Li, A Two-Stage Route to Coaxial Cubic–Aluminum–Nitride–Boron–Nitride Composite Nanotubes, *Adv. Mater.*, 2004, **16**, 929–933.

46 Y.-C. Zhu, Y. Bando, D.-F. Xue, F.-F. Xu and D. Golberg, Insulating tubular BN sheathing on semiconducting nanowires, *J. Am. Chem. Soc.*, 2003, **125**, 14226–14227.

47 K. Suenaga, C. Colliex, N. Demoncy, A. Loiseau, H. Pascard and F. Willaime, Synthesis of nanoparticles and nanotubes with well-separated layers of boron nitride and carbon, *Science*, 1997, **278**, 653–655.

48 N. P. Bansal, J. B. Hurst and S. R. Choi, Boron Nitride Nanotubes-Reinforced Glass Composites, *J. Am. Ceram. Soc.*, 2006, **89**, 388–390.

49 Q. Huang, Y. Bando, X. Xu, T. Nishimura, C. Zhi, C. Tang, F. Xu, L. Gao and D. Golberg, Enhancing superplasticity of engineering ceramics by introducing BN nanotubes, *Nanotechnology*, 2007, **18**, 485706.

50 A. Leela Mohana Reddy, A. E. Tanur and G. C. Walker, Synthesis and hydrogen storage properties of different types of boron nitride nanostructures, *Int. J. Hydrogen Energy*, 2010, **35**, 4138–4143.

51 G. Mpourmpakis and G. E. Froudakis, Why boron nitride nanotubes are preferable to carbon nanotubes for hydrogen storage?: An *ab initio* theoretical study, *Catal. Today*, 2007, **120**, 341–345.

52 S. Hu, E.-J. Kan and J. Yang, First-principles study of interaction between H molecules and BN nanotubes with BN divacancies, *J. Chem. Phys.*, 2007, **127**, 164718.

53 S. Shevlin and Z. Guo, Hydrogen sorption in defective hexagonal BN sheets and BN nanotubes, *Phys. Rev. B: Condens. Matter Mater. Phys.*, 2007, **76**, 024104.

54 E. Durgun, Y.-R. Jang and S. Ciraci, Hydrogen storage capacity of Ti-doped boron-nitride and B/Be-substituted

carbon nanotubes, *Phys. Rev. B: Condens. Matter Mater. Phys.*, 2007, **76**, 073413.

55 B.-C. Wang, M.-H. Tsai and Y.-M. Chou, Comparative theoretical study of carbon nanotubes and boron-nitride nanotubes, *Synth. Met.*, 1997, **86**, 2379–2380.

56 T. Oku, N. Koi and K. Suganuma, Electronic and optical properties of boron nitride nanotubes, *J. Phys. Chem. Solids*, 2008, **69**, 1228–1231.

57 H. Chen, Y. Chen, C. P. Li, H. Zhang, J. S. Williams, Y. Liu, Z. Liu and S. P. Ringer, Eu-doped Boron Nitride Nanotubes as a Nanometer Sized Visible Light Source, *Adv. Mater.*, 2007, **19**, 1845–1848.

58 B. Berzina, L. Trinkler, V. Korsak, R. Krutohvostov, D. Carroll, K. Ucer and R. Williams, Exciton luminescence of boron nitride nanotubes and nano arches, *Phys. Status Solidi B*, 2006, **243**, 3840–3845.

59 W.-Q. Han, H.-G. Yu, C. Zhi, J. Wang, Z. Liu, T. Sekiguchi and Y. Bando, Isotope effect on band gap and radiative transitions properties of boron nitride nanotubes, *Nano Lett.*, 2008, **8**, 491–494.

60 H. Chen, Y. Chen, Y. Liu, C.-N. Xu and J. S. Williams, Light emission and excitonic effect of boron nitride nanotubes observed by photoluminescent spectra, *Opt. Mater.*, 2007, **29**, 1295–1298.

61 M. Silly, P. Jaffrennou, J. Barjon, J.-S. Lauret, F. Ducastelle, A. Loiseau, E. Obraztsova, B. Attal-Tretout and E. Rosencher, Luminescence properties of hexagonal boron nitride: cathodoluminescence and photoluminescence spectroscopy measurements, *Phys. Rev. B: Condens. Matter Mater. Phys.*, 2007, **75**, 085205.

62 R. B. Chen, F. L. Shyu, C. P. Chang and M. F. Lin, Optical properties of boron nitride nanotubes, *J. Phys. Soc. Jpn.*, 2002, **71**, 2286–2289.

63 P. Jaffrennou, J. Barjon, J. S. Lauret, A. Maguer, D. Golberg, B. Attal Trétout, F. Ducastelle and A. Loiseau, Optical properties of multiwall boron nitride nanotubes, *Phys. Status Solidi B*, 2007, **244**, 4147–4151.

64 B. Berzina, L. Trinkler, R. Krutohvostov, R. Williams, D. Carroll, R. Czerw and E. Shishonok, Photoluminescence excitation spectroscopy in boron nitride nanotubes compared to microcrystalline h-BN and c-BN, *Phys. Status Solidi C*, 2005, **2**, 318–321.

65 G. Ciofani, V. Raffa, A. Menciassi and A. Cuschieri, Cytocompatibility, interactions, and uptake of polyethyleneimine coated boron nitride nanotubes by living cells: confirmation of their potential for biomedical applications, *Biotechnol. Bioeng.*, 2008, **101**, 850–858.

66 G. Ciofani, V. Raffa, A. Menciassi and P. Dario, Preparation of boron nitride nanotubes aqueous dispersions for biological applications, *J. Nanosci. Nanotechnol.*, 2008, **8**, 6223–6231.

67 G. Ciofani, V. Raffa, A. Menciassi and A. Cuschieri, Boron nitride nanotubes: an innovative tool for nanomedicine, *Nano Today*, 2009, **4**, 8–10.

68 G. Ciofani, V. Raffa, J. Yu, Y. Chen, Y. Obata, S. Takeoka, A. Menciassi and A. Cuschieri, Boron nitride nanotubes: a novel vector for targeted magnetic drug delivery, *Curr. Nanosci.*, 2009, **5**, 33–38.

69 X. Chen, P. Wu, M. Rousseas, D. Okawa, Z. Gartner, A. Zettl and C. R. Bertozzi, Boron Nitride Nanotubes are Noncytotoxic and can be Functionalized for Interaction with Proteins and Cells, *J. Am. Chem. Soc.*, 2009, **131**, 890–891.

70 G. Ciofani, S. Danti, D. D'Alessandro, L. Ricotti, S. Moscato, G. Bertoni, A. Falqui, S. Berrettini, M. Petrini and V. Mattoli, Enhancement of neurite outgrowth in neuronal-like cells following boron nitride nanotube-mediated stimulation, *ACS Nano*, 2010, **4**, 6267–6277.

71 J. Wang, C. H. Lee and Y. K. Yap, Recent advancements in boron nitride nanotubes, *Nanoscale*, 2010, **2**, 2028–2034.

72 M. Liao and Y. Koide, Carbon-based materials: growth, properties, MEMS/NEMS technologies, and MEM/NEM switches, *Crit. Rev. Solid State Mater. Sci.*, 2011, **36**, 66–101.

73 P. Ahmad, M. U. Khandaker, Z. R. Khan and Y. M. Amin, A simple technique to synthesize pure and highly crystalline boron nitride nanowires, *Ceram. Int.*, 2014, **40**, 14727–14732.

74 J. Li, R. Dahal, S. Majety, J. Lin and H. Jiang, Hexagonal boron nitride epitaxial layers as neutron detector materials, *Nucl. Instrum. Methods Phys. Res., Sect. A*, 2011, **654**, 417–420.

75 P. Ahmad, M. U. Khandaker and Y. M. Amin, Synthesis of highly crystalline multilayers structures of 10BNNTs as a potential neutron sensing element, *Ceram. Int.*, 2015, **41**, 4544–4548.

76 P. Ahmad, N. M. Mohamed and Z. A. Burhanudin, A review of nanostructured based radiation sensors for neutron, in *AIP Conference Proceedings*, 2012, p. 535.

77 A. M. Cassell, J. A. Raymakers, J. Kong and H. Dai, Large scale CVD synthesis of single-walled carbon nanotubes, *J. Phys. Chem. B*, 1999, **103**, 6484–6492.

78 C. J. Lee, D. W. Kim, T. J. Lee, Y. C. Choi, Y. S. Park, Y. H. Lee, W. B. Choi, N. S. Lee, G.-S. Park and J. M. Kim, Synthesis of aligned carbon nanotubes using thermal chemical vapor deposition, *Chem. Phys. Lett.*, 1999, **312**, 461–468.

79 O. R. Lourie, C. R. Jones, B. M. Bartlett, P. C. Gibbons, R. S. Ruoff and W. E. Buhro, CVD growth of boron nitride nanotubes, *Chem. Mater.*, 2000, **12**, 1808–1810.

80 C. Tang, Y. Bando, T. Sato and K. Kurashima, A novel precursor for synthesis of pure boron nitride nanotubes, *Chem. Commun.*, 2002, 1290–1291.

81 C. Zhi, Y. Bando, C. Tan and D. Golberg, Effective precursor for high yield synthesis of pure BN nanotubes, *Solid State Commun.*, 2005, **135**, 67–70.

82 R. S. Wagner and W. C. Ellis, Vapor Liquid Solid Mechanism of Single Crystal Growth, *Appl. Phys. Lett.*, 1964, **4**, 89–90.

83 A. Pakdel, C. Zhi, Y. Bando, T. Nakayama and D. Golberg, A comprehensive analysis of the CVD growth of boron nitride nanotubes, *Nanotechnology*, 2012, **23**, 215601.

84 C. H. Lee, J. Wang, V. K. Kayatsha, J. Y. Huang and Y. K. Yap, Effective growth of boron nitride nanotubes by thermal

chemical vapor deposition, *Nanotechnology*, 2008, **19**, 455605.

85 P. Ahmad, M. U. Khandaker and Y. M. Amin, Synthesis of boron nitride nanotubes by argon supported thermal chemical vapor deposition, *Phys. E*, 2015, **67**, 33–37.

86 I. Narita and T. Oku, Synthesis of boron nitride nanotubes by using YB_6 powder, *Solid State Commun.*, 2002, **122**, 465–468.

87 A. Loiseau, F. Willaime, N. Demoncy, G. Hug and H. Pascard, Boron nitride nanotubes with reduced numbers of layers synthesized by arc discharge, *Phys. Rev. Lett.*, 1996, **76**, 4737.

88 A. Loiseau, F. Willaime, N. Demoncy, N. Schramchenko, G. Hug, C. Colliex and H. Pascard, Boron nitride nanotubes, *Carbon*, 1998, **36**, 743–752.

89 J. Cumings and A. Zettl, Mass-production of boron nitride double-wall nanotubes and nanococoons, *Chem. Phys. Lett.*, 2000, **316**, 211–216.

90 D. Goldberg, Y. Bando, M. Eremets, K. Takemura, K. Kurashima, K. Tamiya and H. Yusa, Boron nitride nanotube growth defects and their annealing-out under electron irradiation, *Chem. Phys. Lett.*, 1997, **279**, 191–196.

91 R. Arenal, O. Stephan, J. L. Cochon and A. Loiseau, Root-growth mechanism for single-walled boron nitride nanotubes in laser vaporization technique, *J. Am. Chem. Soc.*, 2007, **129**, 16183–16189.

92 D. Golberg, A. Rode, Y. Bando, M. Mitome, E. Gamaly and B. Luther-Davies, Boron nitride nanostructures formed by ultra-high-repetition rate laser ablation, *Diamond Relat. Mater.*, 2003, **12**, 1269–1274.

93 D. Golberg, Y. Bando, M. Eremets, K. Takemura, K. Kurashima and H. Yusa, Nanotubes in boron nitride laser heated at high pressure, *Appl. Phys. Lett.*, 1996, **69**, 2045–2047.

94 G. W. Zhou, Z. Zhang, Z. G. Bai and D. P. Yu, Catalyst effects on formation of boron nitride nano-tubules synthesized by laser ablation, *Solid State Commun.*, 1999, **109**, 555–559.

95 D. Golberg, Y. Bando, M. Eremets, K. Kurashima, T. Tamiya, K. Takemura and H. Yusa, High-resolution analytical electron microscopy of boron nitrides laser heated at high pressure, *J. Electron Microsc.*, 1997, **46**, 281–292.

96 M. Cau, N. Dorval, B. Attal-Trétout, J. Cochon, B. Cao, L. Bresson, P. Jaffrennou, M. Silly, A. Loiseau and E. Obraztsova, LASER-based diagnostics applied to the study of BN nanotubes synthesis, *J. Nanosci. Nanotechnol.*, 2008, **8**, 6129–6140.

97 S. Komatsu, Y. Shimizu, Y. Moriyoshi, K. Okada and M. Mitomo, Preparation of boron nitride nanocapsules by plasma-assisted pulsed laser deposition, *J. Appl. Phys.*, 2002, **91**, 6181–6184.

98 V. Naumov, F. Kosyrev, V. Vostrikov, N. Arutyunyan, E. Obraztsova, V. Konov, H. Jiang, A. Nasibulin and E. Kauppinen, Synthesis of boron nitride multi-walled nanotubes by laser ablation technique, *Laser Phys.*, 2009, **19**, 1198–1200.

99 M. W. Smith, K. C. Jordan, C. Park, J.-W. Kim, P. T. Lillehei, R. Crooks and J. S. Harrison, Very long single-and few-walled boron nitride nanotubes via the pressurized vapor/condenser method, *Nanotechnology*, 2009, **20**, 505604.

100 Y. Wang, Y. Yamamoto, H. Kiyono and S. Shimada, Highly ordered boron nitride nanotube arrays with controllable texture from ammonia borane by template-aided vapor-phase pyrolysis, *J. Nanomater.*, 2008, **2008**, 72.

101 D. Golberg, Y. Bando, M. Mitome, K. Kurashima, T. Sato, N. Grobert, M. Reyes-Reyes, H. Terrones and M. Terrones, Preparation of aligned multi-walled BN and B/C/N nanotubular arrays and their characterization using HRTEM, EELS and energy-filtered TEM, *Phys. B*, 2002, **323**, 60–66.

102 D. Golberg, Y. Bando, K. Kurashima and T. Sato, Ropes of BN multi-walled nanotubes, *Solid State Commun.*, 2000, **116**, 1–6.

103 W. Han, P. Redlich, F. Ernst and M. Rühle, Synthesizing boron nitride nanotubes filled with SiC nanowires by using carbon nanotubes as templates, *Appl. Phys. Lett.*, 1999, **75**, 1875–1877.

104 X. Wang, Q. Wu, Z. Hu and Y. Chen, Template-directed synthesis of boron nitride nanotube arrays by microwave plasma chemical reaction, *Electrochim. Acta*, 2007, **52**, 2841–2844.

105 W.-Q. Han, W. Mickelson, J. Cumings and A. Zettl, Transformation of $B_xC_yN_z$ nanotubes to pure BN nanotubes, *Appl. Phys. Lett.*, 2002, **81**, 1110–1112.

106 K. B. Shelimov and M. Moskovits, Composite nanostructures based on template-grown boron nitride nanotubules, *Chem. Mater.*, 2000, **12**, 250–254.

107 Y. Wang, S. Shimada, Y. Yamamoto and N. Miyaura, Preparation of h-BN nano-tubes, -bamboos, and-fibers from borazine oligomer with alumina porous template, *Mater. Res. Bull.*, 2008, **43**, 251–256.

108 M. Bechelany, S. Bernard, A. Brioude, D. Cornu, P. Stadelmann, C. Charcosset, K. Fiaty and P. Miele, Synthesis of boron nitride nanotubes by a template-assisted polymer thermolysis process, *J. Phys. Chem. C*, 2007, **111**, 13378–13384.

109 W. Han, Y. Bando, K. Kurashima and T. Sato, Synthesis of boron nitride nanotubes from carbon nanotubes by a substitution reaction, *Appl. Phys. Lett.*, 1998, **73**, 3085.

110 F. L. Deepak, C. Vinod, K. Mukhopadhyay, A. Govindaraj and C. Rao, Boron nitride nanotubes and nanowires, *Chem. Phys. Lett.*, 2002, **353**, 345–352.

111 W. Q. Han, P. J. Todd and M. Strongin, Formation and growth mechanism of BN nanotubes via a carbon nanotube-substitution reaction, *Appl. Phys. Lett.*, 2006, **89**, 173103.

112 J. Q. Bi, W. L. Wang, Y. X. Qi, Y. J. Bai, L. L. Pang, H. L. Zhu, Y. Zhao and Y. Wang, Large-scale synthesis of BN nanotubes using carbon nanotubes as template, *Mater. Lett.*, 2009, **63**, 1299–1302.

113 D. Golberg, Y. Bando, K. Kurashima and T. Sato, MoO_3-promoted synthesis of multi-walled BN nanotubes from C nanotube templates, *Chem. Phys. Lett.*, 2000, **323**, 185–191.

114 J. Dai, L. Xu, Z. Fang, D. Sheng, Q. Guo, Z. Ren, K. Wang and Y. Qian, A convenient catalytic approach to synthesize straight boron nitride nanotubes using synergic nitrogen source, *Chem. Phys. Lett.*, 2007, **440**, 253–258.

115 G. Rosas, J. Sistos, J. Ascencio, A. Medina and R. Pérez, Múltiple-walled BN nanotubes obtained with a mechanical alloying technique, *Appl. Phys. A: Mater. Sci. Process.*, 2005, **80**, 377–380.

116 L. Xu, Y. Peng, Z. Meng, W. Yu, S. Zhang, X. Liu and Y. Qian, A co-pyrolysis method to boron nitride nanotubes at relative low temperature, *Chem. Mater.*, 2003, **15**, 2675–2680.

117 P. Cai, L. Chen, L. Shi, Z. Yang, A. Zhao, Y. Gu, T. Huang and Y. Qian, One convenient synthesis route to boron nitride nanotube, *Solid State Commun.*, 2005, **133**, 621–623.

118 Y. Chen, L. T. Chadderton, J. F. Gerald and J. S. Williams, A solid-state process for formation of boron nitride nanotubes, *Appl. Phys. Lett.*, 1999, **74**, 2960–2962.

119 J. Yu, Y. Chen, R. Wuhrer, Z. Liu and P. Simon, *In situ* formation of BN nanotubes during nitriding reactions, *Chem. Mater.*, 2005, **17**, 5172–5176.

120 Y. Chen, M. Conway, J. Williams and J. Zou, Large-quantity production of high-yield boron nitride nanotubes, *J. Mater. Res.*, 2002, **17**, 1896–1899.

121 H. Chen, Y. Chen, Y. Liu, L. Fu, C. Huang and D. Llewellyn, Over 1.0 mm-long boron nitride nanotubes, *Chem. Phys. Lett.*, 2008, **463**, 130–133.

122 S. Singhal, A. Srivastava, R. Pant, S. Halder, B. Singh and A. K. Gupta, Synthesis of boron nitride nanotubes employing mechanothermal process and its characterization, *J. Mater. Sci.*, 2008, **43**, 5243–5250.

123 L. Li, C. P. Li and Y. Chen, Synthesis of boron nitride nanotubes, bamboos and nanowires, *Phys. E*, 2008, **40**, 2513–2516.

124 S. Yong Bae, H. Won Seo, J. Park, Y. Sang Choi, J. Chul Park and S. Young Lee, Boron nitride nanotubes synthesized in the temperature range 1000–1200 °C, *Chem. Phys. Lett.*, 2003, **374**, 534–541.

125 Y. Chen, J. Fitz Gerald, J. Williams and S. Bulcock, Synthesis of boron nitride nanotubes at low temperatures using reactive ball milling, *Chem. Phys. Lett.*, 1999, **299**, 260–264.

126 T. Terao, Y. Bando, M. Mitome, K. Kurashima, C. Zhi, C. Tang and D. Golberg, Effective synthesis of surface-modified boron nitride nanotubes and related nanostructures and their hydrogen uptake, *Phys. E*, 2008, **40**, 2551–2555.

127 C. Tang, Y. Bando and T. Sato, Catalytic growth of boron nitride nanotubes, *Chem. Phys. Lett.*, 2002, **362**, 185–189.

128 M. J. Kim, S. Chatterjee, S. M. Kim, E. A. Stach, M. G. Bradley, M. J. Pender, L. G. Sneddon and B. Maruyama, Double-walled boron nitride nanotubes grown by floating catalyst chemical vapor deposition, *Nano Lett.*, 2008, **8**, 3298–3302.

129 C. Tang, X. Ding, X. Huang, Z. Gan, S. Qi, W. Liu and S. Fan, Effective growth of boron nitride nanotubes, *Chem. Phys. Lett.*, 2002, **356**, 254–258.

130 Z. Gan, X. Ding, Z. Huang, X. Huang, C. Cheng, C. Tang and S. Qi, Growth of boron nitride nanotube film *in situ*, *Appl. Phys. A: Mater. Sci. Process.*, 2005, **81**, 527–529.

131 J. Wang, V. K. Kayastha, Y. K. Yap, Z. Fan, J. G. Lu, Z. Pan, I. N. Ivanov, A. A. Puretzky and D. B. Geohegan, Low temperature growth of boron nitride nanotubes on substrates, *Nano Lett.*, 2005, **5**, 2528–2532.

132 C. Tang, Y. Bando and D. Golberg, Multi-walled BN nanotubes synthesized by carbon-free method, *J. Solid State Chem.*, 2004, **177**, 2670–2674.

133 M. Bechelany, A. Brioude, P. Stadelmann, S. Bernard, D. Cornu and P. Miele, Preparation of BN microtubes/nanotubes with a unique chemical process, *J. Phys. Chem. C*, 2008, **112**, 18325–18330.

134 M. Terauchi, M. Tanaka, K. Suzuki, A. Ogino and K. Kimura, Production of zigzag-type BN nanotubes and BN cones by thermal annealing, *Chem. Phys. Lett.*, 2000, **324**, 359–364.

135 L. Guo and R. Singh, Selective growth of boron nitride nanotubes by plasma-enhanced chemical vapor deposition at low substrate temperature, *Nanotechnology*, 2008, **19**, 065601.

136 R. Sen, B. Satishkumar, A. Govindaraj, K. Harikumar, G. Raina, J.-P. Zhang, A. Cheetham and C. Rao, B–C–N, C–N and B–N nanotubes produced by the pyrolysis of precursor molecules over Co catalysts, *Chem. Phys. Lett.*, 1998, **287**, 671–676.

137 L. Cao, X. Zhang, H. Tian, Z. Zhang and W. Wang, Boron nitride nanotube branched nanojunctions, *Nanotechnology*, 2007, **18**, 155605.

138 T. Oku, N. Koi, K. Suganuma, R. V. Belosludov and Y. Kawazoe, Formation and atomic structure of boron nitride nanotubes with a cup-stacked structure, *Solid State Commun.*, 2007, **143**, 331–336.

139 T. Oku, N. Koi and K. Suganuma, Synthesis and nanostructure of boron nitride nanotubes grown from iron-evaporated boron, *Diamond Relat. Mater.*, 2008, **17**, 1805–1807.

140 J. Fu, Y. Lu, H. Xu, K. Huo, X. Wang, L. Li, Z. Hu and Y. Chen, The synthesis of boron nitride nanotubes by an extended vapour–liquid–solid method, *Nanotechnology*, 2004, **15**, 727.

141 C. Tang, Y. Bando, X. Ding, S. Qi and D. Golberg, Catalyzed collapse and enhanced hydrogen storage of BN nanotubes, *J. Am. Chem. Soc.*, 2002, **124**, 14550–14551.

142 A. Ganguly, S. Chattopadhyay, K.-H. Chen and L.-C. Chen, Production and Storage of Energy with One-Dimensional Semiconductor Nanostructures, *Crit. Rev. Solid State Mater. Sci.*, 2014, **39**, 109–153.

143 J. Kong, A. M. Cassell and H. Dai, Chemical vapor deposition of methane for single-walled carbon nanotubes, *Chem. Phys. Lett.*, 1998, **292**, 567–574.

144 M. Su, B. Zheng and J. Liu, A scalable CVD method for the synthesis of single-walled carbon nanotubes with high catalyst productivity, *Chem. Phys. Lett.*, 2000, **322**, 321–326.

145 E. Couteau, K. Hernadi, J. W. Seo, L. Thien-Nga, C. Mikó, R. Gaal and L. Forro, CVD synthesis of high-purity

multiwalled carbon nanotubes using $CaCO_3$ catalyst support for large-scale production, *Chem. Phys. Lett.*, 2003, **378**, 9–17.

146 K.-E. Kim, K.-J. Kim, W. S. Jung, S. Y. Bae, J. Park, J. Choi and J. Choo, Investigation on the temperature-dependent growth rate of carbon nanotubes using chemical vapor deposition of ferrocene and acetylene, *Chem. Phys. Lett.*, 2005, **401**, 459–464.

147 C. Tang, M. Lamy de la Chapelle, P. Li, Y. Liu, H. Dang and S. Fan, Catalytic growth of nanotube and nanobamboo structures of boron nitride, *Chem. Phys. Lett.*, 2001, **342**, 492–496.

148 D. Golberg, Y. Bando, C. Tang and C. Zhi, Functional boron nitride nanotubes, in *Nanoelectronics Conference (INEC), 2010 3rd International*, IEEE, 2010, pp. 47–48.

149 Y. Huang, J. Lin, C. Tang, Y. Bando, C. Zhi, T. Zhai, B. Dierre, T. Sekiguchi and D. Golberg, Bulk synthesis, growth mechanism and properties of highly pure ultrafine boron nitride nanotubes with diameters of sub-10 nm, *Nanotechnology*, 2011, **22**, 145602.

150 L. Li, X. Liu, L. H. Li and Y. Chen, High yield BNNTs synthesis by promotion effect of milling-assisted precursor, *Microelectron. Eng.*, 2013, **110**, 256–259.

151 C. Zhi, Y. Bando, C. Tang, S. Honda, H. Kuwahara and D. Golberg, Boron nitride nanotubes/polystyrene composites, *J. Mater. Res.*, 2006, **21**, 2794–2800.

152 M. Yamaguchi, D.-M. Tang, C. Zhi, Y. Bando, D. Shtansky and D. Golberg, Synthesis, structural analysis and *in situ* transmission electron microscopy mechanical tests on individual aluminum matrix/boron nitride nanotube nanohybrids, *Acta Mater.*, 2012, **60**, 6213–6222.

153 D. Golberg, P. M. Costa, O. Lourie, M. Mitome, X. Bai, K. Kurashima, C. Zhi, C. Tang and Y. Bando, Direct force measurements and kinking under elastic deformation of individual multiwalled boron nitride nanotubes, *Nano Lett.*, 2007, **7**, 2146–2151.

154 X. Wei, M. S. Wang, Y. Bando and D. Golberg, Tensile Tests on Individual Multi-Walled Boron Nitride Nanotubes, *Adv. Mater.*, 2010, **22**, 4895–4899.

155 M. Yamaguchi, A. Pakdel, C. Zhi, Y. Bando, D.-M. Tang, K. Faerstein, D. Shtansky and D. Golberg, Utilization of multiwalled boron nitride nanotubes for the reinforcement of lightweight aluminum ribbons, *Nanoscale Res. Lett.*, 2013, **8**, 1–6.

156 V. K. Kayastha, S. Wu, J. Moscatello and Y. K. Yap, Synthesis of Vertically Aligned Single- and Double-Walled Carbon Nanotubes without Etching Agents, *J. Phys. Chem. C*, 2007, **111**, 10158–10161.

157 C. H. Lee, M. Xie, V. Kayastha, J. Wang and Y. K. Yap, Patterned growth of boron nitride nanotubes by catalytic chemical vapor deposition, *Chem. Mater.*, 2010, **22**, 1782–1787.

158 C. J. Lee, J. H. Park and J. Park, Synthesis of bamboo-shaped multiwalled carbon nanotubes using thermal chemical vapor deposition, *Chem. Phys. Lett.*, 2000, **323**, 560–565.

159 T. H. Ferreira, P. R. O. da Silva, R. G. dos Santos and E. M. B. de Sousa, A novel synthesis route to produce boron nitride nanotubes for bioapplications, *J. Biomater. Nanobiotechnol.*, 2011, **2**, 426–434.

160 D. Seo, J. Kim, S.-H. Park, Y.-U. Jeong, Y.-S. Seo, S.-H. Lee and J. Kim, Synthesis of boron nitride nanotubes using thermal chemical vapor deposition of ball milled boron powder, *J. Ind. Eng. Chem.*, 2012, **19**, 1117–1122.

161 D. Özmen, N. A. Sezgi and S. Balcı, Synthesis of Boron Nitride Nanotubes from Ammonia & a Powder Mixture of Boron & Iron Oxide, *Chem. Eng. J.*, 2012, **219**, 28–36.

162 R. Ma, Y. Bando and T. Sato, CVD synthesis of boron nitride nanotubes without metal catalysts, *Chem. Phys. Lett.*, 2001, **337**, 61–64.

163 R. Ma, Y. Bando, T. Sato and K. Kurashima, Thin boron nitride nanotubes with unusual large inner diameters, *Chem. Phys. Lett.*, 2001, **350**, 434–440.

164 R. Ma, Y. Bando, T. Sato and L. Bourgeois, Novel BN tassel-like and tree-like nanostructures, *Diamond Relat. Mater.*, 2002, **11**, 1397–1402.

165 C. Tang, Y. Bando, Y. Huang, S. Yue, C. Gu, F. Xu and D. Golberg, Fluorination and electrical conductivity of BN nanotubes, *J. Am. Chem. Soc.*, 2005, **127**, 6552–6553.

166 D. Golberg, Y. Bando, C. Tang and C. Zhi, Boron nitride nanotubes, *Adv. Mater.*, 2007, **19**, 2413–2432.

167 L. Guo and R. Singh, Catalytic growth of boron nitride nanotubes using gas precursors, *Phys. E*, 2009, **41**, 448–453.

168 C.-Y. Su, W.-Y. Chu, Z.-Y. Juang, K.-F. Chen, B.-M. Cheng, F.-R. Chen, K.-C. Leou and C.-H. Tsai, Large-scale synthesis of boron nitride nanotubes with iron-supported catalysts, *J. Phys. Chem. C*, 2009, **113**, 14732–14738.

169 R. Wagner and W. Ellis, Vapor liquid solid mechanism of single crystal growth, *Appl. Phys. Lett.*, 1964, **4**, 89–90.

170 C. Tang, Y. Bando and T. Sato, Synthesis and morphology of boron nitride nanotubes and nanohorns, *Appl. Phys. A: Mater. Sci. Process.*, 2002, **75**, 681–685.

171 C. Y. Zhi, Y. Bando, C. C. Tang, R. G. Xie, T. Sekiguchi and D. Golberg, Perfectly dissolved boron nitride nanotubes due to polymer wrapping, *J. Am. Chem. Soc.*, 2005, **127**, 15996–15997.

172 C. Zhi, Y. Bando, C. Tang, S. Honda, K. Sato, H. Kuwahara and D. Golberg, Covalent Functionalization: Towards Soluble Multiwalled Boron Nitride Nanotubes, *Angew. Chem., Int. Ed.*, 2005, **44**, 7932–7935.

173 C. Y. Zhi, Y. Bando, C. C. Tang, S. Honda, K. Sato, H. Kuwahara and D. Golberg, Purification of boron nitride nanotubes through polymer wrapping, *J. Phys. Chem. B*, 2006, **110**, 1525–1528.

174 C. Zhi, Y. Bando, C. Tang, D. Golberg, R. Xie and T. Sekiguchi, Large-scale fabrication of boron nitride nanohorn, *Appl. Phys. Lett.*, 2005, **87**, 063107.

175 W. Meng, Y. Huang, Y. Fu, Z. Wang and C. Zhi, Polymer composites of boron nitride nanotubes and nanosheets, *J. Mater. Chem. C*, 2014, **2**, 10049–10061.

176 B. Saner Okan, Z. L. O. Z. Kocabaş, A. Nalbant Ergün, M. Baysal, I. Letofsky-Papst and Y. Yürüm, Effect of Reaction Temperature and Catalyst Type on the

Formation of Boron Nitride Nanotubes by Chemical Vapor Deposition and Measurement of their Hydrogen Storage Capacity, *Ind. Eng. Chem. Res.*, 2012, **51**, 11341–11347.

177 R. Ma, Y. Bando, T. Sato and K. Kurashima, Growth, morphology, and structure of boron nitride nanotubes, *Chem. Mater.*, 2001, **13**, 2965–2971.

178 L. Bourgeois, Y. Bando and T. Sato, Tubes of rhombohedral boron nitride, *J. Phys. D: Appl. Phys.*, 2000, **33**, 1902.

179 T. Ishii, T. Sato, Y. Sekikawa and M. Iwata, Growth of whiskers of hexagonal boron nitride, *J. Cryst. Growth*, 1981, **52**, 285–289.

180 I. Willems, Z. Konya, J.-F. Colomer, G. Van Tendeloo, N. Nagaraju, A. Fonseca and J. Nagy, Control of the outer diameter of thin carbon nanotubes synthesized by catalytic decomposition of hydrocarbons, *Chem. Phys. Lett.*, 2000, **317**, 71–76.

181 R. Ma, D. Golberg, Y. Bando and T. Sasaki, Syntheses and properties of B–C–N and BN nanostructures, *Philos. Trans. R. Soc., A*, 2004, **362**, 2161–2186.

182 H. Dai, A. G. Rinzler, P. Nikolaev, A. Thess, D. T. Colbert and R. E. Smalley, Single-wall nanotubes produced by metal-catalyzed disproportionation of carbon monoxide, *Chem. Phys. Lett.*, 1996, **260**, 471–475.

183 S. Sinnott, R. Andrews, D. Qian, A. Rao, Z. Mao, E. Dickey and F. Derbyshire, Model of carbon nanotube growth through chemical vapor deposition, *Chem. Phys. Lett.*, 1999, **315**, 25–30.

184 Z. Zhang, B. Wei, G. Ramanath and P. Ajayan, Substrate-site selective growth of aligned carbon nanotubes, *Appl. Phys. Lett.*, 2000, **77**, 3764–3766.

185 B. Wei, R. Vajtai, Z. Zhang, G. Ramanath and P. Ajayan, Carbon nanotube-magnesium oxide cube networks, *J. Nanosci. Nanotechnol.*, 2001, **1**, 35–38.

186 Y. C. Choi, Y. M. Shin, Y. H. Lee, B. S. Lee, G.-S. Park, W. B. Choi, N. S. Lee and J. M. Kim, Controlling the diameter, growth rate, and density of vertically aligned carbon nanotubes synthesized by microwave plasma-enhanced chemical vapor deposition, *Appl. Phys. Lett.*, 2000, **76**, 2367–2369.

187 L. Ci, L. Song, C. Jin, D. Jariwala, D. Wu, Y. Li, A. Srivastava, Z. Wang, K. Storr and L. Balicas, Atomic layers of hybridized boron nitride and graphene domains, *Nat. Mater.*, 2010, **9**, 430–435.

188 L. Song, L. Ci, H. Lu, P. B. Sorokin, C. Jin, J. Ni, A. G. Kvashnin, D. G. Kvashnin, J. Lou and B. I. Yakobson, Large scale growth and characterization of atomic hexagonal boron nitride layers, *Nano Lett.*, 2010, **10**, 3209–3215.

189 Y. Shi, C. Hamsen, X. Jia, K. K. Kim, A. Reina, M. Hofmann, A. L. Hsu, K. Zhang, H. Li and Z.-Y. Juang, Synthesis of few-layer hexagonal boron nitride thin film by chemical vapor deposition, *Nano Lett.*, 2010, **10**, 4134–4139.

190 K. K. Kim, A. Hsu, X. Jia, S. M. Kim, Y. Shi, M. Hofmann, D. Nezich, J. F. Rodriguez-Nieva, M. Dresselhaus and T. Palacios, Synthesis of monolayer hexagonal boron nitride on Cu foil using chemical vapor deposition, *Nano Lett.*, 2011, **12**, 161–166.

191 P. Ahmad, M. U. Khandaker, Y. M. Amin and N. Muhammad, Synthesis and characterization of boron nitride microtubes, *Mater. Express*, 2015, **5**, 249–254.

192 P. Ahmad, M. Khandaker and Y. Amin, Simple technique to synthesise vertically aligned boron nitride nanosheets at 1200 °C, *Adv. Appl. Ceram.*, 2014, DOI: 10.1179/1743676114y.0000000225.

CHAPTER 3

PUBLICATIONS

3.1 Contributions of Authors

The author of current thesis, I am (Pervaiz Ahmad) the main author of all the published papers. As a main author, I designed the experimental set up, carried out all the experimental work, characterized the as-synthesized products, analyzed and interpreted the as-characterized results and wrote manuscripts for publications. All the co-authors have significant contributions in the published work. The contributions of each co-author are described as follows:

Associate Professor Dr. Mayeen Uddin Khandaker and Professor Dr. Yusoff Mohd Amin supervised the current research work. Associate Professor Dr. Mayeen Uddin Khandaker helped in the development of experimental set up and ideas for the synthesis of h-BN nanostructures (BNNTs, ^{10}BNNTs, BNNWs, BNMTs and BNNS etc.) whereas Professor Dr. Yusoff Mohd Amin provided the concepts and logics for the Argon-supported thermal CVD and optimizing experimental parameters for the synthesis of BNNTs, ^{10}BNNTs, BNNWs, BNMTs and BNNS etc. Dr. Ziaul Raza Khan helped in the editing, formation and technical review of Paper 1, 6 and 8 before submission to the journal whereas Dr. Nawshad Muhammed provided technical assistance in drawing and explaining the wide scan B 1s and N 1s XPS spectra in paper 7. Associate Professor Dr. Mayeen Uddin Khandaker and Professor Dr. Yusoff Mohd Amin helped in explaining the results, writing, editing and reviewing all the papers before their submission to the journals and also provided guidance and expertise for reviewer's comments before acceptance of all the papers.

3.2 Publications

A list of eight research publications is given in the following. All these publications have collectively contributed to achieve the main goals and objectives of the current thesis. The author of this thesis (Pervaiz Ahmad) is the first author of all the publications. A brief description of the contents of each of these publications is already given in Chapter 1, section 1.3.

Publication 2nd is the reprint of our paper, "Synthesis of boron nitride nanotubes by Argon supported Thermal Chemical Vapor Deposition" as it published in *Physica E: Low-dimensional Systems and Nanostructures, Volume 67, 2015, pages 33-37,* authored by P. Ahmad, M.U. Khandaker and Y.M. Amin.

Publication 3rd is the reprint of our paper, "A comprehensive study of boron nitride nanotubes multiple synthesis from a single precursor" as it published in *Indian Journal of Physics, Volume* 89, *2015, pages 209-216,* authored by P. Ahmad, M.U. Khandaker and Y.M. Amin.

Publication 4th is the reprint of our paper, "Effective Synthesis of Vertically Aligned Boron Nitride Nanotubes via a Simple CCVD" as it published in *Materials and Manufacturing Processes,* 2014, authored by P. Ahmad, M.U. Khandaker and Y.M. Amin.

Publication 5th is the reprint of our paper, "Synthesis of highly crystalline multilayers structures of ^{10}BNNTs as a potential neutron sensing element" as it published in *Ceramics International, Volume 41, Issue 3, part B, 2015, pages 4544-4548,* authored by P. Ahmad, M.U. Khandaker and Y.M. Amin.

Publication 6th is the reprint of our paper, “A simple technique to synthesize pure and highly crystalline boron nitride nanowires” as it published in *Ceramics International*, *Volume 40, Issue 9, part B, 2015, pages 14727-14732*, authored by P. Ahmad, M.U. Khandaker, Z.R. Khan and Y.M. Amin.

Publication 7th is the reprint of our paper, “Synthesis and characterization of boron nitride microtubes” as it published in *Materials Express*, *Volume 5, Issue 3, 2015, pages 249-254*, authored by P. Ahmad, M.U. Khandaker, Y.M. Amin and N. Muhammad.

Publication 8th is the reprint of our paper, “Synthesis of Boron Nitride Microtubes and Formation of Boron Nitride Nanosheets” as it published in *Materials and Manufacturing Processes*, *Volume* 30, *Issue 2*, *2014*, *pages 184-188*, authored by P. Ahmad, M.U. Khandaker, Y.M. Amin and Z R. Khan .

Publication 9th is the reprint of our paper, “A simple technique to synthesise vertically aligned boron nitride nanosheets at 1200° C” as it published in *Advances in Applied Ceramics*, *Volume* 114, *Issue 5, 2015*, *pages 267-272*, authored by P. Ahmad, M.U. Khandaker and Y.M. Amin.

Physica E 67 (2015) 33–37

Contents lists available at ScienceDirect

Physica E

journal homepage: www.elsevier.com/locate/physe

Synthesis of boron nitride nanotubes by Argon supported Thermal Chemical Vapor Deposition

Pervaiz Ahmad, Mayeen Uddin Khandaker*, Yusoff Mohd Amin

Department of Physics, Faculty of Science, University of Malaya, 50603 Kuala Lumpur, Malaysia

GRAPHICAL ABSTRACT

The use of Ar gas as a reaction atmosphere has made BNNTs synthesis easy and ~ 18 % cost effective as compare to any other technique.

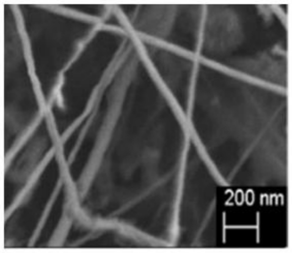

ARTICLE INFO

Article history:
Received 12 August 2014
Received in revised form
15 October 2014
Accepted 7 November 2014
Available online 11 November 2014

Keywords:
Argon supported thermal CVD
BN
Longer BNNTs
Cost effective experimental set up

ABSTRACT

Thermal Chemical Vapor Deposition technique is modified with the use of Argon gas flow inside the chamber as an alternative for vacuum and orientation of one end closed quartz test tube. The use of Argon gas not only simplified the experimental set up, but also made it ~ 18 % cost effective compared to the conventional set up. Field Emission Scanning Electron Microscopy micrographs show straight and long BNNTs along with some cotton like morphologies. Transmission electron microscopy revealed bamboo like structure inside the tube and ~0.34 nm interlayer spacing for highly crystalline nature of boron nitride nanotubes. X-ray photon spectroscopy shows B 1s peak at 191.08 eV and N 1s peak at 398.78 eV that represents h-BN. Whereas, Raman spectrum indicates a major peak at ~1379.60 (cm^{-1}) that correspond to E_{2g} mode of h-BN.

1. Introduction

Hexagonal boron nitride (h-BN) is a wide band gap semiconductor [1], with a direct band gap of 5.97 eV [2]. It is the normal phase of Boron Nitride (BN) that is stable at room temperature and pressure. Its structure is similar to that of graphite but alternative boron and nitrogen atoms substitutes for carbon atoms [1].

Boron Nitride Nanotubes (BNNTs) are the cylindrical structures of boron nitride having diameter in the range of below 100 nm and length up to several micrometers [3]. They were theoretically predicted in 1994 [4] and experimentally discovered in 1995 [5]. Their discovery has opened new ways for making devices with excellent properties. Properties of BNNTs are almost similar to Carbon Nanotubes (CNTs), however, CNTs can be conductor or semiconductor dependent on the chirality or helicity whereas, BNNTs are large band gap semiconductors independent of helicity [6].

---

* Corresponding author. Fax: +60 379674146.
E-mail addresses: mu_khandaker@yahoo.com, mu_khandaker@um.edu.my (M.U. Khandaker).

http://dx.doi.org/10.1016/j.physe.2014.11.003
1386-9477/© 2014 Elsevier B.V. All rights reserved.

BNNTs are found to be very useful material for different biomedical applications such as therapeutic or diagnostic due to its possible non-cytotoxic nature [7–9]. In boron nitride capture therapy, BNNTs are proposed to be the boron carriers. The BNNTs are first injected, and then transferred into the tumor cell, where it produces localized charged particles by the interaction of neutron beam from an external source. The as produced charge particles may then further be used to kill the tumor cells and cure the patient. The uniform distribution of Fe_3O_4 nanoparticles on the BNNTs surface introduced magnetic behavior in BNNTs. This behavior of BNNTs might be very useful in Micro-Electro Mechanical System (MEMS) and targeted drug delivery [10]. Moreover, BNNTs being nanostructure with improved properties can be effectively used as a neutron sensing element in a solid state neutron detector [11].

All these features and advantages of BNNTs for different application are dependent on its purity, size and alignment which in turn depend on the synthesis methods. The synthesis methods being used for BNNTs are Arc-discharge, Laser ablation, Template synthesis, Auto clave, Ball milling and Chemical vapor deposition using borazine as precursor [12]. However, all of these techniques either operate at higher temperature with complex and expensive experimental set up or require toxic and dangerous precursors. The BNNTs thus formed contained different materials as impurities. A major breakthrough, regarding the synthesis of pure BNNTs occurred with the development of Boron Oxide CVD (BOCVD) technique by Tang et al. [13]. This technique utilizes B, MgO and other metal oxides as precursors, and specially designed induction furnace with rapid heating and large temperature gradient as an experimental set up. The precursors are first heated at a temperature above 1300 °C. The B_xO_y vapors thus generated are transferred into the reaction area with the help of Ar (gas) career, where it reacts with NH_3 to form BNNTs [13]. Zhi et al. further developed the BOCVD technique with the introduction of B, MgO and FeO as an effective precursor [14]. Working on the same idea, Lee et al. [15] established thermal CVD technique for the synthesis of BNNTs. In this technique, induction furnace is replaced with a conventional horizontal tube furnace. Additionally, one end closed quartz test tube is used inside the chamber to get vapor trapped for growing of the BNNTs. During the experiment, the chamber is first evacuated to a certain level. Then, a 2:1:1 ratio of the precursor (B, MgO and FeO) is heated up to 1200 °C to form B_2O_2 vapors. At this temperature, NH_3 gas is introduced into the system. The B_2O_2 vapors react with NH_3 and form BNNTs [15]. The as-developed thermal CVD technique [15] is further applied for the pattern growth of the BNNTs by the same group. No change has been made in the previously used set up [15], except, the ratio of the precursors, growth duration, gases flow rates and nature of the substrate. Changes in these parameters with previously developed technique [15] was claimed to be used for controlled growth of the BNNTs [16]. Pakdel et al. studied the effects of precursor's ratios (1:1:1, 2:1:1 and 4:1:1) and temperature (1200, 1300 and 1400 °C) on the size and morphology of the BNNTs [17]. The major difference in their experimental set up and Lee et al. [16] was the use of inner quartz test tube. In the Lee et al. [16] work, the inner test tube used was closed at one end whereas the one used by Pakdel et al. was opened at both ends [17]. The use of both end opened inner quartz tube by Pakdel et al. [17] also denies the claim of Lee et al. [15] that BNNTs cannot be synthesized via their developed technique if the one end closed quartz tube is replaced with the one having both ends open. Both of these groups utilized vacuum or evacuation as a reaction atmosphere inside the chamber. The work of Pakdel et al. [17] on one side shows the effectiveness of thermal CVD technique for BNNTs growth, and on the other side suggests changes for further developments. To improve the quantity of the final product, Seo et al. [18] combined ball milling and annealing process (of the precursors) with thermal CVD (introduced by Lee et al. [15]). In their work, a mixer of milled precursors (B, MgO and FeO) was annealed in the presence of a gases mixer (N_2: 95% and NH_3: 5%) for 6 h. BNNTs were synthesized by the reaction of N_2 with solid phase of B. The production of impurities in the final product was a great concern. It was concluded that the quality of the final product can be improved by controlling the reaction parameters like: precursors, temperature and annealing time. Ozmen et al. [19] used thermal CVD with mass spectrometer, and synthesized BNNTs from the reaction of ammonia with powder mixer of boron and iron oxides in a wide temperature range of 900–1400 °C. Ar gas was used to purge the system before and after the experimental run. Also, during the experiment, Ar gas was used to remove the oxygen from the system [19]. Along with the lower quality of the final product, the as-used thermal CVD set up was a bit complex and expensive regarding the prices of mass spectrometer and arrangements for online analysis.

In the present study, thermal CVD technique [15] is further simplified with the use of Ar inert gas as an alternative for vacuum or evacuation (inside quartz tube chamber). This has also eliminated the use of vacuum pump in thermal CVD technique. Furthermore, the use of Ar gas prevents the oxidation of materials during a reaction [20]. Thus its (Ar gas) use on one side reduces the price of experimental set up by eliminating the use of vacuum pump, and on the other side, helps in growing longer BNNTs by preventing the oxidation of as produced Mg and Fe catalysts or their alloys.

2. Experimental details

A simple experimental setup is designed in the light of the work done by Lee et al. [15] and successfully used for the synthesis of BNNTs in the present work. A conventional horizontal dual zone quartz tube furnace along with one end closed quartz test tube is used as a major part of the experimental set up. During the experiment, Ar (inert gas) is used as an alternative for vacuum or evacuation.

Amorphous Boron powder, MgO and γ-Fe_2O_3 nanopowder of 99.9+% purities were bought from MTI Corporation and used as precursors. The aforementioned precursors having a total weight of 400 mg were first mixed at a weight ratio of 2:1:1 in an alumina combustion boat. The boat was covered with a few Si substrates and placed inside one end closed quartz tube near the closed end. The one end closed quartz test tube was then placed inside the quartz tube chamber of dual zone furnace in such a way that its open end was toward the gas inlet [21], as shown in Fig. 1(a). Furthermore, it was made sure that the precursors in the boat were exactly beneath the heating element. 2 min prior to the experimental run, Ar gas (with a flow rate of 100 sccm) was passed through the system to remove the dust particle and to create an inert atmosphere. Afterwards, the precursors were heated up to 1100 °C in the presence of Ar gas flow [19] at a rate of 100 sccm. At 1100 °C Ar flow was replaced by NH_3 at a rate of 100–200 sccm, and the precursors were heated up to 1200 °C. At 1200 °C, the system was kept for 1-h in the presence of ammonia gas flow.

After then, NH_3 gas flow was stopped, and the system was allowed to cool down to room temperature in the presence of Ar gas flow. At room temperature, white color BNNTs were found, deposited on Si substrate and the inner wall of alumina boat, as shown in Fig. 1(b).

The as synthesized samples are then characterized with the help of: Field Emission Scanning Electron Microscope (FESEM, Model: Zeiss Supra 55 VP) to study its surface morphology, Transmission Electron Microscope (Model: Zeiss Libra 200FE) to

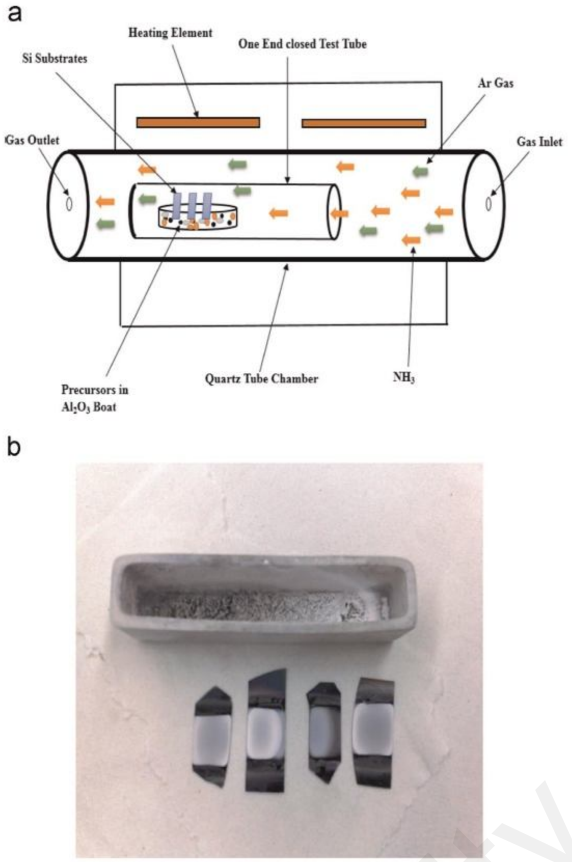

Fig. 1. (a) A sketch of the experimental setup used for synthesis of BNNTs (b) as synthesized Boron nitride nanotubes in Al_2O_3 boat and on Si substrate by thermal CVD technique.

analyze the tubular structure and crystallinity, Raman Spectroscopy (Model: Horiba Jobin Yvon HR800) and X-ray photon spectroscopy (Model: Thermo Scientific K-Alpha) to find out the elemental composition.

The details of all the characterization are given in the next section.

3. Results and discussion

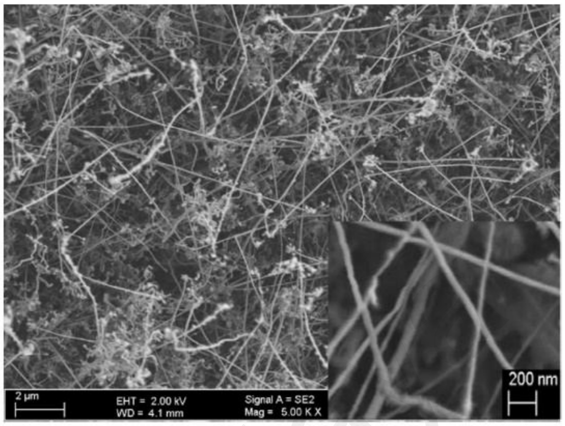

Fig. 2. Lower magnification FESEM micrograph shows randomly aligned BNNTs with some other cotton like morphologies. The inset shows magnified image of the same BNNTs synthesized in the present study.

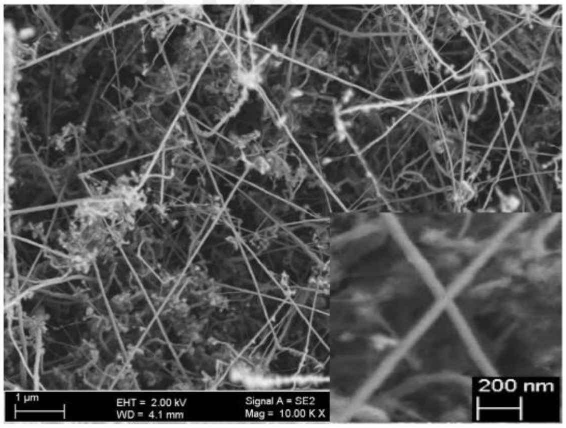

Fig. 3. High magnification FESEM micrograph shows randomly aligned BNNTs with some other cotton like morphologies. The inset shows magnified image of the same BNNTs synthesized in the present study.

Field Emission Scanning Electron Microscopy (FESEM) was used to study the morphology of the synthesized BNNTs. Figs. 2 and 3 show the lower and high magnification images of the BNNTs synthesized at 1200 °C. In lower magnification FESEM micrograph shown in Fig. 2, the BNNTs look like dried grass straws with some white species randomly distributed in between BNNTs on the Si substrate. A magnified inset image on the bottom right hand corner of Fig. 2 gives a clear view of the straight and long BNNTs randomly aligned in different directions [22]. At high magnification micrograph shown in Fig. 3, the straw like structures are more clear. The white species look like cotton packs hanged with different parts of the tubes. A high magnified inset micrograph on the bottom right hand corner of Fig. 3 further clarify the morphology of the randomly aligned straight and long BNNTs. The inset image also gives a good view of the white cotton like morphologies stuck with the BNNTs [22]. The diameter of the BNNTs can be calculated with the help of the scale shown in the inset images and found to be below 100 nm with a length of greater than 10 µm [15].

The tubular structure of the BNNTs was analyzed with the help of Transmission electron microscope (TEM). The analysis shows a tubular structure with a total diameter of 57 nm including 10.072 nm internal diameter and 23.516 nm external diameter or wall-thickness. The details of the tubular structure of the BNNTs are given in Figs. 4 and 5 in lower and higher resolution respectively. At lower resolution image shown in Fig. 4, the TEM shows bamboo like structures that grow from the bottom to top [23]. This bamboo like structure is separately shown in the inset image, on the upper right hand corner of Fig. 4. The tubular morphology of the BNNT is further confirmed from the high resolution TEM image shown in Fig. 5. The high resolution image not only shows the tubular morphology of the BNNT but also some parallel lines on the outer diameter of the tube. The appearance of these parallel lines shows that the as grown BNNTs are multi-walled with interlayer spacing of ~0.34 nm (see in Fig. 5). This interlayer spacing is the evidence of high crystalline nature of BNNTs and also the characteristics of $d_{(002)}$ spacing of h-BN [17,23]. Due to this high

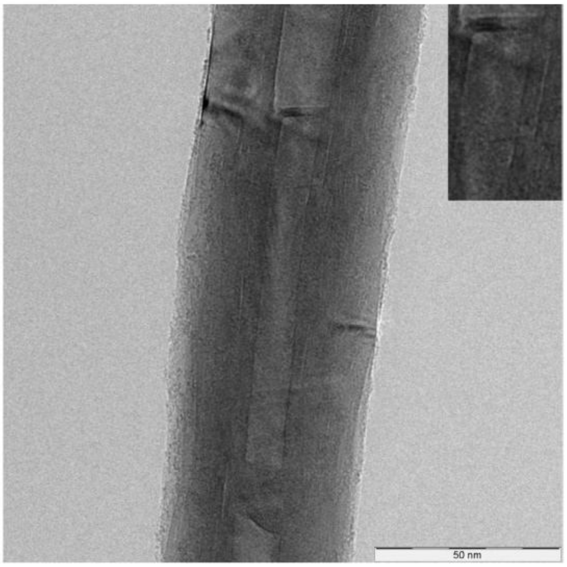

Fig. 4. TEM image of the BNNT shows internal bamboo like structure inside the tubular area. The inset image gives a clearer view of the bamboo like structure.

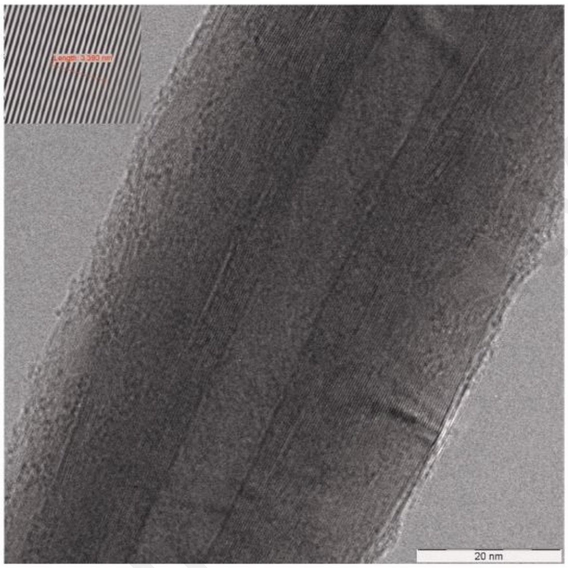

Fig. 5. High resolution TEM image of the BNNT shows some parallel line along with tubular structure. The inset image shows-0.34 nm interlayer spacing, which is the characteristic of $d_{(002)}$ spacing of h-BN..

crystalline nature of BNNTs, it is found to be of great importance in solid state neutron detector [22,24].

X-ray photon spectroscopy (XPS) was used to determine the elemental composition of the BNNTs sample synthesized in the present study. The XPS survey thus obtained is shown in Fig. 6. The survey shows two peaks at 191.08 eV and 398.78 eV respectively. The B 1s peak at 191.08 eV and N 1s peak at 398.08 eV correspond to h-BN [25,26].

Raman spectroscopy was further employed to confirm the elemental composition of the BNNTs sample synthesized in the present work. Raman spectrum of the synthesized BNNTs sample was collected by using laser excitation of 514 nm over the spectral range of 800 (cm^{-1}) to 1600 (cm^{-1}). Two peaks have been observed in the Raman spectrum given in Fig. 7. The high intensity dominant peak at ~1379.60 (cm^{-1}) corresponds to the E_{2g} mode of h-BN [27,28] and the lower intensity peak at 1129.98 (cm^{-1}) corresponds to boric acid. This might have formed by the spontaneous reaction of boron and B_2O_3 (left during the synthesis of BNNTs) with moisture and oxygen in the air [29].

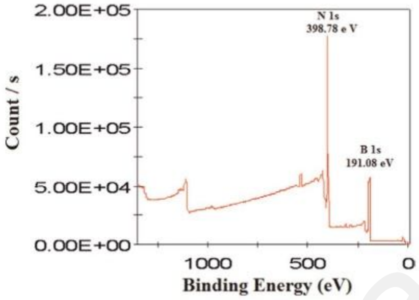

Fig. 6. X-ray photon spectroscopy survey shows B 1s peak 191.08 eV and N 1s peak at 398.78 eV that collectively correspond to h-BN.

Vacuum is normally one of the basic requirements in CVD technique due to the following two main reasons: (1) to remove oxygen and dust particles etc. that might result in undesirable physical or chemical reactions, (2) to deposit a uniform thin film of the desired material by increasing the mean free path of the precursor gases [30]. Most of the CVD techniques used for the synthesis of BNNTs have employed vacuum or evacuation during the experimental run because of the above two mentioned reasons [15,17]. When vacuum or evacuation is required, all the experimental set up used during the synthesis of BNNTs required to have vacuum pumps and gauges. Vacuum pump is used to create vacuum or evacuation inside the chamber whereas gauge is used to measure that particular vacuum needed specifically for that purpose. In 2008, Lee et al. [15] introduced the most efficient, simple and relatively cheap experimental set up for the synthesis of high quality BNNTs. Specifically, the experimental set up were consisted of mainly a conventional horizontal tube furnace with quartz tube and vacuum pump. Since no particular model of either conventional horizontal tube furnace, or vacuum pump is mentioned in their publication, therefore it is assumed from the sketch of the conventional horizontal tube furnace [15] that the type of used furnace was, "1200 °C Dual Zone Split Tube Furnace with Vacuum

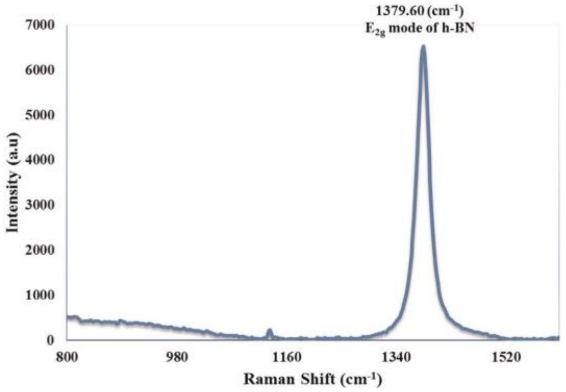

Fig. 7. Raman spectrum showing a major peak at ~1379.60 (cm^{-1}) correspond to E_{2g} mode of h-BN.

Flanges and 3.15" (80 mm) Quartz Tube-OTF-1200X-80-II, and from the mentioned value of the created vacuum (30 mTorr), the used vacuum pump was considered as Rotary pump. Then both of them have an online market price of USD 8455.00, that included USD 6895.00 for the furnace [31] and USD 1560 for the Rotary pump [32].

Although, in the present work, the same model of the horizontal dual zone split tube furnace has been used [31], but, vacuum or use of Rotary pump (for vacuum creation) has been eliminated by Ar (inert) gas flow at a rate of 100 sccm. The quantity of the used Ar gas during the whole experiment is much more less expensive than even the voltage utilized by the Rorary pump for the same duration [20,32]. Furthermore, Ar gas act as a shield against oxidation [20]. Therefore, it is more probable that use of Ar gas during the present experiment not only helped in removing the dust particles or creating an inert atmosphere but also helped in prevention of the oxidation of Mg or Fe catalysts. The availability of the catalysts in a relatively long duration thus helped in growing longer BNNTs as long as it (catalyst) is not oxidized or removed from the tube [17].

The use of the Ar gas as an alternative to vacuum has reduced the price of the experimental set up (by eliminating the use of Rotary vacuum pump) by an amount of USD 1560 (market price of Rotary pump), which is ~ 18 % of the combined price of tube furnace and Rotary pump. Thus, this replacement has not only helped in simplifying the experimental set up but also helped in making it cost effective as compared to Lee et al. [15]. This is a further reduction of experimental expenditure because, the Lee et al. [15] technique is more simple and economical as compared to other thermal CVD techniques introduced by Seo et al. [18] and Ozmen et al. [19]. Seo et al. [18] utilized milling facility combined with thermal CVD, larger amount of precursors and higher flow rates (700–750 sccm) of gases (N_2: 95 vol%, NH_3: 5 vol%) for longer annealing duration of 6 h. Similarly, Ozmen et al. [19] used mass spectrometer with thermal CVD and other facilities for online chemical analysis in a growth duration of 135 min and temperature range of 900–1400 °C. Thus these techniques are more complex and approximately 25–35% more expensive as compared to the technique used in the present study. Along with complex procedure and high prices of the extra facilities in these techniques, the quality of the final product was also not very good.

4. Conclusions

The successful synthesis of BNNTs in the presence of Ar gas as internal environment in the quartz tube chamber of a conventional horizontal tube furnace showed that the flow of Ar gas is a good alternative for high quality BNNTs synthesis. The used of Ar gas has eliminated the use of vacuum pump which in other words has reduced the price of the experimental set up by ~ 18 %. Ar gas has a very cheap price in the market, which is even smaller than the power consumption of rotary pump during a single experiment. It prevents the oxidation of the material during the experimental process. Thus along with economic benefits, Ar gas can help in producing longer BNNTs by preventing the oxidation of as produced Mg and Fe catalyst. Furthermore, it is predicted that a continuous supply of Ar gas along with the availability of precursor may grow longer, high quality and large quantity of the BNNTs.

The synthesized BNNTs in the present study is found to be of great interest in different fields like biomedical applications such as therapeutic or diagnostic, Micro Electro Mechanical System, targeted drug delivery and solid state neutron detector.

Acknowledgements

This research has been carried out under University of Malaya, 50603 Kuala Lumpur, Malaysia Research Grants: RP006D-13AFR and PG076-2014A.

References

[1] Y.N. Xu, W. Ching, Calculation of ground-state and optical properties of boron nitrides in the hexagonal, cubic, and wurtzite structures, Phys. Rev. B 44 (1991) 7787.
[2] Y. Huang, Y. Bando, C. Tang, C. Zhi, T. Terao, B. Dierre, T. Sekiguchi, D. Golberg, Thin-walled boron nitride microtubes exhibiting intense band-edge UV emission at room temperature, Nanotechnology 20 (2009) 085705.
[3] X. Chen, X. Gao, H. Zhang, Z. Zhou, W. Hu, G. Pan, H. Zhu, T. Yan, D. Song, Preparation and electrochemical hydrogen storage of boron nitride nanotubes, J. Phys. Chem. B 109 (2005) 11525–11529.
[4] A. Rubio, J.L. Corkill, M.L. Cohen, Theory of graphitic boron nitride nanotubes, Phys. Rev. B 49 (1994) 5081–5084.
[5] N.G. Chopra, R. Luyken, K. Cherrey, V.H. Crespi, M.L. Cohen, S.G. Louie, A. Zettl, Boron nitride nanotubes, Science 269 (1995) 966–967.
[6] M. Ishigami, S. Aloni, A. Zettl, Properties of boron nitride nanotubes, in: Proceedings of AIP Conference, 2003, pp. 94–99.
[7] G. Ciofani, V. Raffa, J. Yu, Y. Chen, Y. Obata, S. Takeoka, A. Menciassi, A. Cuschieri, Boron nitride nanotubes: a novel vector for targeted magnetic drug delivery, Curr. Nanosci. 5 (2009) 33–38.
[8] X. Chen, P. Wu, M. Rousseas, D. Okawa, Z. Gartner, A. Zettl, C.R. Bertozzi, Boron nitride nanotubes are noncytotoxic and can be functionalized for interaction with proteins and cells, J. Am. Chem. Soc. 131 (2009) 890–891.
[9] G. Ciofani, S. Danti, D. D'Alessandro, L. Ricotti, S. Moscato, G. Bertoni, A. Falqui, S. Berrettini, M. Petrini, V. Mattoli, Enhancement of neurite outgrowth in neuronal-like cells following boron nitride nanotube-mediated stimulation, ACS nano 4 (2010) 6267–6277.
[10] J. Wang, C.H. Lee, Y.K. Yap, Recent advancements in boron nitride nanotubes, Nanoscale 2 (2010) 2028–2034.
[11] P. Ahmad, N.M. Mohamed, Z.A. Burhanudin, A review of nanostructured based radiation sensors for neutron, in: Proceedings of the AIP Conference Proceedings, 2012, pp. 535.
[12] C. Zhi, Y. Bando, C. Tang, D. Golberg, Boron nitride nanotubes, Mater. Sci. Eng. R: Rep. 70 (2010) 92–111.
[13] C. Tang, Y. Bando, T. Sato, K. Kurashima, A novel precursor for synthesis of pure boron nitride nanotubes, Chem. Commun. (2002) 1290–1291.
[14] C. Zhi, Y. Bando, C. Tan, D. Golberg, Effective precursor for high yield synthesis of pure BN nanotubes, Solid State Commun. 135 (2005) 67–70.
[15] C.H. Lee, J. Wang, V.K. Kayatsha, J.Y. Huang, Y.K. Yap, Effective growth of boron nitride nanotubes by thermal chemical vapor deposition, Nanotechnology 19 (2008) 455605.
[16] C.H. Lee, M. Xie, V. Kayastha, J. Wang, Y.K. Yap, Patterned growth of boron nitride nanotubes by catalytic chemical vapor deposition, Chemistry of Materials 22 (2010) 1782–1787.
[17] A. Pakdel, C. Zhi, Y. Bando, T. Nakayama, D. Golberg, A comprehensive analysis of the CVD growth of boron nitride nanotubes, Nanotechnology 23 (2012) 215601.
[18] D. Seo, J. Kim, S.-H. Park, Y.-U. Jeong, Y.-S. Seo, S.-H. Lee, J. Kim, Synthesis of boron nitride nanotubes using thermal chemical vapor deposition of ball milled boron powder, J. Ind. Eng. Chem. 19 (2014) 1117–1122.
[19] D. Özmen, N.A. Sezgi, S. Balcı, Synthesis of boron nitride nanotubes from ammonia & a powder mixture of boron & iron oxide, Chem. Eng. J. 219 (2012) 28–36.
[20] ⟨http://periodictable.com/Elements/018/⟩, (23/05/2014).
[21] P. Ahmad, M.U. Khandaker, Y.M. Amin, Effective synthesis of vertically aligned boron nitride nanotubes via a simple CCVD, Mater. Manuf. Process. (2014) (accepted for publication).
[22] J. Li, J. Lin, X. Xu, X. Zhang, Y. Xue, J. Mi, Z. Mo, Y. Fan, L. Hu, X. Yang, Porous boron nitride with a high surface area: hydrogen storage and water treatment, Nanotechnology 24 (2013) 155603.
[23] J. Wang, L. Zhang, G. Zhao, Y. Gu, Z. Zhang, F. Zhang, W. Wang, Selective synthesis of boron nitride nanotubes by self-propagation high-temperature synthesis and annealing process, J. Solid State Chem. 184 (2011) 2478–2484.
[24] J. Li, R. Dahal, S. Majety, J. Lin, H. Jiang, Hexagonal boron nitride epitaxial layers as neutron detector materials, Nucl. Instrum. Methods Phys. Res. Sec. A: Accel. Spectrom. Detect. Assoc. Equip. 654 (2011) 417–420.
[25] B. Zhong, L. Song, X. Huang, G. Wen, L. Xia, Synthesis of boron nitride nanotubes with SiC nanowire as template, Mater. Res. Bull. 46 (2011) 1521–1523.
[26] P. Ahmad, M.U. Khandaker, Y.M. Amin, Z.R. Khan, Synthesis of boron nitride microtubes and formation of boron nitride nanosheets, Mater. Manuf. Process. (2014) (accepted for publication).
[27] L. Guo, R. Singh, Catalytic growth of boron nitride nanotubes using gas precursors, Phys. E: Low-Dimens. Syst. Nanostruct. 41 (2009) 448–453.
[28] P. Ahmad, M.U. Khandaker, Z.R. Khan, Y.M. Amin, A simple technique to synthesize pure and highly crystalline boron nitride nanowires, Ceram. Int. 40 (2014) 14727–14732.
[29] R. Arenal, A. Ferrari, S. Reich, L. Wirtz, J.-Y. Mevellec, S. Lefrant, A. Rubio, A. Loiseau, Raman spectroscopy of single-wall boron nitride nanotubes, Nano Lett. 6 (2006) 1812–1816.
[30] X.-T. Yan, X. Yongdong, Chemical Vapour Deposition: An Integrated Engineering Design for Advanced Materials, Springerverlag, London, 2010.
[31] ⟨http://www.mtixtl.com/DualZoneSplitTubeFurnace80mmQuartz-OTF-1200X-80-II.aspx⟩, (23/05/2014).
[32] ⟨http://www.mtixtl.com/vacuumpumptwostepsrotar yvanehighspeedvacuumpump220v226lmwithoil-2.aspx⟩, (23/05/2014).

Indian J Phys (March 2015) 89(3):209–216
DOI 10.1007/s12648-014-0545-z

ORIGINAL PAPER

A comprehensive study of boron nitride nanotubes multiple synthesis from a single precursor

P Ahmad*, M U Khandaker and Y M Amin

Department of Physics, Faculty of Science, University of Malaya, 50603 Kuala Lumpur, Malaysia

Received: 04 March 2014 / Accepted: 13 July 2014 / Published online: 5 August 2014

Abstract: Importance of boron nitride nanotubes due to its applications in the fields of biomedical, microelectronic mechanical systems and solid state neutron detectors has greatly increased the demand for high quality and large scale synthesis of boron nitride nanotubes. The idea of using a single precursor for multiple synthesis has been utilized and boron nitride nanotubes are synthesized from fresh as well as residual material left after first and second experimental runs. For the first time, experimental results are characterized and analyzed for their size, morphology and quality of the final product. Results thus obtained are likely to be steps toward the high yield and large scale synthesis of boron nitride nanotubes.

Keywords: BNNTs; CNTs; Residual materials; Synthesis

PACS No.: 81.07.De

1. Introduction

Nanotechnology has greatly changed the properties of materials by reducing their size from bulk to nano. At nano scale, the surface atoms dominate properties of the materials due to quantum effects. These properties include electrical, mechanical, optical etc. [1, 2]. All these properties of the materials can be changed to obtain the desired properties by only reducing their size from bulk to nano [3–5]. These nano size materials have greatly improved the performance of modern electronics devices and sensors. These developments in modern technology have highly increased the demand for synthesis of these small and nano size materials [6, 7]. To fulfill this demand of modern technology, different nanostructure materials have been developed. These nanostructure materials include nanowires, nanoparticles and nanotubes etc. Carbon nanotube (CNT) is one of such nanostructure materials that has remarkable chemical, electrical and mechanical properties dependent on the geometry of the tube [8–10].

These diameter dependent properties of CNTs have made these unsuitable to be used in different microelectronic mechanical system with uniform electronic properties. The need for the discovery of a new kind of material with uniform electronic properties is strongly felt. Boron nitride nanotubes (BNNTs) are large band semiconductor, theoretically predicted in 1994 [11] and experimentally discovered in 1995, [12] are found to have diameter independent [13, 14] uniform electronic properties [15, 16]. These properties have made it a very important material for different applications in modern technologies. These technologies include biomedical and microelectronic mechanical systems etc. [8]. Boron nitride (BN) has large cross-section area for thermal neutron that is expected to be further increased in case of BNNTs due to its nanostructure properties. This property of BNNTs has made it a very important material to be used in development of solid state neutron detectors [17]. All these properties for their respective applications are dependent on the size and purity of as synthesized BNNTs. Different techniques have been tried to synthesize BNNTs with the desired purity and size. These techniques include Arc-discharge, Laser ablation, Template synthesis, Auto clave, Ball milling and chemical vapor deposition (CVD) etc. The BNNTs obtained by almost all of the above techniques contain different precursor materials and some raw products as impurities [18]. These impurities are very difficult to separate from the final

---

Electronic supplementary material The online version of this article (doi:10.1007/s12648-014-0545-z) contains supplementary material, which is available to authorized users.

*Corresponding author, E-mail: pervaiz_pas@yahoo.com product. Also most of the techniques involved at a relatively higher temperature that make the desire quality and quantity very difficult to achieve [18]. CVD techniques are used with different precursor, catalysts and experimental set up to synthesize BNNTs in desired quality and quantity. Majority of these techniques are used with health risk precursor and complex experimental set ups that have made it very difficult for the new researchers to reproduce the desired products [19]. New and effective precursors are reported after successful synthesis of BNNTs of extremely high quality. These precursors are predicted to be used for several syntheses [20]. However no appreciable experimental result is shown to support the arguments. In the present work a simple CVD set up is used to synthesize BNNTs from a particular precursor. The residual materials left in the boat are used for two more consecutive syntheses.

2. Experimental details

Three different samples of Boron nitride nanotubes are synthesized from the fresh precursor and the residual materials left in the boat after first and second experimental runs. The experimental set up used in the present work, is a bit different from those previously described [20–23]. Initially a 400 mg mixture of Boron, MgO and γ-Fe_2O_3 (nano-size amorphous) powders with 99.9 % purity are used as precursor. A 2:1:1 ratio of the precursor in alumina boat, covered with a few Si substrates, are placed inside one end closed quartz tube near the closed-end [22]. The quartz tube is then inserted inside the horizontal quartz tube furnace in such a way that the open end of the inner quartz tube is toward the gas inlet. The precursors are then heated up to 1,200 °C in the presence of Ar gas flow [24]. At 1,200 °C, Ar flow is replaced by NH_3 flow at the same rate of 100–200 sccm. The system is maintained at this condition for 1 h. After 1 h NH_3 flow is again replaced by Ar gas flow and the system is allowed to cool down to room temperature. At room temperature white BNNTs are found deposited on the inner walls of the boat and on the top of precursor in alumina boat [22]. The white layer of BNNTs are successfully removed from the top of precursor in the boat. The residual Blackish-brown material in alumina boat of weight $\sim$370 mg from the first experimental run is then remixed with the help of a conventional stirrer and used for another synthesis in the same boat covered with a few new Si substrates. The rest of the processes remained the same. The Blackish-brown color powder of $\sim$345 mg left in the boat after 2nd experimental run is then used for 3rd synthesis under the same experimental conditions. All the BNNT samples thus deposited on Si-substrates look like the same when observed with the naked eyes but are totally different when observed with FE-SEM and other characterization instruments. The detailed description of all the characterization results is given in the next section.

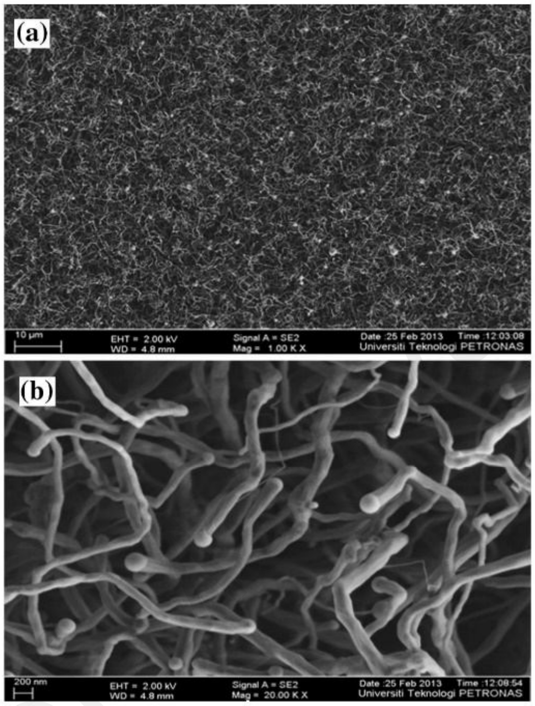

Fig. 1 (**a**) Low and (**b**) high magnification FESEM images of BNNTs synthesized from fresh precursor material at 1,200 °C

3. Results and discussion

3.1. Morphology

Figure 1(a) and 1(b) show the low and high magnification FE-SEM images of BNNTs synthesized from the fresh (unused) precursor materials. At lower magnification the BNNTs look like small insects or pieces of fabric wires randomly cut and dispersed on a particular surface. The as grown BNNTs (at higher magnification) are seem to bent (from different parts) and aligned in random directions. Each BNNT has a clear entangled curve like morphology with a spherical ball like structure (tip) at the top end. This ball like structure or tip is assumed to be the catalyst particle with closed tip end. This closed tip end encapsulated catalyst particle is found to play a key role in the growth of BNNTs as long as it is available in the original form [25]. The as grown each individual tube has almost uniform diameter. The overall diameter of the BNNTs varies from tube to tube within a wide range of 70–170 nm.

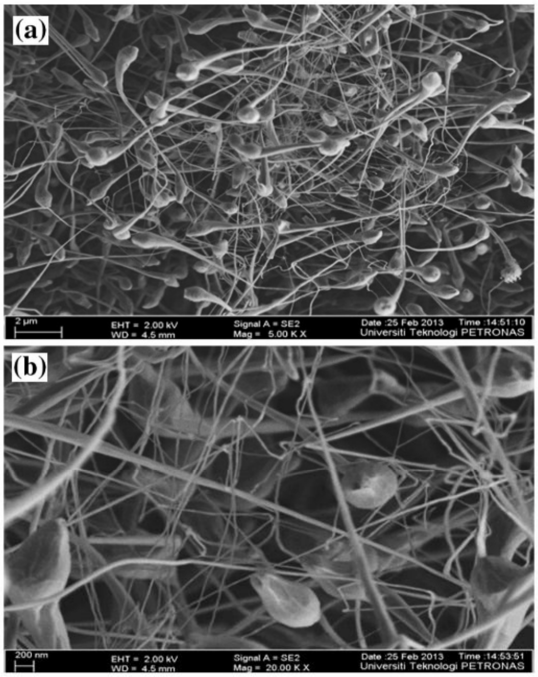

Fig. 2 (**a**) Low and (**b**) high magnification FESEM images of BNNTs synthesized from residual material left in the boat, after first experimental run at 1,200 °C

Almost the same morphologies are previously reported in the diameter range of ~50–150 nm. However the experimental set up, temperature (1,300 °C), ratio (4:1:1) [21] and nature (fresh or residual) of the precursor are totally different from the one used in the present work [21].

The morphology and diameter of the BNNTs synthesized from the residual material left after the first experimental run, is completely different from the BNNTs synthesized from the fresh precursor materials. The structure shown in Fig. 2(a) is the low magnification FE-SEM image of as synthesized BNNTs. The BNNTs look like the shape of blooming flowers. The blooming part at top of each BNNT is assumed to be catalytic tip considered to be responsible for the growth. The size of the "blooming flower" like structure is very large as compared to the spherical tip observed in case of Fig. 1(a) and 1(b). This increase may be due to cumulative catalytic particles on the substrate, which might have formed a larger catalyst particle [21] that can ultimately be seen in the present form. This kind of BNNTs differ from the previous one as shown in Fig. 1(a) and 1(b), in apparent look, size and shape of the tip and its orientation. Apparently most of the BNNTs are straight with continuously decreasing diameter from top to bottom. All the tubes have either closed or opened tip end (varies from tube to tube) encapsulated catalyst particle. The apparent look of these tip changes in higher magnification image shown in Fig. 2(b) and looks like large size electric bulb. Some small sizes BNNTs with diameter in the range of 40–100 nm can also be observed at this magnification. These BNNTs have almost uniform diameter (for each single BNNT) from top to bottom. Some of these BNNTs are straight while others are irregularly bent in different direction throughout the sample. The overall diameter of BNNTs in the sample varies continuously from top to bottom (within single BNNT) and from tube to tube (within the sample) in a huge range of ~40–450 nm. The large diameter of the tube near the tip end actually suggests that the catalyst tip provides a pattern for the BNNTs growth. A similar phenomena has been previously reported [21] with a tube diameter of ~200 nm near the tip end. However that phenomenon is observed by increasing the temperature above 1,200 °C (up to 1,300 °C) and metal oxides to B content in a 2:1 ratio in the sample. Also BNNTs films are reported with diameter in the range of ~100–500 nm (any single BNNT may have diameter with in the mentioned range) at 1300 °C by using 1:1:1 ratio of the precursor [21] whereas in the present sample it (change in diameter) is observed just by reusing the residual material (previously used in 2:1:1 ratio) left in the boat after the first experimental run at 1,200 °C.

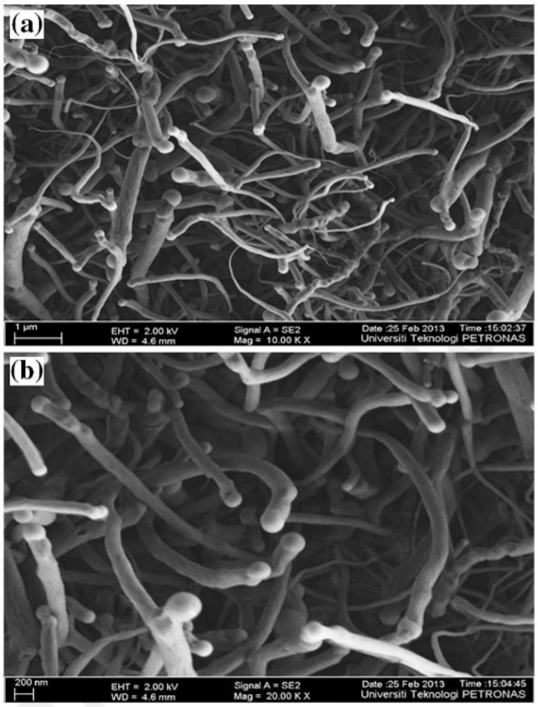

Fig. 3 (**a**) Low and (**b**) high magnification FESEM images of BNNTs synthesized from residual material left in the boat after second experimental run at 1,200 °C

Figure 3(a) shows the FESEM image of BNNTs synthesized from the residual material left after the 2nd experimental

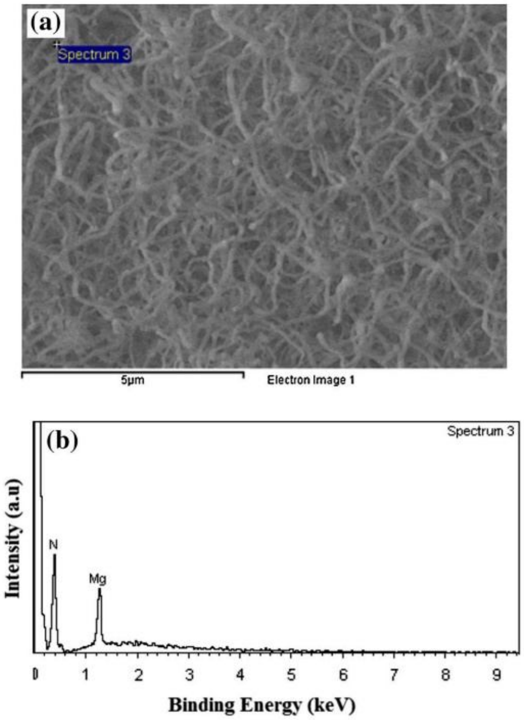

Fig. 4 (**a**) Electron image and (**b**) EDX spectrum of BNNT-tip synthesized from fresh precursor material

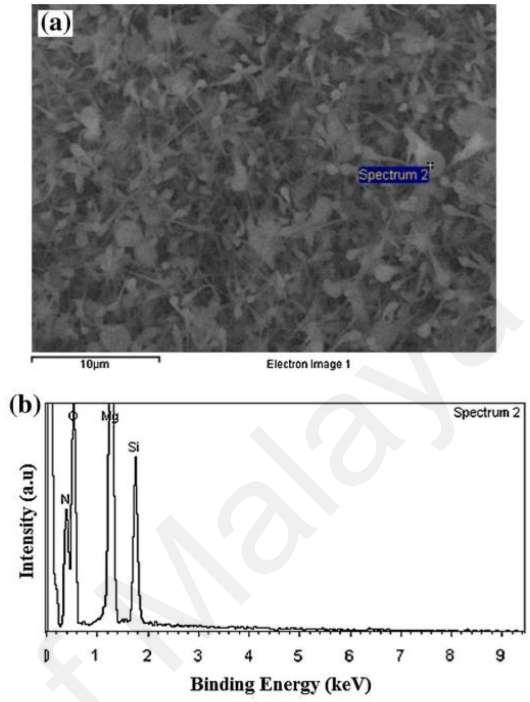

Fig. 5 (**a**) Electron image and (**b**) EDX spectrum of BNNT-tip synthesized from residual material left after first experimental runs

run. All BNNTs can be seen and observed seperatly from each other. In Fig. 3(b) apparently from the top (in higher magnification) the BNNTs look like exactly the same as shown in Fig. 1(b) with almost similar spherical tip at the top [21]. Below the tip, up to a certain point BNNTs seem to have uniform diameter. Below that particular point the diameter decreases gradually up to ∼50 nm at the bottom. This kind of morphology is similar to the one shown in Fig. 2(a) and 2(b). So the present structure of BNNT look like a combination of BNNT in Figs. 1 and 2. Some of the BNNTs have twisted rope like morphology while other have curved structure like earth worm moving in a forward direction as shown in Fig. 3(b). The diameter of BNNTs is highly non-uniform and continuously varies not only from tube to tube but also with in a single tube from top to bottom. A BNNT with a maximum diameter of ∼400 nm at the top and decreases continuously downward to a limit of ∼40 nm.

3.2. Tip analysis

EDX analysis is used to find out the composition of the tip or ball-like structure found at the top ends of the BNNTs synthesized from the fresh and residual materials left after first and second experimental run. Figure 4(a) and 4(b) show the electron image and the EDX spectrum of the BNNT tip synthesized from the fresh precursor materials. The spectrum has shown a peak for Mg along with N. No peak has been detected in the present spectrum for oxygen, which means that the catalyst particle has not yet been oxidized and still available for further growth dependents on the presence of precursor materials or higher temperature [21]. However some of the contents in the sample (tip) show presence of Oxygen that may refer to oxidation of catalyst particles in the sample. This might have stopped further catalytic growth of the corresponding BNNTs.

Figure 5(a) and 5(b) show electron image and EDX spectrum of a particular BNNT-tip synthesized from the residual materials left in the boat after first experimental run. Since the tip is very large as compared to previous sample, therefore comparatively more amount of Mg is found due to cumulative catalytic particles on the substrate, which might have formed a larger catalyst particle. The presence of oxygen is also reported by the EDX spectrum in a huge quantity in the current sample. Due to limitation of EDX analysis, possible compounds formed by reaction of oxygen with lighter element (H and B etc.) are not be fully reported here. However it is assumed that reported

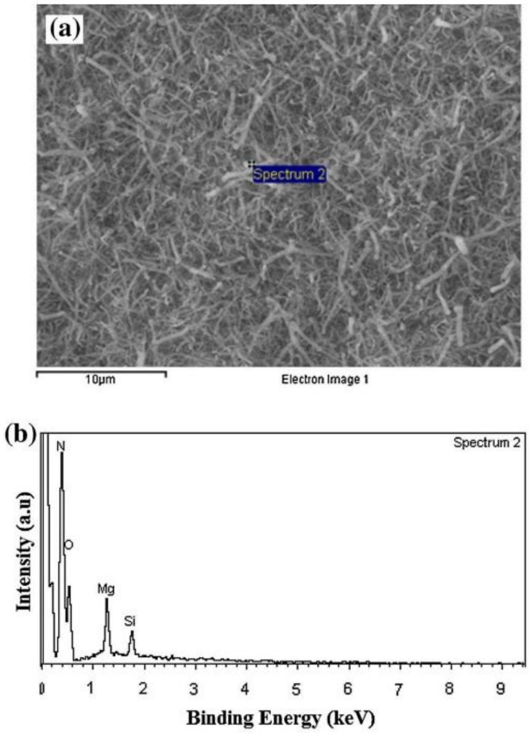

Fig. 6 (**a**) Electron image and (**b**) EDX spectrum of BNNT-tip synthesized from residual material left in the boat after second experimental run

oxygen might have oxidized the Mg catalyst to MgO and growth might have been stopped or decreased afterward [25]. The larger size of the tip due to larger content of oxidized catalyst. BNNT is found to have a larger diameter near the top end as compared to the bottom. Therefore it can be concluded here that size of the catalyst enclosed in tip acts as a pattern for BNNT morphology and size. However the role of Gravity cannot be ignored here, as it might have caused the observed decrease in diameter with increasing length by stretching it downward due to its weight [21].

Figure 6(a) and 6(b) show electron image and EDX analysis of BNNT tips grown from the residual material left after 2nd experimental run. The spectrum shows a magnesium (Mg) peak along with oxygen. The quantity of Mg reported here is very low as compared to the spectra shown in Fig. 4(a) and 4(b). The presence of oxygen again indicates either oxidation of Mg catalyst or formation of some kind of compound with lighter elements that cannot be fully detected with the help of EDX analysis.

A comparison of all three kinds of BNNTs is shown in Table 1. According to comparative analysis shown in Table 1, it is clear that nature of precursor has great impact on the size and morphology of BNNTs in a CVD technique. The diameter of any individual BNNT synthesized from fresh precursor material may remain uniform due to smooth and uniform catalytic activity of as used catalysts. The presence of unoxidized catalytic particles at the tip of some BNNTs, suggests that these BNNTs can grow further lengthy as long as nature of the catalyst is not change [26, 27]. After first experimental run residual material left in the boat (when white BNNTs layer is carefully removed) might have change from amorphous to crystalline form due to high temperature (1,200 °C) [28]. This crystalline nature of the precursor (after 1st and 2nd experimental run) may be responsible for a possible increase in length and purity of the tubes [29]. Due to high temperature, nanosize catalysts may have agglomerated into a relative bigger size, which might have caused an increase in diameter of the tube near tip. The change in morphology of BNNT in the present work may be due to the size, shape, amount and nature of the catalytic materials found in the tip.

Table 1 Comparision of BNNTs Synthesized from fresh precursor and residual material left in the boat after 1st and 2nd experimental run

S.No	Nature of precursor	Diameter (nm)	Morphology	Nature of catalytic content in the tip
1	Fresh	70 to ~170 (from tube to tube)	Entangled curve	Mix oxidized and unoxidized
2	Residual material left after 1st experimental run	~40 to 450 (from top to bottom and tube to tube)	Blooming flowers like	Oxidized
3	Residual material left after 2nd experimental run	~40 to 450 (from top to bottom and tube to tube)	Curved like twisted rope or earth worm	Oxidized

3.3. Tubular analysis

Transmission electron microscopy (TEM) is used to analyze tubular structure of all three kinds of BNNTs. Figure 7(a) shows a clear tubular structure of BNNT synthesized from fresh precursor materials. An internal bamboo like structure can also be found inside tubular part of BNNT. The BNNT has a diameter of 42.143 nm that contained ~15 nm internal diameter and ~13 nm external diameter. The as synthesized BNNTs are found to have an interplanar spacing of 0.34 nm that correspond to d_{0002}

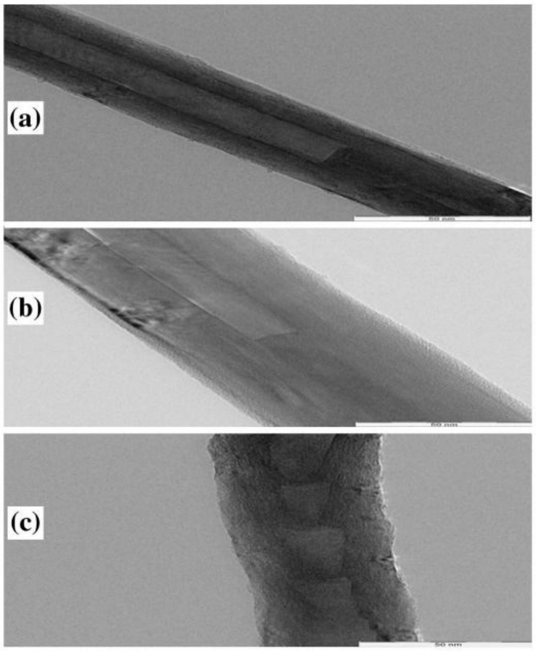

Fig. 7 TEM images of BNNTs synthesized from (**a**) fresh precursor materials, (**b**) residual material left after first syntheses and (**c**) residual material left after second synthesis

spacing of h-BN [1]. It is also a proof of highly crystalline nature of as synthesized BNNTs [2].

An almost similar structure with a same internal bamboo like morphology [30] can be seen in Fig. 7(b). The figure shows BNNT synthesized from the residual materials left after first experimental run. It seems to have a bit of dust on its external part. This dusty view seems to be only apparent difference between present BNNT and previous BNNT. The tube is found to have an internal diameter of ~15 nm and external diameter of 27 nm. Both tubes (one synthesized from fresh materials and other synthesized from the residual materials) have almost same internal diameter but their external diameter differ by a magnitude twice that of first one. Both tubes have same interplanar spacing of ~0.34 nm [21, 31], which is consistent with the crystal structure of h-BN and BNNTs [22, 32]. Figure 7(c) shows TEM image of as synthesized BNNT from residual material left after 2nd experimental run. The BNNT structure shown here is different from other two BNNTs in the sense that it has more bamboos and these bamboos are very close to each other [19]. Due to frequent bamboos inside BNNT internal and external diameter varies continuously form point to point [24]. Therefore average values are calculated for both external and internal diameter. The internal diameter is found to have an average value of ~13 nm and external diameter with an average value of ~15.5 nm. This average value of internal diameter is smaller than other two previously mentioned BNNTs (synthesized from fresh precursor materials and residual material after first experimental run). However the external average diameter for the present BNNT is larger than the BNNT synthesized from the fresh precursors materials and smaller than BNNT synthesized from the residual materials left after 1st experimental run. The interlplanar spacing of the present BNNT is ~0.36 nm, which is a bit larger than other two previously mentioned BNNTs (0.34 nm). This increase in interlayer spacing may possibly be due to frequent and closely related bamboos that seem to emerge from each other in a direction from bottom to top.

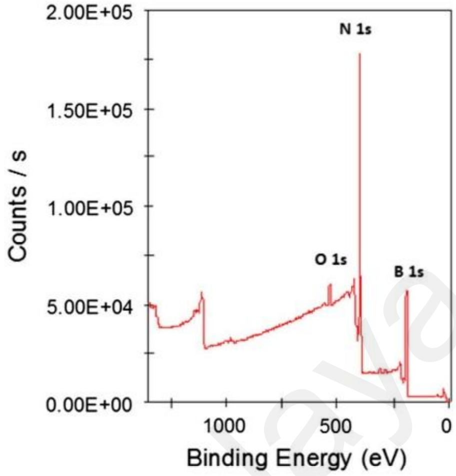

Fig. 8 XPS survey shows B 1 s, N 1 s and O 1 s peaks for the BNNTs sample synthesized form the fresh precursor material

3.4. Compositional analysis

The elemental composition of all BNNTs samples are carried out with help of X-ray Photon Spectroscopy (XPS) and Raman spectroscopy analysis as shown in Figs. 8 and 9. The XPS survey (for BNNTs synthesized from fresh precursor material) reports B 1 s, N 1 s and O 1 s peaks at 191 eV, 398.7 eV and 533.18 eV, respectively. The B 1 s, N 1 s peaks at 191 eV, 398.7 eV, correspond to h-BN, which is consistent with literature [33, 34]. The O 1 s peak at 533.18 eV, corresponds to content of oxygen, which may possibly be referred to formation of other Boron compounds like B_2O_3 and H_3BO_3 etc. [35]. The content of oxygen may also refer to oxidation of Mg to MgO as indicated by EDX analysis; however not enough information is reported by XPS analysis in this regard.

The XPS survey of BNNTs sample synthesized from residual material left after first experimental run reports

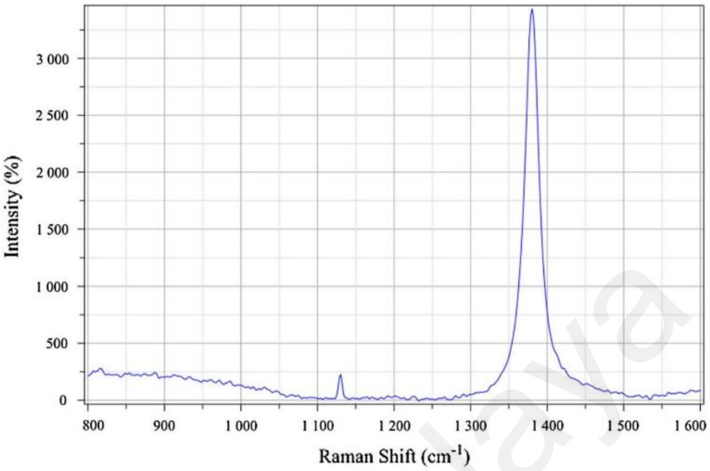

Fig. 9 Raman spectrum of the as synthesized BNNTs form the fresh precursor materials

almost the same information like the previous sample. The survey shows B 1 s, N 1 s peaks at 191.3 eV, 398.5 eV, which may correspond to h-BN [33, 34]. Whereas O 1 s peak at 533.3 eV, represents content of oxygen, which is consistent with EDX results of same sample. Along with O 1 s peak at 533.3 eV, B 1 s peak reported at 193.8 eV, corresponds to formation of B_2O_3 [35]. The high content of oxygen may also refer to oxidation of Mg to MgO as indicated by EDX analysis however, again no proper evidence is found in this regard from XPS analysis.

The XPS survey of BNNTs sample synthesized from residual material left after second experimental run also contains almost similar information like previous one (sample synthesized from the residual material left after first experimental run) however, intensity of N 1 s peak is a bit higher as compare to last one.

The as synthesized BNNT samples are also characterized with the help of Raman spectroscopy. A major peak at Raman spectroscopy is reported at $\sim$1,379.6 (cm^{-1}) that corresponds to E_{2g} mode of h-BN, which is in good agreement with available literature [36–39]. A smaller peak is reported in Raman spectrum at $\sim$1,130 (cm^{-1}) that corresponds to boric acid that might have formed by spontaneous reaction of B_2O_3 moisture and oxygen in the air. Almost similar peaks for h-BN and H_3BO_3 have been obtained for other two samples synthesized from residual material left after first and second experimental run, which show that all samples have almost the same compositional materials [36] which are consistent with XPS results of the same samples.

4. Conclusions

The present work not only demonstrates the variation of size and morphology of BNNTs with nature of the precursor but also guides towards large and continuous production of BNNTs. The demonstration of BNNTs synthesis from residual materials and study of as synthesized structures reveal that quantity and size of the BNNTs can be increased to any desire level by just doing a few simple modifications in the experimental set up in such a way that can easily prevents the blockage of the precursors in the boat due to as synthesized BNNTs. With such a modifications, BNNTs synthesized are not only in high quality or quantity but also have a length even up to centimeter scale.

Acknowledgments We are extremely grateful to Prof. Dr. Norani Muti Mohamed, Director of COINN and MOR Nanotechnology, University of Technology PETRONAS Malaysia for providing Lab and characterization facilities. We are also grateful to Skim Bright Spark Program, University of Malaya 50603 Kuala Lumpure Malaysia for providing funds and facilities for our research work.

References

[1] J Lauret et al. *Phys. Rev. Lett.* **94** 037405 (2005).
[2] S Mitra et al. *Indian J.Phys.* **85** 649 (2011).
[3] P Jaffrennou et al. *Chem. Phys. Lett.* **442** 372 (2007).
[4] C Zhi, Y Bando, C Tang, D Golberg, R Xie and T Sekigushi *Appl. Phys. Lett.* **86** 213110 (2005).
[5] S Karan, D Dutta Majumder and A Goswami *Indian J.Phys.* **86** 667 (2012).
[6] Y Huang et al. *Nanotechnology* **20** 085705 (2009).
[7] E Purushotham and N G Krishna *Indian J.Phys.* **88** 157 (2014).
[8] M Ishigami, S Aloni and A Zettl *AIP Conf. Proc.* Art. 94 (2003).
[9] F Taleshi, A A Hosseini, M Mohammadi and M Pashaee *Indian J.Phys.* **87** 873 (2013).
[10] F Taleshi and A A Hosseini *Indian J.Phys.* **87** 425 (2013).
[11] A Rubio, J L Corkill and M L Cohen *Phys. Rev. B* **49** 5081 (1994).
[12] N G Chopra et al. *Science* **269** 966 (1995).
[13] D Golberg, Y Bando, C Tang and C Zhi *Adv. Mater.* **19** 2413 (2007).

[14] X Blase, A Rubio, S Louie and M Cohen *Europhys. Lett.* **28** 335 (1994).

[15] C H Lee, M Xie, V Kayastha, J Wang and Y K Yap *Chem. Mat.* **22** 1782 (2010).

[16] A Maguer, E Leroy, L Bresson, E Doris, A Loiseau and C Mioskowski *J. Mater. Chem.* **19** 1271 (2009).

[17] P Ahmad, NM Mohamed and Z A Burhanudin *AIP Conf. Proc.* Art. 535 (2012).

[18] C Zhi, Y Bando, C Tang and D Golberg *Mater. Sci. Eng. R- Rep.* **70** 92 (2010).

[19] R Ma, Y Bando and T Sato *Chem. Phys. Lett.* **337** 61 (2001).

[20] C Zhi, Y Bando, C Tan and D Golberg *Solid State Commun.* **135** 67 (2005).

[21] A Pakdel, C Zhi, Y Bando, T Nakayama and D Golberg *Nanotechnology* **23** 215601 (2012).

[22] C H Lee, J Wang, VK Kayatsha, J Y Huang and Y K Yap *Nanotechnology* **19** 455605 (2008).

[23] D Seo et al. *J. Ind. Eng. Chem.* **19** 1117 (2013).

[24] D Özmen, N A Sezgi and S Balcı *Chem. Eng. J.* **219** 28 (2013).

[25] A Pakdel, X Wang, Ybando and D Golberg *Acta Mater.* **61** 1266 (2013).

[26] C Tang, Y Bando and T Sato *Chem. Phys. Lett.* **362** 185 (2002).

[27] C Tang, Y Bando, T Sato and K Kurashima *Chem. Commun* 1290 (2002).

[28] S Balcı, N Sezgi and E Eren *I&ECR* **51** 11091 (2012).

[29] J Kim, S Lee, D Seo and Y S Seo *Mater. Chem. Phys* **137** 182 (2012).

[30] J Wang et al. *J. Solid State Chem.* **184** 2478 (2011).

[31] A E Tanur, J Wang, A L M Reddy, D N Lamont, Y K Yap and G C Walker *J. Phys. Chem. B* **117** 16 (2013).

[32] H Ghassemi, C Lee, Y Yap and R Yassar *J. Appl. Phys.* **108** 024314 (2010).

[33] S Sinnott et al. *Chem. Phys. Lett.* **315** 25 (1999).

[34] C Y Su et al. *J. Phys. Chem. C* **113** 14732 (2009).

[35] B P Martins *Frontiers in superconductivity research* (New York : Nova Publishers) (2003).

[36] R Arenal et al. *Nano Lett.* **6** 1812 (2006).

[37] C Y Zhi et al. *J. Phys. Chem. B* **110** 1525 (2006).

[38] L Guo and R N Singh *Physica E* **41** 448 (2009).

[39] B Fakrach, A Rahmani, H Chadli, K Sbai and J L Sauvajol *Physica E* **41** 1800 (2009).

Materials and Manufacturing Processes, 30: 706–710, 2014
Copyright © Taylor & Francis Group, LLC
ISSN: 1042-6914 print/1532-2475 online
DOI: 10.1080/10426914.2014.941874

Taylor & Francis
Taylor & Francis Group

Effective Synthesis of Vertically Aligned Boron Nitride Nanotubes via a Simple CCVD

PERVAIZ AHMAD, MAYEEN UDDIN KHANDAKER, AND YUSOFF MOHD AMIN

Department of Physics, Faculty of Science, University of Malaya, Kuala Lumpur, Malaysia

A simple catalytic chemical vapor deposition technique based on the combined logic of previously synthesized vertically aligned carbon nanotubes and pattern growth of boron nitride nanotubes (BNNTs) along with a few simple modifications in the experimental setup is successfully used for the synthesis of vertically aligned BNNTs. Field emission scanning electron microscope images show the top and side view of the as grown pure BNNTs. High-resolution transmission electron microscope images confirm the tubular structure as well as the highly crystalline nature of the tubes. X-ray photon spectroscopy and Raman spectroscopy indicate h-BN as a main constituent of BNNTs synthesized in the present work.

Keywords Align; BNNTs; CNTs; Setup; Synthesis.

INTRODUCTION

Boron nitride nanotubes (BNNTs) are sought to be a good and effective alternative for carbon nanotubes (CNTs) [1] due to its diameter independent electronic properties. However, there are certain restrictions which slow down the research and applications of BNNTs. These include high growth temperatures, low production yield, and impurities in the final product. Purity of the BNNTs is very important regarding its applications in nanotechnology, however, vertically aligned BNNTs grown in a particular pattern can be used for application without purification [2]. Due to this advantage different techniques have been tried to achieve the growth of BNNTs in the vertically aligned format. Some of them also claimed to have achieved the BNNTs in the vertically aligned format, however, the as reported vertically aligned format was not like the one reported for CNTs [2]. Some of the researchers have also tried and discovered some other techniques like pattern growth; however, majority of these techniques resulted only in partially aligned BNNTs. These BNNTs were not strong enough to hold even against a slight mechanical compression [3, 4].

Therefore, some of the ideas for the synthesis of vertically aligned BNNTs in the present work have also been taken from the strategies used for the synthesis of vertically aligned CNTs [5, 6] and pattern growth of BNNTs [7]. In these works, it has been noticed that, before deposition or growth of CNTs or BNNTs, some thin layers of catalytic materials are first deposited on Si substrate. Different reasons have been given for the deposition of these catalytic layers on Si substrate prior to the growth of CNTs or BNNTs. In the case of CNTs, Ni-coated Si substrate results in nanotubes of diameter about 100 nm, whereas the one grown on Co-coated substrate results in nanotubes of about 200 nm. In both of these cases, the as produced nanotubes are not vertically aligned. However, it has been shown that an alloy of these materials (Co–Ni alloy) results in faster etching rate of Ni particles as compared to Co in the presence of NH_3 dry etching. This faster etching of Ni particles helped in increasing the densities of nucleation sites which further helped in growing an array of vertically aligned CNTs [5]. In the case of pattern growth of BNNTs, an alumina buffer layer is first deposited on Si substrate followed by thin layers (15–30 nm) of catalyst material (MgO, Ni, or Fe). The alumina buffer layer acts as a diffusion barrier which prevents the reaction of catalysts with Si substrate which otherwise results in loss of their catalytic activity [7].

In the present work both the ideas are combined to some extent in order to synthesize vertically aligned BNNTs successfully. For this purpose, an alumina thin film is first deposited on Si substrate, to work as a diffusion barrier and to prevent the as produced Mg, Fe particles or their alloy to react with Si substrate to save their catalytic activity [7]. The as produced Mg and Fe particles (during the reaction of B, MgO, and FeO) or their alloy (Fe–Mg) are assumed to be deposited on the top of the alumina layer whereas the as produced growth precursor (B_2O_2) remains suspended in the inside atmosphere. When NH_3 is introduced into the system, it reacts separately with as deposited catalysts or their alloy and growth precursor simultaneously. When NH_3 passes the deposited catalysts, it etches away the Fe particles, with a high rate which results in an increase, in density of nucleation sites within Mg particles. The

---

Received April 21, 2014; Accepted June 9, 2014

Address correspondence to Mayeen Uddin Khandaker, Department of Physics, Faculty of Science, University of Malaya, 50603 Kuala Lumpur, Malaysia; E-mail: mu_khandaker@um.edu.my

Color versions of one or more of the figures in the article can be found online at www.tandfonline.com/lmmp.

subsequent reaction of NH_3 with a growth precursor produces a sufficient amount of BN species that diffused on the substrate. With the passage of time these species super saturate. When their vapor pressure is sufficiently increased, they grow in the form of nanotubes from Mg particles [8]. The details are mentioned in the following sections.

MATERIALS AND METHODS

Vertically aligned BNNTs are synthesized via a very simple catalytic chemical vapor deposition (CCVD). B, MgO, and γ-Fe_2O_3 [9, 10] in the form of nanoscale amorphous powder are used as precursor. A total of 100 mg precursor, containing 50 mg of boron, 25 mg of MgO, and 25 mg of γ-Fe_2O_3 (with 2:1:1 ratio) are mixed in alumina boat [9], with a conventional stirrer. An approximately 1.5 μm alumina thin film is first deposited on the shinning surface of Si substrate with the help of an e-beam evaporator. The boat is partially covered with a few Si substrates in such a way that the thin film deposited side is downward toward the precursor. The boat is then slowly placed inside one end close quartz tube near the closed end and is inserted into quartz tube chamber of a conventional horizontal tube furnace in such a way that the open end of the one end closed quartz tube is toward the gas inlet.

To remove the dust particles and create an inert atmosphere, Ar gas is flown through the system before the experimental run. The precursor is then heated in the presence of Ar gas inert atmosphere up to 1000°C with a heating rate of 10°C/min. Ar gas flow is replaced by NH_3 gas flow at 1000°C, and the system is heated up to 1200°C. After keeping the system for 60 min in such a condition, it is allowed to cool down to room temperature in the presence of Ar gas flow. At room temperature, Ar gas flow is stopped, and white color BNNTs are found deposited on Si substrate and inside alumina boat (in powder form).

RESULTS AND DISCUSSION

Figure 1(a) shows the top view of the as synthesized BNNTs in vertically aligned format. BNNTs of different sizes and morphologies can be seen in this image. Some of the BNNTs were very small in diameter (under 100 nm) whereas the other observed in the majority are seemed to be very thick (with a diameter above 100 nm). The smaller size BNNTs are seemed to be uniform in diameter, whereas the larger size BNNTs are found to have a highly non-uniform diameter. It is found that some of the larger size (diameter wise) BNNTs have steadily grown round sharp ends at the top. The top view further shows that after being grown to a certain extent, BNNTs are not able to maintain a vertical align format. Instead of being vertically aligned, most of the BNNTs are seemed to be only partially vertically aligned. This situation is somehow similar to previously synthesized vertically aligned CNTs [11], which suggest that during the growth in vertically aligned format, BNNTs (like CNTs) continuously need some kind of support to hold them in the desired format (vertical) till the end of the reaction or growth [5]. The suggestion is logical because even the CNTs grown in vertical align format have not been observed individually; rather they have been observed in the form of an array in such a way that no apparent space can be seen among them [12].

The higher magnification image shown in Fig. 1(b) gives a more clear top view of the as synthesized BNNTs. Along with sharp ends some other morphologies of the BNNTs can also be seen in the present sample. Like the previous image, BNNTs in the present image are also partially vertically aligned from a certain point.

Figure 2 shows the side view of the as synthesized vertically aligned BNNTs. In general, the image gives a good view of the vertically aligned BNNTs, however, when clearly observed, some broken morphologies of

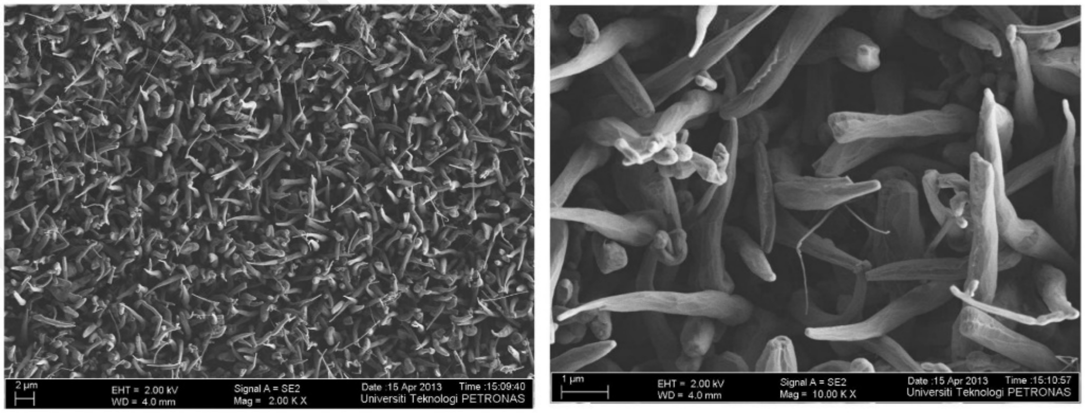

(a) (b)

FIGURE 1.—(a) Low and (b) high magnification FE-SEM images show the top view of the as synthesized vertically aligned BNNTs.

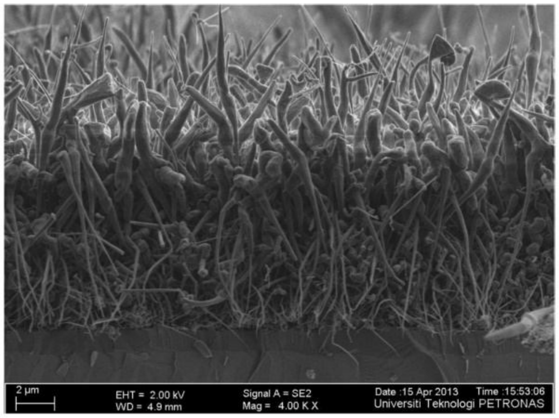

FIGURE 2.—FE-SEM image (side view) of the as synthesized BNNTs in vertically aligned format.

the BNNTs can also be seen in the given picture. The broken or randomly scattered species of the BNNTs might be due to the strong disturbance, when force was applied to break the substrate with deposited sample in order to have the vertical view (analysis) of the as synthesized BNNTs. The BNNTs thus grown are not very long and have an average length only up to ~14 µm.

The diameter of the BNNTs is highly non-uniform and found to vary continuously from top to bottom. At the bottom up to 4 µm (lengthwise) the average diameter can be found less than 100 nm. Above 4 µm in length, the diameter is found to vary continuously and reaches to a maximum range of ~580 nm and then decreases in the form of sharp round edge at the top and is estimated again to be less than 100 nm. It means that different growth mechanisms have been followed by the as synthesized BNNTs in the present sample. It is believed that, from the start up to 10 µm, tip growth mechanism might have been followed. During this process, the growth might have started with a huge diameter and then decreases continuously with increasing length of the tube. At around 10 µm, the tubes are found to have maximum diameter (~580 nm). It is believed that initially the growth might have started with this diameter. During this stage, no space was available among the BNNTs which caused them to grow only in the vertical direction. The decrease in diameter with increasing length creates some empty spaces between BNNTs. Due to these empty spaces BNNTs lose each other's support (to remain vertical) and acquire a bit curly shape. This situation is almost the same as previously observed in suggested growth mechanism for the CNTs [5]. Above the thickest point (~580 nm) in diameter, BNNTs are assumed to have followed base growth mechanism [13]. During this stage the diameter decreases gradually and reaches again under 100 nm in the form of sharp ends at the top. Thus the maximum diameter (at around 10 µm) between the two minimum diameters suggests that there might be a third growth stage which may start from the maximum diameter zone and will have both tip and base growth at the same time. During this stage rapid growth of BNNTs is assumed to occur demanding high temperature or larger growth duration [8]. As a result of this growth, the diameter of the tubes will further be decreased and will thus create more space among them. Thus the as synthesized BNNTs will either be partially vertically aligned or a bit curved up in different directions. This situation may easily be overcome by carefully optimizing the growth precursor, as

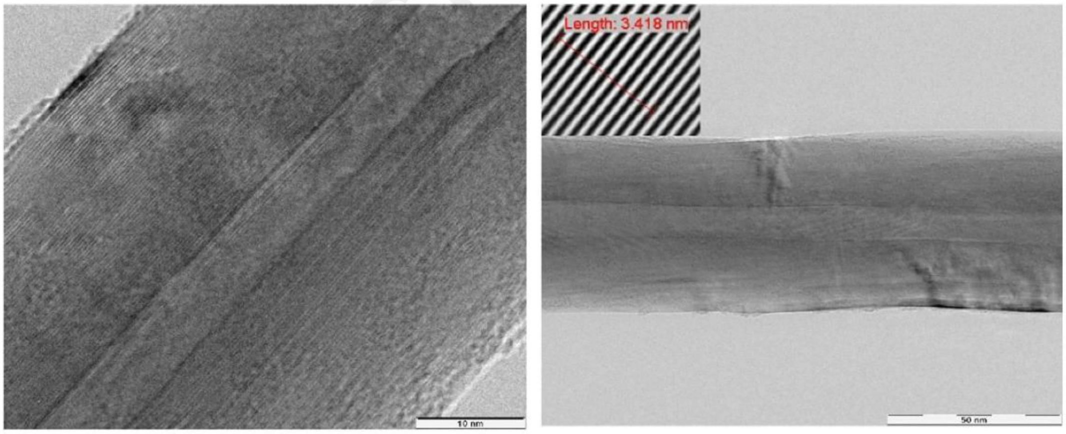

(a) (b)

FIGURE 3.—(a) HR-TEM image shows a smaller internal diameter as compared to the external diameter. (b) Lower magnification HR-TEM image of another BNNT with the same characteristics. The inset shows interplainer spacing of the BNNT.

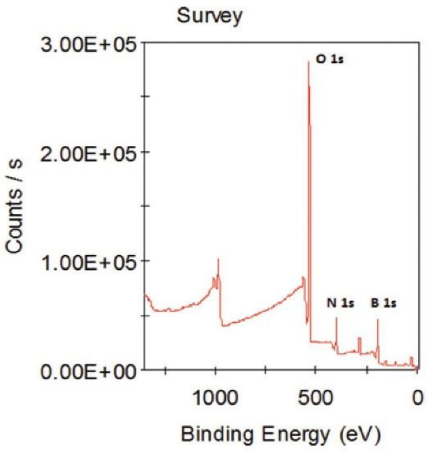

FIGURE 4.—XPS survey showing peaks for the main constituents in the as synthesized BNNTs sample.

used catalysts, affective role of etching agent, and growth duration or further increase in temperature above 1200°C.

The tubular structure of the as synthesized vertically aligned BNNTs is confirmed with the help of high-resolution transmission electron microscope (HR-TEM). The HR-TEM image of the as synthesized BNNT is shown in Fig. 3(a). The image shows that the internal diameter of the BNNT is very small as compared to the external diameter. The external part of BNNT is also found to have some parallel lines. These parallel lines are quite visible at this magnification which is the sign of highly crystalline nature of the BNNTs synthesized in the present work [14]. Figure 3(b) is HR-TEM image of another BNNT collected from the same sample. The image shows a non-uniform external and internal diameter. Like the previous one, the internal diameter of the present BNNT is also quite small and almost equal to half of the external diameter. The inset on the upper left-hand corner of Fig. 3(b) shows that the tube has an interplainer spacing of 0.34 nm which is the characteristic of d_{0002} spacing of h-BN [15], and also a proof of the crystalline nature of the as synthesized BNNTs [14].

The elemental compositions of the BNNTs sample synthesized in the present work is analyzed with the help of an X-ray photon spectroscopy (XPS). An XPS survey for the BNNTs sample synthesized in the present work is shown in Fig. 4. Several peaks have been reported in the XPS survey at 191.18, 193.68, 534.14, and 398.8 eV. The peaks at 191.18 and 398.8 eV [13, 16] represent h-BN in the as synthesized sample whereas the other peaks at 193.68 and 534.14 eV correspond to B_2O_3 or $B(OH)_3$ in the present sample [17].

To verify the constituents as reported by XPS, the as synthesized sample is further characterized with the help of Raman spectroscopy in the spectral range of 800–1600 cm^{-1}. The obtained Raman spectrum is shown in Fig. 5. The main constituents of the present sample are confirmed by a high intensity peak at 1376.56 cm^{-1} in the Raman spectrum that corresponds to E_{2g} mode of h-BN [2, 18]. An extremely smaller intensity peak is also detected at 1126.33 cm^{-1} that corresponds to boric acid which might have formed by the spontaneous reaction of boron and B_2O_3 with moisture and oxygen in the air [19]. Thus the reported values by Raman analysis are in good agreement with the XPS results.

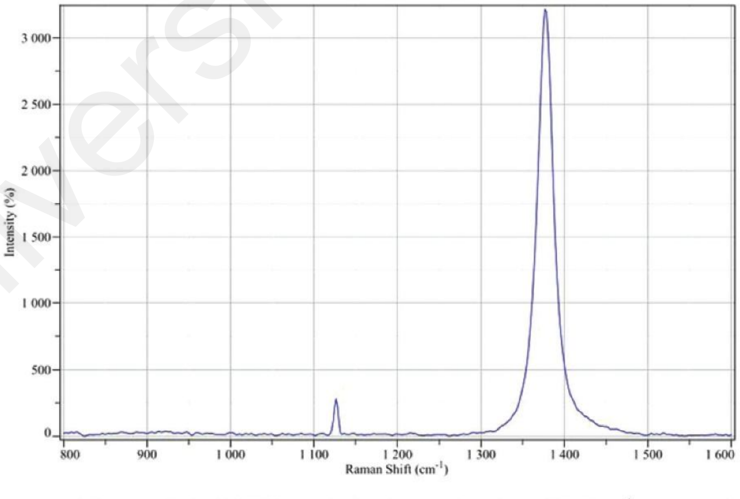

FIGURE 5.—Raman spectrum of the as synthesized BNNTs sample showing a main peak at 1376.56 cm^{-1}, correspond to E_{2g} mode of h-BN.

CONCLUSIONS

The results obtained in the present work showed that the nanotubes alignment depends on the density of the nucleation sites which further depends on etching rate of the as deposited catalysts or their alloy on the diffusion layer. The reduced etching ability of NH_3 due to its simultaneous reaction with B_2O_2 to provide nitrogen for the formation of BN-species may be the possible reason for the non-uniform diameter or relatively partially aligned nature of BNNTs in the present work, which may easily be overcome by carefully optimizing the growth precursor, as used catalysts, affective role of etching agent, and growth duration or further increase in temperature above 1200°C.

FUNDING

We are extremely grateful to Skim Bright Spark Program, University of Malaya, 50603 Kuala Lumpur, Malaysia, for providing funds and facilities for our research work.

REFERENCES

1. Oku, T.; Narita, I.; Nishiwaki, A. Synthesis, atomic structures and electronic states of boron nitride nanocage clusters and nanotubes. *Materials and Manufacturing Processes* **2004**, *19*, 1215–1239.
2. Wang, J.; Xie, M.; Khin Yap, Y. Optimum growth of vertically-aligned boron nitride nanotubes at low temperatures. *APS Meeting Abstracts* **2007**, *1*, 31008.
3. Boinovich, L.B.; Emelyanenko, A.M.; Pashinin, A.S.; Lee, C.H.; Drelich, J.; Yap, Y.K. Origins of thermodynamically stable superhydrophobicity of boron nitride nanotubes coatings. *Langmuir* **2012**, *28*, 1206–1216.
4. Lee, C.H.; Wang, J.; Kayatsha, V.K.; Huang, J.Y.; Yap, Y.K. Effective growth of boron nitride nanotubes by thermal chemical vapor deposition. *Nanotechnology* **2008**, *19*, 455605.
5. Lee, C.J.; Kim, D.W.; Lee, T.J.; Choi, Y.C.; Park, Y.S.; Lee, Y.H.; Choi, W.B.; Lee, N.S.; Park, G.-S.; Kim, J.M. Synthesis of aligned carbon nanotubes using thermal chemical vapor deposition. *Chemical Physics Letters* **1999**, *312*, 461–468.
6. Paul, A.; Bhattacharya, B. DNA functionalized carbon nanotubes for nonbiological applications. *Materials and Manufacturing Processes* **2010**, *25*, 891–908.
7. Lee, C.H.; Xie, M.; Kayastha, V.; Wang, J.; Yap, Y.K. Patterned growth of boron nitride nanotubes by catalytic chemical vapor deposition. *Chemistry of Materials* **2010**, *22*, 1782–1787.
8. Pakdel, A.; Zhi, C.Y.; Bando, Y.; Nakayama, T.; Golberg, D. A comprehensive analysis of the cvd growth of boron nitride nanotubes. *Nanotechnology* **2012**, *23*, 215601–215610.
9. Zhi, C.Y.; Bando, Y.; Terao, T.; Tang, C.C.; Kuwahara, H.; Golberg, D. Towards thermoconductive, electrically insulating polymeric composites with boron nitride nanotubes as fillers. *Advanced Functional Materials* **2009**, *19*, 1857–1862.
10. Zhi, C.; Bando, Y.; Tan, C.; Golberg, D. Effective precursor for high yield synthesis of pure bn nanotubes. *Solid State Communications* **2005**, *135*, 67–70.
11. Lee, C.J.; Park, J.; Kang, S.Y.; Lee, J.H. Growth and field electron emission of vertically aligned multiwalled carbon nanotubes. *Chemical Physics Letters* **2000**, *326*, 175–180.
12. Zhang, W.D.; Wen, Y.; Min Liu, S.; Tjiu, W.C.; Qin Xu, G.; Ming Gan, L. Synthesis of vertically aligned carbon nanotubes on metal deposited quartz plates. *Carbon* **2002**, *40*, 1981–1989.
13. Wang, J.S.; Kayastha, V.K.; Yap, Y.K.; Fan, Z.Y.; Lu, J.G.; Pan, Z.W.; Ivanov, I.N.; Puretzky, A.A.; Geohegan, D.B. Low temperature growth of boron nitride nanotubes on substrates. *Nano Letters* **2005**, *5*, 2528–2532.
14. Tanur, A.E.; Wang, J.; Leela Mohana Reddy, A.; Lamont, D.N.; Yap, Y.K.; Walker, G.C. Diameter-dependent bending modulus of individual multiwall boron nitride nanotubes. *The Journal of Physical Chemistry C* **2013**, *117*, 4618–4625.
15. Huang, Y.; Lin, J.; Tang, C.; Bando, Y.; Zhi, C.; Zhai, T.; Dierre, B.; Sekiguchi, T.; Golberg, D. Bulk synthesis, growth mechanism and properties of highly pure ultrafine boron nitride nanotubes with diameters of sub-10 nm. *Nanotechnology* **2011**, *22*, 145602.
16. Ciofani, G.; Genchi, G.G.; Liakos, I.; Athanassiou, A.; Dinucci, D.; Chiellini, F.; Mattoli, V. A simple approach to covalent functionalization of boron nitride nanotubes. *Journal of Colloid and Interface Science* **2012**, *374*, 308–314.
17. Wagner, C.; Muilenberg, G. *Handbook of x-ray photoelectron spectroscopy*. Perkin-Elmer Corporation Physical Electronics Division: Eden Prairie, MN, 1979.
18. Xu, Z.; Golberg, D.; Bando, Y. In situ TEM-STM recorded kinetics of boron nitride nanotube failure under current flow. *Nano Letters* **2009**, *9*, 2251–2254.
19. Arenal, R.; Ferrari, A.C.; Reich, S.; Wirtz, L.; Mevellec, J.Y.; Lefrant, S.; Rubio, A.; Loiseau, A. Raman spectroscopy of single-wall boron nitride nanotubes. *Nano Letters* **2006**, *6*, 1812–1816.

Available online at www.sciencedirect.com
ScienceDirect
Ceramics International 41 (2015) 4544–4548
CERAMICS INTERNATIONAL
www.elsevier.com/locate/ceramint

Synthesis of highly crystalline multilayers structures of ^{10}BNNTs as a potential neutron sensing element

Pervaiz Ahmad, Mayeen Uddin Khandaker*, Yusoff Mohd Amin

Department of Physics, Faculty of Science, University of Malaya, 50603 Kuala Lumpur, Malaysia

Received 15 November 2014; received in revised form 26 November 2014; accepted 27 November 2014
Available online 6 December 2014

Abstract

Highly crystalline multilayers structures of ^{10}B-enriched boron nitride nanotubes (^{10}BNNTs) are synthesized via a simple technique at 1200 °C. Field emission scanning electron microscopy images show randomly aligned ^{10}BNNTs with some cotton like morphologies. Transmission electron microscopy indicates highly crystalline nature of the BNNTs with internal bamboo-like structures. X-ray photon spectroscopy spectrum confirms Boron and Nitrogen elemental components of ^{10}BNNTs, whereas Raman spectroscopy reports a peak at 1390 (cm^{-1}) that relates to E_{2g} mode of ^{10}BNNTs. The synthesized ^{10}BNNTs can effectively be used as a neutron sensing element in a solid state neutron detector with a 100% suggested efficiency.

Keywords: BNNTs; ^{10}B; ^{10}BNNTs; Synthesis

1. Introduction

Hexagonal boron nitride (h-BN) is an important material for different modern and microelectronic devices. It is a wide band gap semiconductor [1–3] with a direct band gap of 5.97 eV [4]. Structure-wise, h-BN is identical to graphite, however, the carbons atoms are replaced by alternative boron and nitrogen atoms in h-BN [4]. Natural boron (B) in h-BN is found to contain ~20% of ^{10}B and ~80% of ^{11}B [5]. Thus the isotopic ratio of ^{10}B and ^{11}B in h-BN and other B-based compounds can significantly alter their physical properties [6]. The rolled up sheets of h-BN with diameter in the nanoscale range constitute the tubular structures of h-BN called boron nitride nanotubes (BNNTs). Theoretically, BNNTs were predicted in 1994 [7] and experimentally synthesized in 1995 [8]. Unlike carbon nanotubes (CNTs), BNNTs are the large band gap semiconductor with properties independent of diameter or helicity [9,10]. These properties have made it a very important material for different applications in the field of biomedical [11–13], microelectronic mechanical system (MEMS) [14] and solid state neutron detectors [15].

BNNTs have been successfully synthesized by various researchers via their own designed experimental setup and precursors. On this basis, all the techniques used for the BNNTs synthesis were named as: arc-discharge, laser ablation, template synthesis, autoclave, ball milling and chemical vapor deposition (CVD) etc. [16]. Some of the above techniques have also been employed for the synthesis of ^{10}BNNTs. Han et al. [5], first synthesized ^{10}BNNTs via CNT-substitution reaction. Commercially available 99% ^{10}B enriched $^{10}B_2O_3$ is heated in the presence of N_2 flow at 1580 °C. During the reaction molybdenum oxide is used as a promoters with MW-CNTs and $^{10}B_2O_3$. The final product is then further heated at 650 °C to separate carbon impurities. Thus the overall process is not only a bit complicated, lengthly and required higher temperature but also contained impurities [5]. Tang et al. [17] and Zhi et al. [1] introduced their own designed experimental procedures and synthesized high quality BNNTs. Their developed technique [1,17] is further employed by Han et al. [18] for the synthesis of ^{10}BNNTs with ^{10}B, MgO

---

*Corresponding author. Tel.: +601115402880; fax: +60379674146.
E-mail addresses: mu_khandaker@yahoo.com, mu_khandaker@um.edu.my (M.U. Khandaker).

http://dx.doi.org/10.1016/j.ceramint.2014.11.150

and SnO as precursors. Beside high temperature and impurities in the final product, the as-used methods were difficult to follow not only because of their complex, lengthy or time consuming procedures but also due to the high prices of as-used experimental setup and its other accessories.

Previously, we studied [19] some of the most prominently used experimental setup and analyzed it for further simplifications [20–25]. In the light of their work, the system designed is used for the synthesis of BNNTs in the presence of Ar gas as a reaction atmosphere and B, MgO and γ-Fe_2O_3 as precursors. By using this technique, high quality of BNNTs were easily synthesized at 1200 °C [19,26]. Han et al. [18] synthesized BNNTs from B, MgO and SnO as precursors. The same experimental conditions were used for the synthesis of ^{10}BNNTs except B in the precursors was replaced by ^{10}B [18]. The same idea has been utilized for the synthesis of ^{10}BNNTs in the present study. The detail of all the efforts done in this regard is fully mentioned in the next section.

2. Experimental details

The methos used for the synthesis of ^{10}BNNTs is similar to our previously reported method for BNNTs [19,26] except B powder is replaced by ^{10}B powder. In short, a 2:1:1 ratio of ^{10}B, MgO and γ-Fe_2O_3 with a total weight of 100 mg is mixed in alumina boat [27] with a conventional stirrer. A few Si substrates are placed at the top of the boat. The boat is then slowly pushed inside one-end close quartz tube. Afterwards, the tube is moved into the chamber of horizontal quartz tube furnace for further processs. Before the experimental run, the ceal closed chamber is flushed with Ar gas to remove the oxygen and dust particles from the system. The Ar gas flow is maintained at a rate of 150–200 sccm and the system is heated up to 1200 °C. When the temperature is reached to 1200 °C, Ar gas flow is stopped and NH_3 gas is introduced in to the system with the same flow rate of 150–200 sccm. The system is maintained in such a condition for 1 h. At the end of 1 h, the flow of NH_3 gas is stopped. Subsequently, the system is slowly brought to room temperature. At room temperature white colour ^{10}BNNTs can be seen deposited at the walls of alumina boat and Si-substrate, as shown in Fig. S1 (Supporting materials). The ^{10}BNNTs sample thus synthesized is characterized by: (1) Scanning Electron Microscope (Model: Zeiss Supra 55 VP) to analyze the morphology and size of the tubes, (2) Transmission Electron Microscope (Model: Zeiss Libra 200FE), to analyze the tubular structure, interlayer spacing and crystallinity, (3) X-ray Photon Spectroscopy (Model: Thermo Scientific K-Alpha) to find out the elemental composition, (4) Raman Spectroscopy (Model: Horiba Jobin Yvon HR800) to find out the crystallographic structure and crystallinity.

3. Results and discussion

Fig. 1 shows lower magnification FESEM micrograph of the ^{10}BNNTs synthesized in the present study. The micrograph shows randomly aligned ^{10}BNNTs along with some cotton like morphologies. Most of these morphologies are stuck with the curves end of the ^{10}BNNTs. These white species with ^{10}BNNTs look like raw cottons packs held with their plants. The inset magnified image on the bottom right hand corner gives a more clear view of the same ^{10}BNNTs.

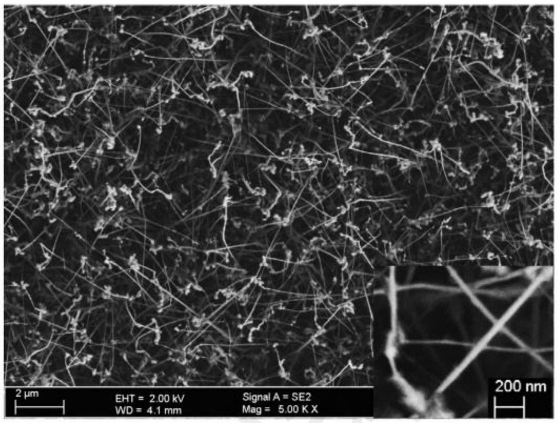

Fig. 1. Lower magnification FESEM micrograph shows randomly aligned ^{10}BNNTs along with some cotton like morphologies mostly stuck with their curves end. The inset magnified image gives a more clear view of the same ^{10}BNNTs.

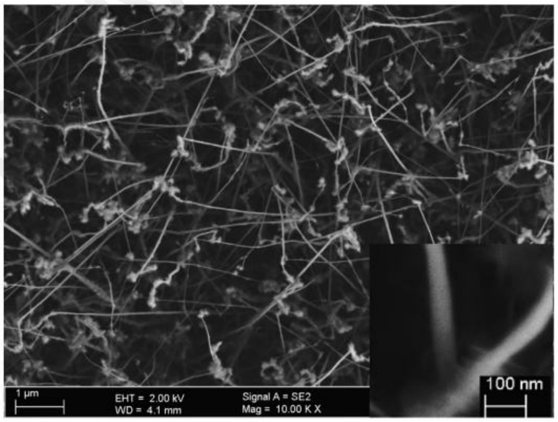

Fig. 2. High magnification FESEM micrograph displays randomly aligned ^{10}BNNTs along with some cotton like morphologies mostly stuck with their curves end. The inset highly magnified image gives a more clear view of the same ^{10}BNNTs.

Fig. 2 shows high magnification FESEM micrograph that further clarify the morphology of the randomly aligned ^{10}BNNTs and cotton like morphologies, previously shown in Fig. 1. The highly magnified inset image on the bottom right hand corner of Fig. 2 shows straight ^{10}BNNTs with cotton like species stuck at their bottom. It has been observed that the diameter of the tubes varies continuously throughout the sample. The scale in the inset image (on the bottom right hand corner of Fig. 2) indicates that the diameter of the tubes can be found in the range of 30–80 nm. The accurately calculated diameter of a few ^{10}BNNTs (in the range of 40 nm to 66 nm) with the help of an FESEM application is

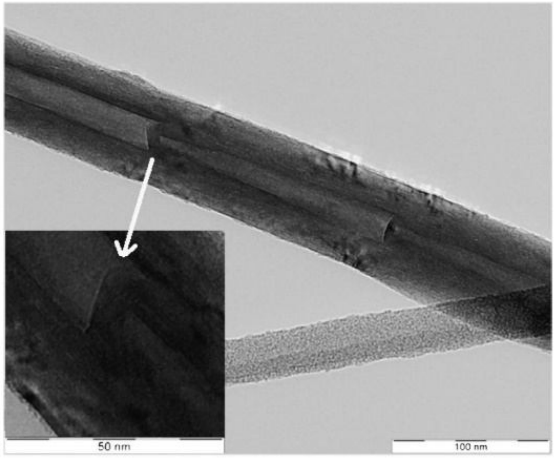

Fig. 3. TEM image shows bamboo-like structures inside ^{10}BNNT at a particular distance. The inset high resolution TEM image further clarifies the bamboo-like structure.

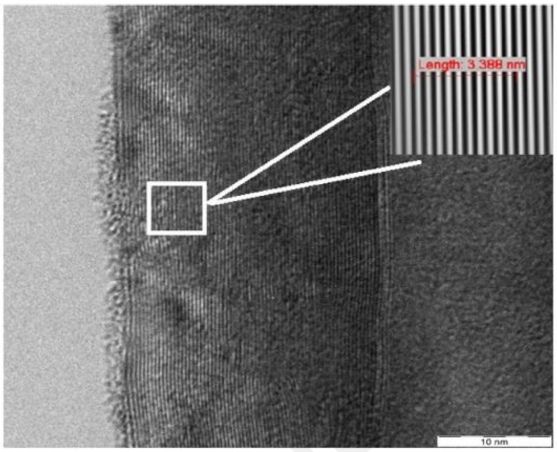

Fig. 4. Higher magnification TEM image shows parallel lines on the outer part of the ^{10}BNNT that refers to its high crystalline nature. The inset image shows that the ^{10}BNNT has an interlayer spacing of ~0.34 nm.

shown in Fig. S2 of the supporting materials. The morphology and size of the ^{10}BNNTs reported in the present study is almost similar to the BNNTs synthesized by Tanur et al. [28] via using the method introduced by Lee et al. [21]. However, it is important to note that, unlike previously reported morphologies of BNNTs [28], comparatively good results are obtained for ^{10}BNNTs in the present study via a simple experimental technique.

The tubular structure of the ^{10}BNNTs is explored via transmission electron microscopy (TEM). The TEM micrographs of the as-synthesized ^{10}BNNTs are shown in Figs. 3 and 4. TEM micrograph in Fig. 3 shows bamboo-like structures inside ^{10}BNNT at a particular distance [29]. The bamboo-like structure is further magnified and separately shown in the inset image on the bottom left hand corner of Fig. 3. The ^{10}BNNT has an average diameter of 64 nm that contained ~22 nm external diameter (or wall thickness) and ~21 nm internal diameter. The measured diameter of the as-synthesized ^{10}BNNT with the help of TEM application is shown in Fig. S3 of the supporting materials. Two bamboos can be seen in the current image at a particular distance [30]. These bamboos seem to proceed in one direction [2].

A higher resolution TEM micrograph in Fig. 4 reveals some parallel lines on the outer surface of the ^{10}BNNTs [30]. These parallel lines have an interlayer spacing of ~0.34 nm, as shown in the inset image on the top right hand corner of Fig. 4. This interlayer spacing is the characteristics of a d_{002} spacing in h-BN [22,31]. Such parallel lines and their separation (~0.34 nm) are the clear evidence of the highly crystalline nature of the ^{10}BNNTs like BNNTs [32].

The BNNTs sample synthesized in our work is also characterized via Raman spectroscopy. A laser excitation of 514 nm is used to collect raman spectrum over a spectral range of 900 to 1600 (cm^{-1}), as shown in Fig. 5. The spectrum shows two peaks (larger and smaller) at ~1390 (cm^{-1}) and ~1121.61 (cm^{-1}). The higher intensity peak at ~1390 (cm^{-1}) resembles with E_{2g} mode of ^{10}BNNTs [18] or hexagonal boron nitride (^{10}h-BN) [33], whereas the smaller peak at 1121.61 (cm^{-1}) represents H_3BO_3 in the as-synthesized sample. The as-found boric acid might be due to interaction of laser with B and moisture in the ambient atmosphere [34].

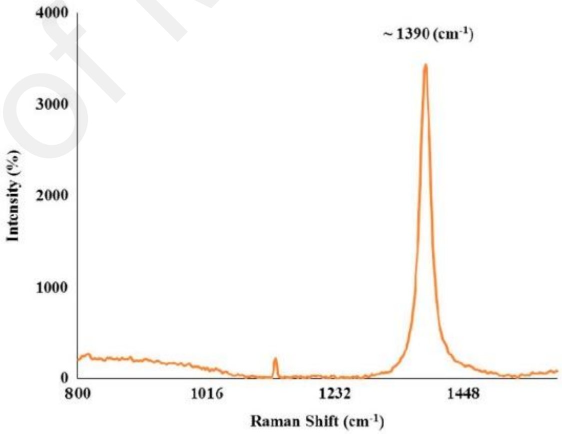

Fig. 5. Raman spectrum showing a major peak at ~1390 (cm^{-1}) for ^{10}BNNTs and a minor peak at 1121.61 (cm^{-1}) for H_3BO_3.

The elemental compositions of the as-synthesized ^{10}BNNTs sample is find out with the help of X-ray photon spectroscopy (XPS). Two peaks are reported in the XPS survey of the as-synthesized ^{10}BNNTs sample shown in Fig. 6. The B 1s peak at the binding energy of 190.5 eV and N 1s peak at 398 eV correspond to h-BN, which is in line with the previous studies [23,35,36].

A study on the use of h-BN as a neutron sensing element has made it an important material for further research in this regard. It has been suggested as a result of experimental work that the neutron detection efficiency can significantly be increased with the

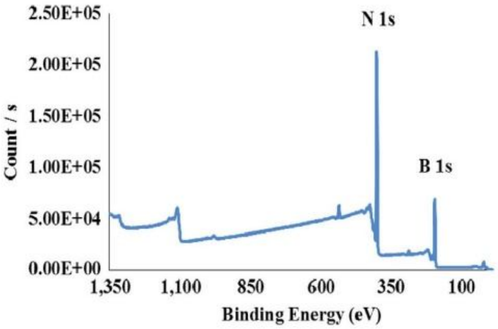

Fig. 6. XPS Spectrum showing B 1s peak at binding energy of 190.5 eV and N 1s peak at 398 eV, both of the peaks represent ^{10}BNNTs in the sample.

use of ^{10}B enriched h-BN layer. As a result, a ^{10}h-BN layer of 200 μm thickness will have the neutron detection of 98.5%, which can otherwise be achieved with a natural h-BN layer of 1 mm thickness [37]. It has further been suggested that the arrangement of ^{10}h-BN in multilayer structure with improved crystalinity can further increase the neutron detection efficiency up to 100% [37]. These suggestions were not only useful for increasing the neutron detection efficiency but also for reducing the size of radiation sensor.

The ^{10}BNNTs synthesized in the present work is different from previously reported ^{10}BNNTs [5] with respect to a few aspects. First, the ^{10}BNNTs synthesized in the present work have internal bamboo like structures whereas TEM showed no internal bamboo in the previous ^{10}BNNTs. Second, previously synthesized ^{10}BNNTs has layered structure with number of walls from one to six whereas the present ^{10}BNNTs are multilayered with number of walls greater than fifty. Furthermore, each wall of the ^{10}BNNTs is separated from the other with a numerical value of ∼0.34 nm. This numerical value is the characteristics of highly crystalline nature of the ^{10}BNNTs [32].

The potential use of natural BNNTs or other nanostructures of h-BN as a neutron sensing element has already been proposed in our previous work [15,36,38] in the light of available literature and experimental work done by Li et al. [37]. However, in the previous case, only nanoscale properties, multilayered structure and crystalline nature of BNNTs etc. was considered. The only 20% of ^{10}B enrichement in natural BNNTs is caused to prevent the cent percent suggested efficiency of solid state neutron detector. The as synthesized ^{10}BNNTs with nanoscale properties, multilayered structure, crystalline nature and ^{10}B enirchement can be an excellent choice as a sensing element in a solid state neutron detector with 100% proposed efficiency [37].

4. Conclusions

The fabrication of ^{10}BNNTs in the present work has proved that the Ar-assisted thermal CVD technique for the BNNTs is equally applicable for the synthesis of ^{10}BNNTs. Thus, the present work will not only encourage the new researchers to efficiently and effectively synthesize ^{10}BNNTs but will also help in further and rapid study of the as-synthesized product for different applications in the field of biomedical, micro electro mechanical system and solid state neutron detectors.

Acknowledgements

We are extremely thankful to Skim Bright Spark Program, University of Malaya, 50603 Kuala Lumpur, Malaysia, for providing funds and facilities for our research work.

Appendix A. Supporting information

Supplementary data associated with this article can be found in the online version at http://dx.doi.org/10.1016/j.ceramint.2014.11.150.

References

[1] C. Zhi, Y. Bando, C. Tan, D. Golberg, Effective precursor for high yield synthesis of pure BN nanotubes, Solid State Commun. 135 (2005) 67–70.
[2] J. Wang, L. Zhang, G. Zhao, Y. Gu, Z. Zhang, F. Zhang, W. Wang, Selective synthesis of boron nitride nanotubes by self-propagation high-temperature synthesis and annealing process, J. Solid State Chem. 184 (2011) 2478–2484.
[3] J. Pouch, S. Alterovitz, A review of: "Synthesis and properties of boron nitride", Mater. Manuf. Processes 6 (1991) 373–374.
[4] A. Pakdel, C. Zhi, Y. Bando, T. Nakayama, D. Golberg, A comprehensive analysis of the CVD growth of boron nitride nanotubes, Nanotechnology 23 (2012) 215601.
[5] W.-Q. Han, P.J. Todd, M. Strongin, Formation and growth mechanism of 10 BN nanotubes via a carbon nanotube—substitution reaction, Appl. Phys. Lett. 89 (2006) (173103-173103-173103).
[6] J. Matsuoka, M. Numaguchi, Y. Fujino, M. Matsuo, S. Kurose, S. Yoshida, N. Soga, Isotope effects on the glass transition phenomena and thermal properties of B_2O_3 glass, J. Non-Cryst. Solids 345 (2004) 542–545.
[7] A. Rubio, J.L. Corkill, M.L. Cohen, Theory of graphitic boron nitride nanotubes, Phys. Rev. B: Condens. Matter 49 (1994) 5081–5084.
[8] N.G. Chopra, R. Luyken, K. Cherrey, V.H. Crespi, M.L. Cohen, S.G. Louie, A. Zettl, Boron nitride nanotubes, Science 269 (1995) 966–967.
[9] M. Ishigami, S. Aloni, A. Zettl, Properties of boron nitride nanotubes, in: AIP Conference Proceedings, 2003, pp. 94–99.
[10] T. Oku, I. Narita, A. Nishiwaki, Synthesis, atomic structures, and electronic states of boron nitride nanocage clusters and nanotubes, Mater. Manuf. Processes 19 (2004) 1215–1239.
[11] C. Tang, Y. Bando, C. Zhi, D. Golberg, Boron–oxygen luminescence centres in boron–nitrogen systems, Chem. Commun. (2007) 4599–4601.
[12] J. Wu, W.-Q. Han, W. Walukiewicz, J. Ager, W. Shan, E. Haller, A. Zettl, Raman spectroscopy and time-resolved photoluminescence of BN and $B_xC_yN_z$ Nanotubes, Nano Lett. 4 (2004) 647–650.
[13] P. Jaffrennou, J. Barjon, T. Schmid, L. Museur, A. Kanaev, J.-S. Lauret, C. Zhi, C. Tang, Y. Bando, D. Golberg, Near-band-edge recombinations in multiwalled boron nitride nanotubes: cathodoluminescence and photoluminescence spectroscopy measurements, Phys. Rev. B: Condens. Matter 77 (2008) 235422.
[14] H. Harutyunyan, T. Gokus, A.A. Green, M.C. Hersam, M. Allegrini, A. Hartschuh, Defect-induced photoluminescence from dark excitonic states in individual single-walled carbon nanotubes, Nano Lett. 9 (2009) 2010–2014.
[15] P. Ahmad, N.M. Mohamed, Z.A. Burhanudin, B. Ari-Wahjoedi, R. Razali, M. Narahari, A review of nanostructured based radiation sensors for neutron, AIP Conf. Proc.-Am. Inst. Phys. (2012) 535.

[16] C. Zhi, Y. Bando, C. Tang, D. Golberg, Boron nitride nanotubes, Mater. Sci. Eng., R 70 (2010) 92–111.

[17] C. Tang, Y. Bando, T. Sato, K. Kurashima, A novel precursor for synthesis of pure boron nitride nanotubes, Chem. Commun. (2002) 1290–1291.

[18] W.Q. Han, H.G. Yu, C. Zhi, J. Wang, Z. Liu, T. Sekiguchi, Y. Bando, Isotope effect on band gap and radiative transitions properties of boron nitride nanotubes, Nano Lett. 8 (2008) 491–494.

[19] P. Ahmad, M. Khandaker, Y. Amin, A comprehensive study of boron nitride nanotubes multiple synthesis from a single precursor, Indian J. Phys., 1–8.

[20] C. Zhi, Y. Bando, C. Tang, D. Golberg, R. Xie, T. Sekigushi, Phonon characteristics and cathodolumininescence of boron nitride nanotubes, Appl. Phys. Lett. 86 (2005) (213110-213110-213113).

[21] C.H. Lee, J. Wang, V.K. Kayatsha, J.Y. Huang, Y.K. Yap, Effective growth of boron nitride nanotubes by thermal chemical vapor deposition, Nanotechnology 19 (2008) 455605.

[22] Y. Huang, J. Lin, C. Tang, Y. Bando, C. Zhi, T. Zhai, B. Dierre, T. Sekiguchi, D. Golberg, Bulk synthesis, growth mechanism and properties of highly pure ultrafine boron nitride nanotubes with diameters of sub-10 nm, Nanotechnology 22 (2011) 145602.

[23] J.S. Wang, V.K. Kayastha, Y.K. Yap, Z.Y. Fan, J.G. Lu, Z.W. Pan, I.N. Ivanov, A.A. Puretzky, D.B. Geohegan, Low temperature growth of boron nitride nanotubes on substrates, Nano Lett. 5 (2005) 2528–2532.

[24] R. Ma, Y. Bando, T. Sato, K. Kurashima, Growth, morphology, and structure of boron nitride nanotubes, Chem. Mater. 13 (2001) 2965–2971.

[25] D. Golberg, Y. Bando, C.C. Tang, C.Y. Zhi, Boron nitride nanotubes, Adv. Mater. 19 (2007) 2413–2432.

[26] P. Ahmad, M.U. Khandaker, Y.M. Amin, Synthesis of boron nitride nanotubes by Argon supported thermal chemical vapor deposition, Physica E 67 (2015) 33–37.

[27] C.Y. Zhi, Y. Bando, T. Terao, C.C. Tang, H. Kuwahara, D. Golberg, Towards thermoconductive, electrically insulating polymeric composites with boron nitride nanotubes as fillers, Adv. Funct. Mater. 19 (2009) 1857–1862.

[28] A.E. Tanur, J. Wang, A.L. Reddy, D.N. Lamont, Y.K. Yap, G.C. Walker, Diameter-dependent bending modulus of individual multiwall boron nitride nanotubes, J. Phys. Chem. B 117 (2013) 4618–4625.

[29] D. Ozmen, N.A. Sezgi, S. Balci, Synthesis of boron nitride nanotubes from ammonia and a powder mixture of boron and iron oxide, Chem. Eng. J. 219 (2013) 28–36.

[30] X.J. Wu, W. An, X.C. Zeng, Chemical functionalization of boron-nitride nanotubes with NH_3 and amino functional groups, J. Am. Chem. Soc. 128 (2006) 12001–12006.

[31] P. Ahmad, M.U. Khandaker, Y.M. Amin, Effective synthesis of vertically aligned boron nitride nanotubes via a simple CCVD, Mater. Manuf. Processes (2014).

[32] A.E. Tanur, J. Wang, A. Leela Mohana Reddy, D.N. Lamont, Y.K. Yap, G.C. Walker, Diameter- dependent bending modulus of individual multiwall boron nitride nanotubes, J. Phys. Chem. C (2013).

[33] Z. Xu, D. Golberg, Y. Bando, In situ TEM-STM recorded kinetics of boron nitride nanotube failure under current flow, Nano Lett. 9 (2009) 2251–2254.

[34] R. Arenal, A.C. Ferrari, S. Reich, L. Wirtz, J.Y. Mevellec, S. Lefrant, A. Rubio, A. Loiseau, Raman spectroscopy of single-wall boron nitride nanotubes, Nano Lett. 6 (2006) 1812–1816.

[35] G. Ciofani, G.G. Genchi, I. Liakos, A. Athanassiou, D. Dinucci, F. Chiellini, V. Mattoli, A simple approach to covalent functionalization of boron nitride nanotubes, J. Colloid Interface Sci. 374 (2012) 308–314.

[36] P. Ahmad, M.U. Khandaker, Y.M. Amin, Z.R. Khan, Synthesis of boron nitride microtubes and formation of boron nitride nanosheets, Mater. Manuf. Processes (2014).

[37] J. Li, R. Dahal, S. Majety, J. Lin, H. Jiang, Hexagonal boron nitride epitaxial layers as neutron detector materials,, Nucl. Instrum. Methods Phys. Res., Sect. A 654 (2011) 417–420.

[38] P. Ahmad, M.U. Khandaker, Z.R. Khan, Y.M. Amin, A simple technique to synthesize pure and highly crystalline boron nitride nanowires, Ceram. Int. 40 (2014) 14727–14732.

Available online at www.sciencedirect.com
ScienceDirect
Ceramics International 40 (2014) 14727–14732
CERAMICS INTERNATIONAL
www.elsevier.com/locate/ceramint

A simple technique to synthesize pure and highly crystalline boron nitride nanowires

Pervaiz Ahmad, Mayeen Uddin Khandaker*, Ziaul Raza Khan, Yusoff Mohd Amin

Department of Physics, Faculty of Science, University of Malaya, 50603 Kuala Lumpur, Malaysia

Received 3 May 2014; received in revised form 11 June 2014; accepted 11 June 2014
Available online 19 June 2014

Abstract

Unlike various complex and extensive experimental procedures available in the literature, a simple experimental technique has been developed to synthesize boron nitride nanowires (BNNWs) on Si substrates in a short growth duration of 30 min via vapor–liquid–solid (VLS) growth mechanism. The surface morphology and diameter of BNNWs were obtained by field emission scanning electron microscopy (FESEM) and high resolution transmission electron microscopy (HR-TEM). The as-grown boron nitride nanowires have a wire-like morphology with diameter in the range of ~20–150 nm. The Raman spectrum of the synthesized BNNWs showed a sharp and intense peak at 1380 (cm^{-1}) corresponds to the E_{2g} mode of vibration in h-BN depicted its highly crystalline nature. This work reveals that a modified CVD technique and short growth duration is suitable to synthesis nanowires with tens of nanometers in diameter.

Keywords: A. Chemical preparation; B. Electron microscopy; B. X-ray methods; E. Sensors; BNNWs

1. Introduction

The study of nanostructured materials has revealed that the electrical, mechanical and optical properties of these materials are totally different from their bulk counterpart due to electrons and holes confinement, surface effects and geometrical confinement of the phonon [1]. Therefore, the desired properties of materials can be achieved for potential applications through their size tailoring from bulk to nano [2,3]. Boron nitride is a promising material due to its remarkable properties for different applications in the modern world. These properties included the hardness, high melting point, low dielectric constant and large band gap etc. It exists in three different crystalline forms; hexagonal (h-BN), cubic (c-BN) and wurtzite (w-BN). Hexagonal boron nitride is a wide band gap semiconductor [4]. It has a direct band gap of 5.97 eV [5]. It is the normal phase of BN which is stable at room temperature and pressure. Its structure is similar to that of graphite but alternative boron and nitrogen atoms substitute for carbon atoms [6]. Boron nitride nanotubes (BNNTs) [7], and BNNWs are the low dimensional structures of h-BN. BNNTs are the hollow cylindrical structures of h-BN with diameter in the nanoscale range and length up to several micrometers [8]. It is found to be a very promising material [9], for different biomedical applications such as therapeutic or diagnostic procedures due to its possible non-cytotoxic nature [10–12]. The uniform distribution of Fe_3O_4 nanoparticles on the BNNTs surface introduced magnetic behavior in BNNTs [13]. This behavior of BNNTs might be very useful in Micro Electro Mechanical System (MEMS) and targeted drug delivery [14]. BNNTs, being nanostructure with improved properties, can be effectively used as a neutron sensing element in a solid state neutron detector [15]. Unlike BNNTs, BNNWs are the filled cylindrical structure of h-BN with at least one dimension in the nanoscale range. Its properties and advantages for different applications are dependent on its purity and size which in turn depends on the synthesis methods. In some of the synthesis methods, BNNWs are reported along with BNNTs. The production

---

*Corresponding author. Tel.: +60 379674099; fax: +60 379674146.
E-mail addresses: mu_khandaker@yahoo.com, mu_khandaker@um.edu.my (M.U. Khandaker).

http://dx.doi.org/10.1016/j.ceramint.2014.06.061
0272-8842/

of the BNNWs in these techniques seem to be unexpected, as no separate method has been described or claimed for their synthesis [16]. BNNWs have been obtained over α-FeB nanoparticles by the reaction of a mixer of NH_3 and N_2; however, this method is a bit complex and quite lengthy as far as the synthesis of α-FeB or FeB and final product is concerned [17]. Ball-milling and annealing methods were also used, and BNNWs were synthesized on a stainless steel substrate covered by B solution [18]; however, again the method shown is quite lengthy and a bit difficult to be followed by other researchers. CVD technique was also utilized, and BNNWs were synthesized directly on stainless steel substrate. Stainless steel was used not only as a substrate but also as a catalyst. The overall method was claimed to be simple and useful for obtaining high quality BNNWs. However, the method is quite lengthy, especially in the milling of initial precursor and somewhat the duration of the final reaction [19]. Some other synthesis methods have also been reported for BNNWs [20–22], however, like all the above techniques, they are either very difficult or complex, or the used precursors are hazardous and may cause serious health problems.

In view of all the lengthy and complex procedures, a very simple and short procedure has been developed for the synthesis of pure BNNWs. The present experimental set up is quite different from the one already reported for the synthesis of BNNTs [23–25]. However, no further modification was done in it after it has been successfully used for the synthesis of BNNTs. The present findings focused on the influence of growth duration on the final product. In this study, we have successfully synthesized BNNWs in a short growth duration of 30 min, and then investigated the surface morphology, structural properties and elemental analysis in details.

2. Experimental details

2.1. Synthesis procedure

Boron nitride nanowires were synthesized via a simple catalytic chemical vapor deposition technique at 1200 °C in growth duration of 30 min. Amorphous Boron, MgO and γ- Fe_2O_3 nano-powder are used as the precursors. First, 400 mg of precursors are mixed in a weight ratio of 2:1:1 in an alumina combustion boat. The boat was covered with a few Si substrates and placed inside one end closed quartz tube near the closed end [26]. The one end closed quartz tube is then inserted into the quartz tube chamber of the dual zone furnace in such a way that the open end of the one end closed quartz tube was toward the gas inlet. Before heating, Ar gas is flown through the system to remove the dust particle, and to create an inert atmosphere [27]. The precursors are then heated up to 1200 °C at a rate of 10 °C/min in the presence of Ar gas flow at a rate of 100–200 sccm. At 1200 °C, Ar gas flow is replaced by NH_3 gas flow at a rate of 200–300 sccm for a growth duration of 30 min. After 30 min NH_3 flow is stopped, and the system was allowed to cool down to room temperature in the presence of Ar gas flow. After cooling the furnace to room temperature, white color BNNWs were found on the Si substrate and on the inner wall of alumina boat (weighted approximately 80 mg in powder form), as shown in Fig. S1 (of the supporting material). The as-synthesized sample on the Si-substrate was then characterized by using FESEM, Raman spectroscopy, X-ray photoelectron spectroscopy and HR-TEM. The details of all the characterizations are discussed in the Results and discussion section.

2.2. Growth mechanism

A cap like morphology of BNNWs in HR-TEM image shown in Fig. 3(b) suggested that the nanowires growth is based on the vapor liquid solid (VLS) mechanism [19]. A detailed schematic diagram of VLS growth mechanism is shown in Fig. 1. The BNNWs have been synthesized by the various researchers based on same growth mechanism. Boron at higher temperature reacts with metal oxides catalyst particles and forms $B_2O_{2(g)}$ vapors, MgB_2 and partially melted Fe catalyst particles. The catalyst (Fe) particles react with Si-substrate and lose it catalytic properties. It then starts working as diffusion barrier that prevents other species or catalysts to react with the Si-substrate [24]. At sufficient partial vapor pressure, the partially melted MgB_2

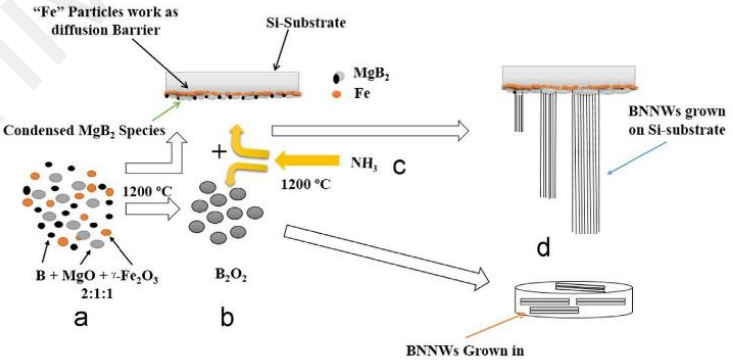

Fig. 1. Schematic diagram of vapor–liquid–solid (VLS) growth mechanism of BNNWs (a) Boron, MgO, γ-Fe_2O_3 are mixed in 2:1:1 ratio. (b) Formation of $B_2O_{2(g)}$ and Diffusion of Fe catalytic particle on Si substrate, condensation of as-formed partially melted MgB_2 species upon Fe catalyst on Si substrate. (c) Flow and decomposition of NH_3 at 1200 °C. (d) Growth of BNNWs from the reaction of MgB_2 and N_2 (from decomposed NH_3) on Si-substrate and from the reaction of B_2O_2 and N_2 (from decomposed NH_3) in Al_2O_3 boat.

species are condensed on the Si-substrate. At higher temperature (1200 °C) $NH_{3\,(g)}$ decomposed into N_2 and H_2. N_2 reacts with MgB_2 to start BNNWs. During the growth process, the melted nano size of Mg drops works as a catalyst/host and pattern for the BNNWs. The growth is assumed to have continued till Mg is either oxidized to MgO or fully covered by the BN species [5]. At the same time $B_2O_{2(g)}$ vapors react with N_2 from decomposed NH_3 and form BNNWs inside the boat.

3. Results and discussion

The aim of the present work was to modify/simplify the well-established experimental set-up and parameters in order to find out its effects on the as-synthesized final product. For this purpose the previously used experimentally set-up [23,24] was modified in such a way that the open end of the one end closed inner quartz tube was toward the gas inlet. Furthermore, Ar gas was used as an alternative for vacuum which has further simplified the experimental set-up by eliminating the use of vacuum pump and gauges. Finally BNNWs were successfully synthesized via a simple and self-modified CVD technique. In the present work, the growth duration was fixed as 30 min which resulted in the form of BNNWs, whereas different sizes and morphologies of the BNNTs have been reported with the same growth duration elsewhere [24]. The modification of experimental set-up w.r.t. the conventional CVD may be the reason of formation of BNNWs in this work. Thus the present work is important not only for the synthesis of BNNWs but also for different experimental parameters which result in different nanostructured materials. A summary of all the possible factors in CVD technique that have resulted in different BN nanostructures is presented in Table 1.

Field Emission Scanning Electron Microscopy (FESEM) was used to study the morphology of the as-synthesized BNNWs. Figs. 2(a) and (b) show the FESEM low and high magnification images of the BNNWs synthesized at 1200 °C within a growth duration of 30 min on Si substrates. At low magnification, the BNNWs look like pieces of silky wires folded and agglomerated in a random direction. At higher magnification, the silky wires-like structures are more clearly observed. The wires are bended from point to point along with varying thickness. Some of the wires are appeared to be very thick along with some other very thin below or in between the thick one. The color of the BNNWs changes from white to blackish white from top to bottom. The diameter of the wires is found to be in the range of 20–150 nm with a length of ~10 μm [28]. The calculated diameter of some of the BNNWs using FE-SEM is shown in Fig. S2 (of the supporting materials).

The as-synthesized BNNWs morphology is also analyzed with the help of high resolution transmission electron microscope (HR-TEM). The details of the wire-like structure of the BNNWs are shown in Figs. 3(a)–(c). In the low resolution HR-TEM image, shown in Fig. 3a, few nanowires with variable diameters can be seen. The HR-TEM image analysis showed a highly non-uniform structure of the BNNWs that vary in diameter from point to point. No tubular structure was

Table 1
A comparison of different experimental parameters and as-produced BN nanostructures.

S. no	Growth duration (min)	Experimental setup			Final product	References
		Inner atmosphere	Inner test tube type	Inner test tube orientation		
1	30	Vacuum	One end closed	Closed end toward gas inlet	BNNTs	[24]
2	30	Vacuum	Both end opened	Both end opened	BNNTs	[40]
3	30	Ar gas	One end closed	Open end toward the gas inlet	BNNWs	Present work

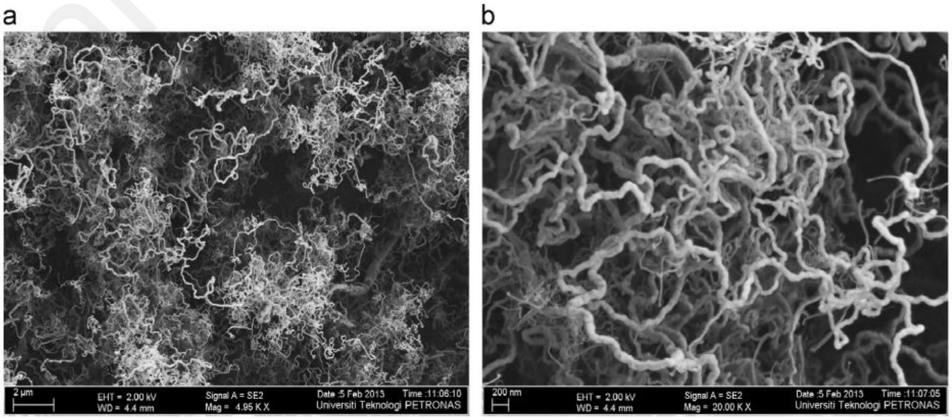

Fig. 2. (a) Low and (b) high magnification FE-SEM images of BNNWs synthesized at 1200 °C.

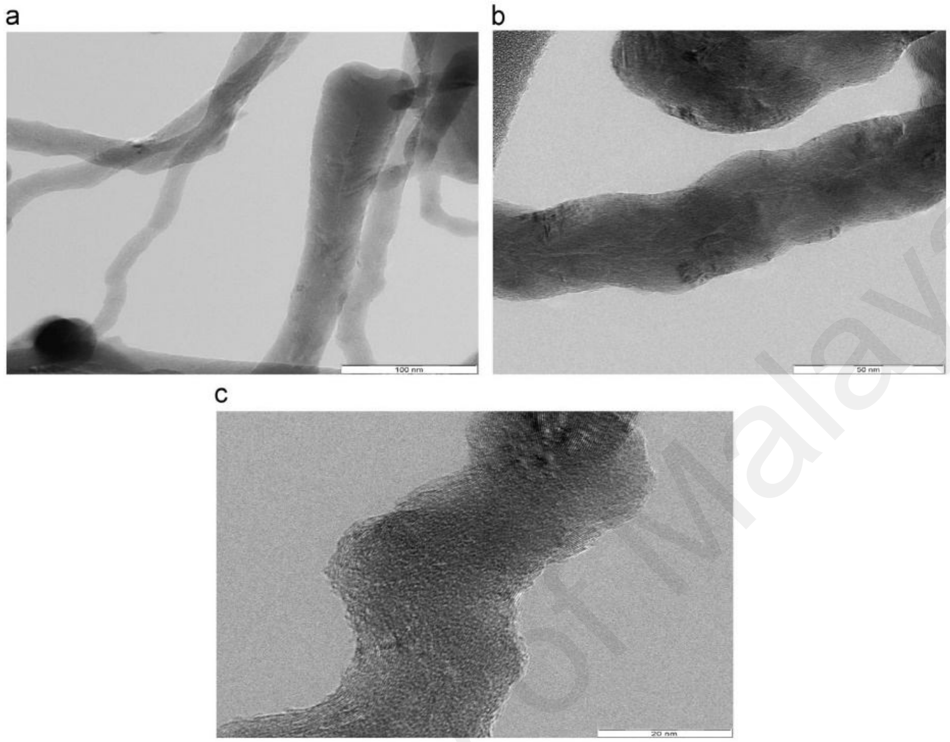

Fig. 3. (a) Low, (b) and (c) high magnification TEM images of BNNWs synthesized at 1200 °C.

observed in the present sample which confirmed that the as-formed structure was a nanowire. This morphology is a bit similar to the one reported earlier [16,29]. The average diameter for some of these BNNWs is calculated from the data given in Fig. S3 (of the supporting material) and found to be 45.64 nm and 24.78 nm respectively, which is consistent with the FE-SEM results. Along with clearly observed wire-like structure, a crack-like sign can also be found lengthwise; however, this crack-like morphology is seemed to be some kind of material (ethanol) that might have left on the BNNW while preparing the TEM copper grid for TEM analysis of the as-synthesized sample. Higher magnification HR-TEM image is shown in Fig. 3(b), the wire-like morphology of the BNNWs was more clearly observed. Along with the wire-like structure, some parallel lines on the outer side of the BNNWs are appeared (shown in Fig. 3(c)). These parallel lines are clearly shown in Fig. S4 of the supporting materials. The appearance of these parallel lines showed that the as-grown BNNWs are multi-walled with inter layer spacing of ~0.35 nm. This interlayer spacing is the evidence of high crystalline nature of BNNWs [4,30]. Due to this high crystalline nature of BNNWs, they are found to be of great importance in solid state neutron detector [31].

X-ray Photon Spectroscopy (XPS) is used to analyze the elemental composition of BNNWs synthesized at 1200 °C within a growth duration of 30 min. The XPS spectrum is shown in Fig. 4. From Fig. 4, it can be seen that several peaks centered at 191.3 eV, 193.8 eV, 398.58 eV and 533.38 eV. The B 1s peak centered at 191.3 eV and N 1s peak at 398.58 eV correspond to h-BN [29,32]. Whereas the peaks at 533.38 eV and 193.8 eV are for the O 1s and B 1s that correspond to B_2O_3 in the as-synthesized sample [33].

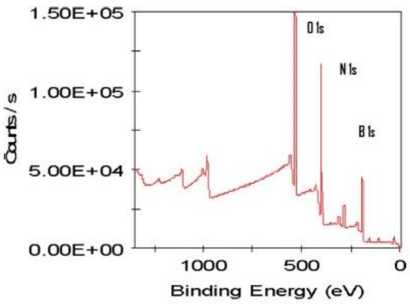

Fig. 4. XPS spectrum of BNNWs synthesized at 1200 °C.

The structural property of as-synthesized BNNWs is investigated using Raman spectroscopy. The Raman spectrum of the as-synthesized BNNWs is recorded by laser excitation of 514 nm over the spectral range of 800–1600 (cm^{-1}). Raman spectrum of BNNWs sample is shown in Fig. 5. Two peaks have been observed in the Raman spectrum with highly intense

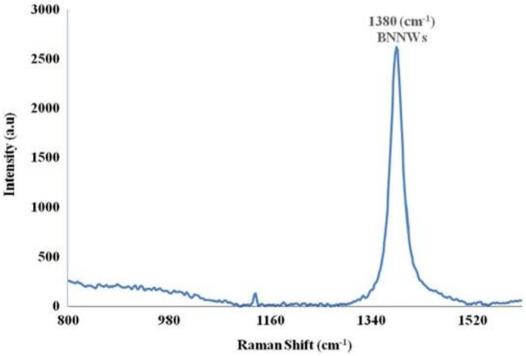

Fig. 5. Raman spectrum of BNNWs synthesized at 1200 °C.

peak centered over ~1380 (cm^{-1}). This high intensity dominant peak at ~1380 (cm^{-1}) corresponds to the E_{2g} mode of h-BN [34]. The Raman shift with sharp and intense peak with smaller value of full width half maxima (FWHM) confirmed the highly crystalline nature of the synthesized BNNWs [9]. The lower intense peak detected at ~1130 (cm^{-1}) corresponds to boric acid (negligible quantity). This small amount of boric acid is assumed to have formed by the spontaneous reaction of boron and B_2O_3 with moisture and oxygen in the air [35].

4. Conclusions

BNNWs have been synthesized by a simple Chemical Vapor Deposition technique at 1200 °C with growth duration of 30 min in a conventional horizontal dual zone quartz tube furnace on Si-substrate and inside alumina boat. The relatively short growth duration and changes in the experimental parameters are considered to be the main reasons for the synthesis of BNNWs in the present work. The Ar gas has proven to be not only effective alternative for vacuum but also helped in simplifying the experimental set up. The as-synthesized BNNWs look like pieces of silky wires folded and agglomerated in a random direction with a diameter in the range of 20–150 nm and length of greater than 10 μm. The wire like morphology of BNNWs has further been confirmed by HR-TEM analysis. XPS and Raman spectroscopy analysis showed that the as-synthesized sample to be made of h-BN. The sharp and intense peak centered at the ~1380 (cm^{-1}) in Raman spectrum reveals that the as-synthesize BNNWs has highly crystalline nature.

Acknowledgments

We are extremely grateful to Prof. Dr. Norani Muti Mohamed, Director of COINN and MOR Nanotechnology, University of Technology PETRONAS Malaysia for providing Lab and characterization facilities, and for her valuable discussion. We are also grateful to Skim Bright Spark Program, University of Malaya, 50603 Kuala Lumpur, Malaysia, for providing funds and facilities for our research work.

Appendix A. Supporting information

Supplementary data associated with this article can be found in the online version at http://dx.doi.org/10.1016/j.ceramint.2014.06.061.

References

[1] J. Lauret, R. Arenal, F. Ducastelle, A. Loiseau, M. Cau, B. Attal-Tretout, E. Rosencher, L. Goux-Capes, Optical transitions in single-wall boron nitride nanotubes, Phys. Rev. Lett. 94 (2005) 037405.
[2] P. Jaffrennou, F. Donatini, J. Barjon, J.-S. Lauret, A. Maguer, B. Attal-Trétout, F. Ducastelle, A. Loiseau, Cathodoluminescence imaging and spectroscopy on a single multiwall boron nitride nanotube, Chem. Phys. Lett. 442 (2007) 372–375.
[3] C. Zhi, Y. Bando, C. Tang, D. Golberg, R. Xie, T. Sekigushi, Phonon characteristics and cathodolumininescence of boron nitride nanotubes, Appl. Phys. Lett. 86 (2005) 213110–213113.
[4] J. Wang, L. Zhang, G. Zhao, Y. Gu, Z. Zhang, F. Zhang, W. Wang, Selective synthesis of boron nitride nanotubes by self-propagation high-temperature synthesis and annealing process, J. Solid State Chem. 184 (2011) 2478–2484.
[5] A. Pakdel, C. Zhi, Y. Bando, T. Nakayama, D. Golberg, A comprehensive analysis of the CVD growth of boron nitride nanotubes, Nanotechnology 23 (2012) 215601.
[6] Y.N. Xu, W. Ching, Calculation of ground-state and optical properties of boron nitrides in the hexagonal, cubic, and wurtzite structures, Phys. Rev. B 44 (1991) 7787.
[7] Y. Huang, J. Lin, C. Tang, Y. Bando, C. Zhi, T. Zhai, B. Dierre, T. Sekiguchi, D. Golberg, Bulk synthesis, growth mechanism and properties of highly pure ultrafine boron nitride nanotubes with diameters of sub-10 nm, Nanotechnology 22 (2011) 145602.
[8] X. Chen, X. Gao, H. Zhang, Z. Zhou, W. Hu, G. Pan, H. Zhu, T. Yan, D. Song, Preparation and electrochemical hydrogen storage of boron nitride nanotubes, J. Phys. Chem. B 109 (2005) 11525–11529.
[9] Y. Huang, J. Lin, C.C. Tang, Y. Bando, C.Y. Zhi, T.Y. Zhai, B. Dierre, T. Sekiguchi, D. Golberg, Bulk synthesis, growth mechanism and properties of highly pure ultrafine boron nitride nanotubes with diameters of sub-10 nm, Nanotechnology 22 (2011).
[10] C. Tang, Y. Bando, C. Zhi, D. Golberg, Boron–oxygen luminescence centres in boron–nitrogen systems, Chem. Commun. (2007) 4599–4601.
[11] J. Wu, W.-Q. Han, W. Walukiewicz, J. Ager, W. Shan, E. Haller, A. Zettl, Raman spectroscopy and time-resolved photoluminescence of BN and B *x* C *y* N *z* Nanotubes, Nano Lett. 4 (2004) 647–650.
[12] P. Jaffrennou, J. Barjon, T. Schmid, L. Museur, A. Kanaev, J.-S. Lauret, C. Zhi, C. Tang, Y. Bando, D. Golberg, Near-band-edge recombinations in multiwalled boron nitride nanotubes: cathodoluminescence and photoluminescence spectroscopy measurements, Phys. Rev. B 77 (2008) 235422.
[13] Y. Huang, J. Lin, Y. Bando, C.C. Tang, C.Y. Zhi, Y.G. Shi, E. Takayama-Muromachi, D. Golberg, BN nanotubes coated with uniformly distributed Fe_3O_4 nanoparticles: novel magneto-operable nanocomposites, J. Mater. Chem. 20 (2010) 1007–1011.
[14] H. Harutyunyan, T. Gokus, A.A. Green, M.C. Hersam, M. Allegrini, A. Hartschuh, Defect-induced photoluminescence from dark excitonic states in individual single-walled carbon nanotubes, Nano Lett. 9 (2009) 2010–2014.
[15] P. Ahmad, N.M. Mohamed, Z.A. Burhanudin, A review of nanostructured based radiation sensors for neutron, in: AIP Conference Proceedings, 2012, pp. 535.
[16] F.L. Deepak, C. Vinod, K. Mukhopadhyay, A. Govindaraj, C. Rao, Boron nitride nanotubes and nanowires, Chem. Phys. Lett. 353 (2002) 345–352.

[17] K. Huo, Z. Hu, F. Chen, J. Fu, Y. Chen, B. Liu, J. Ding, Z.L. Dong, T. White, Synthesis of boron nitride nanowires, Appl. Phys. Lett. 80 (2002) 3611–3613.

[18] L. Li, C.P. Li, Y. Chen, Synthesis of boron nitride nanotubes, bamboos and nanowires, Phys. E: Low-Dimens. Syst. Nanostruct. 40 (2008) 2513–2516.

[19] Y. Chen, Z. Tong, L. Luo, Boron nitride nanowires produced on commercial stainless steel foil, Chin. J. Chem. Eng. 16 (2008) 485–487.

[20] K. Huo, Z. Hu, F. Chen, J. Fu, Y. Chen, B. Liu, J. Ding, Z. Dong, T. White, Synthesis of boron nitride nanowires, Appl. Phys. Lett. 80 (2002) 3611–3613.

[21] T. Sekiguchi, Q. Liu, T. Tanaka, J. Hu, Y. Zhu, Y. Bando, Cathodoluminescence study of widegap-semiconductor nanowires, Eur. Phys. J. Appl. Phys. 27 (2004) 107–109.

[22] N. Koi, T. Oku, M. Inoue, K. Suganuma, Structures and purification of boron nitride nanotubes synthesized from boron-based powders with iron particles, J. Mater. Sci. 43 (2008) 2955–2961.

[23] C.H. Lee, J. Wang, V.K. Kayatsha, J.Y. Huang, Y.K. Yap, Effective growth of boron nitride nanotubes by thermal chemical vapor deposition, Nanotechnology 19 (2008) 455605.

[24] C.H. Lee, M. Xie, V. Kayastha, J. Wang, Y.K. Yap, Patterned growth of boron nitride nanotubes by catalytic chemical vapor deposition, Chem. Mater. 22 (2010) 1782–1787.

[25] C. Zhi, Y. Bando, C. Tan, D. Golberg, Effective precursor for high yield synthesis of pure BN nanotubes, Solid State Commun. 135 (2005) 67–70.

[26] Y. Murakami, B. Lu, S. Kazaoui, N. Minami, T. Okubo, S. Maruyama, Photoluminescence sidebands of carbon nanotubes below the bright singlet excitonic levels, Phys. Rev. B 79 (2009) 195407.

[27] M.J. O'connell, S.M. Bachilo, C.B. Huffman, V.C. Moore, M.S. Strano, E.H. Haroz, K.L. Rialon, P.J. Boul, W.H. Noon, C. Kittrell, Band gap fluorescence from individual single-walled carbon nanotubes, Science 297 (2002) 593–596.

[28] G. Mpourmpakis, G.E. Froudakis, Why boron nitride nanotubes are preferable to carbon nanotubes for hydrogen storage? An ab initio theoretical study, Catal. Today 120 (2007) 341–345.

[29] V. Naumov, F. Kosyrev, V. Vostrikov, N. Arutyunyan, E. Obraztsova, V. Konov, H. Jiang, A. Nasibulin, E. Kauppinen, Synthesis of boron nitride multi-walled nanotubes by laser ablation technique, Laser Phys. 19 (2009) 1198–1200.

[30] S. Hu, E.-J. Kan, J. Yang, First-principles study of interaction between H molecules and BN nanotubes with BN divacancies, J. Chem. Phys. 127 (2007) 164718.

[31] J. Li, R. Dahal, S. Majety, J. Lin, H. Jiang, Hexagonal boron nitride epitaxial layers as neutron detector materials, Nucl. Instrum. Methods Phys. Res Sect. A: Accel. Spectrom. Detect. Assoc. Equip. 654 (2011) 417–420.

[32] G. Ciofani, G.G. Genchi, I. Liakos, A. Athanassiou, D. Dinucci, F. Chiellini, V. Mattoli, A simple approach to covalent functionalization of boron nitride nanotubes, J. Colloids Interface Sci. 374 (2012) 308–314.

[33] O. Dugne, S. Prouhet, A. Guette, R. Naslain, R. Fourmeaux, K. Hssein, J. Sevely, C. Guimon, D. Gonbeau, G. Pfister-Guillouzo, AES, XPS and TEM characterization of boron nitride deposited under chemical vapor infiltration (CVI) conditions, J. Phys. Colloq. 50 (1989) (C5-333-C335-341).

[34] Z. Xu, D. Golberg, Y. Bando, In situ TEM-STM recorded kinetics of boron nitride nanotube failure under current flow, Nano Lett. 9 (2009) 2251–2254.

[35] R. Arenal, A. Ferrari, S. Reich, L. Wirtz, J.-Y. Mevellec, S. Lefrant, A. Rubio, A. Loiseau, Raman spectroscopy of single-wall boron nitride nanotubes, Nano Lett. 6 (2006) 1812–1816.

Materials Express

2158-5849/2015/5/249/006
doi:10.1166/mex.2015.1229
www.aspbs.com/mex

Synthesis and characterization of boron nitride microtubes

Pervaiz Ahmad[1], **Mayeen Uddin Khandaker**[1,*], **Yusoff Mohd Amin**[1], **and Nawshad Muhammad**[2]

[1] *Department of Physics, Faculty of Science, University of Malaya, 50603 Kuala Lumpur, Malaysia*
[2] *Interdisciplinary Research Centre in Biomedical Materials (IRCBM) COMSATS Institute of Information Technology, Lahore, 54000, Pakistan*

ABSTRACT

Boron nitride microtubes (BNMTs) are successfully synthesized via a simple technique at 1200 °C. The method and logics used in the present study are relatively different and easy in comparison to previously synthesized boron nitride nanotubes, boron nitride microtubes and boron-carbon-nitride microtubes regarding the choice of precursors, experimental set up and reaction atmosphere. Field emission scanning electron microscopy (FESEM) shows a unique pipe-like morphology of the as-synthesized BNMTs with thin wall structure and larger internal space. X-ray photoelectron spectroscopy (XPS) survey shows B 1s and N 1s peaks at 190.8 eV and 398.5 eV that represent hexagonal boron nitride (h-BN) composition of synthesized microtubes. Raman spectroscopy demonstrates a peak at 1372.53 (cm^{-1}) that corresponds to E_{2g} mode of h-BN.

Keywords: BNMT, Experimental Setup, Reaction Atmosphere, Growth Duration.

1. INTRODUCTION

Hexagonal boron nitride is a wide band gap semiconductor,(1) with a direct band gap of 5.97 eV.(2) It is a normal phase of BN, stable at room temperature and pressure with a structure similar to that of graphite, but alternative boron and nitrogen atoms substituted for carbon atoms.(3)

The demand for the preparation of micro or nanosize materials with high quality is increasing due to their frequent use in the development of small size optoelectronic devices.(4, 5) The synthesis of carbon nanotubes (CNTs) or boron nitride nanotubes (BNNTs) to some extent have fulfilled this demand of modern technology. BNNTs are the cylindrical structures of hexagonal boron nitride with diameter in the range of 1–100 nm and length up to several micrometers.(6–8) They were theoretically predicted in 1994,(9) and experimentally discovered in 1995.(10) The discovery of BNNTs has opened new ways for making devices with excellent properties. These properties of BNNTs are almost similar to carbon nanotubes;(11) however, CNTs can be conductor or semiconductor dependent on the chirality or helicity of the tube whereas BNNTs are large band gap semiconductors with electronic properties independent of helicity or diameter.(12–14) Helicity independent electronic properties of BNNTs have made it an excellent choice for making (electronic) devices with uniform electronic properties.(4, 12, 15, 16)

An almost similar relation exists between boron nitride microtubes (BNMTs) and BNNTs i.e., BNMTs have almost all the features and advantages of BNNTs.(4) BNMTs due to their ionic origin are large band gap semiconductor with electronic properties independent of geometry or morphology of the tube. They have nanoscale walls (10–100 nm) and larger internal space, which make a unique pipe like morphology. This pipe like morphology (of BNMTs) can efficiently be used (like carbon microtubes) as a carrier of larger size bio-molecules, and inorganic nanoparticles in micro-reactors, micro-fluids devices and targeted drug delivery systems.(17–19) BNMTs with thin

---

[*] Author to whom correspondence should be addressed.
Emails: mu_khandaker@yahoo.com, mu_khandaker@um.edu.my

walls, made of h-BN layers have high chemical stability, excellent mechanical properties and high thermal conductivity. Due to their reduced wall curvatures they have better crystallinity as compare to BNNTs.(17) Further, they exhibit an intense deep Ultra Violet (UV) emission, which can be observed even at room temperature.(4, 17) The better crystallinity and large cross-section area for thermal neutron have made it an excellent choice as a neutron sensing element in a solid state neutron detector. The detector thus develops is predicted to have much better efficiency than any other solid state neutron detector.(20, 21)

BNMTs have previously been synthesized from Li_2CO_3 and B at ~1350 °C,(4) however the experimental set up used is not only a bit complex but also relatively expensive. Furthermore, due to induction heating the size and morphology of the final product is very difficult to control at a desired location.(22) Therefore a relative simple experimental set up has been designed and used for the control synthesis of BNNTs.(22, 23) This experimental set up is further simplified with a few simple modifications and is successfully used for the synthesis of BNMTs at a relative low temperature of 1200 °C (as compare to 1350 °C,(4)). In order to avoid any other complication, same type and precursor's ratio are used for the current synthesis of BNMTs.(22) But, for the hope of better results, the as used precursors were selected in nanoscale dimension. The full details are mentioned in the following sections.

2. EXPERIMENTAL DETAILS

An extremely simple technique is used to synthesize boron nitride microtubes at 1200 °C. B, MgO and γ-Fe_2O_3 of 99.9% purity are used as a precursor. By the intension of getting some improvement in the final results, some modifications have been made in the experimental setup, quantity and size of the previously used precursors and internal environment.(22) Experimental setup is used without vacuum or evacuation. Instead of vacuum, NH_3 gas is used as a reaction atmosphere inside the chamber.

A total of 400 mg of precursors in the form of nanoscale amorphous powder were used during the experiment for the synthesis of BNMTs. All these precursors were mixed in 2:1:1 ratio inside an alumina boat. The boat is covered with a few Si-substrates and placed inside one end closed quartz tube near the closed end. The tube is then inserted into the quartz tube chamber of the furnace in such a way that the open end of the inner quartz tube is toward the gas inlet. The furnace is then sealed closed and turned on to heat up the precursors up to 1200 °C in the presence of NH_3 gas flow at a rate of 200 sccm. At 1200 °C, the system is kept in such a condition for one hour. After 1-hour the system is allowed to cool down to room temperature.

At room temperature, white color BNMTs are found deposited on Si substrate and on the inner walls of alumina boat, as shown in Figure 1. The synthesized sample is then characterized with the help of Variable Pressure Scanning Electron Microscope (VP-FESEM or FESEM, Model: Zeiss Supra 55 VP), Raman Spectroscopy (Model: Horiba Jobin Yvon HR800) and X-ray Photon Spectroscopy (XPS, Model: Thermo Scientific K-Alpha). The details are given in the following section.

Fig. 1. A photograph of as-synthesized BNMTs (white color) in alumina boat and on Si substrate.

3. RESULTS

Unlike previously reported BNMTs,(4, 24) a bit different mechanism based on the idea behind previously synthesized vertically aligned CNTs,(25) is effectively used for the synthesis of BNMTs in the present study. Both MgO and Fe_2O_3 are selected as precursors with B, because they are effective producer of B_2O_2 and catalysts.(26) During the experimental run, the precursors are heated up to 1200 °C. During this stage, MgO and Fe_2O_3 react with B to produce B_2O_2, Fe and Mg particles. Subsequently the as produced Fe and Mg particles make Mg–Fe alloys and deposited at the top of Si-substrate. The flow of ammonia etch away Mg particle from the deposited Mg–Fe alloys on Si-substrate and thus produces nucleation sites in Fe particles (remained deposited) on Si-substrate. At higher temperature NH_3 decomposes into nitrogen and hydrogen. Nitrogen reacts with B_2O_2 and produces BN species. These BN species diffuses into the nucleation sites on Si-substrate. When their partial vapor pressure is sufficient enough, they grow in the form of microtubes following the nucleation sites as pattern.

The FESEM analysis of the size and morphology of the synthesized sample is shown in Figures 2 and 3. Figure 2 shows a low magnification FESEM image of the synthesized BNMTs on Si-substrate. The tubular morphology of the synthesized BNMTs can clearly be seen in the as shown micrograph. Such a unique tubular morphology of the BNMTs with FESEM result has rarely been reported by other researcher in the past.(24) Normally TEM is used to analyze the tubular morphology in such cases,(4) however, in the present work the tubular structure of the synthesized sample is shown with the help of FESEM.

From the top view, two kinds of morphologies can be seen in the synthesized sample. First, clear view of the

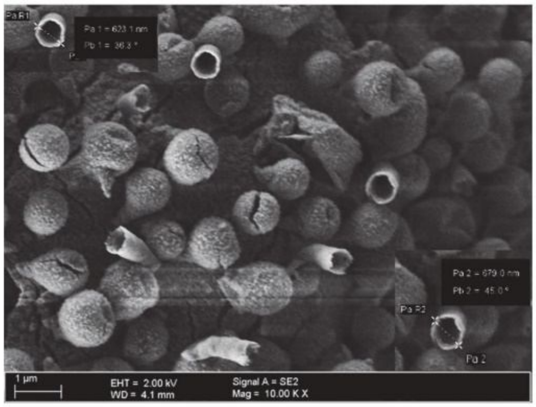

Fig. 2. Low magnification FESEM micrograph shows a clear tubular view of the synthesized BNMTs on Si-substrate at 1200 °C. The inset images on the upper left hand corner and bottom right hand corner show the calculated diameter of the BNMTs with help of FESEM measuring tools.

tubular structures and second, ball-like or button mushroom like morphology. Both kinds of structures are seemed to be embedded in a layer of materials deposited on Si substrate. This layer may possibly be made of either diffused catalysts, their alloys (Fe, Mg or Mg–Fe alloys),(27) or secondary species formed as by-products during the reaction of Boron with metal oxides catalysts. Crakes can also be found in the empty part or spaces between BNMTs and ball-like or button mushroom like morphologies. Some of these crakes can even be observed on the top of these morphologies. The appearances of these crakes are believed to be a precursor for the final and full tabular structure of the BNMTs. The inset images on the upper left hand corner and bottom right hand corner show the calculated diameter of the BNMTs with the help of FESEM measurement tools. The measurement shows an average diameter of 651.05 nm of the BNMTs synthesized in the present study.

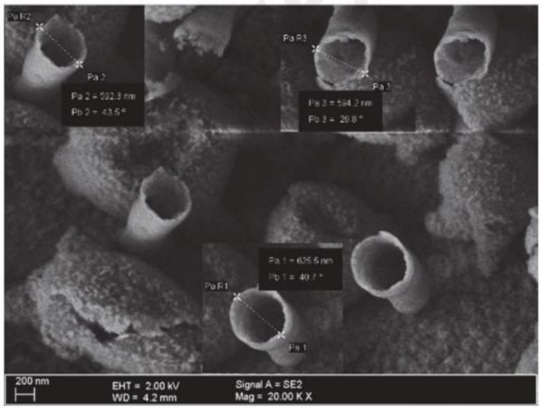

Fig. 3. High magnification FESEM micrograph shows a unique pipe like morphology of the synthesized BNMTs on Si-substrate at 1200 °C. The inset images show the calculated diameter of the BNMTs with help of FESEM measuring tools.

Figure 3 is the higher magnification FESEM image of the same sample, showing a clear view of the tubular morphology of the BNMTs. Here again, the diameters of the tubes are calculated with the help of FESEM measuring tools, as shown in the inset images of Figure 3. The tubes are found to have and average diameter of 604.01 nm, which is smaller than the average diameter of the BNMTs shown in Figure 2. It means that the BNMTs in the present sample are not uniform in diameter and wall thickness. The diameter vary from tube to tube in the range of 580–690 nm (with an overall average of 627.52 nm) whereas the wall thickness from 10–100 nm. The button mushroom like morphologies lying around these tubes are assumed to have either cut off from the top of these tubes or still stick to their original position. At higher magnification, the top of these species and the spaces or empty locations are still found to have crakes and apparently look like to be covered with a black and white wool carpet. It has also been observed in Figure 2 that the diameter of the lower part of the tube is relatively small as compared to the upper part of the tube. It might be due to the presence of ball like or button mushroom like morphology which is assumed to have cut off from the tube later on.

The elemental compositions of the synthesized BNMTs were analyzed with the help of X-ray Photoelectron Spectroscopy (XPS) with an X-ray source of Al K Alpha. The full range XPS survey thus obtained is shown in Figure 4. The survey shows several peaks at binding energies of 190.8, 398.5 and 533.18 eV. The B 1s peak centered at 190.8 eV (inset: upper left of Fig. 4) and N 1s at 398.5 eV (inset: upper right of Fig. 4) correspond to h-BN according to available literature.(28–32) The O 1s peak at 533.18 eV may either be due to the as-used Si substrate or formation of B_2O_3 in the sample,(33) which might be the secondary species or by-product observed in the FESEM micrographs shown in Figures 2 and 3.

The synthesized sample of BNMTs is also characterized together with the Raman spectroscopy to confirm its constituents and phase. The Raman spectrum is shown in the Figure 5. The major peak at 1372.53 (cm^{-1}) reported here, corresponds to the E_{2g} mode of h-BN,(25–28) with a Full Width and Half Maxima (FWHM) of ~19 (cm^{-1}). This result is a bit broader as compared to the one reported for the bulk h-BN. This broadening of the peak is a sign of small micro-size crystallites of h-BN.(34) A smaller peak has also been observed at 1122.15 (cm^{-1}) that correspond to H_3BO_3, which might have formed by the interaction of laser with moisture and oxygen in the air and B_2O_3 in the sample.(34) In Figure 2, there were some undeveloped or powder like morphologies in between the microtubes, which can rightly be assigned to the presence of B_3O_3 (which has already been verified by the XPS analysis) that later on leads to the formation of H_3BO_3 during the Raman spectroscopy of the sample.(34)

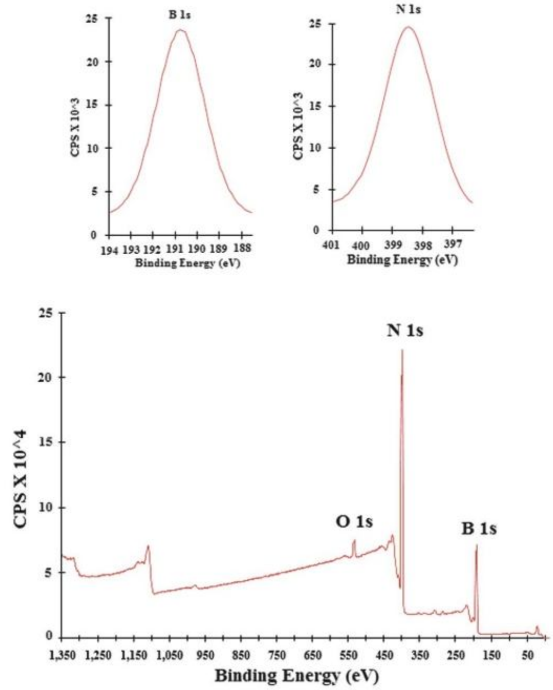

Fig. 4. Full range XPS survey of Boron nitride microtubes synthesized in the present study. The B 1s peak centered at 190.8 eV (inset: upper left) and N 1s peak at 398.5 eV (inset: upper right) correspond to h-BN (BNMTs).

4. DISCUSSION

Though BNMTs synthesis with a bit larger diameter and length have been reported previously,(4) however, the present work is unique with respect to a few aspects. First, the precursors type and ratio used is the same as in the synthesis of BNNTs,(22, 27) but different from those used for the synthesis of BNMTs and B-C-NMTs.(4, 17) Second, the experimental set up used is self-modified, extremely simple without any vacuum or inert gases. This kind of the experimental set up is a bit different from the one used for synthesis of BNNTs,(22, 27) or BNMTs.(4) Third, the use of NH_3 gas as a reaction atmosphere.

Changes in the experimental parameters are the possible reason for current morphology and diameter of the synthesized BNMTs. The main experimental parameters which can cause a change in quality, quantity, size and morphology of any nanostructure material are precursor's type, ratio, experimental set up, reaction atmosphere, final temperature and growth duration etc. A change in any of the above parameters will result a change in the diameter of any as produced final product. Such a change in diameter with respect to experimental parameters has been observed during the synthesis of BNNTs,(2) BNMTs,(4) and B–C–N ternary microtubes.(17) The analysis of such a change has been summarized in Table I.

According to the comparative analysis shown in Table I, only the development of a single precursor (Li_2O for Li_2CO_3) and an increased growth duration (3-h instead of 2-h) makes a huge difference in the diameter of synthesized BN products.(4, 35) However in either of these work,(4, 35) no apparent role of growth duration at final temperature has been discussed to be responsible for such a huge change in the diameter of the final product. Since no role of Carbon from Li_2CO_3 has been stated in the formation mechanism for BNMTs, (4) therefore, in the light of their further work,(35) it is strongly believed that only the growth duration was responsible for their results (BNMTs). Also in the light of our experimental work it is believed that the same results for BNMTs,(4) can easily be reproduced by using B and Li_2O (instead of B and Li_2CO_3) as precursors in a reduced growth duration but with similar experimenters' parameters.(4) Furthermore, synthesis of B–C–N ternary microtubes have been reported at 1200 °C by using similar precursor and experimental conditions, except BN-crucible, which was replaced with graphite crucible. Carbon for the formation of B–C–N is claimed to be supplied by CO/CO_2 formed through the oxidation of graphite crucible.(17) But it is also a fact that the majority of the graphite crucibles are designed in such a way that it can easily withstand with a temperature above 1200 °C. Further it has mentioned that Carbon from Li_2CO_3 decomposition was available at lower temperature.(17) Therefore, it is assumed that lower temperature (1200 °C) is responsible for utilizing C from Li_2CO_3 for the formation of B–C–N microtubes instead of CO/CO_2 due to oxidation of graphite crucible. It has also been stated that the precursors were used in 1:1 ratio,(17) so if C is claimed to be included due to oxidation of graphite crucible then it would have highly effected the as used ratio of the precursor and the final product would have been some other compounds with a lot of carbon-containing impurities.

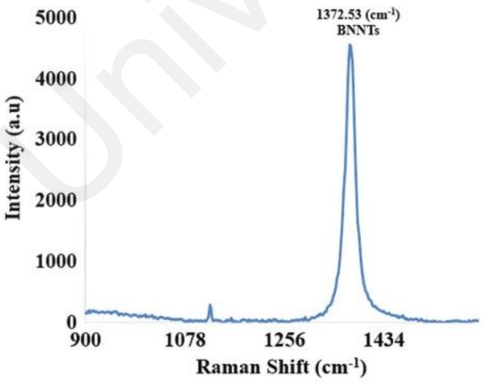

Fig. 5. Raman spectrum of the BNMTs sample synthesized at 1200 °C shows a high intensity peak at 1372.53 (cm^{-1}) that corresponds to E_{2g} mode of h-BN.

Table I. A comparative analysis of Experimental parameters and their effects on the diameter of the final product.

			Experimental parameters							
			Experimental setup							
			Vertical induction furnace			Horizontal tube furnace				
S. no	Precursors	Ratio	Reaction atmosphere	Final temperature (°C)	Growth duration	Reaction atmosphere	Final temperature (°C)	Growth duration	Diameter (of final material)	References
1	B, Li_2CO_3	1:1 (in BN-Crucible)	Vacuum: $\sim 2 \times 10^{-1}$ Torr	1100–∼1350	2-h	×	×	×	1–3 μm (BNMTs)	[4]
2	B, Li_2O	1:1 (in BN-Crucible)	Vacuum: $\sim 2 \times 10^{-1}$ Torr	1100–∼1350	3-h	×	×	×	Sub–10 nm (BNNTs)	[35]
3	B, Li_2CO_3	1:1 (in graphite Crucible)	Vacuum: $\sim 2 \times 10^{-1}$ Torr	∼1200	2-h	×	×	×	1–5 μm (BCNMTs)	[17]
4	B, Fe_2O_3, MgO	2:1:1 (in Al_2O_3 boat)	×	×	×	Vacuum: ∼30 mTorr	1200	1-h	10–100 nm (BNNTs)	[22]
5	B, Fe_2O_3, MgO	2:1:1 (in Al_2O_3 boat)	×	×	×	NH_3 gas	1200	1-h	580–690 nm (BNMTs)	Present work

In the present work, a bit different logic has been used and applied. Instead of changing the precursor's type, their ratio or growth duration, change in the diameter of the final product was sought on the basis of modification in previously used experimental set up and reaction atmosphere inside the chamber.(22) Unlike the previous Experimental set up,(22) the open end of the inner test tube, was turned toward the gas inlet. Further, it has been used without any vacuum or inert gases. Instead of vacuum or inert gases, NH_3 gas was used as a reaction atmosphere inside the chamber. Thus the present work not only gives us BNMTs but also a few more logics; First, the precursor types and ratios used for the synthesis of BNNTs,(22, 27) can also be used for BNMTs synthesis (as in this work) with a simple modification in an experimental set up and its internal environment. Second, the same precursor type, ratio and experimental set up but with Ar gas flow as an internal environment can be used for synthesis of BNNTs. Third, further modification in the Experimental set up with the same precursors type and their ratio and Ar gas (as an alternative for vacuum) can be used for the synthesis of other BN nanostructures like Boron nitride nanowires(5) and nanosheet etc.

5. CONCLUSION

The successful synthesis of BNMTs in the present work and its analysis with previously synthesized BNMTs, BNNTs, and B–C–NMTs, showed that the synthesis of these materials not only depends on the experimental setup, precursor types and their ratios but also on growth duration and internal environment inside the experimental set up during the experiment. Elongation of the growth duration resulted in the synthesis of BNNTs, instead of BNMTs in the past whereas the change of internal atmosphere with ammonia gas flow, instead of inert gases or vacuum, resulted in BNMTs in the present work. The synthesized BNMTs are found to be of high importance as a neutron sensing element in a solid state neutron detector, neutron capture therapy, micro-fluids devices and targeted drug delivery etc.

Acknowledgments: We are extremely grateful to IPPP (Grant Number: PG076-2014A), University of Malaya, 50603 Kuala Lumpur, Malaysia, for providing financial assistance and facilities for our research work.

References and Notes

1. J. Wang, L. Zhang, G. Zhao, Y. Gu, Z. Zhang, F. Zhang, and W. Wang; Selective synthesis of boron nitride nanotubes by self-propagation high-temperature synthesis and annealing process; *J. Solid State Chem.* 184, 2478 **(2011)**.
2. A. Pakdel, C. Zhi, Y. Bando, T. Nakayama, and D. Golberg; A comprehensive analysis of the CVD growth of boron nitride nanotubes; *Nanotechnology* 23, 215601 **(2012)**.
3. Y. N. Xu, and W. Ching; Calculation of ground-state and optical properties of boron nitrides in the hexagonal, cubic, and wurtzite structures; *Phys. Rev. B.* 44, 7787 **(1991)**.
4. Y. Huang, Y. Bando, C. Tang, C. Zhi, T. Terao, B. Dierre, T. Sekiguchi, and D. Golberg; Thin-walled boron nitride microtubes exhibiting intense band-edge UV emission at room temperature; *Nanotechnology* 20, 085705 **(2009)**.
5. P. Ahmad, M. U. Khandaker, Z. R. Khan, and Y. M. Amin; A simple technique to synthesize pure and highly crystalline boron nitride nanowires; *Ceram. Int.* 40, 14727 **(2014)**.
6. X. Chen, X. Gao, H. Zhang, Z. Zhou, W. Hu, G. Pan, H. Zhu, T. Yan, and D. Song; Preparation and electrochemical hydrogen storage of boron nitride nanotubes; *J. Phys. Chem. B* 109, 11525 **(2005)**.
7. P. Ahmad, M. Khandaker, and Y. Amin; A comprehensive study of boron nitride nanotubes multiple synthesis from a single precursor; *Indian J. Phys.* 89, 209 **(2014)**.
8. P. Ahmad, M. U. Khandaker, and Y. M. Amin; Effective synthesis of vertically aligned boron nitride nanotubes via a simple CCVD; *Mater. Manuf. Process* **(2014)**.
9. A. Rubio, J. L. Corkill, and M. L. Cohen; Theory of graphitic boron nitride nanotubes; *Phy. Rev. B* 49, 5081 **(1994)**.

10. N. G. Chopra, R. Luyken, K. Cherrey, V. H. Crespi, M. L. Cohen, S. G. Louie, and A. Zettl; Boron nitride nanotubes; *Science* 269, 966 **(1995)**.

11. K. S. Kim, C. T. Kingston, A. Hrdina, M. B. Jakubinek, J. Guan, M. Plunkett, and B. Simard; Hydrogen-catalyzed, pilot-scale production of small-diameter boron nitride nanotubes and their macroscopic assemblies; *ACS Nano.* 8, 6211 **(2014)**.

12. M. Ishigami, S. Aloni, and A. Zettl; Properties of boron nitride nanotubes; *AIP Conference Proceedings*, Melville, NY, USA **(2003)**, p. 94.

13. B. Saner Okan, Z.Ö. Kocabaş, A. Nalbant Ergün, M. Baysal, I. Letofsky-Papst, and Y. Yürüm; Effect of reaction temperature and catalyst type on the formation of boron nitride nanotubes by chemical vapor deposition and measurement of their hydrogen storage capacity; *Ind. Eng. Chem. Res.* 51, 11341 **(2012)**.

14. A. Fathalizadeh, T. Pham, W. Mickelson, and A. Zettl; Scaled synthesis of boron nitride nanotubes, nanoribbons, and nanococoons using direct feedstock injection into an extended-pressure, inductively-coupled thermal plasma; *Nano Lett.* 14, 4881 **(2014)**.

15. L. Guo, and R. N. Singh; Catalytic growth of boron nitride nanotubes using gas precursors; *Physica E* 41, 448 **(2009)**.

16. S. Chatterjee, M. J. Kim, D. N. Zakharov, S. M. Kim, E. A. Stach, B. Maruyama, and L. G. Sneddon; Syntheses of boron nitride nanotubes from borazine and decaborane molecular precursors by catalytic chemical vapor deposition with a floating nickel catalyst; *Chem. Mater.* 24, 2872 **(2012)**.

17. J. Lin, Y. Huang, C. Tang, Y. Bando, J. Zou, and D. Golberg; Thin-walled B–C–N ternary microtubes: From synthesis to electrical, cathodoluminescence and field-emission properties; *J. Mater. Chem.* 22, 8134 **(2012)**.

18. J. Hu, Y. Bando, F. Xu, Y. Li, J. Zhan, J. Xu, and D. Golberg; Growth and field-emission properties of crystalline, thin-walled carbon microtubes; *Adv. Mater.* 16, 153 **(2004)**.

19. J. Goldberger, R. Fan, and P. Yang; Inorganic nanotubes: A novel platform for nanofluidics; *Accounts Chem. Res.* 39, 239 **(2006)**.

20. J. Li, R. Dahal, S. Majety, J. Lin, and H. Jiang; Hexagonal boron nitride epitaxial layers as neutron detector materials; *Nucl. Instrum. Methods Phys. Res. Sect. A-Accel. Spectrom. Dect. Assoc. Equip.* 654, 417 **(2011)**.

21. P. Ahmad, N. M. Mohamed, and Z. A. Burhanudin; A review of nanostructured based radiation sensors for neutron; *AIP Conference Proceedings*, Kuala Lumpur, Malaysia **(2012)**, p. 535.

22. C. H. Lee, J. Wang, V. K. Kayatsha, J. Y. Huang, and Y. K. Yap; Effective growth of boron nitride nanotubes by thermal chemical vapor deposition; *Nanotechnology* 19, 455605 **(2008)**.

23. C. H. Lee, M. Xie, V. Kayastha, J. Wang, and Y. K. Yap; Patterned growth of boron nitride nanotubes by catalytic chemical vapor deposition; *Chem. Mater.* 22, 1782 **(2010)**.

24. M. Bechelany, A. Brioude, P. Stadelmann, S. Bernard, D. Cornu, and P. Miele; Preparation of BN microtubes/nanotubes with a unique chemical process; *J. Phy. Chem. C.* 112, 18325 **(2008)**.

25. W. D. Zhang, Y. Wen, S. Min Liu, W. C. Tjiu, G. Qin Xu, and L. Ming Gan; Synthesis of vertically aligned carbon nanotubes on metal deposited quartz plates; *Carbon* 40, 1981 **(2002)**.

26. C. Zhi, Y. Bando, C. Tan, and D. Golberg; Effective precursor for high yield synthesis of pure BN nanotubes; *J. Solid State Chem.* 135, 67 **(2005)**.

27. A. Pakdel, C. Y. Zhi, Y. Bando, T. Nakayama, and D. Golberg; A comprehensive analysis of the CVD growth of boron nitride nanotubes; *Nanotechnology* 23, 215601 **(2012)**.

28. C. Wagner and G. Muilenberg; Handbook of X-ray Photoelectron Spectroscopy; Perkin-Elmer, Eden Prairie, MN, USA **(1979)**.

29. B. Zhong, X. Huang, G. Wen, H. Yu, X. Zhang, T. Zhang, and H. Bai; Large-scale fabrication of boron nitride nanotubes via a facile chemical vapor reaction route and their cathodoluminescence properties; *Nanoscale Res. Lett.* 6, 36 **(2011)**.

30. L. Song, L. Ci, H. Lu, P. B. Sorokin, C. Jin, J. Ni, A. G. Kvashnin, D. G. Kvashnin, J. Lou, and B. I. Yakobson; Large scale growth and characterization of atomic hexagonal boron nitride layers; *Nano Lett.* 10, 3209 **(2010)**.

31. J. F. Moulder, W. F. Stickle, P. E. Sobol, and K. D. Bomben; Handbook of X-ray Photoelectron Spectroscopy, Perkin Elmer Eden Prairie, MN **(1992)**.

32. K. S. Park, D. Y. Lee, K. J. Kim, and D. W. Moon; Observation of a hexagonal BN surface layer on the cubic BN film grown by dual ion beam sputter deposition; *Appl. Phys. Lett.* 70, 315 **(1997)**.

33. O. Dugne, S. Prouhet, A. Guette, R. Naslain, R. Fourmeaux, K. Hssein, J. Sevely, C. Guimon, D. Gonbeau, and G. Pfister-Guillouzo; AES, XPS and TEM characterization of boron nitride deposited under chemical vapor infiltration (CVI) conditions; *J. Phy.vColloques.* 50, 335 **(1989)**.

34. R. Arenal, A. Ferrari, S. Reich, L. Wirtz, J.-Y. Mevellec, S. Lefrant, A. Rubio, and A. Loiseau; Raman spectroscopy of single-wall boron nitride nanotubes; *Nano Lett.* 6, 1812 **(2006)**.

35. Y. Huang, J. Lin, C. C. Tang, Y. Bando, C. Y. Zhi, T. Y. Zhai, B. Dierre, T. Sekiguchi, and D. Golberg; Bulk synthesis, growth mechanism and properties of highly pure ultrafine boron nitride nanotubes with diameters of sub-10 nm; *Nanotechnology* 22, 9 **(2011)**.

Received: 15 August 2014. Revised/Accepted: 17 February 2015.

Materials and Manufacturing Processes, 30: 184–188, 2015

ISSN: 1042-6914 print/1532-2475 online
DOI: 10.1080/10426914.2014.952041

Synthesis of Boron Nitride Microtubes and Formation of Boron Nitride Nanosheets

PERVAIZ AHMAD, MAYEEN UDDIN KHANDAKER, YUSOFF MOHD AMIN, AND ZIAUL RAZA KHAN

Department of Physics, Faculty of Science, University of Malaya, Kuala Lumpur, Malaysia

Boron nitride microtubes are synthesized in a dual zone quartz tube furnace at 1200°C with ammonia as a reaction atmosphere. Field emission scanning electron microscopy (FE-SEM) results show a unique cone-like morphology of the tubes with larger internal space and thin walls structure. The diameters of the tubes were found to be in the range of 1 to ~2 μm with the walls thickness estimated to be from 10 to 100 nm. XPS survey shows N 1 s and B 1 s peaks at 398.7 and 191 eV, respectively, that represent h-BN in the sample. Raman spectroscopy indicates a high-intensity peak at 1372.53 (cm^{-1}) that corresponds to the E_{2g} mode of h-BN. Along with the novel tubular morphology of boron nitride microtubes, the present work also explains a mechanism for the formation of boron nitride nanosheets (from boron nitride microtubes) found in the FE-SEM results of the current sample.

Keywords BNMTs; BNNTs; CMTs; CNTs; CVD.

INTRODUCTION

Boron nitride microtubes (BNMTs) are the pipe-like morphologies of hexagonal boron nitride (h-BN) with diameter and length in micro-scale and walls thickness in the range of 1–100 nm. In the present study, the walls thicknesses mean the external diameter of the tubes whereas the diameter includes both internal space and external diameter. The unique cone-like morphology with larger internal space and length in micro-scale range offers exceptional applications in the field of biomedical as a carrier of larger size biomolecules and inorganic nanoparticles in micro-reactors, micro-fluids devices, and targeted drug delivery systems. Previously, carbon microtubes (CMTs) were suggested for this purpose [1–3]; however; the diameter-independent, excellent properties of the BNMTs make it more suitable as compared to CMTs. The nanosize walls-thickness of BNMTs also combine the excellent properties of nanoscale materials due to electron and holes confinement [4], surface effects and geometrical confinement of phonon [5, 6]. The novel morphology of the BNMTs with larger internal space and nanoscale walls can further enhance its effects during neutron capture therapy to kill the tumor cell and cure the patient. The larger internal space helps in carrying larger scale biomolecules or medicine to the tumor site (like CMTs). This condition may help to protect the healthy tissues and control the side effects during the destruction of tumor cell due to the contact of charged particles produced by the interaction of a neutron with BNMTs from an external source [1–3]. A study of solid state neutron detector suggests that a 200 μm thick ^{10}B-enriched h-BN layer can capture 98.5% of the neutron as compared to the one made of 1 mm thick natural h-BN. It has further been suggested that the development of multiple ^{10}B-enriched h-BN layer (epilayer) with improved crystallinity can enhance the neutron detection efficiency up to 100% [7]. A study of boron nitride nanotubes (BNNTs) and BNMTs showed that these materials are multilayer structures of h-BN with highly crystalline nature [8]. Though ^{10}B enrichment of these materials is not confirmed, still they are believed to be an excellent choice for neutron-sensing applications in solid state neutron detector due to their nanoscale properties [9]. BNMTs are made of h-BN layers with thin walls have high chemical stability, excellent mechanical properties, and high thermal conductivity. All these properties make it a very useful material in the fabrication of different electronic devices that can be used in high-temperature environment. BNMTs as compared to BNNTs have better crystallinity due to their reduced wall curvatures. Also, they exhibit an intense, deep ultraviolet (UV) emission, which can be observed even at room temperature [10].

Previously BNMTs were synthesized by using Li_2CO_3 and B at ~1350°C; however, their tubular morphology has not been claimed or visualized with the help of SEM or FE-SEM results. TEM was the ultimate source to confirm their tubular structure [10]. Furthermore, the experimental setup used is relatively expensive and a bit complex. Also, the size and morphology of the final product is very difficult to control at a desired location due to inductive heating [11]. Previously, a simple experimental setup was used for the effective growth of BNNTs [11]. Later on, achievement of control synthesis

---

Received July 5, 2014; Accepted July 29, 2014

Address correspondence to Mayeen Uddin Khandaker, Department of Physics, Faculty of Science, University of Malaya, 50603 Kuala Lumpur, Malaysia; E-mail: mu_khandaker@yahoo.com, mu_khandaker@um.edu.my

Color versions of one or more of the figures in the article can be found online at www.tandfonline.com/lmmp.

of BNNTs at a desired location was claimed with the same setup [12]. Therefore, this experimental setup along with as-used precursors for BNNTs synthesis are carefully analyzed and sought for further developments in BNMTs synthesis [13, 14]. To avoid any other complexity, the same precursors and their ratio [11] have been selected for the synthesis of BNMTs in the present study. However, to utilize the nanoscale properties of the materials, all the precursors used in the present work were selected in nanoscale dimensions [15]. The full details of all the other experimental parameters are presented in the following sections.

MATERIALS AND METHODS

Boron nitride microtubes are synthesized in a dual zone quartz tube furnace at 1200°C. Nanosize amorphous powder of B, MgO, and γ-Fe_2O_3 were bought from MTI Corporation (Richmond, CA, USA) and used as precursors. All the precursors were properly weighed (B 200 mg, γ-Fe_2O_3 100 mg, MgO 100 mg) and mixed in an alumina boat in 2:1:1 ratio [11]. The boat is slowly moved into a one-end-closed quartz tube toward the closed end. The one-end-closed quartz tube is then placed inside a quartz tube chamber of the dual zone furnace in such a way that the boat inside the one-end-closed quartz is positioned exactly beneath the heating filament. Furthermore, the one-end-closed quartz tube is positioned inside the furnace in such a way that the open end is toward the gas inlet. After sealed closed, the system is heated up to 1200°C in the presence of NH_3 gas flow at a rate of 200 sccm. At 1200°C, it is maintained in such a condition for one hour. After one hour, the system is allowed to cool down to room temperature.

At room temperature, white color species of BNMTs were found inside the alumina boat and on its inner walls. These white color species (~80 mg) were physically isolated from the top of the alumina boat and characterized with different characterization instruments. The details of all the characterizations are presented in the following section.

RESULTS AND DISCUSSION

A mixture of MgO and boron powder was found to be an effective source of B_2O_2, it is extremely difficult to increase the yield by simply raising the temperature. Thus, the success rate for the synthesis of BNMTs remains low due to the rigorous growth conditions. In addition, the formation of $Mg_2B_2O_5$ after a single experimental run stopped further chemical activity of the MgO–boron precursor. Therefore, the need to find out a good substitution for the precursor arose. Due to the common use of transition metals as catalysts and the need of oxygen for B_2O_2 production, FeO has been used with boron powder to obtain a high-quality result. However, it was discovered that the chemical reaction effectiveness of B and FeO was not satisfying and very little amount of B_2O_2 was produced in this reaction at a higher temperature. In order to combine the effect of both MgO and FeO, they were collectively used with boron powder, because they are effective B_2O_2 -producers and catalysts, respectively [16].

During the BNMTs synthesis, the reaction of the precursors produces Fe and Mg catalyst particles. Fe particles react with Si-substrate and lose its catalytic activity. It then works as a diffusion barrier and prevents other catalysts to react with the Si-substrate, whereas Mg works as a catalyst and plays an active role during the growth.

In the present case, other metal oxides have not been tested for obtaining similar results, because while studying the literature for BNNTs synthesis, it has been found that majority of these metal oxides have produced unsatisfactory results with a lot of impurities whereas the best results were obtained with B, Fe_2O_3, and MgO [17]. Therefore, only these precursors (B, Fe_2O_3, and MgO) were tried for the synthesis of BNMTs.

Also, it has been found that a mixer of Li_2CO_3 and B has successfully been used for the synthesis of BNMTs [10]. It should be noted that while using these precursors for BNMTs synthesis, it required a specifically designed induction furnace that is quite expensive and complex compared to the one used in the present work. Furthermore, they have reported BNMTs whose tubular morphology can only be observed from their TEM result, whereas in the present work the tubular morphology is quite clear from FE-SEM results.

Figure 1 shows the lower magnification FE-SEM image of the as-synthesized BN structures in the present study. Different kinds of structures and morphologies can be seen and observed in this image. Microtubes are the most obvious structures that can clearly be observed at this magnification; however, some undeveloped morphologies of unknown nature can also be seen here. The as-seen tubular structures with a cone-like morphology are vertically aligned. Their diameters are found to be in the range of 1 to ~2 µm with the wall

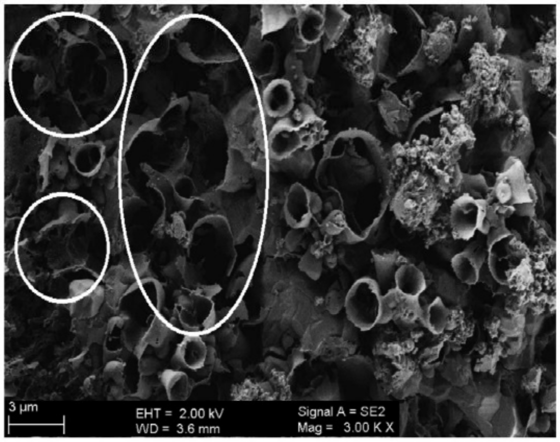

FIGURE 1.—Lower-magnification FE-SEEM image showing as-formed sheet-like morphologies, indicated by white circles. The synthesized microtubes seem to have a cone-like morphology.

thickness estimated to be in the range of 10–100 nm. The observations showed an increase in diameter with an increasing length of the tubes. Due to increasing diameter with the increasing length, the tubes acquired a cone-like morphology. It is believed that the increasing length and diameter of the tube causes a decrease in the wall thickness. The decrease in the wall thickness may be most probably due to the unavailability of the further growth species due to the blockage of precursors in the boat by the as-synthesized BN structures [16]. Thus the growth occurs at the cost of previously available growth species. A time comes when no further growth species are available. At this time the increase in length and diameter occurs at the cost of decreasing wall thickness. This process continues until the tube splits apart and assumes a sheet-like morphology. Majority of the as-formed sheets-like structures (indicated by white circles in Fig. 1) are vertically aligned; however, some of these pieces can also be seen lying randomly among other morphologies. The thickness of these sheets-like structures are most likely to be found in the range of 10–100 nm with the rest of the analogies with the tubes remaining the same.

Figure 2 shows a high-magnification micrograph of the as-synthesized BN structures. The image shows a clear view of the cone-like morphology of the synthesized tubes developed due to a continuous increase in diameter with its increasing length. Cracks can also be found at the top or sides of some of the tubes. These cracks are clearly indicated with the help of white circles in Fig. 2. Though sheets are not observed in the present image, however, the cracks (indicated by white circles) at the top or sides of these tubes are most likely to be considered as the precursor for the formation of sheets.

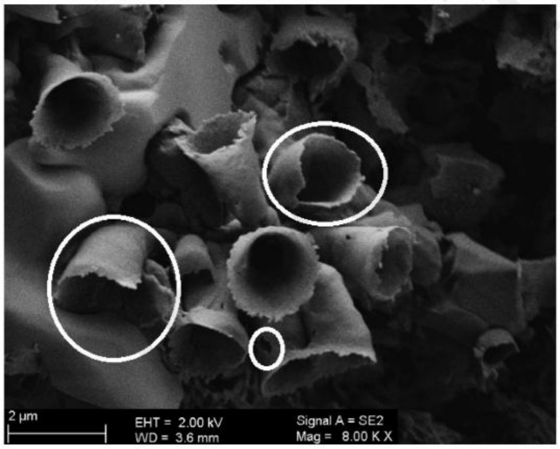

FIGURE 2.—High-magnification FE-SEM image showing a clear view of a cone-like morphology of the synthesized tubes developed due to a continuous increase in diameter with its increasing length. The white circles indicate the cracks or splitting of the tubes, which are considered to be the precursor for the formation of sheets.

Although the synthesis of BNMTs have already been reported by some researchers in the past [10], the tubular structure with a clear cone-like morphology in FE-SEM image has never been reported earlier by any other group. TEM or HR-TEM was normally used to confirm the tubular morphology of such materials [10]; however, due to the clearly visible tubular structure in the FE-SEM results, no need for further verification of tubular structure with TEM or HR-TEM arises.

An X-ray photon spectroscopy (XPS) with an X-ray source of Al Kα is used to find out the composition of the synthesized microtubes. Results of the XPS survey thus obtained are shown in Fig. 3. The survey shows two main peaks at 398.7 and 191 eV. The N 1 s and B 1 s peaks at 398.7 and 191 eV correspond to h-BN in the sample [18].

The constituents and phase of the as-synthesized BN structures (BNMTs and boron nitride nanosheets) in the present study were further confirmed with the help of Raman spectroscopy. The Raman spectrum for the present sample was obtained in the spectral range of 900 (cm^{-1}) to 1600 (cm^{-1}), as shown in Fig. 4. Two peaks have been reported in the spectrum. The high-intensity peak at 1372.53 (cm^{-1}) represents the main constituent of the as-synthesized sample. This high-intensity peak corresponds to the E_{2g} mode of h-BN [17, 19]. Whereas the lower-intensity peak shown at 1122.15 (cm^{-1}) corresponds to the formation of H_3BO_3. This might have formed due to the interaction of laser with moisture and oxygen in the air and B_2O_3 in the sample [20].

The successful characterization of the as-synthesized BNMTs showed that the present work is unique not only due to the synthesis of novel tubular structure of BNMTs and formation of boron nitride nanosheets (BNNS), but also due to few additional experimental parameters. In this regard, the experimental setup is

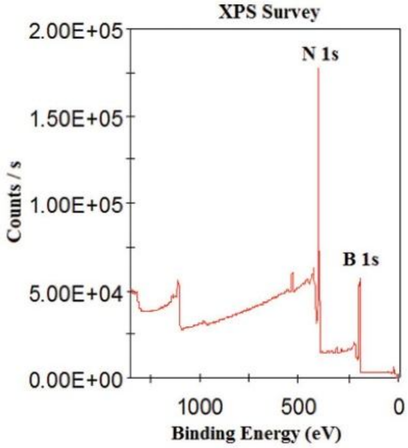

FIGURE 3.—XPS Survey of as-synthesized BNMT sample showing B 1 s (at 191 eV) and N 1 s (at 398.7 eV) peaks that correspond to h-BN.

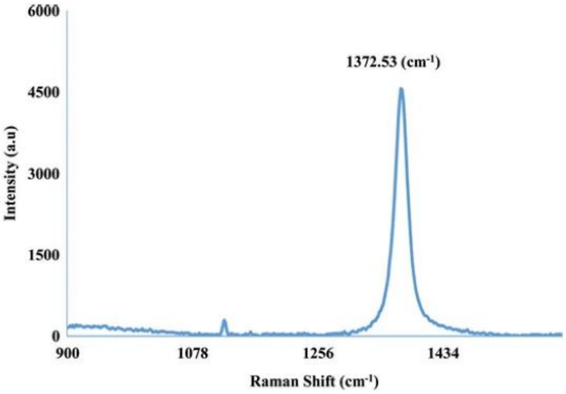

FIGURE 4.—Raman spectrum of the BNMTs sample synthesized at 1200°C, showing a high-intensity peak at 1372.53 (cm^{-1}) that corresponds to the E_{2g} mode of h-BN.

modified to the extent that it can be used without vacuum or inert gases as an internal atmosphere. Instead of vacuum or inert gases, ammonia gas can be used as reaction atmosphere inside the reaction chamber. The setup thus developed is different from the one previously used for the synthesis of BNNTs [11, 17] and BNMTs [10]. The precursor's types and their ratio are selected on the basis of its successful use for the synthesis of BNNTs in some of the earlier works [11, 17]. A critical analysis of the synthesis of BNNTs and BNMTs [6, 10] showed that the growth duration is the only possible reason that makes a huge difference in the structure and morphology of the as-synthesized BN structures. However, it has also been found that other experimental parameters like precursor's types, their ratio, experimental setup, and increase in temperature above 1200°C have a great effect on the size and morphology of the synthesized BN products [6, 11, 16, 17].

Unlike all of the above logics and strategies, a bit different plan based on a slight modification in our successful work on the synthesis of BNNTs and the idea behind previously synthesized vertically aligned CNTs [21] has been effectively used for the synthesis of BNMTs in the present study. As a modification, vacuum or use of inert gasses is eliminated with the use of ammonia as an internal atmosphere inside the quartz tube chamber. Both MgO and Fe_2O_3 are selected as precursors with B, because they are effective producers of B_2O_2 and catalysts [16]. During the experimental run, the precursors are heated up to 1200°C. During this stage, they are assumed to produce B_2O_2 in the vapor form and Mg–Fe alloys on the top of precursors in the boat and on its inner walls. At a higher temperature, NH_3 reacts with as-formed Mg–Fe alloys and B_2O_2. NH_3 works as an etching agent for Mg–Fe alloys. It etches away the Fe particles and thus produces nucleation sites in Mg particles. The creation of the nucleation sites depends on the etching rate, i.e., higher the etching rate the further will nucleation sites produce in Mg particles. The reaction of NH_3 with B_2O_2 produces a BN species that diffuses in Mg particles. With the passage of time, it supersaturates and grows in the form of tubular structures from nucleation sites in Mg particles. Majority of the BNMTs thus grown are vertically aligned following almost the same logics and mechanism previously described for vertically aligned CNTs [21].

CONCLUSIONS

The successful synthesis of BNMTs showed that the experimental setup and adjustments of certain experimental parameters play a key role in the synthesis of different BN nanostructures. In the present work, it has been found that the elimination of vacuum or inert gases as an internal environment causes the material to grow in the form of microtubes instead of nanotubes. Further, it has been noted that the elongation of growth duration once a particular structure has been developed results in another structure (i.e., from microtubes to nanosheet). The growth continues smoothly as long as the growth precursors are available in a particular growth duration. The unavailability of the growth precursor causes the microtubes walls to grow thinner and thinner in particular growth duration until it becomes a sheet. More structures of nanoscale BN can be synthesized with further changes in the experimental parameters. The synthesized BNMTs are found to be of great importance as a neutron-sensing element in a solid state neutron detector, neutron capture therapy, micro-fluids devices, targeted drug delivery etc.

ACKNOWLEDGMENTS

We are extremely grateful to Prof. Dr. Norani Muti Mohamed, MOR Nanotechnology and Director of COINN, (University of Technology PETRONAS, 31750 Tronoh Perak Malaysia) for her fruitful discussion and providing lab (Nanotechnology) and characterization facilities (CAL) for our research work.

FUNDING

We are grateful to Skim Bright Spark Program, University of Malaya, 50603 Kuala Lumpur, Malaysia, for providing financial assistance and facilities for our research work.

REFERENCES

1. Lin, J.; Huang, Y.; Tang, C.; Bando, Y.; Zou, J.; Golberg, D. Thin-walled B-C-N ternary microtubes: from synthesis to electrical, cathodoluminescence and field-emission properties. *Journal of Materials Chemistry* **2012**, *22*, 8134–8138.
2. Hu, J.; Bando, Y.; Xu, F.; Li, Y.; Zhan, J.; Xu, J.; Golberg, D. Growth and field-emission properties of crystalline. *Advanced Materials* **2004**, *16*, 153–156.
3. Goldberger, J.; Fan, R.; Yang, P. Inorganic nanotubes: A novel platform for nanofluidics. *Accounts of Chemical Research* **2006**, *39*, 239–248.
4. Golberg, D.; Bando, Y.; Tang, C.; Zhi, C. Functional boron nitride nanotubes. In *Nanoelectronics Conference (INEC), 2010 3rd International*, IEEE, 3–8 January, 2010; pp. 47–48.

5. Grossman, J.C.; Zettl, A.K.; Wagner, L. Google Patents 2009.
6. Huang, Y.; Lin, J.; Tang, C.; Bando, Y.; Zhi, C.; Zhai, T.; Dierre, B.; Sekiguchi, T.; Golberg, D. Bulk synthesis, growth mechanism and properties of highly pure ultrafine boron nitride nanotubes with diameters of sub-10 nm. *Nanotechnology* **2011**, *22*, 145602.
7. Li, J.; Dahal, R.; Majety, S.; Lin, J.; Jiang, H. Hexagonal boron nitride epitaxial layers as neutron detector materials. *Nuclear Instruments and Methods in Physics Research Section A: Accelerators, Spectrometers, Detectors and Associated Equipment* **2011**, *654*, 417–420.
8. Oku, T.; Narita, I.; Nishiwaki, A. Synthesis, atomic structures, and electronic states of boron nitride nanocage clusters and nanotubes. *Materials and Manufacturing Processes* **2004**, *19*, 1215–1239.
9. Ahmad, P.; Mohamed, N.M.; Burhanudin, Z.A. A review of nanostructured based radiation sensors for neutron. In *AIP Conference Proceedings*, Kuala Lumpur, Malaysia, 12–14, 2012; pp. 535.
10. Huang, Y.; Bando, Y.; Tang, C.; Zhi, C.; Terao, T.; Dierre, B.; Sekiguchi, T.; Golberg, D. Thin-walled boron nitride microtubes exhibiting intense band-edge UV emission at room temperature. *Nanotechnology* **2009**, *20*, 085705.
11. Lee, C.H.; Wang, J.; Kayatsha, V.K.; Huang, J.Y.; Yap, Y.K. Effective growth of boron nitride nanotubes by thermal chemical vapor deposition. *Nanotechnology* **2008**, *19*, 455605.
12. Lee, C.H.; Xie, M.; Kayastha, V.; Wang, J.; Yap, Y.K. Patterned growth of boron nitride nanotubes by catalytic chemical vapor deposition. *Chemistry of Materials* **2010**, *22*, 1782–1787.
13. Lee, C.J.; Kim, D.W.; Lee, T.J.; Choi, Y.C.; Park, Y.S.; Lee, Y.H.; Choi, W.B.; Lee, N.S.; Park, G.-S.; Kim, J.M. Synthesis of aligned carbon nanotubes using thermal chemical vapor deposition. *Chemical Physics Letters* **1999**, *312*, 461–468.
14. Paul, A.; Bhattacharya, B. DNA functionalized carbon nanotubes for nonbiological applications. *Materials and Manufacturing Processes* **2010**, *25*, 891–908.
15. Ahmad, P.; Khandaker, M.U.; Khan, Z.R.; Amin, Y.M. A simple technique to synthesize pure and highly crystalline boron nitride nanowires. *Ceramics International* **2014**, *40* (9) Part B, November 2014, 14727–14732.
16. Zhi, C.; Bando, Y.; Tan, C.; Golberg, D. Effective precursor for high yield synthesis of pure BN nanotubes. *Solid State Communications* **2005**, *135*, 67–70.
17. Pakdel, A.; Zhi, C.; Bando, Y.; Nakayama, T.; Golberg, D. A comprehensive analysis of the CVD growth of boron nitride nanotubes. *Nanotechnology* **2012**, *23*, 215601.
18. Ciofani, G.; Genchi, G.G.; Liakos, I.; Athanassiou, A.; Dinucci, D.; Chiellini, F.; Mattoli, V. A simple approach to covalent functionalization of boron nitride nanotubes. *Journal of Colloid and Interface Science* **2012**, *374*, 308–314.
19. Wang, J.; Xie, M.; Yap, Y.K. Optimum Growth of Vertically-aligned Boron Nitride Nanotubes at Low Temperatures. In *APS Meeting Abstracts 2007*; pp. 31008.
20. Arenal, R.; Ferrari, A.; Reich, S.; Wirtz, L.; Mevellec, J.-Y.; Lefrant, S.; Rubio, A.; Loiseau, A. Raman spectroscopy of single-wall boron nitride nanotubes. *Nano Letters* **2006**, *6*, 1812–1816.
21. Zhang, W.D.; Wen, Y.; Min Liu, S.; Tjiu, W.C.; Qin Xu, G.; Ming Gan, L. Synthesis of vertically aligned carbon nanotubes on metal deposited quartz plates. *Carbon* **2002**, *40*, 1981–1989.

A simple technique to synthesise vertically aligned boron nitride nanosheets at 1200°C

P. Ahmad, M. U. Khandaker* and Y. M. Amin

In order to make the synthesis of boron nitride nanosheets (BNNS) easier and safe, a very simple technique is introduced in the present study. In this technique BNNS are synthesised in a conventional horizontal dual zone quartz tube furnace at 1200°C. Field emission scanning electron microscopy image shows the morphology of synthesised BNNS like spread out cotton packs. Transmission electron microscopy (TEM) images show highly crystalline nature of synthesised nanosheets of boron nitride with an interlayer spacing of 0.34 nm. Raman spectrum shows a major peak at 1366 (cm^{-1}) that corresponds to E_{2g} mode of h-BN. X-ray photon spectroscopy survey shows B 1s (at 191 eV) and N 1s (at 398 eV) peaks that verify the boron and nitrogen contents in synthesised nanosheets.

Keywords: BNNS, BNNTs, Synthesis

Introduction

The study of the nanostructured materials has revealed that the properties (electrical, mechanical, optical, etc.) of these materials are totally different from their bulk counterpart due to electrons and holes confinement,[1] surface effects and geometrical confinement of the phonon. So any desired property for a bulk material can be achieved through their size reduction from bulk to nano.[2,3]

Hexagonal boron nitride (h-BN) is a wide band gap semiconductor,[4] with a direct band gap of 5.97 eV.[5] It is the normal phase of BN that is stable at room temperature and pressure. Its structure is similar to that of graphite, but alternative boron and nitrogen atoms substitute for carbon atoms.[4]

Boron nitride nanosheets (BNNS) are the two-dimensional nanostructure of h-BN with excellent physiochemical properties. The structure of BNNS is similar to the nanosheets of graphene; however, in case of BNNS, alternative boron and nitrogen atoms substitute for carbon atoms. In addition to its similar mechanical properties and thermal conductivity to graphene,[6] BN has some excellent properties as compared to its carbon counterpart. These properties included a constant band gap of 5–6 eV, thermal stability, higher chemical inertness and resistance to oxidation etc.[7] All these properties have made BNNS a very useful and attractive material for use in a wide range of applications. The devices thus developed with BNNS will be highly capable of operating in oxidative and high temperature environment. Further, it can be used as insulating composites of high mechanical properties and thermal conductivity.[6,8]

All the features and advantages of BNNS for different applications are dependent on its purity, size and alignment, which in turn depend on the synthesis methods. In the absence of a well known synthetic method for the preparation of BNNS, its properties and applications have mostly remained unexplored.

Chemical vapour deposition techniques have successfully been introduced to synthesise BNNS on different substrates.[9,10] Though, high quality BNNS in vertically aligned format have been synthesised via this technique;[9] however, the high price and complicated steps involved during the synthesis have made it difficult to be easily followed by other researchers. Furthermore, BF_3 gas was used in precursors,[9] which is highly toxic and can cause serious health problems.[11] Therefore, additional precaution measures are needed during its use. The corrosive nature of BF_3[12] is also a serious threat to the experimental set-up and its other accessories. Thus, further facilities and special arrangements are needed to overcome these problems. Therefore, the synthesis of BNNS in the form of thin film via a simple, easy and relatively safe technique was a great challenge regarding the choice of precursors, experimental set-up and substrate's type.

A simple thermal chemical vapour deposition technique with B, MgO and FeO as precursors was introduced for the synthesis of boron nitride nanotubes (BNNTs) by Lee *et al.*[13,14] This technique is a bit modified by turning the open end of the one closed inner quartz test tube towards the gas inlet. The synthesis of BNNS was claimed with this experimental set-up and B, MgO and FeO as precursors at 900, 1000, 1100 and 1200°C in a growth duration of 30 and 60 min.[15] The increased vapour pressure of B_xO_y due to the trapped growth vapours in their synthesis conditions was considered the most probable reason for the synthesis of BNNS.[15]

Unlike Pakdel *et al.*,[15] the Lee *et al.*[13] technique is further simplified in our previous works with the use of NH_3 or Ar gas as a reaction atmosphere instead of

---

Department of Physics, Faculty of Science, University of Malaya, 50603 Kuala Lumpur, Malaysia

*Corresponding author, email mu_khandaker@um.edu.my

Published by Maney on behalf of the Institute
Received 29 August 2014; accepted 6 December 2014
DOI 10.1179/1743676114Y.0000000225

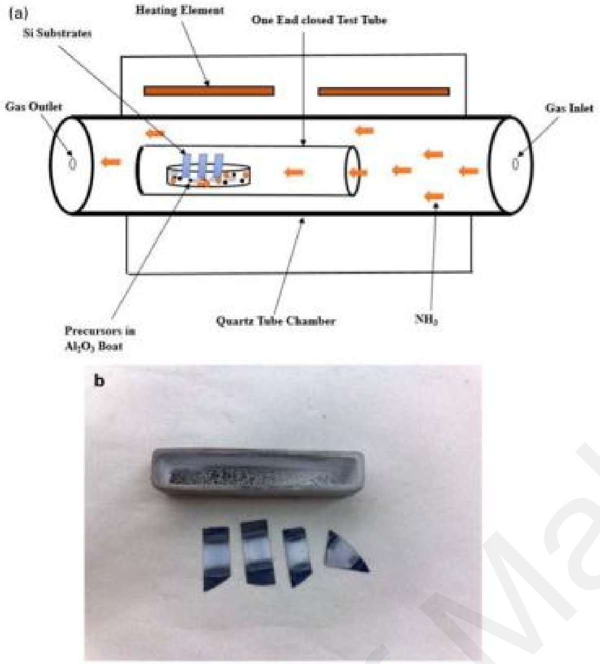

1 ***a*** **sketch of experimental set-up used for synthesis of BNNS;** ***b*** **white spots on Si substrate and inside alumina boat are as synthesised BNNS**

vacuum or evacuation.[16,17] As a result, no vacuum pump is needed to be bought or operates with the experimental set-up. This simplification has not only reduced the required expertise for running the vacuum pump with the experimental set-up but also made it ~18% cost effective.[17]

It has been concluded in our previous work[16] on the synthesis of boron nitride microtubes (BNMTs) and formation of BNNS that the unavailability of further growth species and an increase in the growth duration or temperature cause the tube to split and form vertically aligned nanosheets.[16] These logics are successfully employed in the present work, and vertically aligned BNNS are synthesised directly on Si substrate in a growth duration of 90 min. The full detail is mentioned in the next section.

Experimental

Vertically aligned BNNS are synthesised at 1200°C in a conventional horizontal dual zone quartz tube furnace. Amorphous boron powder, magnisium oxides (MgO) and maghemite (γ-Fe_2O_3) nanopowder of 99.9+ % purities were bought from MTI Corporation and used as precursors. A total of 100 mg of precursors that contained 50 mg of B, 25 mg of MgO and 25 mg of γ-Fe_2O_3 is uniformly mixed in alumina boat. The boat (with precursor inside) is covered with a few Si substrates (cut in 2.5 × 1.2 cm dimension from monocrystaalline Si wafer, IC Grade, size: 3–8″, Conductive type: P, Dopant: boron) and placed inside one end closed quartz test tube near the closed end.

The one end closed quartz tube is then placed inside the quartz tube chamber of dual zone furnace in such a way that its open end is toward the gas inlet, as shown in Fig. 1*a*. Furthermore, it is made sure that the precursors in the boat are exactly beneath the heating element. Afterwards, the precursors are heated up to 1200°C in the presence of NH_3 flow at a rate of 200 sccm. The system is kept in such a condition for 90 min at 1200°C.

After that, NH_3 flow is stopped, and the system is allowed to cool down to room temperature. At room temperature, white colour BNNS are found deposited on Si substrate and on the inner wall of alumina boat, as shown in Fig. 1*b*.

The as synthesised sample is then characterised with the help of different characterisation instruments to study its surface morphology and crystallinity and to find out its elemental composition.

The surface morphology is investigated using field emission electron microscopy (model FESEM Quanta 200). Transmission electron microscope (TEM) measurements are recorded using Philips CM 300 (300 kV) instruments to reveal diameter and crystallinity. The Raman spectrum of the sample is obtained (for composition, phase and crystallinity) with the help of Horiba Jobin Yvon 800 UV Micro-Raman Spectrometer using Ar+ laser source with the wavelength of 514.5 nm. The X-ray photoelectron spectrometer (XPS) analyses of the sample (for finding the compositions) are performed on a PHI 5600 with a monochromatic Al K_α source at 14 kV and 350 W, and photoelectron take off angle of 450.

Results and discussion

Figure 2 shows FESEM image of vertically aligned BNNS synthesised in a growth duration of 90 min. The synthesised nanosheets of hexagonal BN have wrinkled

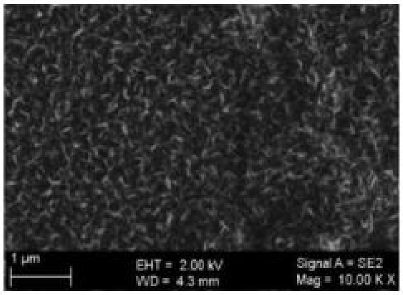

2 Image (FESEM) of vertically aligned BNNS synthesised in growth duration of 90 min

morphology and are vertically aligned on silicon substrate. It has been observed that the wrinkled or bent morphology of the BNNS is due to their smaller size and high residual stresses generated during the growth at high temperatures.

The as synthesised BNNS sample is further characterised with TEM to confirm its sheet-like morphology and crystallinity. The images thus obtained are shown in Fig. 3. The lower resolution TEM image shown in Fig. 3*a* reveals that most of the nanosheets are bended and scrolled[9] without any tapered edge morphology. Such a morphology of the BNNS is somehow similar to that of carbon nanosheets.[18] It has frequently been reported that bending and scrolling is an intrinsic property of the two-dimensional nanostructures.[9] The individual morphology of each BN nanosheet can clearly be seen in high resolution TEM image shown in Fig. 3*b*. The scale on the image shows that the diameter of the BNNS can be found in the range of 15–40 nm. By further increasing the resolution (of BNNS in high resolution TEM images), there appears lattice fringes (lengthwise) on BNNS, as shown in Fig. 3*c* and *d*. These lattice fringe have an interlayer spacing of 0.34 nm, as shown in Fig. 3*e*. This interlayer spacing (0.34 nm) is the characteristics of $d_{(002)}$ spacing of h-BN and its highly crystalline nature.[19,20]

Raman spectroscopy was employed to find out the elemental composition and phase and to confirm the crystalline nature of synthesised nanosheets of h-BN. Raman shift of the synthesised nanosheets of BN was searched in the spectral range of 900 to 1600 (cm^{-1}) using laser excitation of 534 nm. The Raman spectrum thus obtained is shown in Fig. 4. The spectrum shows two peaks: the high intensity peak at 1366 (cm^{-1}) corresponds

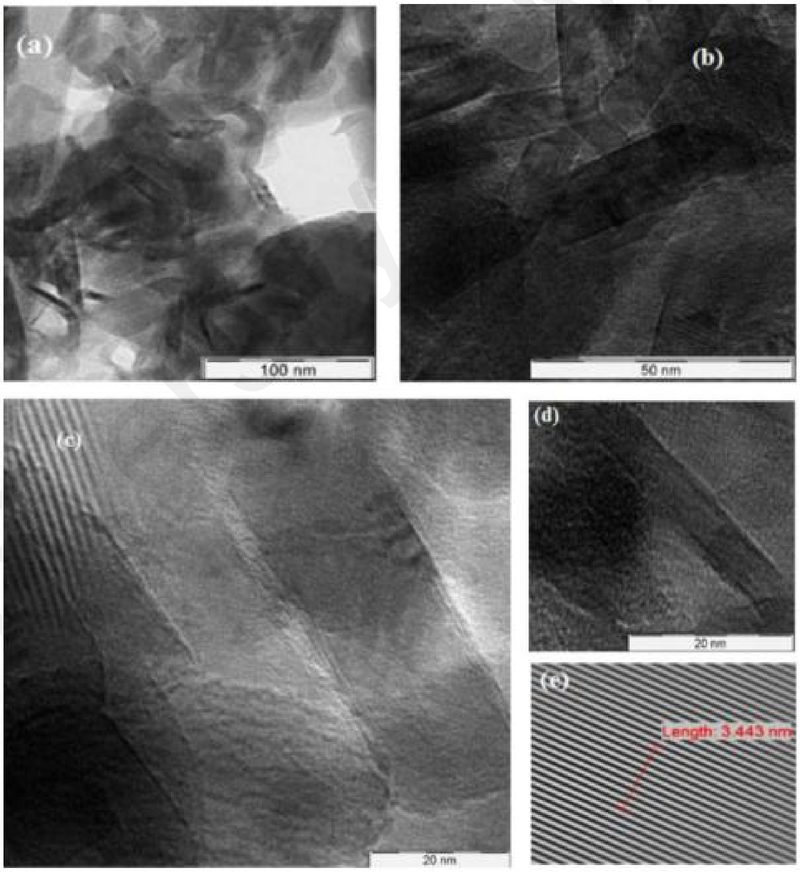

a lower and *b* high magnification TEM images show several BNNS; *c* higher magnification TEM image of BNNS with some parallel line; *d* higher magnification TEM image of single BNNS; *e* image shows that sheet has interlayer spacing of 0.34 nm that shows highly crystalline nature of synthesised

3 Images (TEM) of BNNS

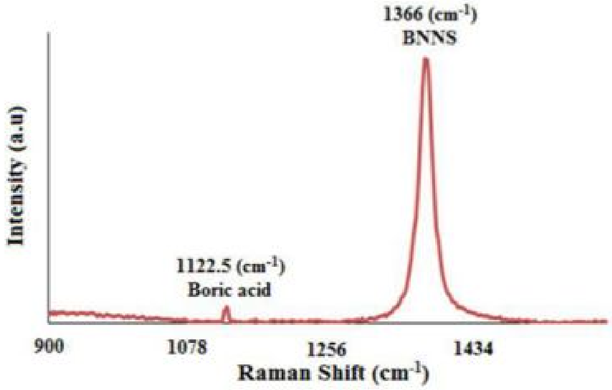

4 Raman spectrum shows high intensity peak at 1366 (cm^{-1}) correspond to E_{2g} mode of h-BN (BNNS); lower intensity peak at 1122.5 (cm^{-1}) represents Boric acid in synthesised sample

to E_{2g} mode of h-BN,[15,21] which represents BNNS in the present sample, whereas a lower intensity peak at 1122.5 (cm^{-1}) represents a minute quantity of boric acid, which might have formed by the spontaneous reaction of boron and B_2O_3 (left during the synthesis of BNNS) with moisture and oxygen in the air.[22] The sharpness of the high intensity Raman peak confirmed the crystalline nature of the synthesised BNNS.[23]

The elemental composition of synthesised BNNS sample was further confirmed with the help of XPS. The as obtained XPS survey is shown in Fig. 5. The survey shows three main peaks at 191, 398 and 535 eV. The peaks at 191 and 398 eV are the B 1s and N 1s peaks that represent h-BN (BNNS) in the sample.[24] The O 1s peak at 535 eV may either be due to the as used Si substrate or B_2O_3 (which later on converted to boric acid by the interaction of laser during Raman spectroscopy[22]).

The main factors responsible for the synthesis of BNNS in the present study are the following: the nature of internal environment inside the chamber of quartz tube furnace (during the synthesis) and increased growth duration. Vacuum or evacuation is normally created with the help of vacuum pump to eliminate the role of impurities during the synthesis of BNNTs.[25] Ar inert gas has also been employed for the same purpose during the synthesis of BNNTs[26] and boron nitride nanowires.[27] Unlike these, NH_3 gas is used as a reaction atmosphere during the synthesis of BNNS in the present study. This is one of the basic reasons for the BNNS synthesis. Along with the elimination of vacuum or inert gases, increased growth duration has also played a key and parallel role during the synthesis of BNNS. Normally, BNNTs are formed with the vacuum[25] or Ar gas[28] as an internal environment in the chamber. As the time passes, the top surface of the precursor in the boat is covered by the initially formed BNNTs.[29] This blockage stops the formation of further growth species. Thus, the internal environment inside the chamber and increased growth duration cause the tube to grow thinner and thinner until it splits and converts into a sheet-like morphology. In our previous study,[16] this phenomenon has been observed in the FESEM results. However, the absence of tubular morphologies or formation of sheet from the tubular structure is not observed in the current FESEM results. This is due to the increased growth duration (90 min instead of 60 min), which have split all the tubular morphologies into sheet-like structures.

Along with the obvious reasons (absence of vacuum or Ar free environment and increased growth duration) for the synthesis of BNNS in the present study, the role

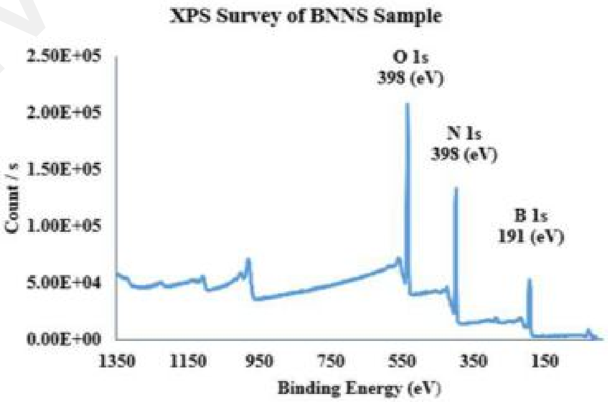

5 Survey (XPS) shows B 1s (at 191 eV) and N 1s (398 eV) peaks that represent BN (BNNS), whereas O 1s peak (at 535 eV) is due to as used Si substrate

of the substrate[30,31] and as produced metallic catalysts or their alloys in the absence of vacuum or Ar free environment cannot be ignored.

Diameter of the as synthesised materials depends on the grain size and morphology of the substrate. By varying the grain size and morphology of the substrate, the diameter of the final product can easily be controlled.[32] Si wafers are properly cut and cleaned before using as a substrate for the synthesis of any nanostructure material. During the cleaning process, the impurities left on the substrate might have modified the morphology of the substrate, which in other words might have resulted in pattern for the synthesis of BNNS in the present study.

In case of carbon nanotubes (CNTs), metal oxide catalysts or their alloys are first deposited on Si substrate. An etching agent is then introduced, which etches away some of the catalysts and thus produces a pattern for the synthesis of vertically aligned CNTs.[33] A bit same concept is used during the synthesis of BNMTs.[16] However, in case of CNTs, metal oxide catalysts are first deposited on Si substrate, and after etching, they are used for the deposition of CNTs.[33] Whereas, in the case of BNMTs,[16] metal oxide catalysts are used as precursor (mixed) with boron powder. At higher temperature (the as formed), metallic catalysts or their alloys are first deposited on the substrate. When ammonia is introduced into the system, it not only provides N_2 through its decomposition for BNMTs synthesis, but before decomposition (at lower temperature), it works as an etching agent and thus produces a pattern for the BNMTs growth. The absence of vacuum or inert gases might have resulted in some kind of different pattern (sheet-like) due to the first interaction of ammonia gas (as an etching agent). This might have helped in growing BN nanostructures in the form of sheet-like morphology due to the reaction of N_2 gas (from decomposed NH_3) with either MgB_2 or Fe_2B.[34]

Conclusion

The results obtained in the present study showed that BNNS can easily be synthesised via a simple, safe and relative economical technique. The synthesised nanosheets of BN thus have a diameter in the range of 15–40 nm.

It has been noted that the nature of the internal environment inside the chamber (of horizontal quartz tube furnace) and growth duration has a key role in the synthesis of BNNS. However, the nature of the substrate and the role of the as formed catalysts or their alloys in the absence of vacuum or Ar free environment cannot be ignored. The synthesised BNNS can be used in the development of devices, which will be capable of operating in oxidative and high temperature environment.

Acknowledgement

We are extremely grateful to the Skim Bright Spark Program, University of Malaya, 50603 Kuala Lumpur, Malaysia, for providing funds and facilities for our research work.

References

1. J. Lauret, R. Arenal, F. Ducastelle, A. Loiseau, M. Cau, B. Attal-Tretout, E. Rosencher and L. Goux-Capes: 'Optical transitions in single-wall boron nitride nanotubes', [redacted], 2005, **94**, 037405.
2. P. Jaffrennou, F. Donatini, J. Barjon, J.-S. Lauret, A. Maguer, B. Attal-Trétout, F. Ducastelle and A. Loiseau: 'Cathodoluminescence imaging and spectroscopy on a single multiwall boron nitride nanotube', [redacted], 2007, **442**, 372–375.
3. C. Zhi, Y. Bando, C. Tang, D. Golberg, R. Xie and T. Sekigushi: 'Phonon characteristics and cathodolumininescence of boron nitride nanotubes', [redacted], 2005, **86**, 213110-213110-213113.
4. Y. N. Xu and W. Ching: 'Calculation of ground-state and optical properties of boron nitrides in the hexagonal, cubic, and wurtzite structures', [redacted], 1991, **44B**, 7787.
5. Y. Huang, Y. Bando, C. Tang, C. Zhi, T. Terao, B. Dierre, T. Sekiguchi and D. Golberg: 'Thin-walled boron nitride microtubes exhibiting intense band-edge UV emission at room temperature', [redacted], 2009, **20**, 085705.
6. Y. Wang, Z. Shi and J. Yin: 'Boron nitride nanosheets: large-scale exfoliation in methanesulfonic acid and their composites with polybenzimidazole', [redacted], 2011, **21**, 11371–11377.
7. C. Y. Zhi, Y. Bando, C. C. Tang, Q. Huang and D. Golberg: 'Boron nitride nanotubes: functionalization and composites', [redacted], 2008, **18**, 3900–3908.
8. D. Golberg, Y. Bando, C. C. Tang and C. Y. Zhi: 'Boron nitride nanotubes', [redacted], 2007, **19**, 2413–2432.
9. J. Yu, L. Qin, Y. Hao, S. Kuang, X. Bai, Y.-M. Chong, W. Zhang and E. Wang: 'Vertically aligned boron nitride nanosheets: Chemical vapor synthesis, ultraviolet light emission, and superhydrophobicity', [redacted], 2010, **4**, 414–422.
10. L. Song, L. Ci, H. Lu, P. B. Sorokin, C. Jin, J. Ni, A. G. Kvashnin, D. G. Kvashnin, J. Lou and B. I. Yakobson: 'Large scale growth and characterization of atomic hexagonal boron nitride layers', [redacted], 2010, **10**, 3209–3215.
11. K.-S. Liu: 'Preparation of fatty acid methyl esters for gas-chromatographic analysis of lipids in biological materials', [redacted], 1994, **71**, 1179–1187.
12. O. P. Strausz, T. W. Mojelsky, J. D. Payzant, G. A. Olah and G. S. Prakash: 'Upgrading of Alberta's heavy oils by superacid-catalyzed hydrocracking', [redacted], 1999, **13**, 558–569.
13. C. H. Lee, J. S. Wang, V. K. Kayatsha, J. Y. Huang and Y. K. Yap: 'Effective growth of boron nitride nanotubes by thermal chemical vapor deposition', [redacted], **2008**, 19, 455605–455609.
14. C. H. Lee, M. Xie, V. Kayastha, J. S. Wang and Y. K. Yap: 'Patterned growth of boron nitride nanotubes by catalytic chemical vapor deposition', [redacted], 2010, **22**, 1782–1787.
15. A. Pakdel, C. Zhi, Y. Bando, T. Nakayama and D. Golberg: 'Boron nitride nanosheet coatings with controllable water repellency', [redacted], 2011, **5**, 6507–6515.
16. P. Ahmad, M. U. Khandaker, Y. M. Amin and Z. R. Khan: 'Synthesis of boron nitride microtubes and formation of boron nitride nanosheets', *Mater. Manuf. Process.*, 2014.
17. P. Ahmad, M. U. Khandaker and Y. M. Amin: 'Synthesis of boron nitride nanotubes by argon supported thermal chemical vapor deposition', [redacted], 2015, **67E**, 33–37.
18. N. G. Shang, P. Papakonstantinou, M. McMullan, M. Chu, A. Stamboulis, A. Potenza, S. S. Dhesi and H. Marchetto: 'Catalyst-free efficient growth, orientation and biosensing properties of multilayer graphene nanoflake films with sharp edge planes', [redacted], 2008, **18**, 3506–3514.
19. A. Pakdel, C. Zhi, Y. Bando, T. Nakayama and D. Golberg: 'A comprehensive analysis of the CVD growth of boron nitride nanotubes', [redacted], 2012, **23**, 215601.
20. J. Wang, L. Zhang, G. Zhao, Y. Gu, Z. Zhang, F. Zhang and W. Wang: 'Selective synthesis of boron nitride nanotubes by self-propagation high-temperature synthesis and annealing process', [redacted], 2011, **184**, 2478–2484.
21. L. Guo and R. Singh: 'Catalytic growth of boron nitride nanotubes using gas precursors', [redacted], 2009, **41E**, 448–453.
22. R. Arenal, A. Ferrari, S. Reich, L. Wirtz, J.-Y. Mevellec, S. Lefrant, A. Rubio and A. Loiseau: 'Raman spectroscopy of single-wall boron nitride nanotubes', [redacted], 2006, **6**, 1812–1816.
23. Y. Huang, J. Lin, C. Tang, Y. Bando, C. Zhi, T. Zhai, B. Dierre, T. Sekiguchi and D. Golberg: 'Bulk synthesis, growth mechanism and properties of highly pure ultrafine boron nitride nanotubes with diameters of sub-10 nm', [redacted], **2011**, 22, 145602–145610.
24. B. Zhong, L. Song, X. Huang, G. Wen and L. Xia: 'Synthesis of boron nitride nanotubes with SiC nanowire as template', [redacted], 2011, **46**, 1521–1523.
25. C. H. Lee, J. Wang, V. K. Kayatsha, J. Y. Huang and Y. K. Yap: 'Effective growth of boron nitride nanotubes by thermal chemical vapor deposition', [redacted], 2008, **19**, 455605.

26. P. Ahmad, M. Khandaker and Y. Amin: 'A comprehensive study of boron nitride nanotubes multiple synthesis from a single precursor', *Indian J. Phys.*, 2014, 1–8.
27. P. Ahmad, M. U. Khandaker, Z. R. Khan and Y. M. Amin: 'A simple technique to synthesize pure and highly crystalline boron nitride nanowires', [redacted], 2014, **40**, 14727–14732.
28. D. Özmen, N. A. Sezgi and S. Balcı: 'Synthesis of boron nitride nanotubes from ammonia & a powder mixture of boron and iron oxide', [redacted], 2013, **219**, 28–36.
29. C. Zhi, Y. Bando, C. Tan and D. Golberg: 'Effective precursor for high yield synthesis of pure BN nanotubes', [redacted], 2005, **135**, 67–70.
30. Z. Zhang, B. Wei, G. Ramanath and P. Ajayan: 'Substrate-site selective growth of aligned carbon nanotubes', [redacted], 2000, **77**, 3764–3766.
31. B. Wei, R. Vajtai, Z. Zhang, G. Ramanath and P. Ajayan: 'Carbon nanotube-magnesium oxide cube networks', [redacted], 2001, **1**, 35–38.
32. Y. C. Choi, Y. M. Shin, Y. H. Lee, B. S. Lee, G.-S. Park, W. B. Choi, N. S. Lee and J. M. Kim: 'Controlling the diameter, growth rate, and density of vertically aligned carbon nanotubes synthesized by microwave plasma-enhanced chemical vapor deposition', [redacted], 2000, **76**, 2367–2369.
33. C. J. Lee, J. Park, S. Y. Kang and J. H. Lee: 'Growth and field electron emission of vertically aligned multiwalled carbon nanotubes', [redacted], 2000, **326**, 175–180.
34. C.-Y. Su, W.-Y. Chu, Z.-Y. Juang, K.-F. Chen, B.-M. Cheng, F.-R. Chen, K.-C. Leou and C.-H. Tsai: 'Large-scale synthesis of boron nitride nanotubes with iron-supported catalysts', *J. Phys. Chem. C*, 2009, **113C**, 14732–14738.

CHAPTER 4

CONCLUSIONS AND FUTURE DIRECTION

4.1 Conclusions

A simple and cost effective experimental technique has been developed for the synthesis of BNNTs. This technique is entitled as Argon-supported thermal CVD. In this technique, vacuum or evacuation inside the chamber is replaced by Argon gas flow as a reaction atmosphere. The used of Ar gas has eliminated the use of vacuum pump which in other words has reduced the price of the experimental set up by ~18 %. It (Ar) prevents the oxidation of the material during the experimental process. Thus along with economic benefits, Ar gas can help in producing longer BNNTs by preventing the oxidation of as produced Mg and Fe catalyst. Furthermore, it has been concluded that a continuous supply of Ar gas along with the availability of precursor may grow longer, high quality and large quantity of the BNNTs.

To study the effects of precursor's nature on size and morphology of h-BN nanostructures, BNNTs are synthesized via Argon-supported CVD technique from fresh as well as residual material left after first and second experimental run. For the first time, the as obtained experimental products synthesized from fresh and residual left in the boat after first and second experimental run are characterized and analyzed for their size, morphology and quality of the final product. The study showed that the precursor's nature not only changes the diameter and length but also the morphology and catalytic content in the tip at the top of the tube. It has been concluded that the quantity and size of the BNNTs can be increased to any desired level by making slight modifications in the experimental set up in such a way that it can easily prevent the blockage of the precursors in the boat due to as synthesized BNNTs. With such modifications, BNNTs synthesized will not only be in high quality or quantity but will also have a length even up to centimeter scale.

The technique for the synthesis of vertically aligned h-BN nanostructures (BNNTs) has been developed by using "Argon-supported thermal CVD" technique with the help of combined logics of previously synthesized vertically aligned CNTs and pattern growth of BNNTs. The results showed that the nanotubes alignment depends on the density of the nucleation sites which further depends on the etching rate of the as-deposited catalysts or their alloys on the substrate layer. The reduced etching ability of NH_3 due to its simultaneous reaction with B_2O_2 to provide Nitrogen for the formation of BN-species may be the possible reason for the non-uniform diameter or relatively partially aligned nature of BNNTs in the present work.

Nanostructures of ^{10}h-BN (^{10}BNNTs) are synthesized by using ^{10}B (Boron-10) as a precursor with MgO and γ-Fe_2O_3 in Argon-supported thermal CVD. The fabrication of ^{10}BNNTs has proved that the Argon-assisted thermal CVD technique for the BNNTs is equally applicable for the synthesis of ^{10}BNNTs. It has been found that the as synthesized ^{10}BNNTs with nanoscale properties, multilayered structure, crystalline nature and ^{10}B enrichment can be an excellent choice as a sensing element in a solid state neutron detector with 100 % proposed efficiency.

Experimental approach has been used to study the main experimental parameters responsible for the synthesis of different nanostructures of h-BN or ^{10}h-BN. In this regard, Argon-supported thermal CVD is tested with growth duration of smaller than 60 min. BNNWs have been formed at 1200 ºC within a growth duration of 30 min. This relatively short growth duration is found be the main reason for the synthesis of BNNWs via Argon-supported thermal CVD. The type and nature of the reaction atmosphere and growth duration have also been proved to play a key role in the synthesis of h-BN nanostructures. Ammonia gas flow is tested as a reaction atmosphere instead of Argon gas or vacuum in thermal CVD technique. Ammonia as a reaction atmosphere resulted in the synthesis of pipe-like morphologies of BNMTs on Si substrate, cone-like morphologies of BNMTs and formation of BNNS inside alumina boat. The change in morphology of the BNMTs and formation of BNNS is found to be due to the nature of the surface, non-availability of the precursors and long growth duration. The formation of BNNS from BNMTs in long growth duration is also verified by the synthesis of BNNS under similar circumstances within a growth duration of 90 min.

Thus, in the current thesis, a simple and cost-effective technique is developed for the synthesis of BNNTs that has further been optimized to study, the effects of precursor's nature, synthesis of vertically aligned BNNTs and synthesis of ^{10}BNNTs. In addition, the experimental parameters are clearly identified for the individual/specific synthesis of BNNWs, BNMTs and BNNS etc.

4.2 Future Directions

As it has been discussed in Chapter 3 that a simple and cost effective Argon-supported thermal CVD is developed for the synthesis of BNNTs; The as-developed Argon-supported thermal CVD is further optimized by changing different experimental parameters which resulted in determining separate parameters responsible for the synthesis of BNNWs, BNMTs and BNNS etc. However, there are several improvements that need to be carried out in the future studies.

In Chapter 3: Paper 2 (Ahmad et al., 2015a) and 3 (Ahmad et al., 2015), it is mentioned that the use of Argon gas as a reaction atmosphere prevents the oxidation of the as-used catalysts and thus helped in growing of longer BNNTs. However, the blockage of precursors in the boat by the initially formed BNNTs not only stops the synthesis of new BNNTs but also prevents further growth of the already formed BNNTs. In future studies, this problem can be solved by replacing the boat with a device (like the one used for concrete mixing) of appropriate size and shape that can keep or separate the as-formed BNNTs layer, and continuously make a homogeneous mixture of the rest of the precursors for further synthesis. This will not only prevent the top of precursor from blocking due to formation of BNNTs layer but also helps to continue synthesis of BNNTs till the precursors are completely utilized.

In Paper 4 (Ahmad, Khandaker, & Amin, 2014), vertically aligned BNNTs are reported with a large and non-uniform diameter. It has been noted that the alignment of the BNNTs depends on the density of nucleation sites produced in the as-deposited catalysts due to ammonia etching. The choice of suitable catalysts deposited at the top of the substrate surface and absence of separate etching with ammonia were considered to be the main reasons for the size, morphology and alignment of the as synthesized BNNTs. Future studies will be focused on the search of the suitable catalysts or their alloys and separate ammonia etching of the as-deposited catalysts or their alloys to produce the desired number of nucleation sites.

In Paper 5 (Ahmad et al., 2015b), highly crystalline multilayered structures of ^{10}BNNTs were reported. ^{10}BNNTs is a potential neutron sensing element and is predicted to have 100 % neutron detection capability. Future studies will be based on the development of a solid state neutron detector with ^{10}BNNTs as a neutron sensing element.

In Paper 6 (Ahmad, Khandaker, Khan et al., 2014), pure and highly crystalline BNNWs synthesis are reported via a simple technique. Future studies will be focused on the practical applications of BNNWs in the field of biomedical, MEMs and solid state neutron detector.

Paper 7 (Ahmad, Khandaker, Amin et al., 2015) and 8 (Ahmad, Khandaker, Amin et al., 2014) describe the synthesis of BNMTs in the presence of ammonia as a reaction atmosphere instead of Argon. The production and deposition of as-produced catalysts on the substrate during the experimental run produce nucleation sites. The size of nucleation sites increases with the passage of time due to ammonia etching. As a result, most of the nucleation sites are destroyed due to longer exposure to ammonia and thus left with a very few sites that results in a small number of BNMTs. Future studies will concentrate on to increase the number and length of BNMTs. In this regard, the etching duration will be optimized to the extent where it will not destroy the already formed nucleation sites. The large number of nucleation sites will help in growing more number of BNMTs. The ideas for growing longer and large quantity of BNNTs described in Paper 2 (Ahmad, Khandaker et al., 2015a) and 3 (Ahmad et al., 2015) can equally be applied for growing longer and large quantity of BNMTs.

Synthesis of BNNS is described via a simple technique in Paper 9 (Ahmad et al., 2014). Future studies will be carried out in testing the as synthesized BNNS for it potential applications in the developments of microelectronics devices. The devices thus developed with BNNS will be highly capable of operating in oxidative and high temperature environment. Further, it can be used as insulating composites of high mechanical properties and thermal conductivity (Golberg et al., 2007; Wang et al., 2011).

REFERENCES

Ahmad, P., Khandaker, M., & Amin, Y. (2014). Simple technique to synthesise vertically aligned boron nitride nanosheets at 1200° C. *Advances in Applied Ceramics, 114*(5): 267-272.

Ahmad, P., Khandaker, M. U., & Amin, Y. M. (2014). Effective Synthesis of Vertically Aligned Boron Nitride Nanotubes via a Simple CCVD. *Materials and Manufacturing Processes, 30*(6): 706-710.

Ahmad, P., Khandaker, M. U., & Amin, Y. M. (2015). A comprehensive study of boron nitride nanotubes multiple synthesis from a single precursor. *Indian Journal of Physics, 89*(3): 209-216.

Ahmad, P., Khandaker, M. U., & Amin, Y. M. (2015a). Synthesis of boron nitride nanotubes by Argon supported Thermal Chemical Vapor Deposition. *Physica E: Low-dimensional Systems and Nanostructures, 67*(0): 33-37.

Ahmad, P., Khandaker, M. U., & Amin, Y. M. (2015c). Synthesis of highly crystalline multilayers structures of 10BNNTs as a potential neutron sensing element. *Ceramics International, 41*(3, Part B): 4544-4548.

Ahmad, P., Khandaker, M. U., Amin, Y. M., & Khan, Z. R. (2014). Synthesis of Boron Nitride Microtubes and Formation of Boron Nitride Nanosheets. *Materials and Manufacturing Processes, 30*(2): 184-188.

Ahmad, P., Khandaker, M. U., Amin, Y. M., & Muhammad, N. (2015). Synthesis and characterization of boron nitride microtubes. *Materials Express, 5*(3): 249-254.

Ahmad, P., Khandaker, M. U., Khan, Z. R., & Amin, Y. M. (2014). A simple technique to synthesize pure and highly crystalline boron nitride nanowires. *Ceramics International, 40*(9, Part B): 14727-14732.

Ahmad, P., Khandaker, M. U., Khan, Z. R., & Amin, Y. M. (2015). Synthesis of boron nitride nanotubes via chemical vapour deposition: a comprehensive review. *Rsc Advances, 5*(44): 35116-35137.

Ahmad, P., Mohamed, N. M., & Burhanudin, Z. A. (2012). *A review of nanostructured based radiation sensors for neutron*. Paper presented at the AIP Conference Proceedings.

Akdim, B., Pachter, R., Duan, X., & Adams, W. W. (2003). Comparative theoretical study of single-wall carbon and boron-nitride nanotubes. *Physical Review B, 67*(24): 245404.

B. Chen, R., L. Shyu, F., P. Chang, C., & F. Lin, M. (2002). Optical properties of boron nitride nanotubes. *Journal of the Physical Society of Japan, 71*(9): 2286-2289.

Bansal, N. P., Hurst, J. B., & Choi, S. R. (2006). Boron Nitride Nanotubes-Reinforced Glass Composites. *Journal of the American Ceramic Society, 89*(1): 388-390.

Berzina, B., Trinkler, L., Korsak, V., Krutohvostov, R., Carroll, D., Ucer, K., & Williams, R. (2006). Exciton luminescence of boron nitride nanotubes and nano-arches. *physica status solidi (b), 243*(14): 3840-3845.

Berzina, B., Trinkler, L., Krutohvostov, R., Williams, R., Carroll, D., Czerw, R., & Shishonok, E. (2005). Photoluminescence excitation spectroscopy in boron nitride nanotubes compared to microcrystalline h-BN and c-BN. *Physica status solidi (c), 2*(1): 318-321.

Cao, G. (2004). *Synthesis, Properties and Applications*: World Scientific.

Chen, H., Chen, Y., Li, C. P., Zhang, H., Williams, J. S., Liu, Y., . . . Ringer, S. P. (2007). Eu-doped Boron Nitride Nanotubes as a Nanometer-Sized Visible-Light Source. *Advanced Materials, 19*(14): 1845-1848.

Chen, H., Chen, Y., Liu, Y., Xu, C.-N., & Williams, J. S. (2007). Light emission and excitonic effect of boron nitride nanotubes observed by photoluminescent spectra. *Optical Materials, 29*(11): 1295-1298.

Chen, X., Gao, X., Zhang, H., Zhou, Z., Hu, W., Pan, G., . . . Song, D. (2005). Preparation and electrochemical hydrogen storage of boron nitride nanotubes. *The Journal of Physical Chemistry B, 109*(23): 11525-11529.

Chen, X., Wu, P., Rousseas, M., Okawa, D., Gartner, Z., Zettl, A., & Bertozzi, C. R. (2009). Boron Nitride Nanotubes Are Noncytotoxic and Can Be Functionalized for Interaction with Proteins and Cells. *Journal of the American Chemical Society, 131*(3): 890.

Chopra, N. G., Luyken, R. J., Cherrey, K., Crespi, V. H., Cohen, M. L., Louie, S. G., & Zettl, A. (1995). Boron-Nitride Nanotubes. *Science, 269*(5226): 966-967.

Ciofani, G., Danti, S., D'Alessandro, D., Ricotti, L., Moscato, S., Bertoni, G., . . . Mattoli, V. (2010). Enhancement of neurite outgrowth in neuronal-like cells following boron nitride nanotube-mediated stimulation. *Acs Nano, 4*(10): 6267-6277.

Ciofani, G., Raffa, V., Menciassi, A., & Cuschieri, A. (2008). Cytocompatibility, interactions, and uptake of polyethyleneimine-coated boron nitride nanotubes by living cells: Confirmation of their potential for biomedical applications. *Biotechnology and Bioengineering, 101*(4): 850-858.

Ciofani, G., Raffa, V., Menciassi, A., & Cuschieri, A. (2009). Boron nitride nanotubes: an innovative tool for nanomedicine. *Nano Today, 4*(1): 8-10.

Ciofani, G., Raffa, V., Menciassi, A., & Dario, P. (2008). Preparation of boron nitride nanotubes aqueous dispersions for biological applications. *Journal of Nanoscience and Nanotechnology, 8*(12): 6223-6231.

Ciofani, G., Raffa, V., Yu, J., Chen, Y., Obata, Y., Takeoka, S., . . . Cuschieri, A. (2009). Boron nitride nanotubes: a novel vector for targeted magnetic drug delivery. *Current Nanoscience, 5*(1): 33-38.

Deepak, F. L., Vinod, C. P., Mukhopadhyay, K., Govindaraj, A., & Rao, C. N. R. (2002). Boron nitride nanotubes and nanowires. *Chemical Physics Letters, 353*(5-6): 345-352.

Durgun, E., Jang, Y.-R., & Ciraci, S. (2007). Hydrogen storage capacity of Ti-doped boron-nitride and B⁄Be-substituted carbon nanotubes. *Physical Review B, 76*(7): 073413.

Golberg, D., Bando, Y., Huang, Y., Terao, T., Mitome, M., Tang, C. C., & Zhi, C. Y. (2010). Boron Nitride Nanotubes and Nanosheets. *Acs Nano*, *4*(6): 2979-2993.

Golberg, D., Bando, Y., Tang, C., & Zhi, C. (2010). „" *Functional boron nitride nanotubes""*. Paper presented at the Nanoelectronics Conference (INEC), 2010 3rd International.

Golberg, D., Bando, Y., Tang, C. C., & Zhi, C. Y. (2007). Boron nitride nanotubes. *Advanced Materials, 19*(18): 2413-2432.

Goldberger, J., Fan, R., & Yang, P. (2006). Inorganic nanotubes: a novel platform for nanofluidics. *Accounts of chemical research, 39*(4): 239-248.

Grossman, J. C., Zettl, A. K., & Wagner, L. (2009). AMORPHOUS SILICON SOLAR CELLS: Google Patents.

Gubin, S. P. (2009). *Magnetic nanoparticles*: John Wiley & Sons.

Han, W.-Q., Todd, P. J., & Strongin, M. (2006). Formation and growth mechanism of 10 BN nanotubes via a carbon nanotube–substitution reaction. *Applied Physics Letters, 89*(17): 173103.

Han, W.-Q., Yu, H.-G., Zhi, C., Wang, J., Liu, Z., Sekiguchi, T., & Bando, Y. (2008). Isotope effect on band gap and radiative transitions properties of boron nitride nanotubes. *Nano letters, 8*(2): 491-494.

Hao, S., Zhou, G., Duan, W., Wu, J., & Gu, B.-L. (2006). Tremendous spin-splitting effects in open boron nitride nanotubes: application to nanoscale spintronic devices. *Journal of the American Chemical Society, 128*(26): 8453-8458.

Hotze, E. M., Phenrat, T., & Lowry, G. V. (2010). Nanoparticle aggregation: challenges to understanding transport and reactivity in the environment. *Journal of environmental quality, 39*(6), 1909-1924.

Hu, J., Bando, Y., Xu, F., Li, Y., Zhan, J., Xu, J., & Golberg, D. (2004). Growth and Field-Emission Properties of Crystalline, Thin-Walled Carbon Microtubes. *Advanced Materials, 16*(2): 153-156.

Hu, S., Kan, E.-J., & Yang, J. (2007). First-principles study of interaction between H molecules and BN nanotubes with BN divacancies. *The Journal of chemical physics, 127*, 164718.

Huang, Q., Bando, Y., Xu, X., Nishimura, T., Zhi, C., Tang, C., . . . Golberg, D. (2007). Enhancing superplasticity of engineering ceramics by introducing BN nanotubes. *Nanotechnology, 18*(48): 485706.

Huang, Y., Bando, Y., Tang, C., Zhi, C., Terao, T., Dierre, B., . . . Golberg, D. (2009). Thin-walled boron nitride microtubes exhibiting intense band-edge UV emission at room temperature. *Nanotechnology, 20*(8): 085705.

Huang, Y., Lin, J., Tang, C. C., Bando, Y., Zhi, C. Y., Zhai, T. Y., . . . Golberg, D. (2011). Bulk synthesis, growth mechanism and properties of highly pure ultrafine boron nitride nanotubes with diameters of sub-10 nm. *Nanotechnology, 22*(14): 145602.

Ishigami, M., Aloni, S., & Zettl, A. (2003). *Properties of boron nitride nanotubes*.

Jaffrennou, P., Barjon, J., Lauret, J. S., Maguer, A., Golberg, D., Attal-Trétout, B., . . . Loiseau, A. (2007). Optical properties of multiwall boron nitride nanotubes. *physica status solidi (b), 244*(11): 4147-4151.

Jaffrennou, P., Donatini, F., Barjon, J., Lauret, J.-S., Maguer, A., Attal-Trétout, B., . . . Loiseau, A. (2007). Cathodoluminescence imaging and spectroscopy on a single multiwall boron nitride nanotube. *Chemical physics letters, 442*(4): 372-375.

Jang, W. S., Kim, S. Y., Lee, J., Park, J., Park, C. J., & Lee, C. J. (2006). Triangular GaN–BN core–shell nanocables: Synthesis and field emission. *Chemical physics letters, 422*(1): 41-45.

Kolodiazhnyi, T., & Golberg, D. (2005). Paramagnetic defects in boron nitride nanostructures. *Chemical physics letters, 413*(1): 47-51.

Lauret, J., Arenal, R., Ducastelle, F., Loiseau, A., Cau, M., Attal-Tretout, B., . . . Goux-Capes, L. (2005). Optical transitions in single-wall boron nitride nanotubes. *Physical review letters, 94*(3): 037405.

Lee, C. H., Wang, J. S., Kayatsha, V. K., Huang, J. Y., & Yap, Y. K. (2008). Effective growth of boron nitride nanotubes by thermal chemical vapor deposition. *Nanotechnology, 19*(45): 455605.

Lee, C. H., Xie, M., Kayastha, V., Wang, J. S., & Yap, Y. K. (2010). Patterned Growth of Boron Nitride Nanotubes by Catalytic Chemical Vapor Deposition. *Chemistry of Materials, 22*(5): 1782-1787.

Lee, C. J., Kim, D. W., Lee, T. J., Choi, Y. C., Park, Y. S., Lee, Y. H., . . . Kim, J. M. (1999). Synthesis of aligned carbon nanotubes using thermal chemical vapor deposition. *Chemical Physics Letters, 312*(5): 461-468.

Leela Mohana Reddy, A., Tanur, A. E., & Walker, G. C. (2010). Synthesis and hydrogen storage properties of different types of boron nitride nanostructures. *International Journal of Hydrogen Energy, 35*(9): 4138-4143.

Li, F., Zhu, Z., Zhao, M., & Xia, Y. (2008). Ab initio calculations on the magnetic properties of hydrogenated boron nitride nanotubes. *The Journal of Physical Chemistry C, 112*(42): 16231-16235.

Li, J., Dahal, R., Majety, S., Lin, J., & Jiang, H. (2011). Hexagonal boron nitride epitaxial layers as neutron detector materials. *Nuclear Instruments and Methods in Physics Research Section A: Accelerators, Spectrometers, Detectors and Associated Equipment, 654*(1): 417-420.

Liao, M., & Koide, Y. (2011). Carbon-based materials: growth, properties, MEMS/NEMS technologies, and MEM/NEM switches. *Critical Reviews in Solid State and Materials Sciences, 36*(2): 66-101.

Lin, J., Huang, Y., Tang, C., Bando, Y., Zou, J., & Golberg, D. (2012). Thin-walled B–C–N ternary microtubes: from synthesis to electrical, cathodoluminescence and field-emission properties. *Journal of Materials Chemistry, 22*(16): 8134-8138.

Lourie, O. R., Jones, C. R., Bartlett, B. M., Gibbons, P. C., Ruoff, R. S., & Buhro, W. E. (2000). CVD growth of boron nitride nanotubes. *Chemistry of Materials, 12*(7): 1808.

Ma, R., Bando, Y., & Sato, T. (2001). CVD synthesis of boron nitride nanotubes without metal catalysts. *Chemical Physics Letters, 337*(1-3): 61-64.

Maragó, O. M., Bonaccorso, F., Saija, R., Privitera, G., Gucciardi, P. G., Iatì, M. A., . . . Denti, P. (2010). Brownian motion of graphene. *Acs Nano, 4*(12), 7515-7523.

Matsuoka, J., Numaguchi, M., Fujino, Y., Matsuo, M., Kurose, S., Yoshida, S., & Soga, N. (2004). Isotope effects on the glass transition phenomena and thermal properties of B< sub> 2</sub> O< sub> 3</sub> glass. *Journal of non-crystalline solids, 345*: 542-545.

Mpourmpakis, G., & Froudakis, G. E. (2007). Why boron nitride nanotubes are preferable to carbon nanotubes for hydrogen storage?: An ab initio theoretical study. *Catalysis today, 120*(3): 341-345.

Oku, T., Koi, N., & Suganuma, K. (2008). Electronic and optical properties of boron nitride nanotubes. *Journal of Physics and Chemistry of Solids, 69*(5): 1228-1231.

Oku, T., & Kuno, M. (2003). Synthesis, argon/hydrogen storage and magnetic properties of boron nitride nanotubes and nanocapsules. *Diamond and related materials, 12*(3): 840-845.

Oku, T., Narita, I., & Nishiwaki, A. (2004). Synthesis, atomic structures, and electronic states of boron nitride nanocage clusters and nanotubes. *Materials and Manufacturing Processes, 19*(6): 1215-1239.

Özmen, D., Sezgi, N. A., & Balcı, S. (2013). Synthesis of boron nitride nanotubes from ammonia and a powder mixture of boron and iron oxide. *Chemical Engineering Journal, 219*: 28-36.

Pakdel, A., Zhi, C., Bando, Y., Nakayama, T., & Golberg, D. (2011). Boron nitride nanosheet coatings with controllable water repellency. *Acs Nano, 5*(8): 6507-6515.

Pakdel, A., Zhi, C., Bando, Y., Nakayama, T., & Golberg, D. (2012). A comprehensive analysis of the CVD growth of boron nitride nanotubes. *Nanotechnology, 23*(21): 215601.

Pouch, J., & Alterovitz, S. (1991). A review of:"Synthesis And Properties Of Boron Nitride". *Material And Manufacturing Process, 6*(2): 373-374.

Rubio, A., Corkill, J. L., & Cohen, M. L. (1994). Theory of graphitic boron nitride nanotubes. *Physical Review B, 49*(7): 5081-5084.

Ryu, K.-S., Kim, Y.-I., Jung, J. K., Chen, Y., & Lee, C. H. (2008). Dynamics of Natural Spin Defects in Boron Nitride Nanotubes. *Journal of Nanoscience and Nanotechnology, 8*(10): 5193-5195.

Seo, D., Kim, J., Park, S. H., Jeong, Y. U., Seo, Y. S., Lee, S. H., & Kim, J. (2013). Synthesis of boron nitride nanotubes using thermal chemical vapor deposition of ball milled boron powder. *Journal of Industrial and Engineering Chemistry, 19*(4): 1117-1122.

Shevlin, S., & Guo, Z. (2007). Hydrogen sorption in defective hexagonal BN sheets and BN nanotubes. *Physical Review B, 76*(2): 024104.

Silly, M., Jaffrennou, P., Barjon, J., Lauret, J.-S., Ducastelle, F., Loiseau, A., . . . Rosencher, E. (2007). Luminescence properties of hexagonal boron nitride: Cathodoluminescence and photoluminescence spectroscopy measurements. *Physical Review B, 75*(8): 085205.

Suenaga, K., Colliex, C., Demoncy, N., Loiseau, A., Pascard, H., & Willaime, F. (1997). Synthesis of nanoparticles and nanotubes with well-separated layers of boron nitride and carbon. *Science, 278*(5338): 653-655.

Tang, C., Bando, Y., Sato, T., & Kurashima, K. (2002). Uniform boron nitride coatings on silicon carbide nanowires. *Advanced Materials, 14*(15): 1046-1049.

Tang, C., Bando, Y., Zhi, C., & Golberg, D. (2007). Boron–oxygen luminescence centres in boron–nitrogen systems. *Chemical Communications*(44): 4599-4601.

Tay, R. Y., Li, H., Tsang, S. H., Jing, L., Tan, D., Wei, M., & Teo, E. H. T. (2015). Facile Synthesis of Millimeter-Scale Vertically Aligned Boron Nitride Nanotube Forests by Template-Assisted Chemical Vapor Deposition. *Chemistry of Materials, 27*(20), 7156-7163.

Wang, B.-C., Tsai, M.-H., & Chou, Y.-M. (1997). Comparative theoretical study of carbon nanotubes and boron-nitride nanotubes. *Synthetic metals, 86*(1): 2379-2380.

Wang, J., Lee, C. H., & Yap, Y. K. (2010). Recent advancements in boron nitride nanotubes. *Nanoscale, 2*(10): 2028-2034.

Wang, J., Zhang, L., Zhao, G., Gu, Y., Zhang, Z., Zhang, F., & Wang, W. (2011). Selective synthesis of boron nitride nanotubes by self-propagation high-temperature synthesis and annealing process. *Journal of Solid State Chemistry, 184*(9): 2478-2484.

Wang, X.-B., Weng, Q., Wang, X., Li, X., Zhang, J., Liu, F., . . . Bando, Y. (2014). Biomass-Directed Synthesis of 20 g High-Quality Boron Nitride Nanosheets for Thermoconductive Polymeric Composites. *Acs Nano, 8*(9): 9081-9088.

Wang, Y., Shi, Z., & Yin, J. (2011). Boron nitride nanosheets: large-scale exfoliation in methanesulfonic acid and their composites with polybenzimidazole. *Journal of Materials Chemistry, 21*(30): 11371-11377.

Wu, J., Han, W.-Q., Walukiewicz, W., Ager, J., Shan, W., Haller, E., & Zettl, A. (2004). Raman Spectroscopy and Time-Resolved Photoluminescence of BN and B x C y N z Nanotubes. *Nano letters, 4*(4): 647-650.

Wu, R., Liu, L., Peng, G., & Feng, Y. (2005). Magnetism in BN nanotubes induced by carbon doping. *Applied physics letters, 86*(12): 122510.

Xu, Y. N., & Ching, W. (1991). Calculation of ground-state and optical properties of boron nitrides in the hexagonal, cubic, and wurtzite structures. *Physical review B, 44*(15): 7787.

Yin, L. W., Bando, Y., Zhu, Y. C., Golberg, D., & Li, M. S. (2004). A Two-Stage Route to Coaxial Cubic-Aluminum-Nitride–Boron-Nitride Composite Nanotubes. *Advanced Materials, 16*(11): 929-933.

Zhang, Y., Suenaga, K., Colliex, C., & Iijima, S. (1998). Coaxial nanocable: silicon carbide and silicon oxide sheathed with boron nitride and carbon. *Science, 281*(5379): 973-975.

Zhang, Z. H., & Guo, W. L. (2009). Tunable Ferromagnetic Spin Ordering in Boron Nitride Nanotubes with Topological Fluorine Adsorption. *Journal of the American Chemical Society, 131*(19): 6874-6879.

Zhi, C., Bando, Y., Tan, C., & Golberg, D. (2005). Effective precursor for high yield synthesis of pure BN nanotubes. *Solid State Communications, 135*(1): 67-70.

Zhi, C., Bando, Y., Tang, C., Golberg, D., Xie, R., & Sekigushi, T. (2005). Phonon characteristics and cathodolumininescence of boron nitride nanotubes. *Applied physics letters, 86*(21): 213110-213113.

Zhi, C. Y., Bando, Y., Tang, C. C., & Golberg, D. (2010). Boron nitride nanotubes. *Materials Science & Engineering R-Reports, 70*(3-6): 92-111.

Zhi, C. Y., Bando, Y., Tang, C. C., Huang, Q., & Golberg, D. (2008). Boron nitride nanotubes: functionalization and composites. *Journal of Materials Chemistry, 18*(33): 3900-3908.

Zhou, G., & Duan, W. (2007). Spin-polarized electron current from carbon-doped open armchair boron nitride nanotubes: Implication for nano-spintronic devices. *Chemical physics letters, 437*(1): 83-86.

Zhou, Z., Zhao, J. J., Chen, Z. F., & Schleyer, P. V. (2006). Atomic and electronic structures of fluorinated BN nanotubes: Computational study. *Journal of Physical Chemistry B, 110*(51): 25678-25685.

Zhu, Y.-C., Bando, Y., Xue, D.-F., Xu, F.-F., & Golberg, D. (2003). Insulating tubular BN sheathing on semiconducting nanowires. *Journal of the American Chemical Society, 125*(47): 14226-14227.

LIST OF PUBLICATIONS AND PAPERS PRESENTED

A. Publications in ISI-cited Q1 and Q2 Journals:

1. Ahmad, P., Khandaker, M. U., Amin, Y. M., & Muhammad, N. (2016). Synthesis of Highly Crystalline Multilayered Boron Niride Microflakes. *Scientific Reports, 6*, 21403.
2. Ahmad, P., Khandaker, M. U., Amin, Y. M., Khan, G., Ramay, S. M., Mahmood, A., . . . Muhammad, N. (2016). Catalytic growth of vertically aligned neutron sensitive 10Boron nitride nanotubes. *Journal of Nanoparticle Research, 18*(1), 1-7.
3. Ahmad, P., Khandaker, M. U., Khan, Z. R., & Amin, Y. M. (2015). Synthesis of boron nitride nanotubes via chemical vapour deposition: a comprehensive review. *Rsc Advances, 5*(44), 35116-35137.
4. Ahmad, P., Khandaker, M. U., & Amin, Y. M. (2015). Synthesis of boron nitride nanotubes by Argon supported Thermal Chemical Vapor Deposition. *Physica E: Low-dimensional Systems and Nanostructures, 67*(0), 33-37.
5. Ahmad, P., Khandaker, M. U., & Amin, Y. M. (2015). A comprehensive study of boron nitride nanotubes multiple synthesis from a single precursor. *Indian Journal of Physics, 89*(3), 209-216.
6. Ahmad, P., Khandaker, M. U., & Amin, Y. M. (2014). Effective Synthesis of Vertically Aligned Boron Nitride Nanotubes via a Simple CCVD. *Materials and Manufacturing Processes, 30*(6), 706-710.
7. Ahmad, P., Khandaker, M. U., & Amin, Y. M. (2015). Synthesis of highly crystalline multilayers structures of 10BNNTs as a potential neutron sensing element. *Ceramics International, 41*(3, Part B), 4544-4548.

8. Ahmad, P., Khandaker, M. U., Khan, Z. R., & Amin, Y. M. (2014). A simple technique to synthesize pure and highly crystalline boron nitride nanowires. *Ceramics International, 40*(9, Part B), 14727-14732.

9. Ahmad, P., Khandaker, M. U., Amin, Y. M., & Muhammad, N. (2015). Synthesis and characterization of boron nitride microtubes. *Materials Express, 5*(3), 249-254.

10. Ahmad, P., Khandaker, M. U., Amin, Y. M., & Khan, Z. R. (2014). Synthesis of Boron Nitride Microtubes and Formation of Boron Nitride Nanosheets. *Materials and Manufacturing Processes, 30*(2), 184-188.

11. Ahmad, P., Khandaker, M. U., & Amin, Y. M. (2015). A simple technique to synthesise vertically aligned boron nitride nanosheets at 1200°C. *Advances in Applied Ceramics, 114*(5), 267-272.

12. Ahmad, P., Khandaker, M. U., & Amin, Y. M. (2015). Synthesis of vertically aligned flower-like morphologies of BNNTs with the help of nucleation sites in Co–Ni alloy. *Materials Science in Semiconductor Processing, 38*(0), 113-118.

13. Ahmad, P., Khandaker, Mayeen U., Mohd Amin, Y., & Raza Khan, Z. (2015). Influence of growth duration on size and morphology of boron nitride nanotubes grown via chemical vapor deposition technique. *Journal of Physics and Chemistry of Solids, 85*(0), 226-232.

14. Ahmad, P., Khandaker, M. U., Amin, Y. M., Muhammad, N., Usman, A. R., & Amin, M. (2015). The effect of reaction atmosphere and growth duration on the size and morphology of boron nitride nanotubes. *New Journal of Chemistry*. doi:10.1039/C5NJ01466B

15. Ahmad, P., Uddin Khandaker, M., Mohd Amin, Y., Amin, M., Imran Irshad, M., & Ud Din, I. (2015). Low temperature synthesis of high quality BNNTs via argon supported thermal CVD. *Ceramics International, 41*(10, Part B), 15222-15226.

16. Ahmad, P., Khandaker, M. U., Amin, Y. M., Muhammad, N., Khan, G., Khan, A. S., . . . Khan, A. (2016). Synthesis of hexagonal boron nitride fibers within two hour annealing at 500 °C and two hour growth duration at 1000 °C. *Ceramics International, 42*(13), 14661-14666.

B. Abstract in Conferences:

1. Ahmad, P., Khandaker, M. U., & Amin, Y. M. (2015). Synthesis of BNNTs from Residual Materials by chemical vapor deposition technique. AFM Conference, Stony Brook University, NY USA, 29th June – 3rd July 2015.

2. Ahmad, P., Khandaker, Mayeen U., Mohd Amin, Y., & Raza Khan, Z. (2014). Boron nitride nanowires synthesis via a simple chemical vapor deposition at 1200 °C. PERFIK Conference, Sunway Resort Kuala Lumpur, Malaysia, 18th November – 19th November 2014.

3. Ahmad, P., Khandaker, M. U., & Amin, Y. M. (2015). A Study on the Synthesis of boron nitride microtubes. ICFMD Conference, New York Hotel, Johor Bahru, Malaysia , 04 August – 06 August 2015.